Evaluation of Corrosion Inhibitors in Chloride Contaminated Reinforced Concrete

By

Roumiana Hristova

A thesis submitted in conformity with the requirements for the Degree of Master of Applied Science in the University of Ottawa

Department of Civil Engineering

Faculty of Engineering

University of Ottawa

August 1996

The M.A.Sc. program in Civil Engineering Program is a joint program with Carleton University, administrated by the Ottawa-Carleton Institute for Civil Engineering

ISBN 0-612-16410-1

Canada

UNIVERSITÉ D'OTTAWA
UNIVERSITY OF OTTAWA

ACKNOWLEDGEMENTS

A deep appreciation to Dr. J. Gardner for his supervision and interest in this study.

Thanks are due to Dr. R. Brousseau for providing the concrete samples, B. Baldock and G. Chan for their help with the experimental apparatus.

A sincere gratitude is expressed to Dr. Ping Gu for his constant encouragement, guidance and support throughout this investigation.

Contents

List of Figures

The circles represent the the experimental data and the solid line is a computer simulation curve. Curves numbered 1, 2 and 3 correspond to the chloride contents of 0, 2 and 4%.

Fig. 32. Impedance spectra and simulation for the reinforced concrete specimens containing 5 % sodium nitrite. (a) Real versus Imaginary plot; (b) enlarged Real versus Imaginary plot; (c) Phase angle vs. frequency plot and (d) modulus vs. frequency plot. The circles represent the experimental data and the solid line is a computer simulation curve. Curves numbered 1, 2 and 3 correspond to the chloride contents of 0, 2 and 4%.

Fig. 33. Impedance spectra and simulation for the reinforced concrete specimens containing 5% dinitrobenzoic acid. (a) Real versus Imaginary plot; (b) enlarged Real versus Imaginary plot; (c) Phase angle vs. frequency plot and (d) modulus vs. frequency plot. The circles represent the experimental data and the solid line is a computer simulation curve. Curves numbered 1,2 and 3 correspond to the chloride contents of 0, 2 and 4%.

Fig. 34. (a) Plot of the R_c versus percentage of pre-mixed chlorides and (b) C_c versus percentage of pre-mixed chlorides. Symbols represent: (A-) control concrete; (B-) concrete containing 5 % sodium nitrite; and (C-) concrete containing 5% dinitrobenzoic acid.

Fig. 35. (a) Plot of the R_i versus percentage of pre-mixed chlorides; (b) C_i versus percentage of pre-mixed chlorides and (c) $1-\alpha_2$ versus percentage of pre-mixed chlorides. Symbols represent: (A-) control concrete; (B-) concrete containing 5 % sodium nitrite; and (C-) concrete containing 5% dinitrobenzoic acid.

Fig. 36. (a) Plot of the R_p versus percentage of pre-mixed chlorides; (b) C_{dl} versus percentage of pre-mixed chlorides and (c) $1-\alpha_3$ versus percentage of pre-mixed chlorides. Symbols represent: (A-) control concrete; (B-) concrete containing 5 % sodium nitrite; and (C-) concrete containing 5% dinitrobenzoic acid.

Fig. 37. (a) Plot of maximum phase angle shift versus percentage of pre-mixed chlorides. . Symbols represent: (A-) control concrete; (B-) concrete containing 5 % sodium nitrite; and (C-) concrete containing 5% dinitrobenzoic acid.

Fig. 38. Plot of corrosion current densities versus percentage of pre-mixed chlorides. (a) corrosion current densities were calculated using Stern-Geary equation with B=50mV and Rp obtained from the impedance spectra simulations; (b) corrosion current densities were determined by linear polarization measurements.

Fig. 39. Plots for the corrosion systems without inhibitor

Fig. 40. Plots for the corrosion systems with 2% $NaNO_2$ and 2% -4% $CaCl_2$

Fig. 41. Plots for the corrosion systems with 5% 3-5, dinitrobenzoic acid and 2-4% $CaCl_2$

List of Tables

ABSTRACT

The report describes research to determine the effectiveness of commercial corrosion-inhibiting admixtures on the corrosion of reinforcing steel in chloride contaminated concrete.

Domestic and foreign publications were reviewed to locate performance data and current practices related to the use, testing and evaluation of corrosion inhibiting admixtures. The study consisted of identification and evaluation of the currently used corrosion-inhibiting admixtures in the United States and other countries. A list of available corrosion-inhibiting admixtures was compiled. The existing test procedures for evaluating the effectiveness of corrosion-inhibiting admixtures were appraised. Consideration was given to performance predictability, practicality, cost, and other pertinent factors.

Five-year old "lollipop" concrete specimens containing sodium nitrite and dinitrobenzoic acid as corrosion inhibitors, and comparison with control specimens were studied using linear polarization and impedance spectroscopy. All mixes had different amounts of calcium chloride added.

An equivalent circuit model considering the physical characteristics of the rebar/concrete interface was used to simulate the impedance spectra. The RC parameters obtained from the impedance simulation, including maximum phase angle shift, surface impedance and capacitive responses, were utilized to characterize the surface corrosion of embedded steel and to evaluate the effect of inhibitors with chloride content. The corrosion current densities determined by impedance measurement were compared with those determined using linear polarization and good agreement between the two methods was obtained.

Chapter 1

1. Introduction

1.1. General

The corrosion of reinforcing steel in concrete structures is a multibillion dollar problem all over the world. It is estimated that approximately half of the 500,000 plus bridges in the U.S. Highway system are in need of repair [1]. The Strategic Highway Research Program (SHRP) suggested that $450 to $500 million per year could be saved by correcting problems in current bridges [2]. In recognition of the problem to assess the extent of corrosion damage, the SHRP program allocated approximately $10 million to this problem [3].

Reinforced concrete has been in use for over 100 years and, in general, the environment provided by concrete provides protection for the embedded steel. Many of the problems associated with corrosion in reinforced concrete can be attributed to the presence of salts from the environment. This association with salt has led to two problems, (1) a misunderstanding of the role of salts in the corrosion process for reinforced concrete structures and (2) a false sense of security for concrete structures in the absence of salt. The reinforcement in concrete, made from hydraulic cements such as Portland cement, is relatively resistant to corrosion in air and water environments without chloride ions. This is because of the high alkalinity of concrete, i.e. a pH of approximately 12.5. In such highly alkaline environments, a protective oxide film is normally developed on the surface of the reinforcing steel which inhibits the corrosion of the steel.

However the frequent high concentrations of chloride ions in the concrete of highway structures or parking garages, originating from deicing salts, will induce corrosion of the reinforcement. The ingress of chloride ions destroys the protective oxide film around the steel reinforcement allowing the steel to corrode, given that oxygen and moisture are present.

A review of the corrosion of reinforcing steel in the concrete literature reveals two possible mechanisms whereby concrete may protect steel from corrosion:

1) Concrete is a base, and bases cause iron and steel to form protective oxides (passive films) which protect the metal from further reaction with their environments.
2) Concrete is a high-resistance electrolyte which limits galvanic corrosion.

The next section is a brief review of each of these possibilities and how they relate to salts, cracking, freeze-thaw cycles, and other environmental concerns.

1.2. Corrosion principles in concrete

1.2.1. Concrete as an Electrolyte

Good-quality concrete provides excellent protection for steel reinforcement. Chemical protection is provided by concrete's high alkalinity and physical protection is afforded by the concrete acting as a barrier to the access of aggressive species. Because of this excellent protective nature, concrete is generally specified only on the basis of its (28-day) strength with little, if any, regard for its durability. However, despite these inherent protective qualities, corrosion of steel reinforcement has become the most common cause of distress in reinforced concrete structures. In structures such as bridges and parking garages, this may be attributed in large part to the use of de-icing salts. In other structures, carbonation of the concrete cover and/or salt penetration from sea spray may be responsible for the corrosion. The unexpected rapidity of these effects may, in turn, be due to a number of factors such as poor specifications and the lack of control in mixing or placing of the concrete.

As it was mentioned above, concrete as a heterogeneous material has two special characteristics related to rebar corrosion, high alkalinity and high electrical resistivity. High Alkalinity: Concrete is a composite material made with cement, sand, aggregates, water and chemical admixtures. Portland cement hydration involves initial dissolution of CaO, $CaSO_4$ hemihydrate or dihydrate, alkalis and aluminate phases etc... This is followed by reactions between the main components, C_3S* and C_2S, and free water resulting in the formation of C-S-H, calcium hydroxide (CH), ettringite and other minor compounds. These reactions bridge the individual particles, fill the capillary pores, bind aggregates together and promote the formation of a rigid microstructure and consequent strength development[4,5] The pore solution of concrete has a pH value between 12-13 due to of the presence of calcium hydroxide along with small amounts of Na_2O and K_2O.

High Electrical Resistivity: The conduction in concrete is principally through the motion of ions, such as Na^+, K^+, OH^-, SO^{2-}_4 and Ca^{++}, in the pore solution. A typical value of the electrical resistivity of pore solution in cement paste is about 25-35 Ω cm [6]. The conventional aggregates used in concrete, however, are relatively good insulators with electrical resistivity values ranging from 10^5 to 10^{14} Ωcm. The resistivity air for air-dried Portland cement paste and concrete is in the region 600-1200 kΩcm. Moist concrete and cement paste have values of 2.5-4.5kΩcm and 1.0-1.3 kΩcm, respectively.

In general, the stone and sand constituents of concrete do not play a significant role in the protection or corrosion (no leachable ions) of reinforcing steel. The presence and transport of the corrosion reactants (water, oxygen, and various ions), the corrosion products, and the passage of the ionic current necessary to support corrosion are normally confined to the cement paste phase. It is, therefore, this phase which will be considered here. To understand the influence of the cement paste on corrosion, it is sufficient to consider the paste as a two-phase system consisting of the hydrated minerals and a liquid phase-the pore solution. From the point of view of reinforcement corrosion, the controlling parameters are: (1) the composition and quantity of the pore solution; (2) the structure and distribution of the pores, and (3) the presence of the $Ca(OH)_2$ in the hardened paste.

1.2.1.1. Cement Paste Pore Solution

The composition of the pore solution is the decisive factor in determining whether embedded steel will be passivated or whether it will actively corrode. In recent years, many laboratories have obtained equipment such as that described in Ref. 7 to extract the solution out of hardened paste, mortar, or concrete and data is being accumulated on the influence of a number of factors on the composition of the pore solution.[8-10]

These investigations have shown that the highly soluble sodium and potassium salts can give the pore solution of ordinary portland cement a pH of greater than 13 while the pH of blended cements is somewhat lower. A major application of the technique has been to determine how much of the total chloride content of the cement is present as free

* C=CaO; S=SiO_2; H=H_2O.

chloride ions in the solution and therefore, is available to attack the reinforcement. How the composition of the cement influences the degree of binding of the chloride ions is also of interest.

1.2.1.2. The Structure and Distribution of Pores

The structure, size distribution, and interconnection of the pores in the cement paste determine the availability of oxygen and moisture at the steel surface, both of which are necessary for the maintenance of a passive film. They also determine the rate of penetration of chlorides and carbon dioxide which, are the two most common culprits in the depassivation of embedded steel.

There are several techniques available for determining the pore-size distribution, those most commonly employed for cement being mercury intrusion porosimetry, vapor adsorption, and vapor desorption. A comparative review of these three techniques is given in reference 11. The major disadvantage of the mercury porosimetry and vapor adsorption techniques is that the cement paste must be thoroughly dried and the drying process alters the pore structure, causing the finer pores to collapse under the capillary forces. Two newer techniques which do not suffer from this disadvantage, and are also able to determine pore sizes over considerably wider range than earlier techniques, are small-angle neutron scattering [12] and low temperature calorimetry [13,14]. The results of these two techniques have, independently, been interpreted as showing a clear bimodal distribution of pore sizes corresponding to the gel and capillary pores. It is the capillary pore system which is responsible for the diffusion and permeation processes and, therefore, of importance for corrosion.

1.2.1.3. The Presence of Calcium Hydroxide

$Ca(OH)_2$ has a very limited solubility in aqueous solutions and the bulk of this hydration reaction product remains as a solid substance embedded in the cement paste. It adds little to the strength of the paste but provides a pH buffer for the pore solution, keeping the solution at a constantly high pH. The higher the concentration of $Ca(OH)_2$, the longer it takes for a carbonation front to penetrate the concrete cover to the steel surface and the greater the pozzolanic content can be without risk of a significant decrease in pH.

It has been reported [15.16] that $Ca(OH)_2$ has a second advantageous effect, namely that of precipitating as a coating over the surface of the steel, the pore walls, the mould walls, and so on. This coating of $Ca(OH)_2$ hexagonal platelets constitutes a physical protection of the bars. This is one of the reasons why reinforcement corrosion tests in solutions cannot be simply extrapolated to the real behavior of steel in concrete.

1.2.2. Passivity

The corrosion process can be considered in the form of an electrical circuit, and, as in any electrical system, the driving force for the reaction is a difference in electrical potential between the anode and cathode. For corroding systems, the driving force is the difference in the electrochemical potentials for the following reactions:

$$Fe \Rightarrow Fe^{2+} + 2e^-$$

$$2H_2O + O_2 + 4e^- \Rightarrow 4\ OH^-$$

These potentials maybe defined as a measure of the ease of charge transfer across the steel-concrete interface and the ease of ionization of the dissolved oxygen, respectively.

It is not possible to determine the absolute value of an electrochemical potential and, therefore, the potential difference between the anode and cathode and a reference electrode is taken as a measure of the actual potential and is quoted in volts relative to the particular reference electrode used. A fixed difference in potential is always established between a metal and a solution containing its ions at an activity of unity. This potential difference is arbitrarily defined as zero for the hydrogen electrode which is used as a reference for all metal potentials. A scale of standard potentials, E^0, of metals in contact with a solution containing their ions at an activity of unity and relative to hydrogen potential may thus be drawn up.

When the solution in contact with the metal does not contain its ions or if their activity is not unity, the Nernst equation allows the actual potential, E, to be determined :

$$E = E^\circ - (RT / nF)\ 1n\ K$$

where R is the gas constant, n the valence, and K the equilibrium constant for the ions present in the solution.

Therefore, the actual potential of a corroding iron piece (known as its open circuit potential, at rest potential, or corrosion potential, E_{corr}) is dependent on a variety of factors, including the equilibrium potentials of the anodic and cathodic half-cell- reactions, the composition of the surrounding electrolyte, the temperature, the polarization the half cells, and the existence, if any, of passivity.

The concept of passivity was reintroduced in 1964 by Cornet and co-workers who cited the then popular concept of potential-pH (Pourbaix) diagrams [17] to explain how concrete, with a pH of approximately 12.8, protects steel from corrosion. These diagrams (see Fig. 4), based on equilibrium thermodynamics, define three regions in potential-pH space:

1. Immunity - the metal is thermodynamically stable and is immune to corrosion.
2. Corrosion - ions of the metal are thermodynamically stable, and, under most conditions, corrosion will occur at a rate which cannot be predicted thermodynamically.
3. Passivity - compounds of the metal are thermodynamically stable. These compounds, or passive films, may protect the substrate from further reactions with the environment and may be protective.

1.2.3. Corrosion of reinforcing steel

As mentioned above, the two major causes of the breakdown of passitivity on steel embedded in concrete, and the consequent initiation of active corrosion, are (a) the presence of chloride ions, either included in the mix with the concrete raw materials or due to penetration from the environment and (b) a decrease in the pH value of the aqueous solution in the concrete pores because of reaction of the cement paste with atmospheric carbon dioxide. These two factors can, and often do work together, having a synergistic effect on each other.

The consequences of the corrosion of reinforcement are: (a) decrease of the bar diameter (weakening their mechanical properties); (b) cracking and spalling of the concrete cover due to the expansive nature of the iron oxides, and (c) decrease of the steel-concrete bond.

It should also be mentioned that, for prestressed or post-tensioned structures, sudden and catastrophic failure can occur due to hydrogen embrittlement of the stressed

steel. This type of failure is a result or corrosion under non-alkaline conditions where the cathodic half-cell reaction evolves hydrogen.

1.3. Threshold concentration of chloride in concrete for the initiation of reinforcement corrosion

In good quality portland cement concrete, steel develops a protective passive layer because of the high alkalinity of the pore solution. In the passive state, the steel corrodes at a insignificantly slow rate, typically of the order of 0.1 mm/year [2]. However chloride ions break down this passivity and allow the steel to actively corrode.

The most common source of chlorides in concrete is from the environment. Chlorides can penetrate all types of concrete and the presence of cracks is not a necessary factor. The most rapid form of penetration occurs by capillary suction of salt water into more or less dry concrete. By this process, the salt water can penetrate several millimeters in a few hours. In wet or highly moist concrete, the penetration occurs more slowly by diffusion of the chloride ions through the cement paste pore solution with the concentration gradient as the driving force. The penetration of a 10 mm thick layer of cement paste by chlorides would takes months.

The critical amount of chloride necessary for the breakdown of the passive film and the onset of active corrosion has been the subject investigation for many years. Moreover, its corollary - the amount of chloride which can be tolerated without risk of corrosion is of major interest to practicing engineers who would like to use accelerators or other chloride-containing additives in concrete , or who must construct in areas where the mixing water or aggregate are contaminated by chlorides (for example in the Middle East).

From the viewpoint of reinforcement corrosion, [18] it is the amount of "free" chloride present in the cement paste pore solution rather than the total chloride concentration which is critical. The difference between these two, the amount or proportion of "bound" chloride determines the concentration of Cl^- in the pore solution which effects the total chloride threshold value for corrosion. Finally, they determine the access of oxygen from the environment and the electrical resistivity of the concrete which, together, control the corrosion rate after initiation.

It should be noted that the exact value of threshold concentration cannot be used

in practice because each part of each construction is likely to have its own unique value. Consequently, the aim of different projects has been to determine the relative influence of the different factors so that the risk of corrosion from penetrating chlorides can be minimized in future constructions.

1.4. Inhibitors in Concrete

The principle function of corrosion-protection systems is to prevent aggressive agents, mainly chloride ions, from attacking the surface of the reinforcing steel. Realkalization or desalination removes chloride ions from the surface of the reinforcing steel by electrical migration. Epoxy coated rebar provides a physical barrier to the ingress of aggressive agents and cathodic protection electrochemically stabilized the steel surface. Use of corrosion-inhibiting admixtures can be considered as a cost-effective solution to the wide spread corrosion problem due to its convenient and economical application to both new structures and repair of existing buildings [4].

The ISO 8044 definition for a corrosion inhibitor is a "Chemical substance which when present in the corrosion system at a suitable concentration decreases the corrosion rate without significantly changing the concentration of any other corrosive agent"[1]. Corrosion inhibitors used in concrete must not have adverse affects on the concrete properties in either the plastic or hardened states.

Ideally when used in appropriate amounts in the concrete it should prevent corrosion of embedded steel with no adverse effects on concrete performance (strength, setting time, bleeding etc.). Corrosion inhibitors may be classified as inorganic, organic, or vapor-phase inhibitors. Corrosion inhibiting admixtures for reinforced concrete typically are categorized as anodic, cathodic, or mixed depending on how the inhibitor effects the corrosion process. Previous studies mainly focused on sodium nitrite, calcium nitrite, potassium chromate, sodium benzoate, stannous chloride. Except calcium nitrite it was found that a remarkable decrease (as high as 20 to 40%) in comparative strengths were observed when these inhibitors were added to the mortars. Tensile strengths were also adversely affected by sodium nitrite and sodium benzoate. Stannous chloride appeared to decrease corrosion in the short term [19].

It should be mentioned that the advantages of using inhibitors are that the inhibitor is distributed throughout the concrete protecting all the steel. and that concrete's low permeability prevents the inhibitor from being lost. A review of early research on inhibitors for steel in concrete is given in the report.

1.5. Objective and Scope

The objective of this research program is to investigate the effectiveness of two different commercial corrosion-inhibiting admixtures and to determine the values of corrosion intensity, which have been measured in laboratory tests using linear polarization and A.C. Impedance techniques .

The following is the scope of the investigation:

1. Literature search and review of domestic and foreign publications, research findings, performance data and current practices related to the use, testing and evaluation of corrosion inhibiting admixtures.

A list of available corrosion-inhibiting admixtures is compiled. The effect of each admixture on the behaviour of fresh and hardened concrete and the mechanism by which each admixture works are summarized.

2. Investigation of the methods of evaluating the corrosion resistance of reinforcing material in the laboratory and in the field.
3. Identification of methods of monitoring existing structures and for evaluating the effectiveness of corrosion- inhibiting admixtures
4. Preparation of an experimental program for testing five years old reinforced specimens.
5. Testing of samples involves using two different electrochemical approaches- linear polarization and A.C. Impedance spectroscopy
6. Evaluation and presentation of results
7. Presentation of research findings relating to the limitations and improvements of the discussed inhibitors.

CHAPTER 2

2. Basic Principles of Corrosion

2.1. Objectives

The objective of this part of the report is to describe the generally accepted processes of corrosion of reinforcement and protection of reinforcement against corrosion. A summary of the principles of metallic corrosion processes in general is presented. The principles are then applied to provide a concise description of the various corrosion states of steel in concrete[5].

2.2. Electrochemical nature of corrosion

It has long been established that the corrosion of base metals in aqueous environments proceeds by an electrochemical mechanism [20-21].

The corrosion process is similar to action which takes place in a flashlight battery and, as in a battery, the corroding system consists of an anode where electrochemical oxidation takes place, a cathode where electrochemical reduction takes place, an electrical conductor, and an electrolyte (in the case of concrete, this is the cement paste pore solution).

For steel in concrete the iron is oxidized at the anode (the negative pole) by one of a number of half dash cell reactions such as:

$$Fe \text{ Þ } Fe^{2+} + 2e^{-}$$

The electrons released at the anode flow through the steel to the cathodic areas, as illustrated in Fig. 1, where they are consumed by the cathodic half-cell reaction.

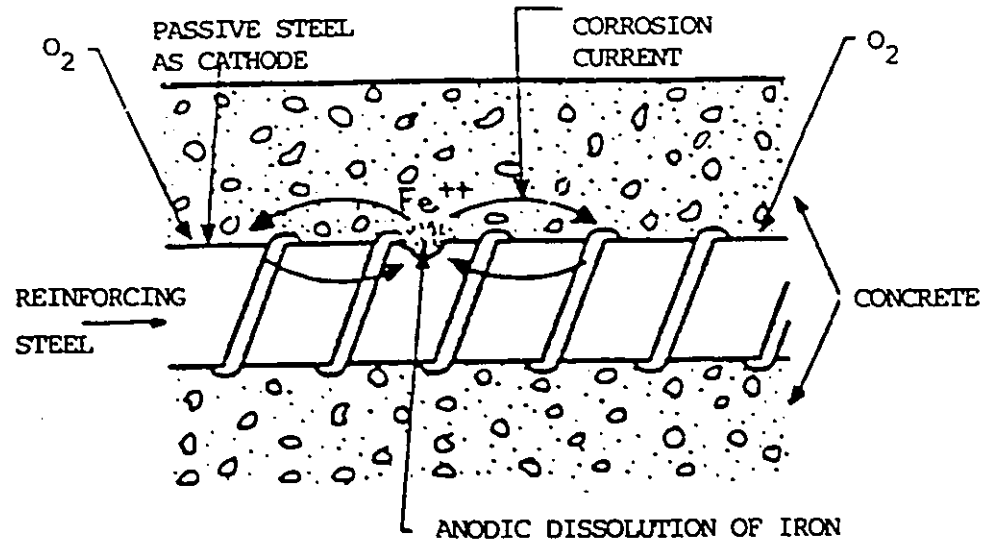

Fig. 1: Schematic representation of the corrosion of steel in concrete. (Ref.21)

In normal concrete structure which the pore solution is alkaline, and a ready access to air, this is the reduction of dissolved oxygen:

$$2H_2O + O_2 + 4e^- \Rightarrow 4\ OH^-$$

The development of anodes and cathodes (regions of different electrochemical potential), is due to the existence of heterogeneities in the corroding system. A common example is that of two different metals which are connected and immersed in the same electrolyte. One will act as an anode, the other as a cathode. Heterogeneities can also exist at the surface of a single metal, due to metallurgical segregation, different grain orientations, etc., or due to local differences in the electrolyte (variations in concentration, aeration, etc.)

When a corrosion cell is established, the net anodic current (the release of electrons by corrosion of the metal) is equal to the net cathodic current (in the case of steel in concrete, the consumption of electrons in the reduction of oxygen).

The corrosion process will depend on the distribution of anodes and cathodes and on their relative areas. Therefore, if the anodes and cathodes are irregularly distributed on the steel surface and change position during the corrosion process, the attack will be more or less uniform. If, on the other hand, the anodes are located at fixed points and the anode/cathode area ratio is very small, localized attack will develop.

The surface of the corroding metal functions as a mixed electrode, upon which coupled anodic and cathodic reactions take place. These processes may be illustrated as shown in figures 2a and 2b, where the corrosion of iron in different environments is represented.

a)

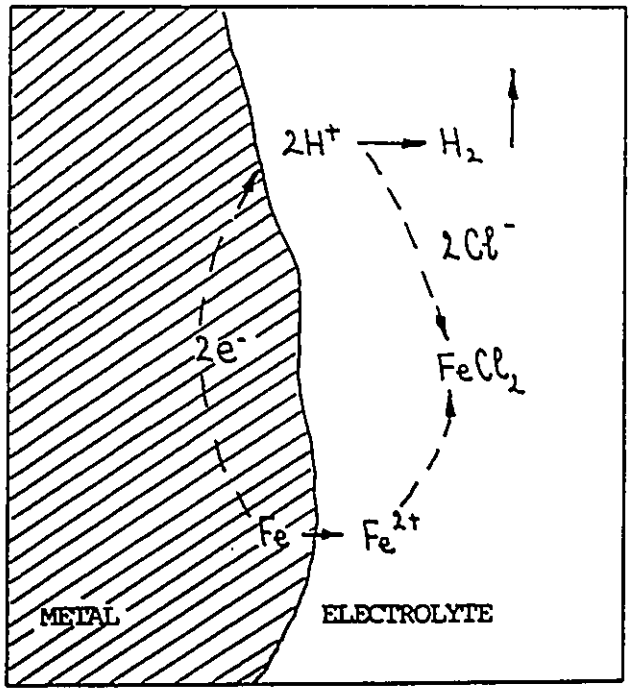

Fig. 2a: Corrosion of iron in hydrochloric acid solution (Ref. 19)

b)

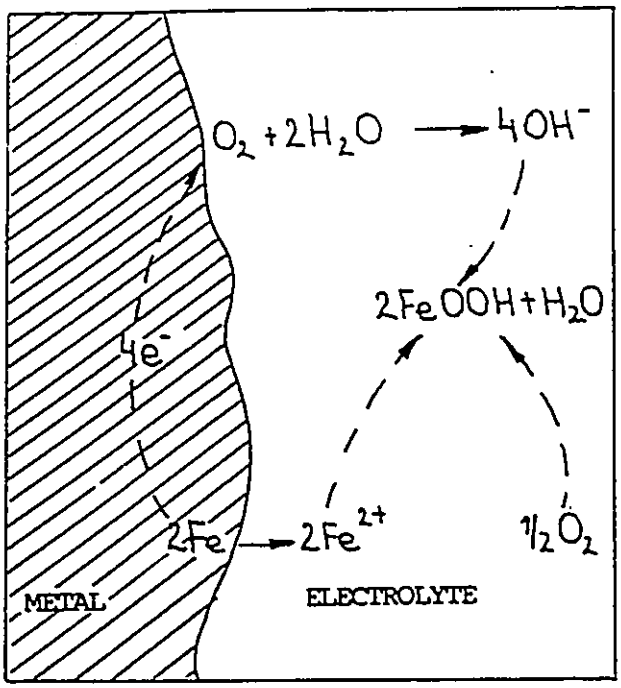

Fig. 2b: Corrosion of iron in oxygenated water (Ref.19)

At anodic sites metal atoms pass into solution as positively charged, hydrated ions (anodic oxidation) and the excess free electrons flow through the metal to cathodic sites where an electron acceptor, such as a hydrogen ion or dissolved oxygen is available to consume them (cathodic reduction). The process is completed by electromigration of ions through the aqueous phase, leading to the formation of a corrosion product which may be soluble (e.g. ferrous chloride) Fig. 2a or insoluble (e.g. rust, hydrated ferric oxide) Fig. 26.

Essential features of the process in each case are as follows:

a) a reactive metal which will oxidize anodically to form soluble ions,

b) a reducible substance which provides the cathodic reactant,

c) an electrolyte which allows ions to move between anodic and cathodic sites.

2.2.1. Electrode Potentials

A direct analogy may be drawn between the behavior of a corroding metal and that of an electrolytic cell. Since current flows between the local anodes and cathodes, electrical potential differences must exist between these sites, as shown in Figure 3.

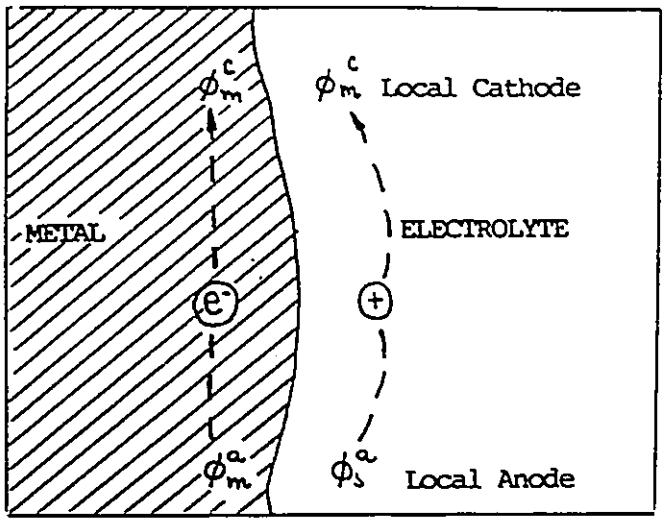

Fig. 3: Relationship between potentials and currents generated in corrosion cell (Ref.19)

If $\varnothing_m$ and $\varnothing_s$ represent the electrical potentials of points at the metal surface and in the surface and in the neighboring solution phase (separated by an electrical double layer consisting of an array of charged particles and oriented water dipoles) and if the superscripts a and c refer to anodic and cathodic sites respectively, then:

$$\varnothing_m^a < \varnothing_m^c \quad , \varnothing_s^a > \varnothing_s^c$$

and therefore:

$$(\varnothing_m^a - \varnothing_s^a) < (\varnothing_m^c - \varnothing_s^c).$$

The quantity $(\varnothing_\mu - \varnothing_s)$, which represents the potential drop across the electrical double layer, is known as the electrode potential and denoted by (E). Thus the electrode potential is always lower at a local anode than at a cathode of corrosion couple.
The difference $(E_c - E_a)$ may be very small if anodes and cathodes are closely spaced and the electrolyte solution is of high conductivity but it may amount to as much as several

hundred millivolts if the anodes and cathodes are separated by a medium of high resistance.

Absolute values of electrode potentials are indeterminate. Relative values can, however be measured and are expressed on scales for which the zero-point is arbitrarily defined by the fixed electrode potential of some reference half-cell. Reference half-cells are reversible electrodes at which single charge transfer reactions are in equilibrium under defined conditions of concentration and temperature.

2.2.2 Corrosion Tendency

Questions as to why a particular metal does or does not tend to corrode in a particular environment may be viewed from the standpoint of chemical thermodynamics.

Thermodynamic data (ΔG° and E° values) for chemical and electrochemical reactions that may influence the corrosion of metals in aqueous environments at 25 ° C have been collected by Pourbaix and co-workers.[17] These provide the means for deciding which of a set of reactions are thermodynamically favored and to predict the most stable reaction products under specified conditions of electrode potential and solution composition.

A convenient form of representation of such information is the Equilibrium Potential/pH diagram (or Pourbaix diagram) in which the axes are electrode potential and solution pH value. The domains of stability of the various substances considered are bounded by lines that represent conditions of equilibrium for the following classes of reaction:

-chemical reactions involving H^+ or OH^- (vertical lines)

-electrochemical reactions involving H^+ or OH^- (sloping lines)

-electrochemical reactions without participation of H^+ or OH^- (horizontal lines).

An important example of an equilibrium potential/pH diagram is that for the system Fe - H_20 at 25 °C, shown in Figure 4, in which the concentrations of dissolved ions, other than H^+ and OH^-, are taken to be 1μmol l^{-1} and solid phases are assumed to be pure.

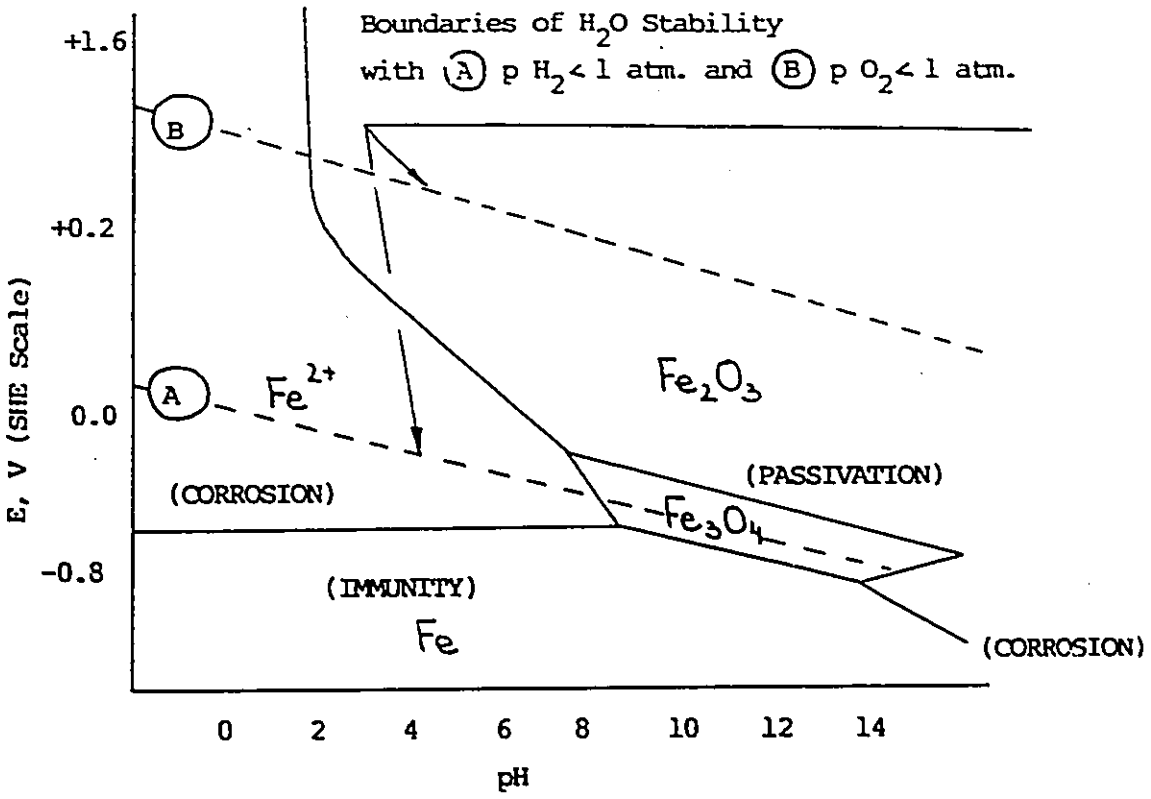

Fig. 4: Pourbaix Diagram for Fe - H_20 at 25 °C (Ref. 17)

The domains over which soluble ions are stable are liable to be associated with corrosion since anodic reactions leading to the formation of Fe^{2+} or Fe0.OH^- are thermodynamically favored:

$$Fe = Fe^{2+} + 2e^-$$

$$Fe + 3OH^- = Fe0.OH^- + H_2O + 2e^-$$

The domains over which the oxides, Fe_3O_4 and Fe_2O_3, are stable and are likely to give rise to a condition termed passivation since significant corrosion may be stifled owing to the anodic formation of a protective oxide layer on the metal surface:

$$3Fe + 4H_2O = Fe_3O_4 + 8H^+ + 8e^-$$

$$2Fe + 3H_2O = Fe_2O_3 + 6H^+ + 6e^-.$$

The domain over which Fe is stable is one of immunity from corrosion where the metal is thermodynamically unable to undergo anodic reactions.

metal is thermodynamically unable to undergo anodic reactions.

Even though the information displayed in an equilibrium potential/pH diagram provides a useful basis for predicting conditions under which particular reactions are liable to influence the corrosion behavior of metals it is necessary to recognize that the approach has certain limitations. In particular, the kinetics of the possible reactions are not considered and, therefore, it is impossible to predict whether a thermodynamically favored reaction, will occur at a significant rate in practice.

Secondly, it is necessary, when applying the information contained in a Pourbaix diagram, to assume that the aqueous solution composition in the vicinity of the corroding surface is known. This presents difficulties when considering real corroding systems in which concentration gradients may be developed.

2.2.3. Polarization of Electrochemical Reactions

The foregoing discussion established that the condition for equilibrium of a single electrode reaction is that the electrode potential (E) takes a value (E_{eq}). At this potential, the rates of the reversible anodic and cathodic processes, represented by current densities i_a and i_c respectively, are equal and opposite:

$$i_a = | i_c | = i_o.$$

(where i_0 is termed the exchange current density for the reaction).

If $E > E_{eq}$, then the anodic process is favored ($i_a > | i_c |$) and if $E < E_{eq}$, the cathodic process predominates ($i_a < | i_c |$). In either case, the electrode is said to be polarized and the driving force for the net anodic or cathodic reaction is related to its overpotential (n_a or n_c) where:

$$n_a = E - E_{eq}$$

$$n_c = E_{eq} - E .$$

The relationships between overpotential and current density for individual electrode processes that play a part in corrosion reactions may be determined experimentally by means of an electrolytic cell arrangement in which the metal under investigation (the working electrode) has its electrode potential controlled by means of

an electronic potentiostat. The resulting graphs of η versus i (or versus log i) are known as polarization curves and the forms that these relationships take are dependent on the nature of the rate-determining step in the electrode process considered (see Figures 5 and 6).

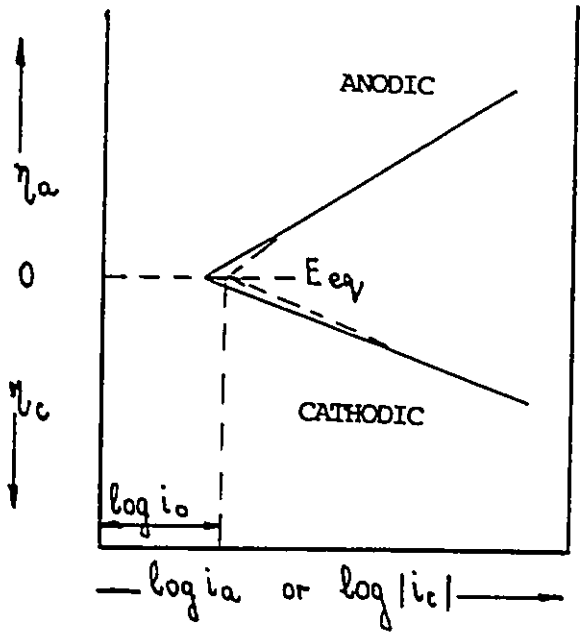

Fig. 5: Polarization curves for an electrode process in which the rate is limited by a step involving thermally activated charge transfer. (Ref. 17)

For $\eta > 50$ mV, the relationship between overpotential and current density is known as the **Tafel Equation:**

$$n_a = \beta_a \log (i_a / i_o)$$

$$n_c = \beta_c \log (i_c / i_o)$$

where the Tafel coefficients, β_a and β_c, are constants for the reaction at given temperature.

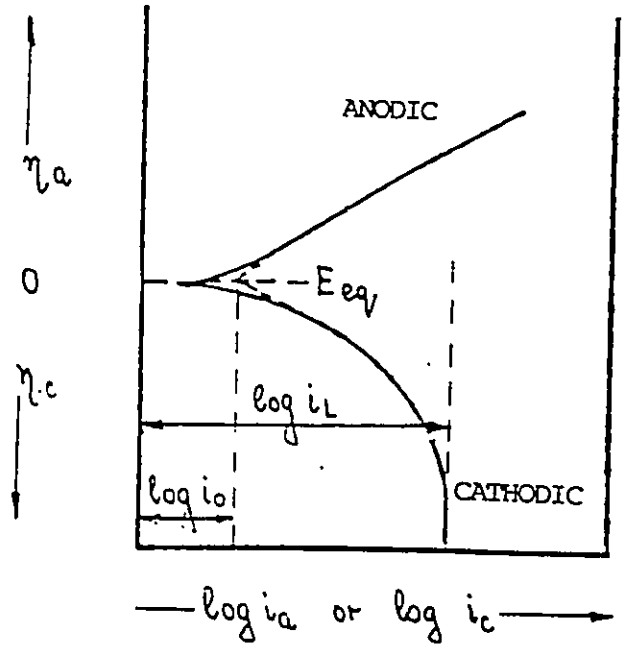

Fig. 6: Polarization curves for an electrode process such as $O_2 + 2H_2O + 4e^- \sim 4OH^-$ (Ref. 17).

In an electrode process such as $O_2 + 2\ H_2O + 4e^- \sim 4\ OH^-$ the rate of the cathodic reaction is limited by mass transport of the reactants by diffusion to the electrode surface, a situation referred to as concentration polarization; at large values of overpotential (η_c), the cathodic current density (i_c), approaches a limiting value (i_L), whose magnitude depends on temperature, stirring of the solution etc. The relationship is of the form: η_c = constant • log $(1 - i_c / i_L)$.

In general, the form of a polarization curve for a **single electrode process** will be expected to reflect the tendency for reaction rate (i) to increase as the driving force for the reaction (η) is increased. If, however, the electrode is capable of sustaining different reactions at different ranges of electrode potential, then apparently anomalous forms of polarization curve may result. Consider, for example, the case of a metal (M) which tends to dissolve anodically forming M^{2+} ions at $E > E_{eq,\ M/M^{2+}}$, $(M = M^{2+} + 2e^-)$, but can form a surface oxide film (MO) at $E > E_{eq,\ M/MO}$, $(M + H_2O = MO + 2H^+ + 2e^-)$. The resultant

surface oxide film (MO) at $E > E_{eq,\ M/MO}$, ($M + H_2O = MO + 2H^+ + 2e^-$). The resultant anodic polarization curve may exhibit features shown in Figure 7. At values of $E < E_{eq,\ M/M^{2+}}$, anodic dissolution is thermodynamically impossible and the metal is **immune** to dissolution. Raising E to values $> E_{eq,\ M/M^{2+}}$ leads to **active** dissolution at a rate which initially increases with increasing overpotential. At some potential more noble than $E_{eq,M/MO}$, however, active dissolution practically ceases owing to the formation of a surface film of oxide which renders the metal **passive** and allows the passage of a small 'leakage current' that increases only slightly with further polarization. If the oxide film is an electron conductor, then the surface may support the anodic formation of oxygen from water ($2H_2O = O_2 + 4H^+ + 4e^-$) at potentials more noble than $E_{eq,\ H_2O/O_2}$, the associated increase in anodic current density being shown in figure 7 by the dashed region of the polarization curve.

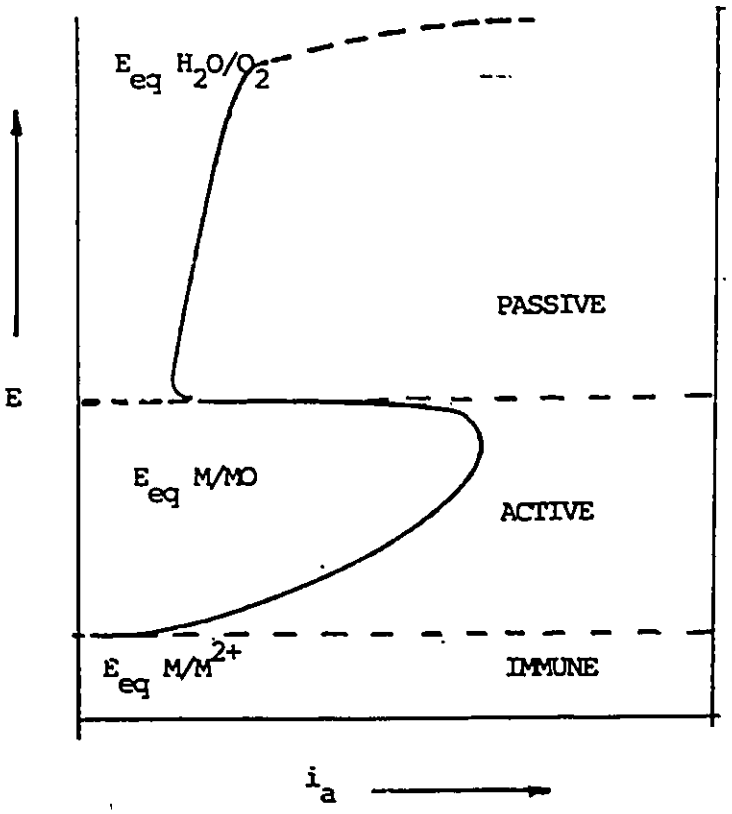

Fig. 7: Anodic polarization curve showing a transition from active dissolution to passivation (Ref. 17).

2.2.4 Corrosion Potentials and Corrosion Rates

The discussion of polarization curves has been concerned with behavior of electrodes that are made to function as net anodes or cathodes of cells in which the driving force is supplied by an external power source (the potentiostat). The situation is different in the case of a freely corroding metal, where separate anodic and cathodic processes are occurring simultaneously at equal rates on the same mixed electrode surface.

The simplest form of corrosion process is one in which a single polarized anodic reaction ($M - Ze^- = M^{Z+}$) and a single polarized cathodic reaction ($X + Ze^- = X^{Z-}$) are coupled to form numerous microcells on the surface of a metal immersed in an electrolyte of high conductivity; it may be represented as shown in figure 8 in what is known as an **Evans diagram** for the corrosion process. This shows the polarization curves for the separate anodic and cathodic reactions intersecting at a point (P) where the mean anodic and cathodic current densities are equal and represent the corrosion rate in terms of a mean corrosion current density (i_{corr}). The electrode potential of the couple at this point is termed the corrosion potential (E_{corr}).

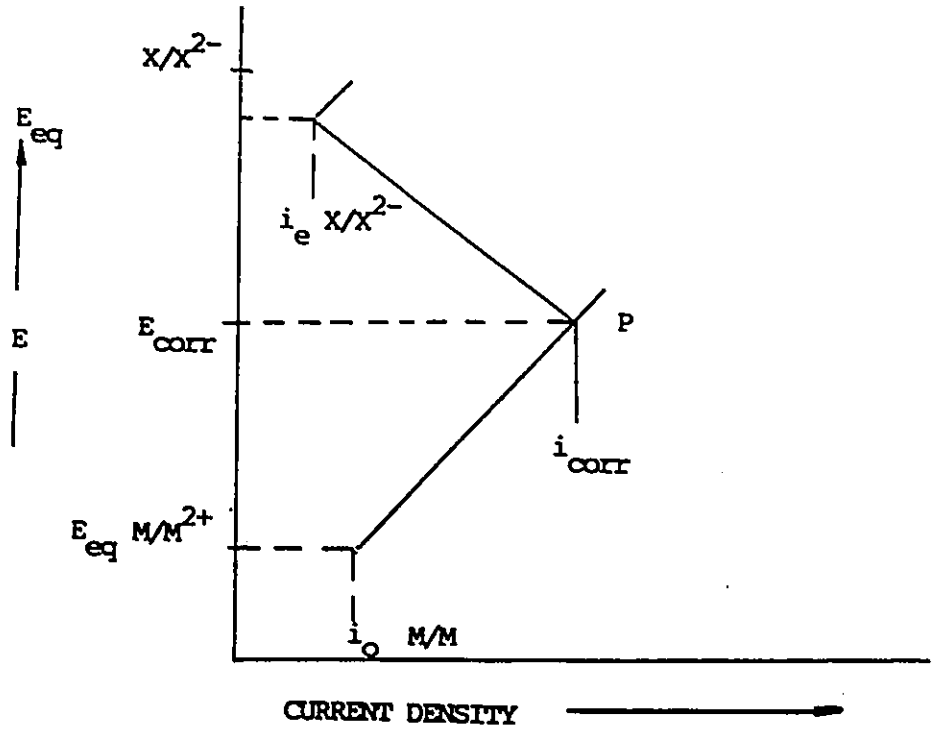

Fig. 8: Evans diagram for simple corrosion couple (Ref.17).

However, there must always be some difference between the electrode potentials developed at anodic and cathodic sites on the metal surface. While the difference is negligible when corrosion takes the form of micro-cell action, it may amount to a significant Ohmic drop (ir) under conditions where corrosion macro-cells are formed when the anodic and cathodic areas are separated by a medium of high electrolytic resistance. In these circumstances, the Evans diagram is modified as shown in Figure 9. The mean corrosion rate, as represented by i_{corr}, is now reduced and the corrosion potential varies with location between the limits E^a_{corr} and E^c_{corr}, positions of local anodes being indicated by the regions of low corrosion potential (E^a_{corr}). This has practical application since surveys of corrosion potential may be used as a means of identifying sites of corrosion damage (anodic regions) in structures where macro-cells develop.

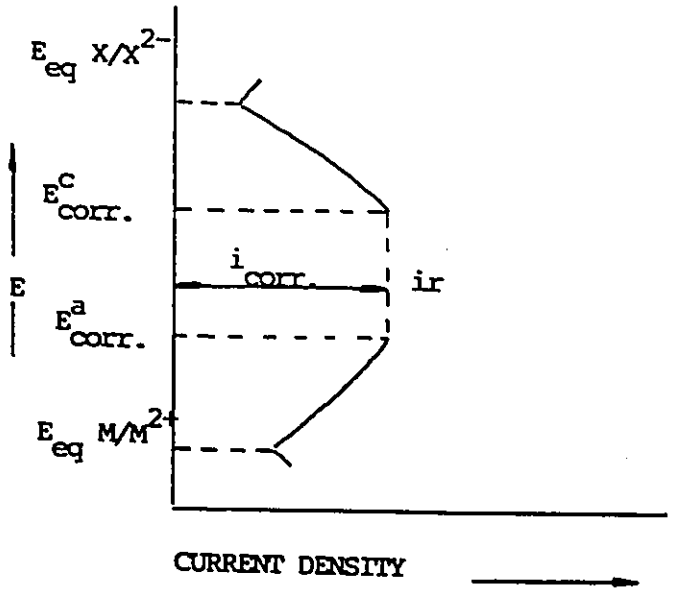

Fig. 9: Evans diagram for corrosion couple with Ohmic drop (Ref.17).

In the absence of significant Ohmic drops, the mean corrosion rate (i_{corr}) depends on the magnitude of the difference between the reversible potentials of the anodic and

cathodic reactions and on the average slopes of the anodic and cathodic polarization curves. If the anodic reaction is steeply polarized (e.g. owing to the presence of a passive film), then i_{corr} is small and E_{corr} assumes a value which is close to the reversible potential of the cathodic reaction (Figure 10). Conversely, if the cathodic reaction is steeply polarized (e.g. owing to limited oxygen availability), the situation is as depicted in Figure 11, with i_{corr} again small but the corrosion potential close to the reversible potential of the anodic reaction.

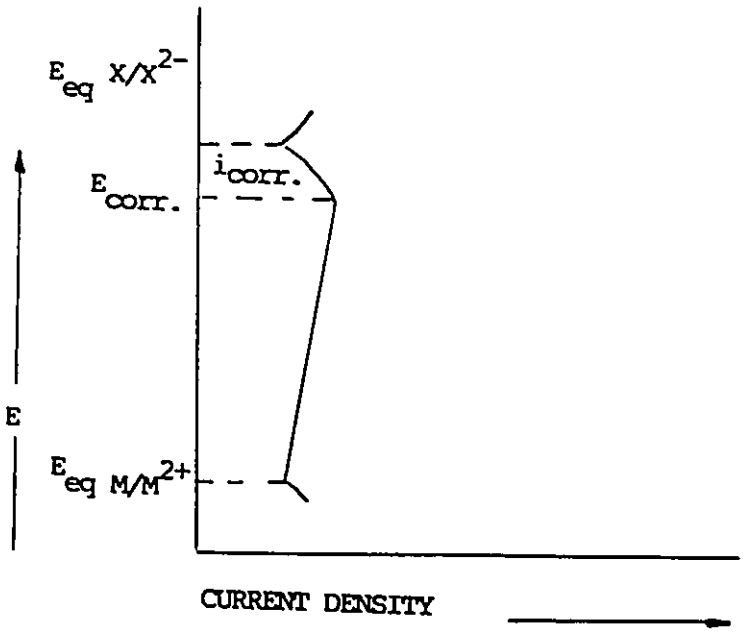

Fig. 10: Evans diagram illustrating corrosion under anodic control (Ref.17).

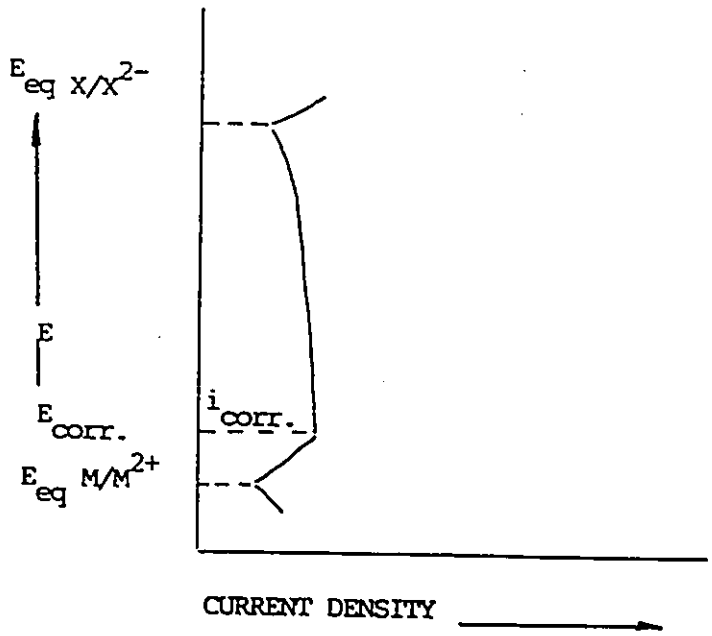

Fig. 11: Evans diagram illustrating corrosion under cathodic control (Ref.17).

It is clear from the previous considerations that the corrosion potential is not a simple property of a corroding system nor a reliable guide to corrosion rate. If, for example, the corrosion potential is observed to shift with time in a negative (base) direction, then this implies either that the anodic reaction is being facilitated, in which case the corrosion rate is increasing, or that the cathodic reaction is being impeded so that the corrosion rate is decreasing. In systems for which it is possible to distinguish between these alternatives it is, of course, reasonable to assume some correlation between corrosion potential and corrosion rate and this may provide the basis for a simple method of corrosion monitoring.

2.3. States of corrosion in concrete

Having reviewed the principles which govern metallic corrosion processes in general, it is possible to give a simple description of the various states of corrosion that may be exhibited by steel in concrete. The conditions that give rise to these different corrosion states will then be examined in more detail in subsequent chapters.

2.3.1. The passive state

Dense concrete, which has not carbonated by reaction with acidic constituents of the atmosphere, contains a highly alkaline solution (pH > 13) within the pores of the hardened cement matrix that surrounds the aggregate particles and the reinforcement. This alkalinity is due to the presence of sodium, potassium and calcium hydroxides, derived from the reactions between the mix water and Portland cement. The pore-water also normally contains a significant level of dissolved oxygen.

In such an environment, as would be predicted from the Pourbaix diagram for iron shown in Figure 4, embedded steel reinforcement is maintained in a passive condition and the corrosion rate is insignificantly low because of the protective oxide film surrounding the metal. The corrosion potential of the steel in this normal, protected state in sound concrete may vary over a wide range, from about +200 mV to -700 mV (SCE scale), depending on the availability of the cathodic reactant, oxygen. Typically, however, for reinforced concrete structures exposed to air, the level of dissolved oxygen will be sufficient to maintain the corrosion potential of passive steel in the range +100mV to -200 mV (SCE scale).

The quality of the concrete and the thickness of cover to the reinforcement both affect the stability of the passive state. They influence the ability of the system to exclude aggressive substances, which tend to alter the pore-water composition endangering the passivity of embedded steel and so induce significant corrosion.

2.3.2. The state of pitting corrosion

The passivity of steel in an alkaline environment may be destroyed by the presence of chloride ions. Pitting corrosion is, therefore, likely to occur in reinforced concrete containing significant levels of chloride salts, derived either from the service environment or from the use of contaminated mix materials. This corrosion state is characterized by galvanic action between relatively large areas of passive steel acting as cathode and small anodic pits where the local environment, within the pits, has a high chloride concentration and a depressed pH value. For pitting to be sustained, it is necessary that a sufficient concentration of oxygen should be available to cause polarization of the cathodes to

potentials more noble than the pitting (breakdown) potential characteristic of the particular environment.

The average corrosion potential of steel reinforcement undergoing pitting is likely to vary between that of the passive state and that of the anodic pitting areas, being typically in the range -200 mV to -500 mV (SCE scale). Anodic sites, which may be identified by corrosion potential mapping as the most negative regions within a structure, are generally surrounded by areas of high potential gradient.

2.3.3. The state of general corrosion

The passivity of steel in non-buffered alkaline electrolytes requires a minimum pH value of about 11.5 to be maintained. (Somewhat lower threshold pH values, ca. 9, can be tolerated in buffered solutions owing to reduced effects associated with hydrolysis of anodic reaction products).

In concrete, general loss of passivity can occur if the pH value of pore-water at the depth of the reinforcement becomes substantially reduced from its initial high level. This can happen as a result of carbonation, which involves penetration in the concrete of CO_2, gases etc. from the surrounding air, and it gives rise to general corrosion of the steel. More or less general corrosion may also be observed in reinforced concrete, which has been contaminated with chloride ions to such an excessive level as to cause virtually complete destruction of the passive film.

The corrosion potential of reinforcement, which is undergoing general corrosion, is usually in the range of -450mV to -600mV (SCE scale), i.e. similar to that of uncoated steel undergoing corrosion in a nearly neutral aqueous environment. Potential gradients within structures in this condition are not usually as large as those associated with pitting corrosion.

2.3.4. The state of active, low potential corrosion

In environments where the availability of oxygen is extremely limited, as is sometimes the case for fully submerged or buried reinforced concrete, the limiting cathodic current density may eventually become insufficient to maintain the passive film.

Under these conditions the metal behaves 'actively' in the highly alkaline environment, undergoing uniform dissolution to form soluble $FeO.OH^-$ ions, as

represented in the Pourbaix diagram for the Fe-H_2O system (Figure 4). The corrosion potential is depressed to a value within the approximate range-850mV to -1000mV (SCE scale) and the rate of metal dissolution is extremely low owing to the restricted availability of the cathodic reactant.

2.4. Types of Corrosion - Controlling Mechanisms

The maximum corrosion current will depend on the shape of the anodic and cathodic branches of the polarization curves. If the cathodic process is the slower one, the corrosion rate is considered to be cathodically controlled (Fig.12(a)). Conversely, if the anodic process is the slower, the corrosion rate is said to be anodically controlled (Fig.12(b)).

The shapes of the anodic and cathodic branches of the polarization curves depend in turn, on the type of polarization process. There are three types of polarization which may act separately or simultaneously, namely activation, concentration, and resistance polarization.

2.4.1. Activation polarization

It occurs due to kinetic hindrance of the rate-controlling step of the electrode reaction. It is related to the activation energy required for the anodic and cathodic half-cell reactions to proceed and is associated with the slower step in the transfer of electrochemical charge. Tafel showed experimentally in 1905 [22] that, for large currents in the absence of concentration and ohmic polarization, the measured polarization is directly proportional to the logarithm of the current density, i:

$$\eta = a + b \log i$$

where a and b are constants known as the Tafel intercept and Tafel slope parameters, respectively, and can be obtained empirically. The parameter "a" is related to the exchange current i_o, which is the equilibrium current flowing back and forth through the electrode-electrolyte interface at equilibrium and is a measure of the reversibility of the reaction. The parameter "b", on the other hand, gives an insight into the mechanism of the electrode reaction. [23]

(a)

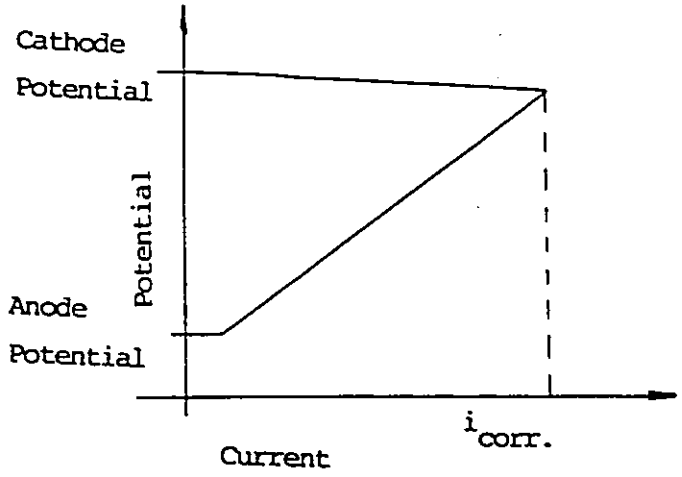

(b)

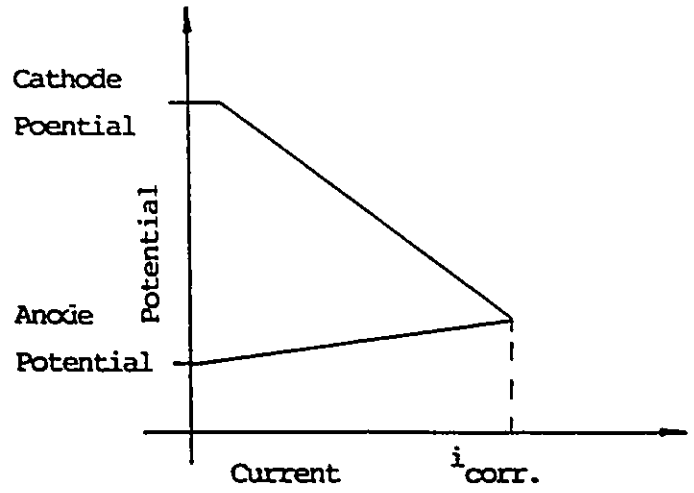

Fig. 12: Potential vs current plots for systems under (a) cathodic control and (b) anodic control

2.4.2. Concentration Polarization

Concentration polarization occurs when the concentration of the electrolyte changes in the vicinity of the electrode. An example of this would be depletion of oxygen at the cathode. The rate of oxygen diffusion through the concrete to the reinforcement determines the rate of corrosion. This is illustrated in Fig.13 for two different rates of oxygen diffusion.

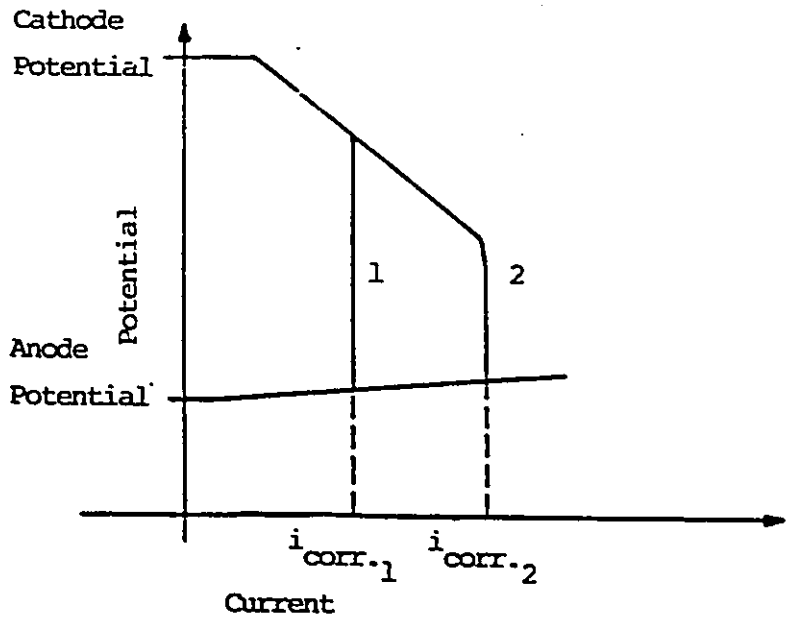

Fig. 13: Potential vs current plot illustrating cathodic diffusion polarization

2.4.3. Ohmic Polarization

Ohmic polarization occurs because of the ohmic resistance of the electrolyte and of any films on the electrode surface. This produces an ohmic (iR) potential drop. Since the electrolyte in concrete is the cement paste pore solution which, at humidities less than 100%, is present as a film on the paste gel, an ohmic polarization is inevitable in concrete and increases significantly with decreasing humidity. Figure 14 illustrates two cases of resistance control, where the potential available for corrosion is the difference in potential between anode and cathode minus the relevant iR loss.

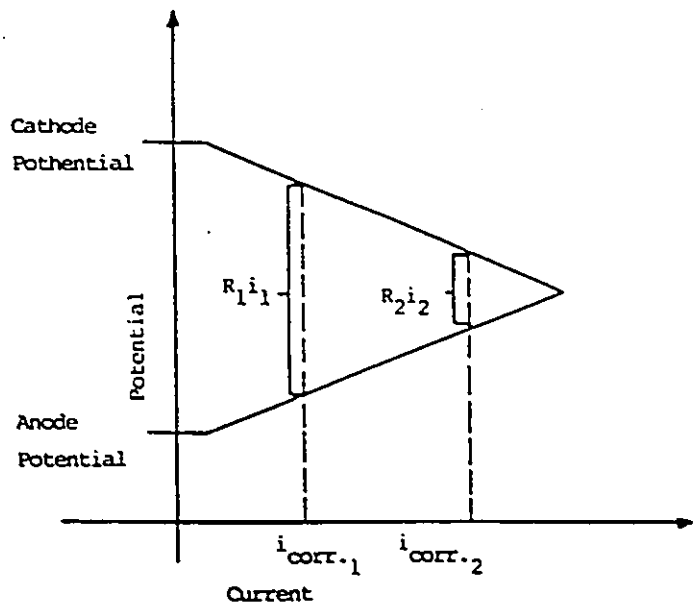

Fig. 14: Potential vs current plot illustrating resistance polarization

2.5. Chlorides in Concrete

As mentioned above, the two major causes of the breakdown of passivity on steel embedded in concrete and the consequent initiation of active corrosion are (a) the presence of chloride ions, either included in the mix with the concrete raw materials or due to penetration from the environment and (b) a decrease in the pH value of the aqueous solution in the concrete pores because of reaction of the cement paste with atmospheric CO_2 (carbonation). These two factors can and often do work together, having a synergistic effect on each other.

The consequences of the corrosion of reinforcement are: (a)decrease of the bar diameter (weakening its mechanical properties); (b) cracking and spalling of the concrete cover due to the expansive nature of the iron oxides, and (c) decrease of the steel/concrete bond. Chlorides can be introduced into concrete via two main routes, (a) as contaminates in the original mix and (b) as a result of post-setting exposure to de-icing salts, sea water or other chloride-bearing liquids. In the case of (a) the presence of chlorides will set up immediate corrosion reactions the severity and extent of which will be described later. In the case of (b) the chloride content of the concrete will build up with

time until the concrete is no longer able to protect the reinforcement from corrosion. As in the case with the ingress of CO_2, the amount of chloride ions will be limited.

2.5.1. Binding of the chlorides

The amount of chloride that can be bound is dependent on the binding capacity of the hydrated cement. Two different types of bond have to be recognized:

- the chemical bond: Chloride ions are incorporated in the lattice of a more or less crystalline product by a reaction between the chloride and hydration products.

- the physical bond: Chloride ions are absorbed at the surface of the hydration product.

Known chloride containing reaction products are:

$$3\ CaO \bullet Al_2O_3 \bullet CaCl_2 \bullet 1OH_2O \text{ (Friedels salt) and}$$

$$3\ CaO \bullet Al_2O_3 \bullet 3CaCl_2 \bullet 32H_2O$$

The amount of chloride that can be chemically bound is, other than the cement type, dependent on the presence of other anions like sulphates and carbonates, the type of cation Ca^{++}, K^+ or Na^+ and dependent on temperature and pH.

As can be seen from the reaction products the binding capacity of the cement will, from the chemical point of view, be determined by the ratio CaO / Al_2O_3. However, as with the penetration of CO_2, the rate of penetration of chloride ions will be more determined by the permeability and resistivity than by the binding capacity of the pore system [24].

The carbonation in concrete in practice only proceeds when the pores are not filled with water. With the diffusion of chlorides the reverse is the case. Diffusion of ions take place only in water. If the concrete is dry, transport of chloride ions is nearly impossible. If the concrete is semi-dry there will be diffusion of chlorides from the surface to the inner concrete.

The total amount of chlorides necessary to ingress to a certain depth to get a certain value in the pore solution at that depth, depends on the binding capacity for chlorides of the concrete per unit volume. In practice the binding capacity for chloride ions is determined by:

- the composition of the cement and

- the amount of cement per m^3

The amount of Cl^- that will diffuse per unit time into the concrete depends on the permeability of the concrete for chloride ions.

This means in practice:

- the composition of the concrete
- the compaction of the concrete
- the curing conditions of the concrete
- the environmental conditions of the concrete

2.5.2. Mechanism of Chloride Attack

While the structure of the passive film and the mechanism of its breakdown by chloride ions is not fully understood, it is generally believed that the chloride ions become incorporated in the passive film, replacing some of the oxygen and increasing both its conductivity and its solubility. The film, therefore, loses its protective character and, because the high potential difference across the film cannot be maintained, the potential measured at the steel surface falls to a value closer to that for the iron electrode.

Chloride ions are rarely distributed homogeneously over the steel surface and the imperfections in the passive film which allow easy incorporation of the chloride ions are also inhomogeneously distributed. The breakdown of the passive film is, thus, a local phenomenon and results in the creation of macrogalvanic cells. The local active areas will act as anodes where the iron will readily dissolve at a relatively low potential, while the remaining passive areas will act as cathodes where oxygen reduction takes place at a higher potential. The effective separation of the anodic and cathodic areas, caused by the localized nature of chloride attack, has significant consequences for the pattern of corrosion. In the concrete adjacent to the anode area, the concentration of positive iron ions increases, that is, the pH falls, whereas the production of the negative hydroxyl ions occurs in the neighborhood of the cathodic areas of the steel. Because of the local drop in pH at the anode, a soluble complex of iron chloride can form. This complex can diffuse away from the anode, permitting corrosion to continue. Some distance from the electrode, where both the pH and the concentration of dissolved oxygen are higher, the complex breaks down, iron hydroxide precipitates, and the chloride ion is free to react

further with ferrous ions at the anode. Since the chloride ions are not used up in this process and the corrosion is not stifled by a high concentration of iron ions in the vicinity of the steel, the process can continue with iron ions migrating away from the steel and reacting further with oxygen to form higher oxides or hydroxides. Consequently, instead of spreading laterally along the reinforcing bar, the corrosion continues at the local anodic areas, causing the development of deep pits and eventual severance of the bar.

As evidence for this sequence of events, it has been reported [25,26] that, when concrete with actively corroding reinforcement is broken open, a light-green semisolid reaction product (probably a mixture of $Fe(OH)_2$ and Fe_3O_4) has been observed near the steel which, on exposure to air, turns black (Fe_3O_4) and subsequently rust red ($Fe(OH)_3 \bullet nH_2O$).

An excellent illustrative representation of the relation between some of these factors and the threshold chloride content is given by CEB[*] and reproduced in Fig.15. The different national standards consider different limits for chlorides, depending on the experience within that country. The value of 0.4% of Cl^- by mass of the cement, suggested in Fig.15, is also considered by RILEM[**] as an appropriate threshold value. In the United States, on the other hand, the Federal Highway Administration has stated[119] that a chloride ion concentration of 0.15% by mass of the cement can be tolerated but that 0.3% is considered dangerous.

---

* Draft CEB Guide to Durable Concrete Structures, "Bulletin d'Information No. 166, ComiteEuro-International d'Beton, May 1985.

** RILEM Committee 60-CSG "Corrosion of Steel in Concrete"; State of the Art Support. Edited by P.Schiessel. Chapman and Hall, London, 1987.

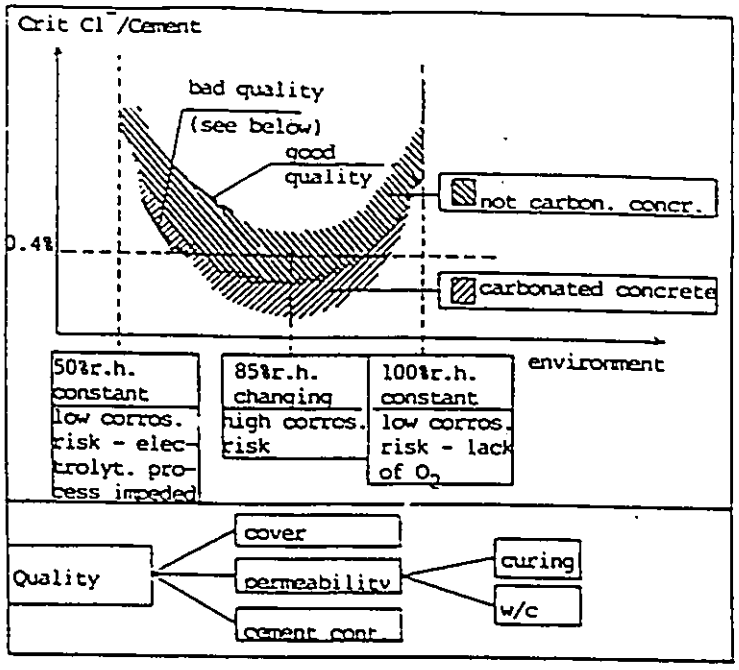

Fig. 15: The critical chloride content according to CEB recommendations (RILEM Committee 60-CSG)

2.6. Carbonation of Concrete

Some acid atmospheric agents react with concrete due to its alkaline nature. This process is usually known as "carbonation" because the main reaction agent is the atmospheric CO_2, but nitrous and sulfurous oxides can also play a role. CO_2 can react with the ions in the pore solution according to the following reactions:

$$Ca(OH)_2 + CO_2 \Rightarrow CaCO_3 + H_2O$$

$$2NaOH + CO_2 \Rightarrow Na_2CO_3 + H_2O$$

The $CaCO_3$ and Na_2CO_3 precipitate inside the pores of the cement, thereby diminishing the permeability of the concrete but also reducing the pH of the pore solution. If carbonation is allowed to continue after neutralization of the pore solution, the solid phases of the cement paste also react with the carbon dioxide, producing in the final state an amorphous Si_2 $Al(OH)_3$, $CaSO_4$, $CaCO_3$, and H_2O.

The change in pH due to carbonation is very abrupt and, therefore, appears as a "carbonation front" which is usually a very narrow zone separating two sides, one toward

the surface with pH values below 8 and the other into the concrete core with pH values above 12.

The carbonation rate is a function of many variables, including cement type, w/c ratio, proportion of cement, and so on, which may together be termed concrete "cover quality", or cover permeability. Although it is not valid in all cases, the carbonation rate may be modeled by a parabolic law, the carbonated cover depth, x , being proportional to the square root of the time "t" of exposure:

$$x = kt^{1/2}$$

The water saturation level of the pores in the cement paste is the second decisive factor in determining the carbonation rate because the CO_2 permeates the concrete most rapidly in the gas phase, but the carbonation reaction takes place in the liquid phase. Thus as Venuat [27] showed, intermediate humidity contents are the most dangerous ones, as illustrated in Figure 16. In a completely dry concrete the CO_2 cannot react because there is no water in the pores.

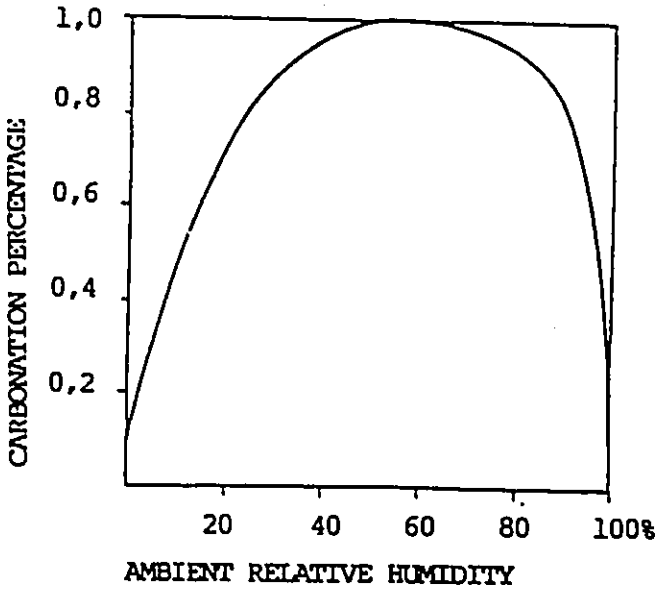

Fig. 16: The degree of carbonation as a function of the relative humidity (Ref. 28).

In a completely saturated concrete, the CO_2 must first dissolve in the pore solution and diffuse through the pores to reach the alkaline substances. Consequently, when the

pores have a layer of moisture on the walls but are not completely saturated, the CO_2 can rapidly reach the vicinity of the pore walls and have enough water to react.

2.6.1 Carbonation-induced Corrosion

When the carbonation front reaches the reinforcement, the passive film is no longer stable and active corrosion initiates. The corrosion process is generalized and homogeneous, producing, over the long term, a reduction in the cross-sectional area of the steel and a significant amount of oxides which may crack the cover or diffuse through the pores to the surface of the concrete.

The depassivation may be followed in laboratory experiments [28-30] using an atmosphere saturated in CO_2 in order to accelerate the process. Figure 17 shows the changes in corrosion current and potential in bars embedded in mortar specimens during accelerated carbonation. When the carbonation front reaches the bars, a dramatic increase in the i_{corr} and a shift of the E_{corr} to active values are recorded. When a corrosion inhibitor, is present, depassivation does not occur and the values of i_{corr} and E_{corr} remain in the passive region.

As mentioned before, however, depassivation of the steel is necessary but not sufficient to shorten the service life of reinforced concrete. The presence of moisture in the pores is crucial for corrosion to occur at a significant rate.

Therefore, the most aggressive environment related to the concrete neutralization will be that with alternate semi-dry and wet cycles. During the semi-dry periods, the carbonation front advances and, during the wet periods, the steel corrodes. A permanently dry environment will provoke depassivation when the carbonation front reaches the steel but no significant corrosion will develop. Constantly wet conditions will avoid carbonation and the steel will remain passive as long as no other depassivating agent is present.

Although the progress of the carbonation front in sound and dense concrete is, fortunately, slow in real situations, two factors may lead to a reduction in the expected service life: too thin a cover and the existence of cracks.

Cover depths of less than 20 mm are considered in different standards, as shown in Figure 18, and the stirrups have ever smaller covers, leading to a risk of premature depassivation due to carbonation.

The situation in the cracks is represented in Figure 19 [31]. The crack surfaces carbonate and depassivation of the steel occurs locally in the neighborhood of the crack. For cracks with opening displacements of up to $\cong$ 0.4 mm, it has been considered, an accepted in most standards, that there is no relationship between crack width and the amount of corrosion. The risk is more a function of the "cover quality" and of the cover/bar diameter ratio. A crack constitutes a risk of corrosion but for crack widths of $\langle$ 0.4 mm the risk is independent of crack width [32].

a)

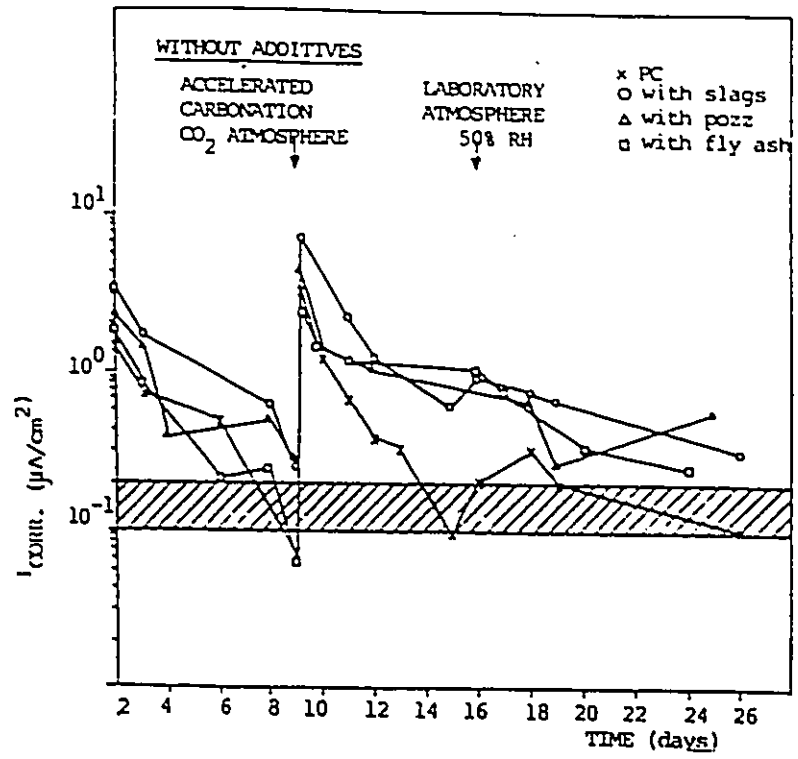

b)

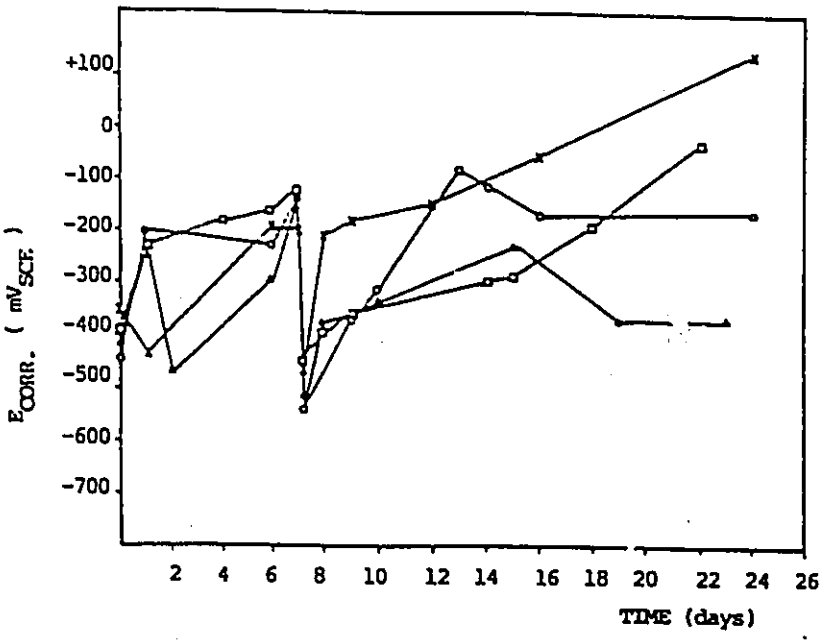

Fig. 17: Variation in i_{corr} and E_{corr} due to accelerated carbonation in a 50% relative humidity atmosphere saturated in CO_2 of steel embedded in mortar made with different types of cement (Ref. 28)

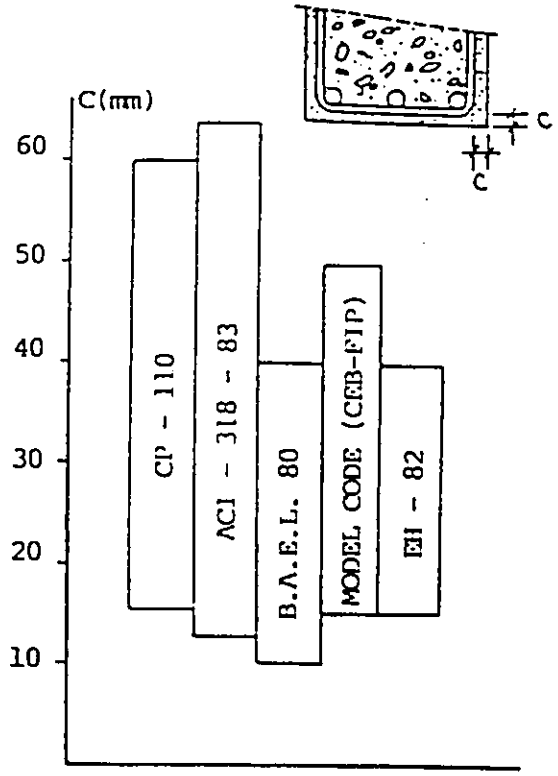

Fig. 18: Cover depths recommended by different codes.

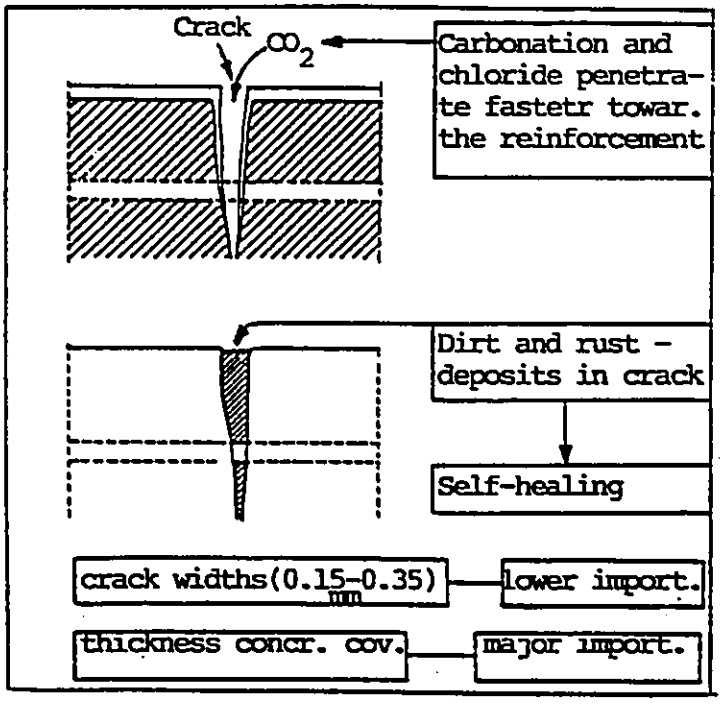

Fig. 19: Carbonation in cracks (Ref. 31).

2.7. Forms of Corrosion

It is useful to classify the forms of corrosion based on the appearance of the corroded rebar. It facilitates determination of the cause to corrosion quickly by visual inspection. Normally, four types of reinforcing steel corrosion are observed in concrete [19].

2.7.1. Pitting

It is a form of extremely localized attack that results in holes in the rebar. A pit maybe described as a cavity or hole with a surface diameter about the same or less than the depth. Pitting is one of the most destructive and insidious forms of corrosion. It causes failure because of perforation with only a small percent weight loss of the entire structure. It is often difficult to detect because of small pit size and because pits are often covered with corrosion products. Pitting could occur in local areas with high chloride concentration.

The electrochemical theory of pitting corrosion is still the subject of research and discussion. Nevertheless some principles of the processes are now generally agreed and the following sections embody those points of general agreement. It is important to recognize, however, that the precise mechanisms of pitting have still to be elucidated and the theories suggested here may have to be adjusted in the light of developing knowledge and understanding.

The propagation of pitting requires continuing activity at specific sites by maintenance of the chloride/hydroxide-ratio above the critical value for initiation, as a with continuing influx of chloride to the site. As pitting continues anodic acidity develops as a result of hydrolysis of the corrosion product so liberating hydrogen ions. The potential in this region becomes more negative. Correspondingly, sites of incipient pitting in the more noble areas are eliminated as the potential falls. At the same time hydroxyl ions are produced as a consequence of the cathodic reactions raising the pH of cathodic areas.

Thus pitting corrosion becomes self-supporting at specific sites by lowering the pH at those sites, with increasing pH at adjacent cathodic areas, so reducing the chance of further attack in these areas.

It will be seen from the foregoing that continuation of the corrosion processes at the active sites requires maintenance of the (Cl)/(OH)-ratio. Thus chloride has to be available at the pitting site to the detriment of hydroxyl ions. It is believed that two major processes of chloride replenishment exist:

1. migration from the pore liquid in the bulk concrete (to maintain specific concentrations relative to hydroxyl in the pitting zone)
2. recycling of chloride processes (Figure 20).

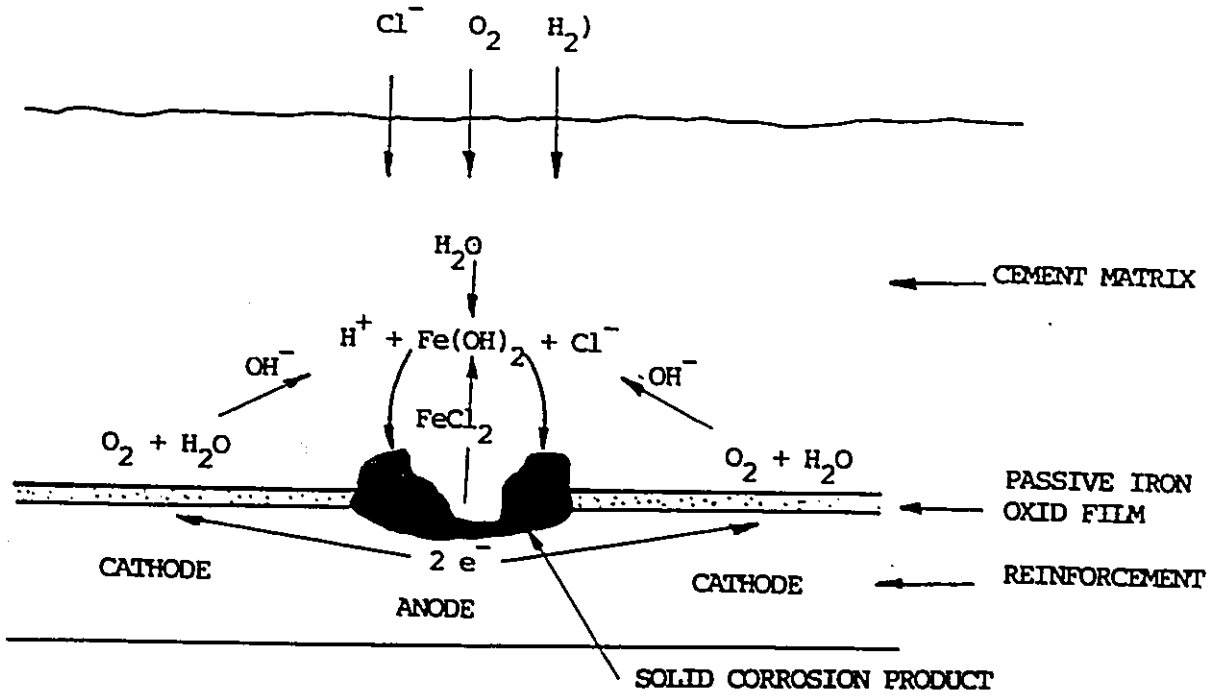

Fig. 20: Effective corrosion product hydrolysis and recycling Cl⁻ on pitting corrosion

As the process of pitting corrosion continues a certain amount of the chloride available from the pore liquid will be consumed, albeit in a transient condition, by the formation of intermediate iron chloride corrosion products which will remain stable only at the lower values of pH found within the pitting zone. These complexes diffuse away from the zone and will be precipitated in the alkaline environment provided by the bulk cement

matrix. Since, at least temporarily, the total chloride concentration in the pore liquid will be reduced by this process chloride will need to be replenished to ensure continuation of the corrosion process. This is achieved partly by the breakdown of chloroaluminate complexes and partly by diffusion of chloride from the bulk pore liquid. Additional recycling of chloride from the hydrolysis of the intermediate iron chloride complexes will replenish chloride in the pore liquid.

However, as the site of pitting grows this process of replenishment becomes more critical and as a result corrosion propagation may be limited by the availability of chloride at a specific site. In such a situation the level of hydroxyl ion also becomes important since reduction of the (Cl)/(OH) will result in depassivation of the propagating site.

The role of hydroxyl ions in imparting stability to the oxide film formed on the surface of steel embedded in concrete has already been considered. In particular the availability of hydroxyl ions is a critical factor in imparting passivity to steel in concrete and increased availability of hydroxyl improves the attainment and retention of passivity. Thus uncorroded steel surfaces are more readily protected than those covered by a rust scale. Likewise this argument also holds when chloride ions are present in concrete and the critical chloride hydroxyl concentration ratio has been breached. In this case the availability, and reserve, of alkalinity is important in re-establishing passivity. Reduced availability, perhaps resulting from discontinuities in the interfacial zone resulting from voids in direct contact with the rusty steel surfaces, or limited diffusion of hydroxyl ions to active sites would encourage corrosion to propagate. Likewise partial carbonation of the cover would reduce the availability of hydroxyl ions [27].

Carbonation would not only reduce availability of hydroxyl ions, it would also influence the stability of the solid chloroaluminate hydrate phases. These phases only maintain their stability at high pH. If the pH is reduced they break down, liberating free chloride to the pore liquid so increasing the aggressivity of the environment in which the steel is embedded and giving a greater risk of corrosion.

Two key factors will influence the propagation of pitting in chloride-bearing concrete are:

1) The availability of chloride which will be influenced by:.

a) the concentration of chloride ions at the pit

b) the recycling of chloride ions

c) the diffusion of chloride ions to the pit

2) The availability of hydroxyl which will be influenced by:

a) the extent of neutralization

b) the rate of hydrolysis

c) the cement composition and content

d) any additions made to the concrete.

Pitting corrosion will be more likely to propagate when both chemical and physical factors in 1) and 2) above, allowing a high mobility of chloride ions, are favourable. Conditions which favour high ionic mobility are mainly associated with the physical characteristics of the cement matrix. In particular the pore size distribution, the level of pore saturation and the interface between the steel and the matrix. Pore size distribution, while related to cement type, is also greatly influenced by the initial water/cement-ratio and the degree of curing; in general low w/c and long-term curing aiding the development of a micro - rather than a macro - porous hydrated structure. This will, in turn, restrict ionic migration. The implications on concreting practice of these features are discussed later.

From the foregoing it will be seen that propagation of pitting corrosion is most likely when chloride in sufficient quantity in the pore liquid to overcome the passivating effects of the hydroxyl ion is sustained at a site of attack by replenishment as a result of diffusion. Depletion of chloride at the active site as a result of partial consumption and limited diffusion will lead to a modification of the anodic polarization characteristics.

As chloride ions are taken up during the pitting process in the formation of ionic complexes, a driving force is developed to maintain ionic equilibrium within the site of attack. This driving force is controlled by the gradient of chloride concentration and the potential developed across the reinforcement/cement interface relative to that in the pit.

It is important to note that the cathodic processes also need to be sustained if pitting is to propagate. Pitting attack will occupy relatively small area of the total

reinforcement surface, and the remainder of the bar will be available for cathodic processes. The efficiency of these cathodic processes in driving the pitting attack will be determined by the availability of oxygen and concrete resistivity. Limiting oxygen diffusion will reduce the cathodic reaction and hence the amount of attack at the anode. However, if the concrete is of low resistivity, the total cathodic process can still stimulate intense local anodic activity and hence significant attack. Therefore, although not a rate determining process, for openly-exposed concrete structures, cathodic reactivity in relation to the resistivity of the concrete is important in encouraging the propagation of pitting attack. Likewise the migration of ions through the electrolyte from anode to cathode [12] is required. Normally , however, conductivity will be high in chloride-contaminated concrete.

2.7.2. Uniform or General Corrosion

General corrosion is normally characterized by a chemical or electrochemical reaction that proceeds uniformly over the entire rebar surface or over a large area. The rebar becomes smaller and eventually fails. Corrosion of an isolated rebar trapped in a cathodic protection system and corrosion caused by carbonation are examples of this form of corrosion.

Very high concentrations of chloride in the pore liquid can produce such active pitting attack that the pitting sites coalesce and give rise to a more general form of corrosion occurring at high rate. However, general corrosion is more likely to be encountered as a result of pH reduction leading to a condition where the alkaline nature of the cement matrix is unable to maintain the stability of the passive film. Propagation of this condition where anodes and cathodes are closely spaced, will depend on a ready availability of oxygen to depolarize the cathodic reaction and sufficient conductivity to allow ionic movement between adjacent anodic and cathodic sites. By implication, since sufficient carbon dioxide will have permeated the matrix to produce carbonation, oxygen will be in ready supply at the cathodic sites. Rates of corrosion will, therefore, be controlled by the resistivity of the electrolyte path between anode and cathode.

Thus general corrosion is likely to be controlled by the 'time of wetness' (a term

accepted in atmospheric corrosion studies) of the concrete. Recent work has shown that relative humilities below 50 % are unlikely to be sufficient to stimulate corrosion of steel in carbonated and chloride-free concrete, whereas humidities approaching 100 % produces high rates of corrosion. The level of moisture sufficient to enable the corrosion reactions has not yet been determined but will be between these two extremes. For example although carbonation to the full depth of cover has been seen in some concrete tests in Middle Eastern countries corrosion has not developed, whereas had this occurred in temperate, damp conditions, corrosion would have been seen.[33]

2.7.3. Macro-Corrosion

Macro-corrosion is the most common form of corrosion in reinforced concrete. It occurs over a relatively large area. Macro-corrosion often occurs in bridge decks involving double mat construction. The whole top rebar mat of becomes a large anode area due to the chloride contamination from the de-icing salt and the chloride free bottom mat forms the cathode.

Micro cells and macro cells are both galvanic corrosion cells driven by an electrochemical potential and balance between the anode and cathode. Formation of a micro cell is usually due to defects in the metal. A macro cell is generally initiated by the environment. Corrosion of rebar is a complex process. It should be noted that these different forms of corrosion can occur individually or in combination.

2.7.4. Micro-Corrosion

Micro-corrosion cells are often formed because of impurities, residual stress or defects in the metal substrate. Corrosion, especially in presence of chloride ions, will be dominated by these local active corrosion cells. Micro-corrosion cells generally operate over short distances, ie, less than 1-2 inches.

CHAPTER 3

3. Literature Review of Corrosion Inhibitors Used in Concrete Construction

For a majority of environments sufficient durability with respect to protection of reinforcement can be gained by an adequate quality of the concrete cover. Only in extremely aggressive environmental conditions may additional protective measures be necessary. However, poor execution has often contributed to the development of corrosion damage. Both aspects have led to an increased interest in providing corrosion protection to the reinforcement additional to that provided by the concrete cover. In particular efforts have been directed towards developments in four main areas, the use of metallic and organic coatings, the use of corrosion resistant alloys for concrete reinforcement, cathodic protection and the use of chemical corrosion inhibitors.

3.1. Definition of corrosion inhibitor

An inhibitor is a substance which retards or slows down a chemical reaction. Thus, a **corrosion inhibitor** is a substance which, when added to an environment, decreases the rate of attack by the environment on a metal. Corrosion inhibitors are commonly added either continuously or intermittently in small amounts to acids, cooling waters, steam, boilers, car radiators, to prevent serious corrosion.

It would be awkward to include mechanisms of inhibition in the definition of a corrosion inhibitor because inhibition can be accomplished by one or more of several mechanisms. Some inhibitors retard corrosion by adsorption to form a thin, invisible film only a few molecules thick; others form visible bulky precipitates which coat the metal and protect it from attack. Another common mechanism causes the metal to corrode in such a way that a combination of adsorption and corrosion product forms a **passive** layer.

One also includes in the definition those substances which, when added to an environment, retard corrosion but do not interact directly with the metal surface. This type of inhibitor causes conditions in the environment to be more favorable for the formation of

protective precipitates or it removes an aggressive constituent from the environment.

To use corrosion inhibitors effectively, the corrosion engineer must, first of all, be able to identify those problems which can be solved by the use of corrosion inhibitors. The compatibility of inhibitor with the system being used must be considered to avoid adverse effects such as foaming, decreases in catalytic activity, degradation of another material, loss of heat transfer, etc.

Of the four components of a corrosion cell (anode, cathode, electrolyte, and electronic conductor), three may be affected by a corrosion inhibitor to retard corrosion. The inhibitor may cause:

1. Increased polarization of the anode (anodic inhibition),
2. Increased polarization of the cathode (cathodic inhibition), or it may
3. Increase the electrical resistance of the circuit by forming a thick deposit on the surface of the metal.

Of course, the bulk film-formers also restrict diffusion of depolarizers (such as dissolved oxygen) to the surface of the metal; hence, they may play a dual role. The resistance of the conductor connecting the anodes and cathodes (i.e., usually the resistance of the metal itself) is very low and cannot be changed by corrosion inhibitors.

3.2. TYPES OF INHIBITORS

3.2.1 Anodic Passifying Inhibitors

Anodic inhibitors which cause a large shift in the corrosion potential are called passivating inhibitors. They are also called dangerous inhibitors because, if used in insufficient concentrations, they cause pitting and sometimes an increase in corrosion rate. There are two types of passivating inhibitors: oxidizing anions such as chromate, nitrite, and nitrate which can passivate steel in the absence of oxygen; and the non oxidizing ions such as phosphate, tungstate, and molybdate which require the presence of oxygen to passivate steel. With careful control passivating inhibitors are frequently used because they are very effective in sufficient quantities.

Passivating inhibitors such as sodium chromate ($Na_2 CrO_4$) and sodium nitrite ($NaNO_2$) do not require oxygen to be effective. They increase the rate of anodic passivation to the extent that the anodes are polarized to a passive potential (or Flade

Potential), indicated by E_f in Figure 21. The cathode will be depolarized, as indicated by the cathodic lines in Figure 21. The depolarized cathodic curve then intersects the anodic curve in the passive region at E_c. Absorption of the inhibitor on anodic areas also plays a part in the process because it decreases the current (or corrosion rate) required for the anode to reach the critical passive potential.

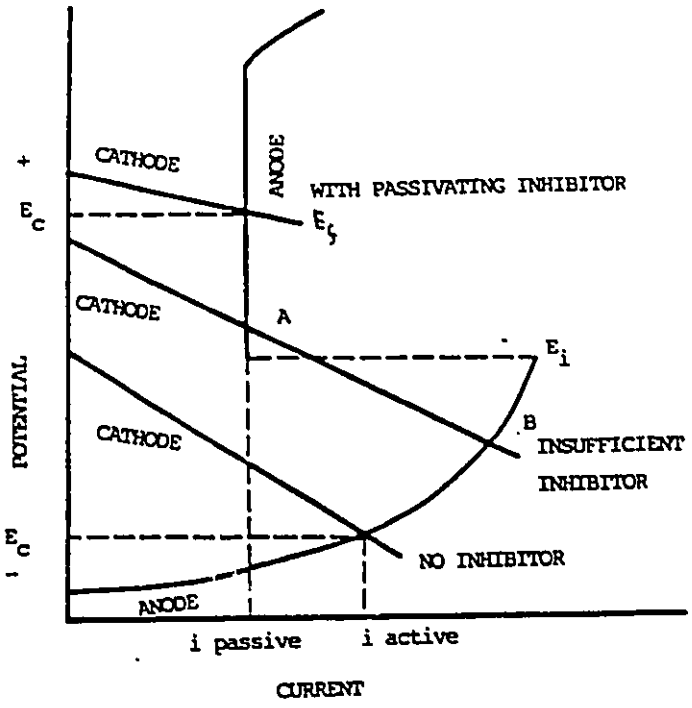

Fig. 21: Effect of passivating inhibitors on the corrosion of iron

When an insufficient amount of inhibitor is used, the cathodic curve will intersect the anodic curve in an active region or in both active and passive regions, indicated by A and B in Figure 21. In the latter case, corrosion will proceed at a high rate; in the former case, passivity is unstable, and the corrosion potential will oscillate between A and B, usually resulting in pitting of the metal. Measurement of the corrosion potential when using passivators is a good way to determine if the inhibitor is doing its job because a large positive shift in potential will occur as the metal passivates. Passivation by

inhibitors is more difficult at higher temperatures, higher salt concentrations, lower pH, and lower dissolved oxygen concentrations.

The mechanism by which chlorate passivates steel has been studied extensively, and it appears likely that protection is afforded by a combination of adsorption and oxide formation on the steel surface. Adsorption helps to polarize the anode to sufficient potentials to form very thin hydrated ferric oxides which protect the steel. Because the oxide film is invisible on steel, articles protected by chromate remain bright in otherwise aggressive environments. The oxide film is a mixture of ferric and chromic oxides and is kept in good repair by adsorption and oxidation with very little loss of metal as long as sufficient chromate remains in solution.

Chromates are accelerators of corrosion at low concentration because they are good cathodic depolarizers. The passive oxide film is conductive and cathodic to steel; therefore passive steel consists almost entirely of cathodic areas. When the passive film is penetrated by scratching or by dissolution, and when insufficient chromate is present to repair the film, the exposed steel becomes a small anodic area on which accelerated localized corrosion can occur, resulting in pitting of the metal. Mechanisms similar to that proposed for chromate are believed to apply to nitrites and nitrates.

It is practical to passivate steel in an aqueous solution, except those which contain easily oxidized substances in solution or high concentrations of chloride ions. For example, chromate should not be used in hydrogen sulfide (H_2S)-containing (or sour) environments because it is lost by oxidation of the sulfide to free sulfur. High concentrations of chloride ions prevent passivation because they compete with chromate for adsorption, thus preventing polarization of the anodes. They also prevent deposition of protective oxides by forming a soluble complex with ferric ions.

For a given concentration of passivating inhibitor, there is a concentration of chloride and sulfate ions which will cause depassivation. Table 1 lists the "critical concentrations" of sodium chloride (NaCl) and sodium sulfate (Na_2SO_4) required to cause pitting of steel in the presence of various concentrations of sodium chromate and sodium

nitrite. [21] The critical concentrations will vary depending on other factors; for example, more chloride or sulfate will be required for depassivation as the temperature is lowered, the oxygen concentration is increased, or the pH is increased.

5-Day Tests, 25 °C, Stagnant Solutions

Inhibitor	Concentration ppm	Critical Concentration, ppm NaCl	Na_2SO_4
Na_2CrO_4	200	12	55
	500	30	120
$NaNO_2$	50	210	20
	100	460	55
	500	2000	450

Table 1- Critical concentration of sodium chloride or sodium sulfate above which pitting of armco iron occurs in chromate or nitrite solution

Non oxidizing passivators such as sodium benzoate or polyphosphate require the presence of oxygen to cause passivation. They do not inhibit corrosion in the absence of oxygen. They apparently function by promoting the adsorption of oxygen on the anodes, thereby causing polarization into the passive region. Non oxidizing passivators are also dangerous when used in insufficient amounts because the oxygen which is required for passivation is a good cathodic depolarizer.

3.2.2. Cathodic Inhibitors

Cathodic inhibitors either slow the cathodic reaction itself, or they selectively precipitate on cathodic areas to increase circuit resistance and restrict diffusion of reducible species to the cathodes. The effects of cathodic inhibitors on cathodic polarization are shown in Figure 21. In this case, where the anodic polarization is unaffected, the corrosion potential is shifted to more negative values from E_c to E''_c.

The cathodic reaction is often the reduction of hydrogen ions to form hydrogen gas. Some cathodic inhibitors make the discharge of hydrogen gas more difficult, and they are said to increase the hydrogen overvoltage. Compounds of arsenic and antimony are examples of this type of inhibitor which are often used in acids or in systems where oxygen is excluded. Another possible cathodic reaction is the reduction of oxygen. The inhibitors for this cathodic reaction are different from those mentioned for the more acidic systems.

Other cathodic inhibitors utilize the increase in alkalinity at cathodic sites to precipitate insoluble compounds on the metal surface. The cathodic reaction, hydrogen ion and/or oxygen reduction, causes the environment immediately adjacent to the cathodes to become alkaline; therefore, ions such as calcium, zinc, or magnesium may be precipitated as oxides to form a protective layer on the metal. Many natural waters are self-inhibiting due to the deposition of a scale on metals by precipitation of naturally occurring ions.

The three main categories of inhibitors which affect cathodic reaction are cathodic poisons, cathodic precipitates, and oxygen scavengers.

3.2.3. Ohmic Inhibitor

Inhibitors which increase the ohmic resistance of the electrolyte circuit already have been considered to some extent in discussions of anodic and cathodic film-forming inhibitors. Because it usually is impractical to increase resistance of the bulk electrolyte, increased resistance is practically achieved by the formation of a film, a microinch thick or more, on the metal surface. If the film is deposited selectively on anodic areas, the corrosion potential shifts to more positive values; if it is deposited on cathodic areas, the shift is to more negative values; and if the film covers both anodic and cathodic areas, there may be only a slight shift in either direction.

3.2.4.Organic Inhibitors

Organic compounds constitute a broad class of corrosion inhibitors which cannot be designated specifically as anodic, cathodic, or ohmic. Anodic or cathodic effects alone are sometimes observed in the presence of organic inhibitors, but, as a general rule, organic inhibitors affect the entire surface of a corroding metal when present in sufficient concentration. Both anodic and cathodic areas probably are inhibited, but to varying

degrees, depending on the potential of the metal, chemical structure of the inhibitor molecule, and size of the molecule.

The typical increase in corrosion inhibition with inhibitor concentration, as shown in Figure 22, suggests that inhibition is the result of adsorption of inhibitor on the metal surface. The film formed by adsorption of soluble organic inhibitors is only a few molecules thick and is invisible [16].

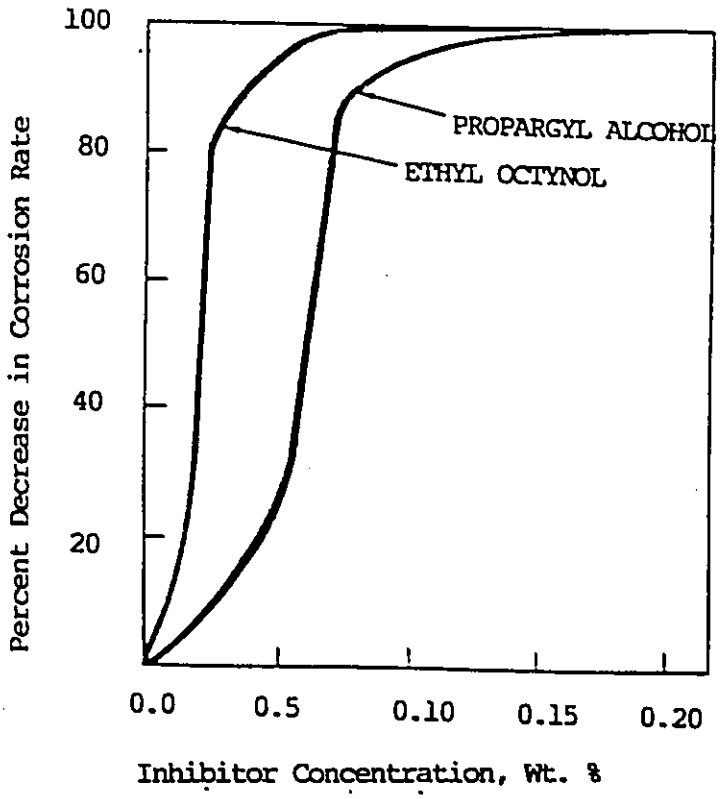

Fig. 22: Effect of concentration of organic inhibitor on corrosion rate

Organic inhibitors will be absorbed according to the ionic charge of the inhibitor and the charge on the metal surface. Cationic inhibitors (positively charged, +), such as amines, or anionic inhibitors (negatively charged, -), such as sulfonates, will be adsorbed preferentially, depending on whether the metal is charged negatively or positively (opposite sign charges attract). The potential at which neither cationic nor anionic molecules are preferred is known as the zero point of charge or ZPC. Thus a

combination of cathodic protection and an inhibitor which is absorbed more strongly at negative potentials gives greater inhibition than either cathodic protection or an inhibitor when used alone.

3.3. Review of Corrosion Inhibitors in Concrete

Many chemical admixtures, both organic and inorganic, have been suggested as specific inhibitors of steel corrosion. Among those compounds reported as inorganic inhibitors are potassium dichromate, stannous chloride, zinc and lead chromates, calcium hypophosphite, sodium nitrite, and calcium nitrite. Organic inhibitors suggested have included sodium benzoate, ethyl aniline, and mercaptobenzothiazole. With some inhibitors, inhibition occurs only at addition rates high enough to counteract the effects of chlorides. Sodium nitrite has been used with apparent effectiveness in Europe, where as calcium nitrite is being used in the United States and the Soviet Union since several side effects of the sodium salt would be avoided, such as low strength, erratic setting times, efflorescence, and an enhanced susceptibility to the alkali-aggregate reaction.[34]

The use of inhibitors in concrete has been reviewed by Griffin [37], Craig and Wood [36], Treadaway and Russell [37], Slater [38], and by Berke [39-40]. With the exception of Berke's reviews the previous reviews were written on work performed before 1980. Early studies looked at numerous inhibitors with the most attention focused on sodium nitrite, potassium chromate, sodium benzoate, and stannous chloride. This part presents a brief review of early work and several new references.

Craig and Wood [36] examined the mechanical properties of mortars produced with sodium nitrite, potassium chromate, sodium benzoate, and calcium chloride. They found a marked decrease (as high as 20 to 40%) in compressive strengths when these inhibitors were added to the mortars. In contrast calcium chloride increased compressive strength. Tensile strengths were adversely affected by sodium nitrite and sodium benzoate, but not by potassium chromate.

Corrosion testing showed that the above inhibitors, with the exception of sodium nitrite, did not work in the presence of chloride. Sodium benzoate and 2% potassium chromate were found to be detrimental in the presence of chloride.

Treadaway [41] and Treadaway and Russell [37] conducted tests of sodium nitrite

and sodium benzoate and found a decrease in compressive strength. Corrosion tests were conducted in alkaline solutions and in cement extracts. In the cement extract experiments they found that sodium nitrite inhibited corrosion in the presence of chlorides, whereas sodium benzoate did not. In their solution testing it was determined that corrosion was uniform with sodium benzoate and pitting occurred with sodium nitrite. Initiation of corrosion was delayed with sodium nitrite, with the delay increasing with inhibitor content.

In good quality concrete, where carbonation is unlikely at the reinforcement level, the mechanism of corrosion in the presence of chloride will be pitting [41,42]. Thus, the sodium nitrite inhibitor did not change the corrosion process into one of pitting, and did protect the steel until carbonation took place.

The reviews of Griffin [35] and Craig and Wood [36] mention the work of Arber and Vivian [43] with stannous chloride, and indicate that it is a corrosion inhibitor. In examining the Arber's and Vivian's experiments one finds that stannous chloride appeared to be a noncorrosive set accelerator. Stannous chloride, in short term testing with/without admixed chlorides, and no further chloride exposure from the environment, did appear to decrease corrosion as measured by tensile strength regression and steel appearance [45] (mild corrosion and tensile loss still occurred). Stannic chloride on the other hand did not behave as an inhibitor.

The authors [43] attributed the improved corrosion resistance to the stannous ion. However, some of it is most likely due to a decrease in chloride content, since stannous chloride is 37% chloride, stannic chloride is 54% chloride, and calcium chloride is 64% chloride. Recent tests by Hope and Ip [44] showed that stannous chloride was not a corrosion inhibitor.

Based upon results of experiments on inhibitors up to the mid 1970's it is not surprising that inhibitors were not in large scale use in concrete. Sodium nitrite was identified as a good inhibitor, but caused severe strength loss. Sodium or potassium salts of chromates and benzoates gave mixed results on inhibition and also reduced strength. Stannous chloride increased strength, but still contained chloride and was relatively expensive.

3.4.1. Calcium Nitrite Corrosion Inhibitor

The commercial production of calcium nitrite as a stable solution of up to 40% dissolved solids encouraged the use of calcium nitrite as a corrosion inhibitor. Unlike sodium nitrite in which the sodium cations are detrimental to strength and alkali-aggregate reactions, calcium nitrite was found to be non-detrimental to mechanical properties. For example, calcium nitrite meets ASTM C494 specifications as a concrete accelerator [48]. Later studies showed that calcium nitrite is compatible with silica fume (microsilica) [49,50].

3.4.1.1. Laboratory Corrosion Testing

In the 1970's numerous corrosion studies were performed documenting the corrosion inhibiting properties of calcium nitrite [44-53]. It was determined that the mechanism of corrosion protection (to be discussed in a later section) was that of anodic inhibition, and that steel in concrete containing chloride fails by pitting. This was later documented by basic research in saturated calcium hydroxide solutions [51].

The first large scale results reported by a government agency (FHWA) were released in 1983 [52]. Even though the FHWA used a water-to-cement (w/c) ratio that was high (>0.5), and added chlorides to the mix water, it was concluded that "...calcium nitrite can provide more than an order of magnitude reduction in the corrosion rate." The final recommendation of this work was that calcium nitrite was effective at chloride to nitrite ratios below 1.0 based on admixed chlorides, and ratios "...higher than 1 might be tolerable..." for chloride ingress into initially chloride free concrete [53]. A recent review on calcium nitrite showed that for nonadmixed chlorides protection ratios are above 1.0 for chloride levels up to 9.5 kg/m3 (16 pcy) [54]. Solution experiments by Hope and Ip indicate that the ratios of chloride to nitrite can be higher than one to one [44].

The South Dakota DOT conducted a study in which rebars were embedded in concrete cylinders with/without admixed chlorides [55]. Cylinders with admixed chlorides went into corrosion immediately (1 day) unless calcium nitrite was present. Samples with calcium nitrite remained passive for 700 days. Calcium nitrite also improved the corrosion resistance of samples without admixed chlorides. For the nonadmixed chloride specimens,

chloride analyses at the reinforcing bar showed the calcium nitrite prevented corrosion at chloride-to-nitrite ratios of 1.6 to 2.2 (chloride contents exceeded 10.7 kg/m^3 or 18 lbs/yd^3).

Additional data supporting the effectiveness of calcium nitrite corrosion inhibitor has recently come from Japan [56,57]. In accelerated tests with wetting and drying cycles at 80°C calcium nitrate was found to be an effective inhibitor [56]. In spite of the high water-to-cement ratios (w/c) calcium nitrite still proved effective [Table 2, 59] Another test of wet/dry cycling at 50°C demonstrated the advantages of using a lower w/c ratio of 0.5 versus 0.6 [56].

Nishibayashi et al [57] document long-term performance of "rust inhibitor," identified as calcium nitrite in their presentation, as a corrosion inhibitor in field marine exposures. They showed that at the 20 l/m^3 (4 lbs/yd^3) addition level of a 30% solution that calcium nitrite reduces corrosion.

Recent experiments by Tomosawa et al [58] also document the effectiveness of a 33% calcium nitrite solution in accelerated laboratory testing of steel reinforced concretes. In addition to tests on admixed chloride at 80°C under wet and dry cyclic exposure, they studied chloride penetration from cyclic immersion in 3% NaCl at 50°C. Calcium nitrite was found to be very effective in improving corrosion resistance as shown in Table 3 of from from their paper.

Though most of the work with calcium nitrite has looked at the protection against chloride ions, work by Andrade et al [59] shows that it also protects steel in carbonated concrete.

3.4.1.2. Calcium Nitrite in Concretes Containing Supplementary Cementitious Materials

Increasing use of pozzolans to prevent corrosion by reducing permeability to chlorides is taking place. Silica fume is one of the most effective pozzolans because its small particle size enables it to act as a filler and increases its chemical reactivity. Studies have shown that it improves the corrosion performance of fly ash concretes [54] and concretes with slag [60].

Calcium nitrite is compatible with silica fume [46] and should provide protection in the presence of chlorides. There is proof of the benefits of combining both silica fume and

calcium nitrite. Based upon data in study [46] one can expect significant decrease in corrosion that occurred for a silica fume containing concrete without calcium nitrite. This occurred even though the AASHTO T277 rapid chloride permeability was under 400 coulombs for the non nitrite specimens [60]. The specimens with calcium nitrite had decreased resistivity and increased permeability but remained passive [60]. Previous studies had showed that even though permeability numbers increased and resistivities decreased, that chloride ingress was not increased [46,47].

3.4.1.3. Calcium Nitrite Effect on Other Metals

In addition to protecting steel in concrete recent tests show that calcium nitrite also protects galvanized steel and aluminum [61]. This study involved the alternate ponding of minibeams with 3% NaCI solutions, and the measurement of corrosion by the macrocell and polarization resistance methods.

3.4.1.4. In Cracked Concrete

Calcium nitrite has been shown to provide benefits in cracked concrete [54,62,63,64]. Cracked samples with calcium nitrite took longer to start corroding or were corroded at substantially reduced rates. Cracks were less than 0.01 inch in width [60]. Visual analysis showed that both the depth of attack as well as the extent of surface attacked were significantly reduced by the addition of calcium nitrite [62]. More recently a study of unnotched beams cracked in flexure showed that calcium nitrite provided enhanced performance to chloride induced corrosion [63].

A recent German study [65] showed that sodium nitrite was also effective in reducing corrosion in cracked specimens, even at much higher than recommended water-to-cement ratios and low dosage rates of inhibitor. Other investigators have shown in general that thin cracking was not a significant factor in corrosion [66,67].

Thus, extensive research shows that calcium nitrite will perform well in cracked concretes. This improved performance is due to several factors. One is that, in concrete produced to proper ACI guidelines and codes, crack sizes at the surface will be less than 0.2 mm (0.008 inch) and covers will be at least 1.5 inches. Under these conditions the

crack size at the rebar will be quite small and the solution will be buffered by the concrete. Good performance was demonstrated for calcium nitrite in this quality of concrete [68,69].

3.4.1.5. Effect of Calcium Nitrite on Chloride Ingress

Studies have shown that calcium nitrite might decrease the resistivity of concrete [47,68]. However, long-term corrosion data show that in spite of the decrease in resistivity, corrosion rates were significantly reduced [47,68,69]. Likewise, increases in ASSHTO T277 chloride permeability values with calcium nitrite were clearly shown to have no negative effects on actual chloride ingress into the concretes [46,47]. The decrease in resistivity and increase in coulomb values in AASHTO T277 are due to the fact that calcium nitrite is an ionic salt and increases the ionic mobility.

3.4.1.6. Laboratory Studies on Nitrite Stability

Several tests were performed to determine the nitrite content of concrete with calcium nitrite as a function of time and environment. Analysis of the nitrite contents in the concretes in reference 58 show that nitrite at the reinforcement level remained high after 4 years of severe chloride exposure.

Another test was performed on concrete cylinders (100 mm in diameter) containing 2% calcium nitrite by mass of cement exposed to a fog room or to 2% NaCl for five years. The w/c ratio was 0.44 and the cement quantity was 375 kg/m^3 (634 lbs/yd^3). While some nitrite is lost at the surface there is no loss in the interior where the reinforcement would be placed. This is not unexpected since the surface typically has a higher porosity than the bulk concrete, and because the surface was in continuous contact with the solution. The fog room specimens had no loss of nitrite at any level indicating that nitrite is extremely stable in concrete.

3.4.1.7. Mechanism for Calcium Nitrite Corrosion Protection

The mechanism by which calcium nitrite protects steel in concrete from chloride induced corrosion was addressed recently by Berke and Rosenberg [54] and Berke and El-Jazairi [37]. A description of the mechanism will be presented here as well as other evidence supporting the mechanism as outlined by these researchers.

The corrosion inhibition by calcium nitrite could be outlined on the basis of the

Pourbaix [70] potential-pH equilibrium diagram, and other studies [51,70-76].

The first reaction that occurs when steel is placed in an alkaline environment, such as concrete, is:

$$Fe \rightarrow Fe^{2+} + 2e^-$$

Later reactions will convert the Fe^{2+} to an $Fe(OH)_2$, or $Fe_3O_4 \bullet nH_2O$, or y-FeOOH passive oxide layer at the steel surface. In the absence of chloride all the oxide phases are stable in alkaline environments. These oxide layers are only a few monolayers thick since once they are formed they prevent further oxidation from occurring. y-FeOOH is the most stable in the presence of chloride or other depassivating ions.

On the microscopic scale there will be regions where the protective oxide is not present. At these locations chloride ions can form a complex with Fe^{2+}. The resulting complex can migrate from the steel surface and subsequently convert into an expansive corrosion product.

Calcium nitrite prevents the continuation of the corrosion reaction by reacting with the ferrous ions, Fe^{2+}(18).

$$2\,Fe^{2+} + 2OH^- + 2NO_2^- \rightarrow 2NO^{2-} + Fe_2O_3 + H_2O$$

or

$$Fe^{2+} + OH^- + NO_2^- \rightarrow NO^{2-} + \text{y-FeOOH}$$

If corrosion reaction (1) occurs, the ferrous ions produced are changed through calcium nitrite to the stable passive layer. Thus, the passivation chemical reaction of nitrite with ferrous ions is to block active corrosion centers by producing a passive ferric oxide protective film. The iron in the ferric state is not complexed by chloride and corrosion is reduced.

It is worth noting here, that the nitrite does not enter into reactions involved in producing the anode, but reacts with the resulting products of the anode. Thus it cannot affect the size of the anode. Also as monolayers of oxides are involved, essentially no nitrites or hydroxide are consumed in forming the initial protective oxides or hydroxide, which is supported by the nitrite concentration data at the reinforcement level given in the previous section.

Note that both Cl^- (or other aggressive anions), NO_2^-, and OH^- are competing at

"flaws" in the oxide for Fe^{2+}. Over time, nitrite and/or an alkaline environment free of chloride will reduce the number of sites where Fe^{2+} ions are formed through formation of a protective coating y-FeOOH or $Fe_2O_3 * nH_2O$.

Recent studies as part of the Strategic Highway Research Program add new evidence supporting the outlined mechanism of protection. These studies showed that nitrite modifies the oxide film on the reinforcing bar to be more protective than it naturally occurs in concrete [77]. They also demonstrated that this improved oxide leads to enhanced corrosion resistance [78].

When chloride is present at extremely high $[Cl^-]/[NO_2^-]$ and/or $[Cl^-]/[OH^-]$ ratios the probability of Cl^- complexing a Fe^{2+} cation is increased. This leads to a $[Cl^-]/[NO_2^-]$ or $[Cl^-]/[OH^-]$ protection ratio beyond which pitting would be likely. The ratios for $[Cl^-]/[OH^-]$ are typically stated to be between 0.27 to 0.57 for the initiation of pitting [85]. In reference 22 an analysis of hundreds of concrete and solution tests was performed showing that the $[Cl^-]/[NO_2^-]$ is approximately 1.5 to 1.

3.4.1.8. Comparisons of Calcium Nitrite and Newly Introduced Products

In 1991 dimethylethanolamine [79] and butyl ester of oleic acid plus amine [80] inhibitors were introduced into the commercial market based upon data in accelerated laboratory tests. These products were compared to calcium nitrite in the ASTM G109 test method [81] in reference [82]. These tests showed that calcium nitrite had the best performance and that dimethylethanolamine was ineffective as can be seen in Figure 9. The butyl ester emulsion reduced macrocell currents, but did not prevent corrosion even though chloride ingress was significantly reduced compared to the control specimens.

Further examination of the butyl ester emulsion product with admixed chloride showed no improvement in corrosion performance in 0.4 w/c concrete, whereas calcium nitrite was very effective [82]. Additional testing in 0.4 w/c concrete also showed no reduction in chloride ingress for the butyl ester emulsion, in contrast with the reductions observed in poorer quality concrete at 0.5 w/c. Cyclic polarization data also showed minimal effect of the butyl ester emulsion or dimethylethanolamine products versus a substantial improvement with calcium nitrite [83].

These results disagree with the published results in poor quality concrete

[80,84,85] in which low cement factors, high w/c ratio and poor curing were utilized. In such concretes a butyl ester emulsion would act to screen chloride and appear to be beneficial. However, even in that case the product could not be universally considered to be a corrosion inhibitor as the chloride levels were significantly reduced [86]. The relatively poor performance of the organic materials testes is not surprising since organic inhibitors are primarily used in acid environments [86].

3.4.2. Sodium Nitrite

Gouda and Monfore [50] showed that an addition of 1 to 2 % sodium nitrite by mass of cement reduced considerably the corrosion susceptibility of steel embedded in concrete containing 2 % admixed calcium chloride. When 0.5 % sodium nitrite was used, steel samples were passivated initially but became active afterwards. The authors cautioned that sodium salt might be undesirable for use with aggregates which are known to be reactive with alkalis. The tests were performed using two anodic polarization methods (constant applied current and variable applied current).

Gouda and Halaka [51-53] showed that an addition of 1 to 2 % sodium nitrite by mass of cement effectively suppressed the corrosion of steel embedded in concrete containing 2% admixed sodium chloride. Compared to other sodium and potassium salts, such as sodium chromate, sodium phosphate, sodium benzoate, sodium silicate, and potassium chromate, sodium nitrite required the lowest dosage to achieve a similar level of protection. The tests were conducted using anodic polarization with a constant applied current.

Gonzalez et al [62] found that an addition of 3 % sodium nitrite by mass of cement reduced considerably corrosion of steel embedded in carbonated mortar. The tests were performed using polarization resistance and half-cell potential measurement.

Chen et al [63] found that corrosion of rebars embedded in concrete containing 2 % admixed sodium nitrite by mass of cement was only half that of rebars embedded in concrete without sodium nitrite. The tests were carried out by visual inspection of rebars after concrete slabs were exposed to seawater for 10 years.

Craig and Wood [87] showed that, while sodium nitrite offered substantial corrosion protection of steel, it caused a decrease in both tensile and compressive

strengths of mortar. The corrosion tests were performed using anodic polarization with a constant applied current.

Treadaway and Russell [37] also concluded that sodium nitrite provided effective corrosion protection of embedded steel but it caused a decrease in concrete strength.

From these test results, corrosion protection offered by sodium nitrite is similar to that of calcium nitrite. This is probably because only nitrite ions are involved in the inhibition process. Sodium nitrite, however, may cause a decrease in strength of concrete and increases the risk of alkali-aggregate reaction for some susceptible aggregates. It may also be more susceptible to leaching and efflorescence than calcium nitrite [49].

3.4.3. Stannous Chloride

Arber and Vivian [43,88] found that an addition of stannous chloride (up to 5 % by mass of cement) effectively suppressed corrosion of steel specimens embedded in mortar containing admixed calcium chloride (up to 4 % by mass of cement) The mortar blocks were steam-cured and corrosion of steel was examined visually after the blocks were broken. Stannous chloride increased the tensile strength of the mortar and acted comparably to calcium chloride in accelerating strength development. A similar result for concrete containing stannous chloride was reported by Treadaway and Russell [37]

From these test results, it appears that stannous chloride, like calcium nitrite, shows promising inhibitory properties and has a beneficial effect on strength development of concrete.

3.4.4. Sodium Benzoate

Lewis et al [65] stated that sodium benzoate might have a more persistent inhibitory effect than calcium nitrite.

Gouda et al [50, 51, 53] found that, compared with sodium nitrite, the dosage of sodium benzoate required to achieve a similar protection level in concrete containing 2 % admixed chloride was about six times higher.

Craig and Wood [54] indicated that sodium benzoate did not display passivity in mortar containing 2 % admixed calcium chloride and it caused a decrease in both tensile and compressive strengths of mortar. The strength decreased more with higher dosages of sodium benzoate.

Based upon these test results, the effectiveness of corrosion protection offered by sodium benzoate is not clear. Sodium benzoate, similar to sodium nitrite, would be expected to cause a decrease in concrete strength.

3.4.5. Other Inorganic Salts

Some sodium and potassium salts (sodium chromate, sodium phosphate, sodium silicate, and potassium chromate) have also been investigated.[50, 51, 53, 54]

Gouda et al [50, 51, 53] found that these salts generally required higher concentrations to achieve a comparable protection level when compared to sodium nitrite.

Craig and Wood [54] indicated that potassium chromate, like sodium benzoate, provided no passivity for steel in mortar with 2 % admixed calcium chloride and it caused a decrease in the compressive strength of mortar.

Based on test results of sodium nitrite and sodium benzoate, all of the above sodium salts would likely cause a decrease in strength of concrete and increase the danger of alkali-aggregate reaction for some types of aggregates. Therefore, these inhibitors appear to be less promising.

The inhibiting action of molybdate, borate and nitrite ions against Cl-induced corrosion of steel embedded in OPC mortar was investigated by impedance spectroscopy and linear polarization techniques[80]. Anion inhibition efficiency is found to vary with cure duration, but after 180 days their inhibition is in the order nitrite > borate > molybdate. Both impedance spectroscopy and electron microscopy analyses indicate that molybdate inhibition is achieved through surface layer formation involving molybdenum participation during the normal thickening of the passivating iron oxide film. Borate is, however, a less satisfactory additive because it inhibits cement hydration.

3.4.6. Sodium Thiocyanate-Based Admixture

Concern over the detrimental effect of calcium chloride on reinforcing steel in concrete has led to the development of non chloride accelerating admixtures.[71-72] One such admixture contains sodium thiacyanate, an inorganic salt. This non chloride admixture has been shown to be effective in accelerating the set of concrete at ambient temperatures as low as 20 °F (-7 °C), thereby reducing the need for some of the typical

requirements for cold-weather concreting such as heavy insulation and jobsite heaters. [73, 74]

Unlike calcium chloride, most of the investigations conducted to study the effect of sodium thiocyanate on the corrosion of steel in concrete were not published until recently. The article "Sodium Thiocyanate and the Corrosion Potential of Steel in Concrete and Mortar" (Concrete International, November 1989) showed that sodium thiocyanate-based admixtures are safe for use in reinforced concrete applications at current recommended dosages.[75].

Chapter 4

4. Methodology

Visual inspection and electrochemical methods may be used to monitor the corrosion of small steel samples in a tap water bath containing corrosion inhibitors and chloride. These types of measurements can be performed quickly and provide information about the inhibiting mechanism and the inhibitor/chloride threshold level.

The anodic polarization methods used in many studies give useful information on the effectiveness of various corrosion inhibitors. The change in steel surface condition due to the large applied potentials or currents is of concern and a new steel sample must be used for each test when these methods are used.

The polarization resistance technique can estimate corrosion rate of steel in an electrolyte. This method minimizes the disturbance of the test sample since only small potential shifts are applied to the test system. In addition, the measurement time of polarization resistance is the fastest among various electrochemical methods (typically 3 minutes or less). However, difficulties arise when determining the Tafel constants (necessary for conversion of polarization resistance to corrosion rate) and applying this technique in more complex electrochemical systems.

The Tafel constants in the polarization resistance equation may be obtained from the linear portions of Tafel plot, which is a plot of applied potential vs the logarithm of the resulting current. Corrosion rate can also be estimated directly from this plot. The potential shift in such a plot is typically 300 mV CSE. Because of the large magnitudes of the applied potentials or currents, the condition of the steel surface would likely be changed and therefore, a new steel sample must be used for each test.

The AC impedance spectroscopy method can provide information on inhibitor performance and passive layer characteristics of steel. In this method, an electrochemical cell is represented by an equivalent electrical circuit. Electrode capacitance and charge-transfer kinetics of the cell are obtained graphically from impedance diagrams, such as Nyquist and Bode plots.

The excitation signal in AC impedance spectroscopy is a small AC signal (typically 10 mV or less) and does not disturb the test system significantly. Therefore, the same steel sample can be monitored continuously to examine changes in passivity of steel corresponding to changes in inhibitor and chloride concentrations. The major disadvantage of this technique has been its complicated and time consuming data aquisition and analysis. However, the acquisition and analysis of data are greatly facilitated using automated measurement systems which have recently become available.

The advantages of electrochemical corrosion-rate measurement are as follows:

1) They permit rapid corrosion rate measurements and can be used to monitor corrosion rate in various process streams.
2) These techniques may be used for accurately measuring very low corrosion rates (less than 0.1 mpy).

   The measurement of low corrosion rates is especially important in nuclear, pharmaceutical, and food processing industries, where trace impurities and contamination are problems.
3) Electrochemical corrosion rate measurements may be used to measure the corrosion rate of structures that cannot be visually inspected or subjected to weight loss tests. Underground pipes and tanks and large chemical plant components are examples.

The techniques used in this research are linear polarization and A.C. impedance spectroscopy.

4.1. Linear Polarization Measurement

4.1.1. Basic Principles

The linear polarization technique involves application of a slow potential scan (usually 0.1 mV/s) close to the corrosion potential, Φ_{corr}, (ranging -20 mV to +20 mV). [89] The response, polarization current density, I, is recorded. The measurement can also be made in a galvanostat mode in which the current is monitored in order to obtain a small polarization potential. The polarization resistance, R_p, of the corroding electrode is defined as the slope of a potential-current density plot at the corrosion potential, Φ_{corr},

$$R_p = \left(\frac{\partial \Delta V}{\partial I} \right)_{\Phi_{corr}}$$

and the corrosion current density is calculated from the Stern-Geary equation [94]:

$$I_{corr} = \frac{B}{R_p}$$

and

$$B = \frac{\beta_a \beta_c}{2.303(\beta_a + \beta_c)}$$

B is a function of the anodic and cathodic Tafel slopes β_a and β_c. Corrosion rate, C.R. (μm consumption of steel per year) can be computed using Faraday's Law as follows: [89]

$$C.R.\ (\mu m/year) = 3.3 I_{corr} M/zd$$

where z = ionic charge (2 for iron), M = atomic weight of metal (56 for iron), d = density of iron, 7.9g/cm^3, and I_{corr}, is in μA/cm^2. Moreover, the reduction of rebar diameter in the steel cross section can be calculated according to: [90]

$$\phi(t) = \phi_i - 0.023 I_{corr}\, t$$

where $\phi(t)$ = remaining diameter (mm) at time t (years), ϕ_i = initial diameter and 0.023 is a factor to convert μA/cm^2 to mm/year.

4.1.2. Advantages

The linear polarization technique is the most successful non-destructive, relatively fast, cost-effective and quantitative approach in field reinforced concrete corrosion assessment to date. It allows the corrosion rate of rebar to be determined and the remaining diameter to be estimated. [91] It is a very useful technique in the field assessment of the remaining service life of the reinforced concrete structure. This technique can locate active corrosion areas with a high accuracy and is valuable for evaluation of the performance of repair patch and maintenance.

4.1.3. Limitations

Corrosion rate surveys employing linear polarization measurements are relatively time consuming since each reading takes about 5-10 minutes depending on the actual corrosion conditions. Time is also required to set up the equipment and carry out other preparatory work such as a rebar connection and electrical continuity checks. However the experience and knowledge of the operator are essential to collect the most useful data for a reasonable expenditure of time and effort.

On line cathodic protection systems, stray current, electrical short circuits, and insulating coatings or overlays may make linear polarization measurements inaccurate or impossible. Unfavorable conditions for measurements such as temperatures below 0°C(32F) or over 50°C (I22F), rain, standing water or humidity exceeding 80% should be avoided [92]. Modification is required for service life prediction modeling of reinforced concrete structures.

4.2. A.C. Impedance Spectroscopy (ACIS)

A.C. Impedance Spectroscopy (ACIS) is a powerful method of characterizing many of the electrical properties of materials and their interfaces. It is widely used in both fundamental and applied electrochemical studies including various aspects of electrode kinetics, battery performance, corrosion and high temperature electrochemistry. This technique has been used in determining the corrosion rate of reinforcing steel in concrete[93, 94]. However, due to the sophistication of the measurement and relatively high cost of the equipment, this technique is more frequently used in laboratory studies rather than in field surveys. Nevertheless, ACIS was validated as a useful tool in field corrosion assessment of reinforced concrete structure in SHRP report WFR-91 -524,1994 and elsewhere. [94] It allows the corrosion rate of rebar to be measured quantitatively, and provides information on rebar corrosion kinetics and insights into corrosion mechanisms which are key requirements to making decisions on repair and maintenance strategies.

4.2.1. Basic Principles

The a.c. impedance spectroscopy technique involves application of a small amplitude sinusoidal voltage or current signal to a system over a range of frequencies. A response current or potential signal is generated is recorded. The impedance of the system is easily evaluated through the analysis of the ratio of the amplitudes and phase shift between the voltage and current.

The impedance is defined as a vector:

$$Z(\omega) = \frac{V}{I}$$

The real component is plotted as the abscissce and the imaginary component as the ordinate in the so-called "complex plane" plot . This leads to definitions of impedance in terms of the complex quantities.

$$Z(\omega) = Z'(w) - jZ''(\omega)$$

$$Z'(\omega) = |Z| \cos(\theta)$$

$$Z''(\omega) = |Z| \sin(\theta)$$

where $|Z|$ is the modulus and (θ) the phase angle. $Z'(\omega)$ is the real component and $Z''(\omega)$ is the imaginary component of the impedance. The complex plane type of plot was first introduced by Cole and Cole and plots of log $|Z|$ and phase angle vs. log [frequency] are referred to as "Bode plots" [95].

4.2.2. Advantages

The ac. impedance technique provides information on corrosion mechanism and kinetic process. In addition to the determination of Rp and corrosion rate of rebar, a.c. impedance measurement provides information relating to steel/concrete interface structure and capacitive constants that other techniques do not. The impedance technique is a relatively fast and non-destructive, quantitative technique.

4.2.3. Limitations

This method requires substantial knowledge and working experience in order to interpret the spectra correctly. The calculation of the corrosion polarization resistance is tedious since the curve fitting is very time consuming. It will therefore have similar difficulties in actual field performance as half-cell potential and linear polarization methods.

4.2.4. Electrical Equivalent Circuit For Steel/Concrete Interface - AC Impedance

Interpretation of an impedance spectrum is difficult due to the complexity of cement paste and concrete microstructural changes taking place on steel surfaces. It requires modeling with a selected equivalent circuit until the electrical response of the parameters is well simulated with the experimental spectra. The usefulness of the analyses is strongly dependent on how the electrical components are selected and the extent to which they represent the microstructure of steel/concrete interface. It is generally accepted the physical model of the steel/concrete interface consists of a layer of compact iron oxide film and an interfacial film adjoined to the concrete matrix. The interfacial film consists of $Ca(OH)_2$ and other cement hydration products deposited onto the surface of steel. It could also involve the change of dielectric constant of this steel/concrete interface due to the diffusion of iron oxides into the steel-concrete interface. Many equivalent circuits have been proposed to describe the physical model of steel/concrete interface including those of Sagoe-Crentsil et al., Wenger, Alonso-Andrade and Hachni et al.

4.2.5. Equivalent Circuit Models for Reinforcing Steel and the Steel/Concrete Interface

A simple parallel combination of a pure resistor and capacitor along with the corresponding impedance plots in the complex plane (Cole-Cole plot) and log $|Z|$ and phase angle vs. log [frequency] (Bode plots) are illustrated in Figures 23a and 23b-d. The impedance of the circuit can be described by the following equation:

$$Z(\omega) = \frac{R}{1 + (\omega C R)^2} - j \frac{\omega C R^2}{1 + (\omega C R)^2}$$

where $\omega = 2\pi f$, and $j = \sqrt{-1}$. A plot of the equation in the complex plane (Figure 23b) gives rise to a perfect semi-circle characterized by a single conductivity relaxation time ($\tau = RC$); the maximum value of the imaginary impedance occurs at the characteristic frequency $f_o = 1/2\pi RC$. An ideal semi-circle is generally not observed in practice.

It is normally an inclined semi-circle with its center depressed below the real axis by an angle α, Figure 24a. This behavior normally associated with a spread of relaxation times cannot be described by the classical Debye equation employing a single relaxation time. A dispersive, frequency-dependent element or so called constant phase element (CPE)[123-124] as depicted in Figure 24b is used to account for the shape of the depressed complex plot. The corresponding impedance, expressed as follows:

$$Z(CPE) = \frac{R}{(1+RC(j\omega)^{\alpha})}$$

(where $0<1-\alpha<1$), α can be used to represent the degree of perfection of the capacitor and represents a measure of how far the arc is depressed below the real impedance axis.

Sagoe-Crentsil et al. and Lemoine et al. and Wanger] have proposed a very similar physical model to describe steel/concrete (or cement) interface as shown in Figure 25. The model consists of a layer of compact iron oxide film and interfacial film adjoined by the concrete matrix. It was suggested that the interfacial film consisted of $Ca(OH)_2$ and other cement hydration products deposited onto the surface of steel. A change of dielectric constant of the steel/concrete interface due to presence of the iron oxides can be considered.

Interpretation of an impedance spectrum requires modeling with a selected equivalent circuit until the response of the elemental microstructure of the cement paste is well simulated. The usefulness of the analyses is strongly dependent on how the electrical components are selected and the extent to which they represent the structure of the steel/concrete interface. Various equivalent circuits for the steel/concrete interface have been proposed by different authors. These are given in Figure 26.

Alonso-Andrade[30] propose an electrical circuit model (Figure 26a) for an activated rebar corrosion system without considering the interfacial film. The model consists of a concrete matrix circuit $R_{conc}//C_{conc}$ in parallel to, $R_p//C_{dl}$. R_p represents the corrosion polarization resistance and C_{dl} double layer capacitance at the electrode/concrete interface. A Warburg impedance, W, is also included to account for slow ionic diffusion effects at the electrode interface. Another electric circuit was also reported by the same

Sagoe-Crentsil et al.[96, 97] John et al[100] and Wenger [98, 99], suggested an electrical circuit to represent the physical model (Figure 17). The equivalent circuit, shown in Figure 26c, consists of three parallel circuits in series, $R_{conc}//C_{conc}$, $R_{inf}//C_{inf}$ and $R_p//C_{dl}$ to represent the concrete matrix, the interfacial film and the compact oxide film. This circuit appears to be more logical in describing the proposed physical model by assuming the layer of films are in series.

Hachani et al. [101, 102] described an electrical circuit as shown in Figure 26d. $R_p//C_{dl}$ is in series with R_{inf}, then in parallel with C_{inf}. This equivalent circuit is often used to describe an electrochemical kinetic process involving one or more adsorbed intermediates.

A modified electrical equivalent circuit similar to the one reported by Sagoe-Crentsil et al. was used in this simulation (Figure 27a). This equivalent circuit consists of three parallel combinations of a pure resistor and a frequency dependent capacitor (which is called a constant phase element (CPE) introduced to account for the shape of the depressed complex plot) to represent the concrete matrix, interface film and steel surface corrosion process arcs in the Real versus Imaginary (or Cole-Cole) plot (Figure 27b). The frequency dependent capacitor is defined as: $C = C_o(j\omega)^{1-\alpha}$, where C_o is a constant representing a pure capacitor, $\omega = 2\pi f$, and $j = \sqrt{-1}$.) The total impedance of the equivalent circuit is:

$$Z_t = Z_c + Z_i + Z_k$$

$$= \frac{R_c}{(1+\tau_c(j\omega)^{1-\alpha 1})} + \frac{R_i}{(1+t_i(j\omega)^{1-\alpha 2})} + \frac{R_p}{(1+\tau_k(j\omega)^{1-\alpha 3})}$$

The terms $\tau = R_cC_c$, $\tau_i = R_iC_i$, $\tau_k = R_pC_{dl}$ are relaxation times, and α_i ($0<\alpha_i<1$) are constants used to represent the degree of perfection of the capacitor and the extent to which the arc is depressed below the real impedance axis. The RC parameters in the given equation are defined elsewhere[9-13] and their abbreviations are given below:

- R_c and C_c -- the concrete resistance and matrix solid/liquid interface capacitance;
- R_i and C_i -- steel/concrete interface film resistance and capacitance;
- R_p and C_{dl} -- rebar polarization resistance and steel surface double layer capacitance.

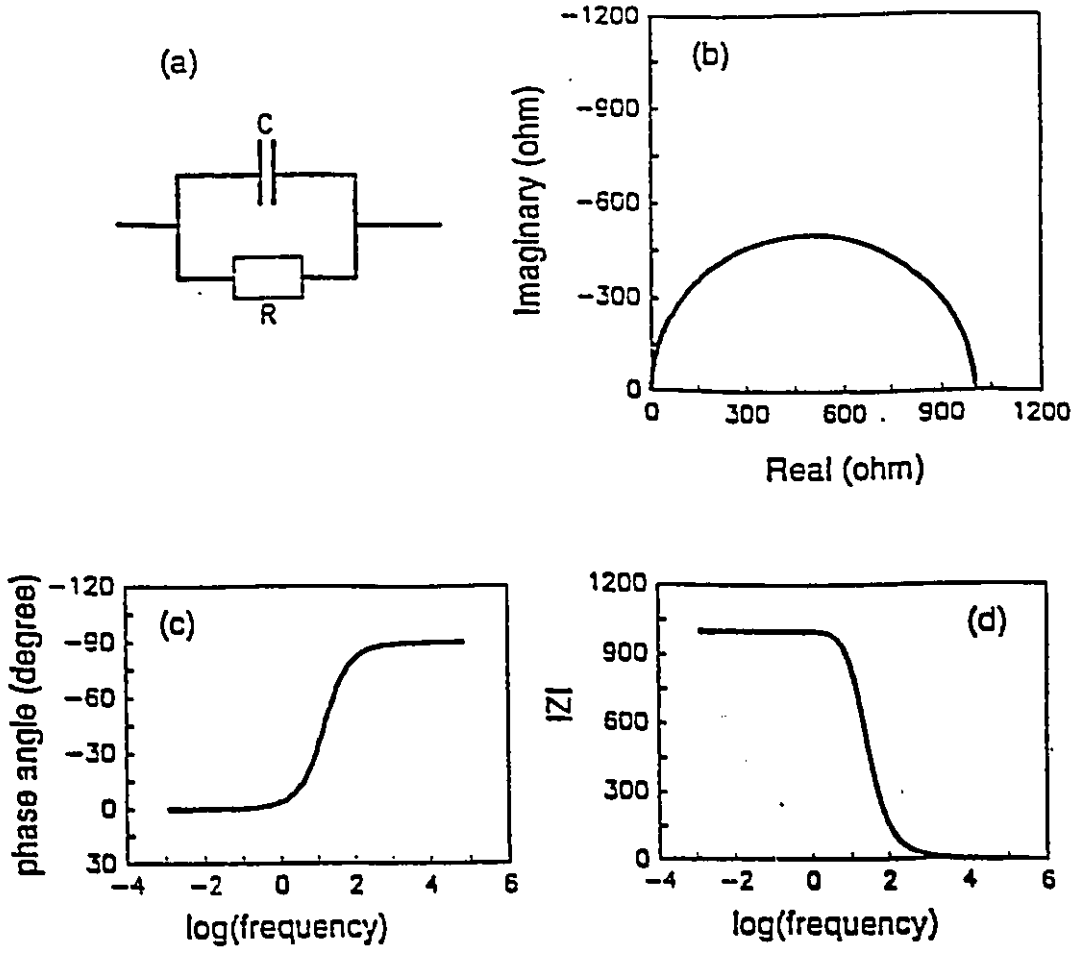

Fig. 23: (a) Simple parallel equivalent RC circuit consisting of a pure resistor and capacitor; (b) corresponding impedance plot in the complex plane (Cole-Cole Plot), (c) Phase angle vs. log (frequency); and (d) |Z| and vs. log (frequency)

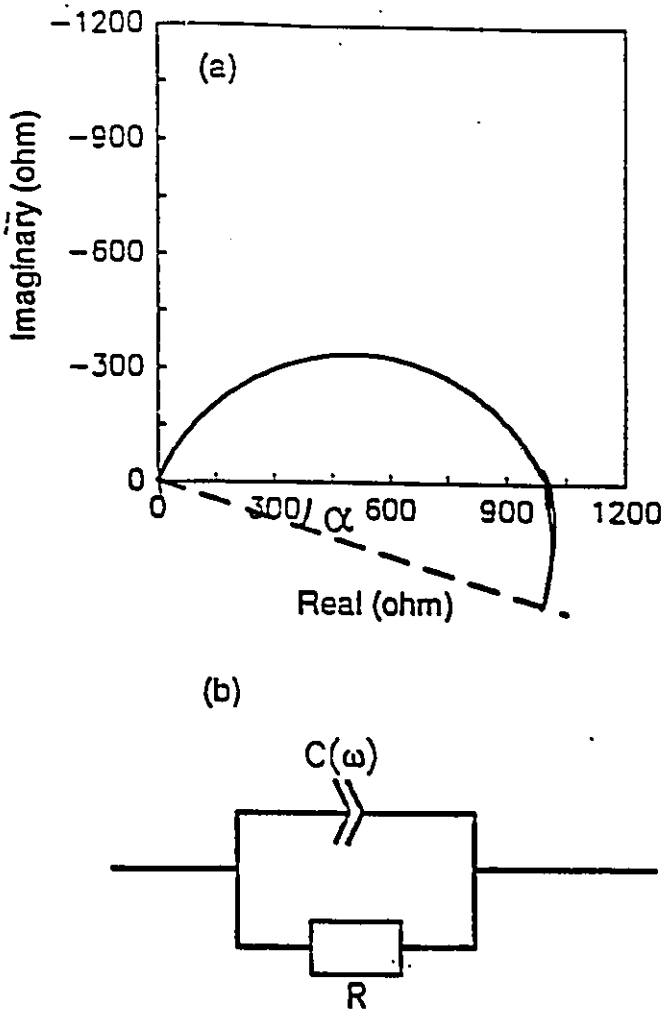

Fig. 24: (a) Impedance plot containing an inclined semi-circle with its center depressed below the real axis by an angle ∝; and (b) an equivalent circuit containing a constant phase element (CPE)

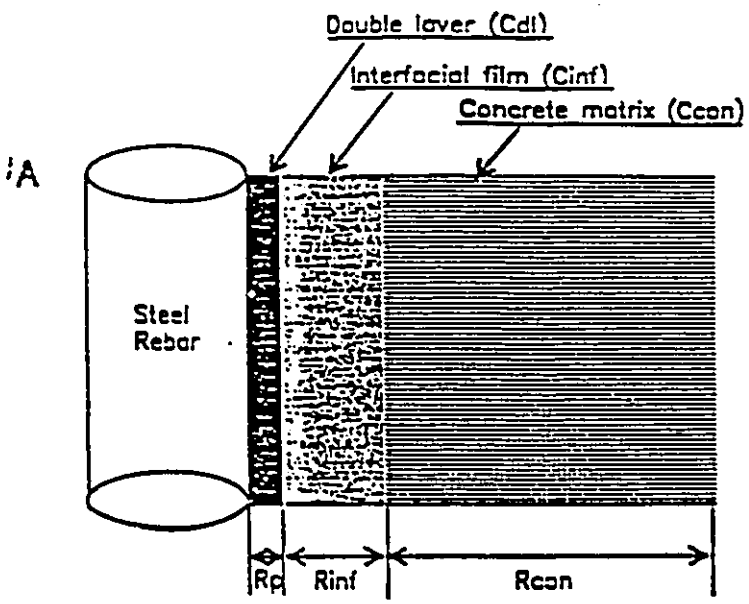

Fig. 25: A physical model to describe the steel/concrete (or cement paste) interface (Ref. 97).

a) Alonso-Andrade

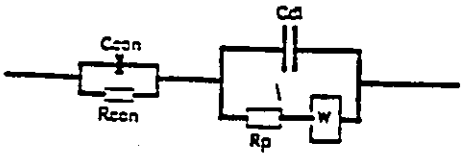

b) Alonso-Andrade

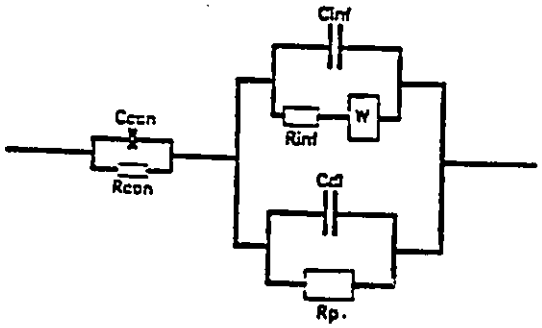

c) Sagoe-Crentsil et al.
John et al.
Wenger

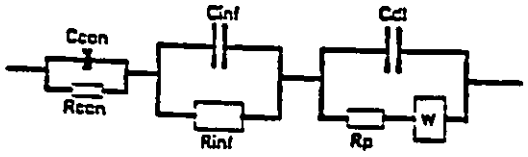

d) Hachni et al.

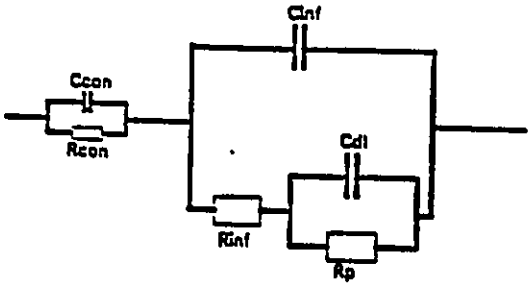

e) modified Sagoe-Crentsil

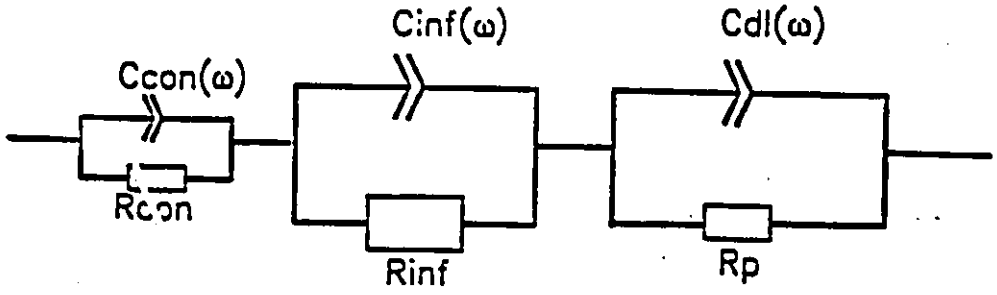

Fig. 26: Various equivalent circuits representing the steel/concrete (or cement paste) interface: (a) and (b) Alonso-Andrade (Ref.51); (c) Sagoe-Crentsil (Ref.52); (d) Hachni et al. (Ref.103).

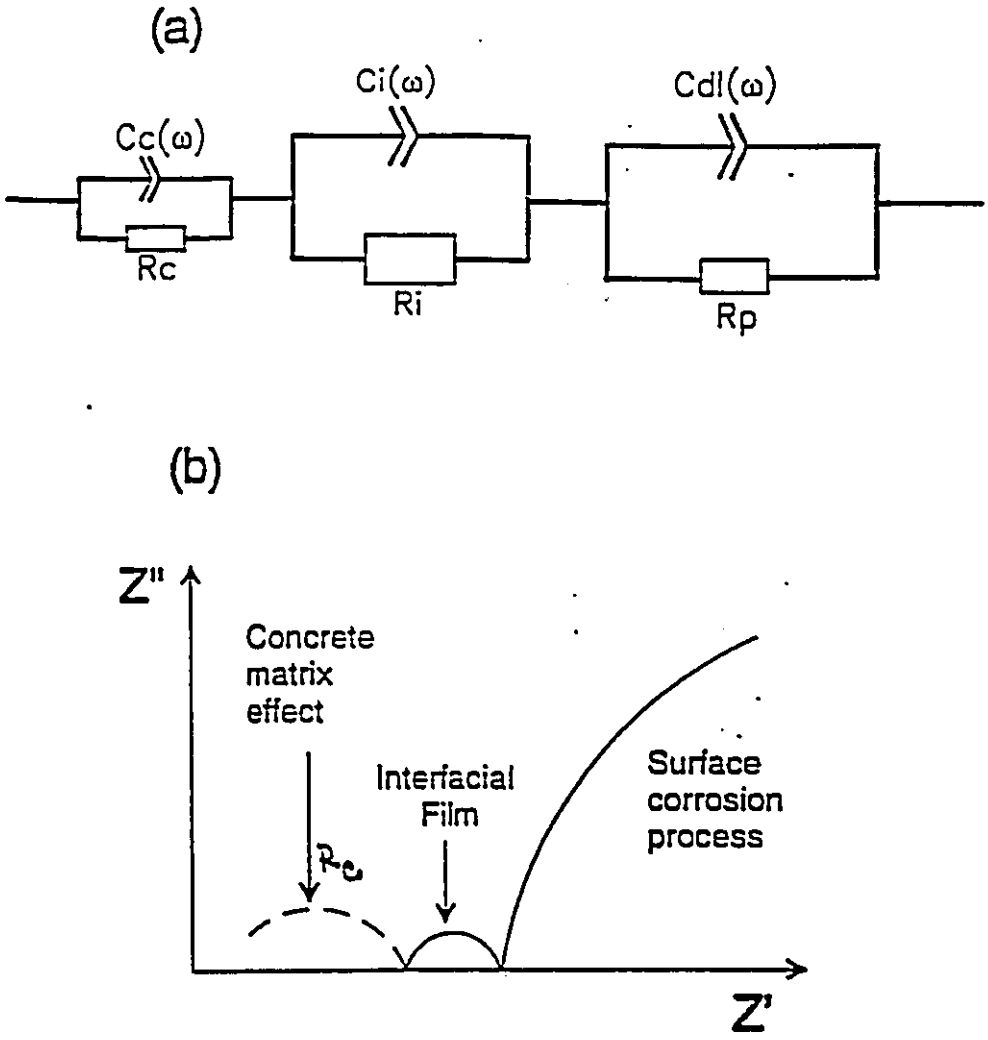

Fig. 27 a,b: (a) Equivalent circuit consisting of three parallel combinations of a pure resistor and a frequency dependent capacitor, (b) Corresponding impedance plot in the complex plane (Cole-Cole Plot).

4.2.6. Characterization of the Steel/Concrete Interface

Concrete Matrix

Figure 27 shows the equivalent circuit used in this work and an identical representation of the impedances in the complex plane (Cole-Cole plot). The three regions in the graph have been identified as concrete matrix effect, interfacial film and the surface corrosion effect.

The concrete matrix high frequency arc is usually observed at a few hundred kHz and higher frequencies. It is noted that the high frequency arc diameter, R_c, decreases with an increase of ionic concentration of the pore solution and porosity of the hydrating cement paste or concrete systems.

Interface Film

Physically, this film is a layer of precipitated cement hydration products including calcium hydroxide, and calcium silicate hydrates, that deposit on the surface of the steel bars. It has been reported that this arc in the Real versus Imaginary plot was not observed for the fresh made or non-corroded reinforced concrete or for steel in calcium hydroxide solution systems.(Fig.27b) This suggests that the chemical and physical properties of this interfacial layer are similar to those of the cement or concrete matrix. This arc therefore can not be distinguished from the matrix arc in most cases in the impedance measurements (except the extreme case of significant microstructural differences existing in the steel/concrete interface zones). However, if the rebar corrosion takes place, the corrosion products ("rust") will diffuse into the steel/concrete interfacial zone, fill the pores and change the pore solution conductivity and dielectric properties. In these situations the change of the electrical properties in this zone is indicated by the appearance of the arc in the kHz frequency range in the impedance spectrum.

Steel Corrosion Process

The third arc is due to the steel surface corrosion process which can normally be represented by a double layer capacitance, C_{dl} and the polarization resistance, R_p in parallel. A complete arc is hard to obtain due to time and equipment limitations especially when measurements at very low frequencies (below 0.01 mHz) are required. However, C_{dl} and R_p can be evaluated using equivalent circuit simulation.

R_p and Corrosion Rate

RC parameters can easily be determined through a computer simulation of the experimental spectra using the electric equivalent analysis method. This applies especially at very low frequencies when data is difficult to obtain experimentally due to time or equipment limitations. The corrosion rate determination involves acquisition of impedance spectra and data processing using electrical equivalent circuit fitting. As an example, Figure 28 shows an impedance spectrum in both Cole-Cole and Bode plots for a mild steel reinforced concrete specimen. The circles represent the experimental data and the solid line is a computer simulation curve. There are three regions in the frequency domain as indicated in the figure. Only a tail of a semi-circle is depicted in the high frequency range. This is attributed to concrete matrix microstructure. The interfacial film is represented by a depressed semi-circle at frequencies ranging from KHz to Hz. The large and incomplete semi-circle in the very low frequency region is due to double layer and polarization resistance contributions.

4.2.7. Effectiveness of Corrosion Inhibitors

The process of reinforcement corrosion in concrete is usually divided into two periods: an initiation period and a propagation period as indicated in Figure 27c. These two periods may be identified qualitatively by observing the changes in the impedance spectrum.

Normally there are two arcs in the impedance spectrum, e.g. the arcs corresponding to the concrete matrix and the steel interface effect in the complex plane. This indicates a non-corroded reinforcement in the initiation period. The appearance of the interface film arc, however, may imply an ongoing propagation period of rebar corrosion (Figure 27c). Moreover, the maximum phase angle shift and polarization resistance can be used to estimate the present corrosion rate of the reinforcement.

The concrete resistance, R_c, and concrete matrix capacitance, C_c, are related to the concrete matrix ionic concentration of the pore solution and porosity of the hydrating concrete systems. The steel surface corrosion process normally is represented by double layer capacitance, C_{dl} and the polarization resistance, R_p, in parallel. A complete arc is hard to obtain due to the time and equipment limitations especially when the measurement

at very low frequencies (below 0.01mHz) is required. However, C_{dl} and R_p can be evaluated using equivalent circuit simulation. The value of R_p decreases significantly with an increase in the amount of pre-mixed chloride.

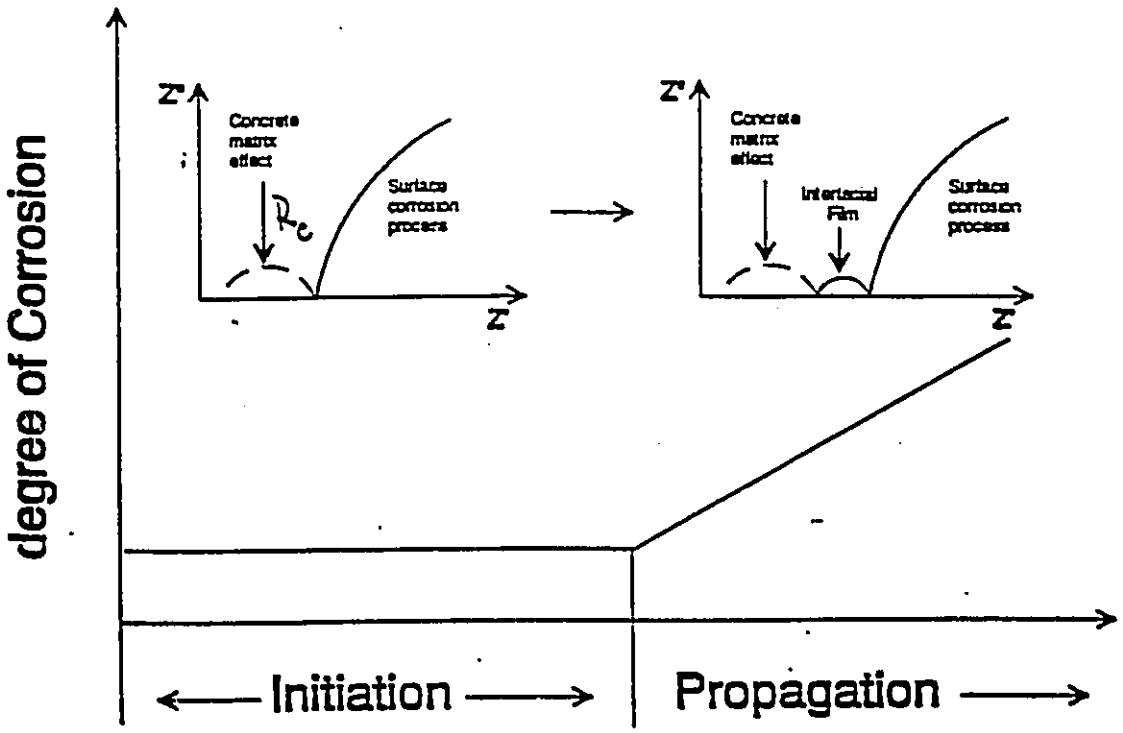

Fig. 27c: A schematic of the reinforcement corrosion mechanism in concrete and the corresponding changes of the impedance spectrum.

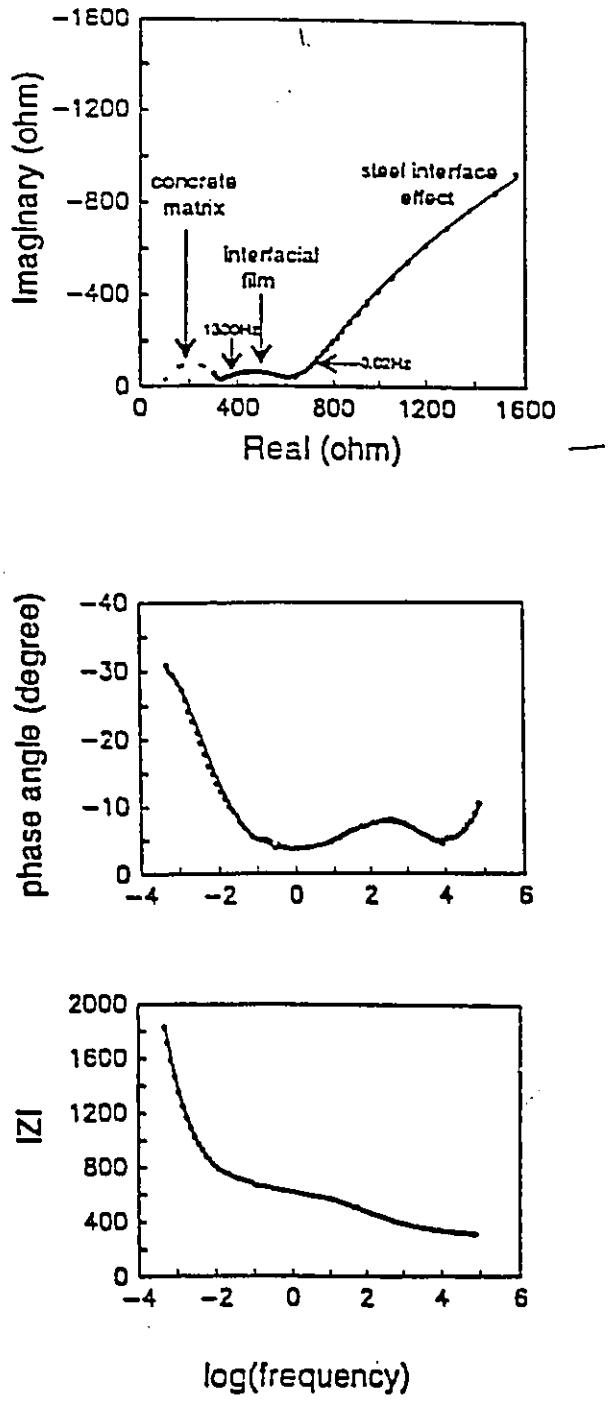

Fig. 28: Typical impedance spectrum of a mild steel reinforced concrete specimen. (a) Cole-Cole; (b) and (c) bode plots. The circles represent the experimental data and the solid line is a computer simulation curve.

Chapter 5

5. Experimental Procedure

The original intent of the experimental program was to trace the changes with time of polarization resistance of reinforcing bars in concretes with various known percentages of calcium chloride and fixed percentages of corrosion inhibitors, stored in artificial sea water. The specimens were cast at the National Research Council on 31.08.90 under the direction of Dr. Rejean Brosseau.

Sodium nitrite ($NaNO_2$) and dinitrobenzoic acid were selected as the corrosion inhibitors. Calcium chloride was used to provoke, or initiate, corrosion.

A third series of specimens without any corrosion inhibitor and similar percentages of calcium chloride were used as control samples.

5.1. Materials

Normal portland cement ASTM Type 1 was used throughout the tests. Coarse and fine aggregates were washed graded materials with a maximum size of 9 mm. The composition of concrete mixtures consisted of one part normal portland cement, three parts coarse aggregate, two parts sand and 0.5 part distilled water (by mass).

Each corrosion inhibitor system consisted of five samples. Each sample contained the inhibitor and one of the following $CaCl_2$ concentrations, 0%, 2%, 4%.

The different corrosion inhibitor systems used in this study were made from three chemical compounds which were introduced in the concrete either alone or in combination. The systems are listed below:

- Sodium Nitrite ($NaNO_2$)
- Dinitrobenzoic Acid
- Calcium Chloride - a widely used accelerator which encourages corrosion of reinforcing steel in concrete

5.2. Test Specimens

Nine series of "lollipop-like" concrete specimens containing 0, 2 and 4% chloride ions and 5% of various corrosion inhibitors (percentages are based on mass of cement) were fabricated. The cement: sand: aggregate ratio was 1:2:3 and water/cement ratio of 0.5 was used Table 2 summarizes the additives to each mix. The fabrication configuration is shown in Figure 29a. Mild steel reinforcing bars (ϕ = 11.7 mm x 146 mm) were sandblasted prior to use. Both ends of the rebar were sealed with silicone. Only the middle section (6.98 cm) of the bar left exposed to concrete. Specimens were moist-cured for seven or more days before they were stored in a 3.4% sodium chloride solution.

Specimen Series	% NaCl (mass of cement)	% Inhibitors (mass of cement)
A1	non	none
A2	2%	none
A3	4%	none
B1	non	5% sodium nitrite
B2	2%	5% sodium nitrite
B3	4%	5% sodium nitrite
C1	non	5% dinitrobenzoic acid
C2	2%	5% dinitrobenzoic acid
C3	4%	5% dinitrobenzoic acid

Table 2: Series Identification

The solution level was kept approximately 6 mm below the top of the concrete.

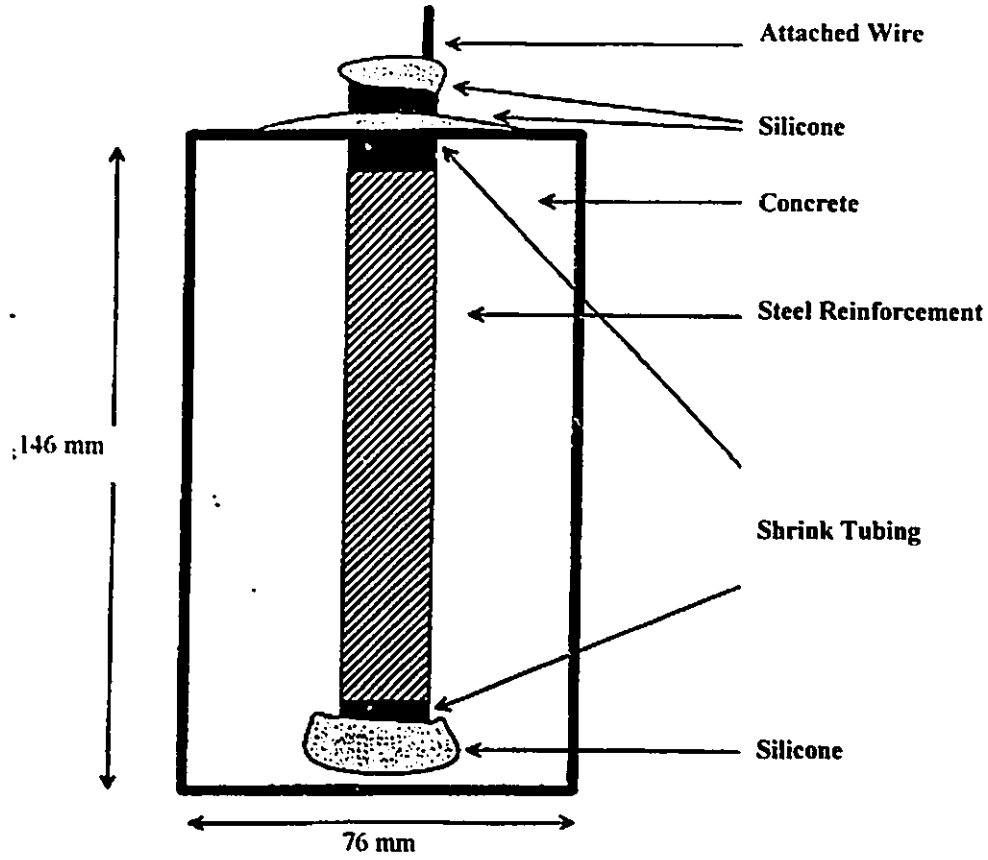

Fig. 29a: Schematic of Test Specimen

5.3. Test Procedure

Test specimens were placed in a tap water bath containing 3.5% sodium chloride. The samples were aerated with air for at least fifteen minutes prior to testing and throughout the tests. A copper/copper sulphate reference electrode 2.54 cm in diameter was used for each test. A stainless steel cylindrical shell 20.32 cm diameter x 15.24 cm long was used to obtain a uniform current distribution. Linear polarization and a.c.

impedance methods were used to determine the corrosion rate of the reinforcing bar. Figure 29b shows the setup for both testing methods.

It was difficult to have confidence in the polarization resistance method. One of the reasons was oxygen depletion in the salt water tanks. New tanks were built with a non-galvanic aeration system. Secondly, a circular counter electrode was used (Figure 29b)

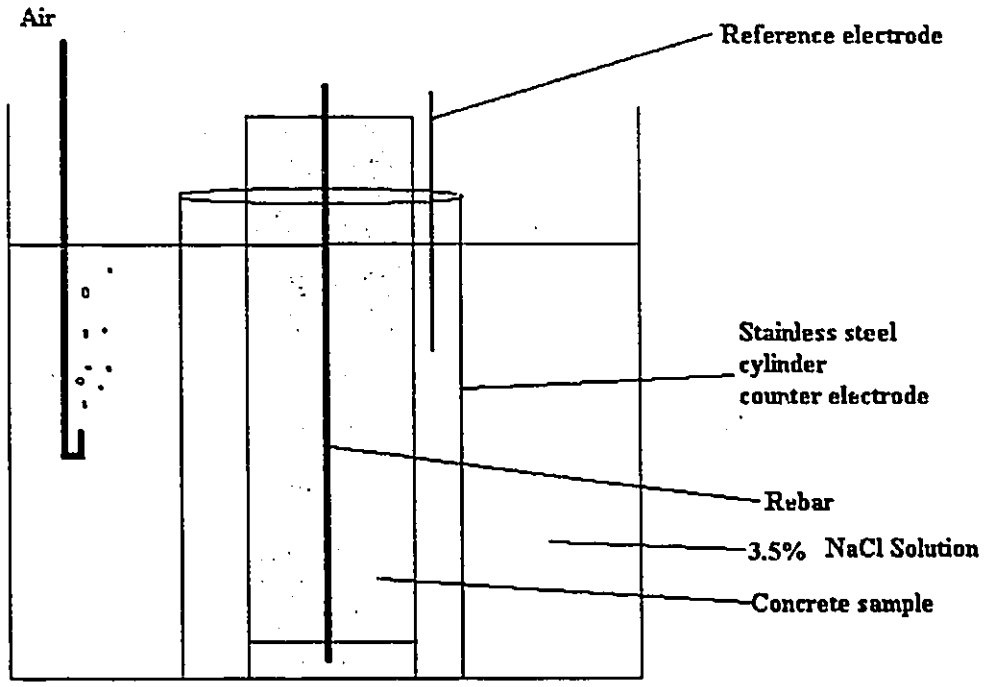

Fig. 29b: Experimental setup for both LP and A.C. Impedance investigations

The linear polarization data was analysed using the software associated with the testing program. The a.c. impedance data were analyzed using a computer fitting model called ZSIM. The relative corrosion resistance of the concrete samples as well as the best method for analysis will be analyzed.

5.3.1. Linear Polarization

A potentiostat is used to displace the equilibrium of the metal as measured relative to the reference electrode, and the current flowing between the reinforcement and a counter electrode is measured (P). These tests were done using an EG&G Princeton Applied Research Potentiostat/Galvanostat Model 273 and an associated software package to control the test procedures and analyze the data. Polarization experiments were performed at a scan rate of 0.1 mV/s and initiated at -20 mV vs. below the corrosion potential and ended at a maximum of +20mV vs. the corrosion potential. Each test took approximately 6 to 7 minutes. Three tests were performed on each specimen. At least 15 minutes was allowed between tests on the same sample to allow the sample to depolarize. The linear polarization results were only used to determine which specimens should be used in the ACIS experiments.

5.3.2. AC Impedance

A small AC voltage signal of 10 mV was applied over the range of frequencies 75000 to 0.0005 Hz and the current required to cause this voltage perturbation was measured. The phase shift of the current and voltage characteristics were measured. A three electrode configuration was used with the reference electrode shorted to the working electrode. These tests were done using a Schulumberger SI 1255 HF Frequency Response Analyzer and a Schulumberger SI 1286 Electrical Interface273 and associated software to control the test procedures and analyze the data. One or two tests were performed on each sample. Each test took slightly less than three hours. The data was analyzed using an equivalent circuit for the steel/concrete interface and are presented in Chapter 6.

Chapter 6

Results and Discussion

6.1 Linear Polarization

The potentiostat is used to measure E corrosion, scans the voltage between E_{corr} - 20mV to E_{corr} +20mV and measures the resulting current. From the experimental results the software associated with the potentiostat calculates the polarization resistance and corrosion current I_{corr}. A typical output of Ya linear polarization data is shown in Figure 30.

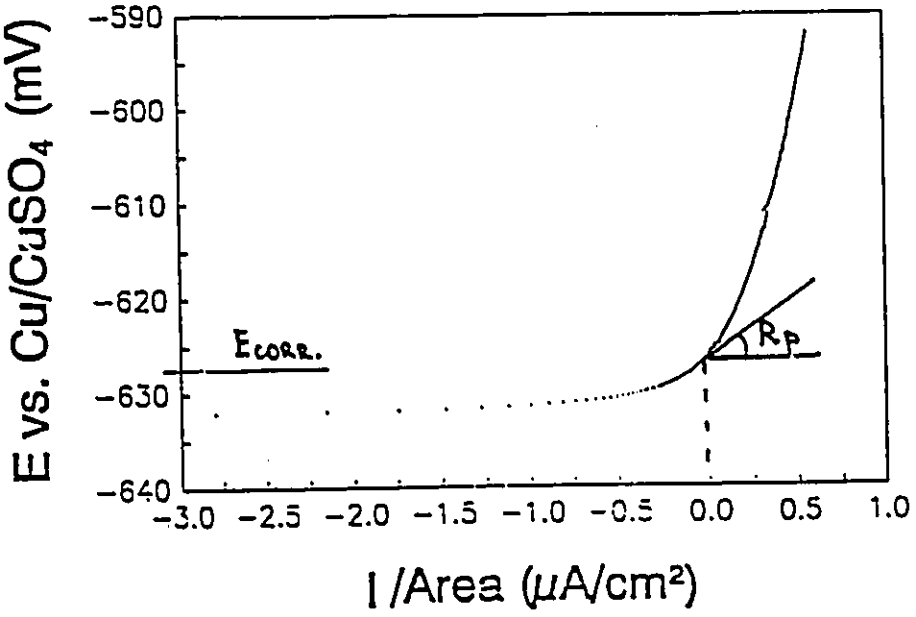

Fig. 30: Sample Graph for Linear Polarization Data

Ideally the voltage against current graph should be a straight line; however this was not observed in any test.

The results of the first set of measurements on all specimens is given in Appendix A. Each measurement was repeated. Table 3 is a reduced set of results for the series which had 5 replicates.

SAMPLE	Ecorr (uV)	Rp (kohms/cm2)	Icorr (μA/cm2)
A_{11-1}	546.07	25.88	1.01
A_{12-1}	487.7	32.78	0.99
A_{13-1}	386.25	24.54	1.24
A_{14-1}	445.53	17.65	1.48
A_{15-1}	481.34	14.66	1.78
MEAN	469.38	23.1	1.3
STD DEV	58.82	7.15	0.165
C of V (%)	12.5	31	13
SAMPLE	**Ecorr**	**Rp**	**Icorr**
A_{21-1}	387.5	11.93	2.18
A_{22-1}	492.23	19.72	1.32
A_{23-1}	369.89	48.84	0.53
A_{24-1}	441.71	15.08	1.73
A_{25-1}	526.39	18.81	1.38
MEAN	443.54	22.88	1.43
STD DEV	66.71	14.84	0.61
C of V (%)	15	65	43
SAMPLE	**Ecorr**	**Rp**	**Icorr**
A_{31-1}	467.73	12.37	2.11
A_{32-1}	450.21	12.11	2.18
A_{33-1}	426.05	12.1	2.15
A_{34-1}	588.23	8.27	3.15
A_{35-1}	360.23	14.55	1.79
MEAN	458.49	11.88	2.28
STD DEV	83.21	2.26	0.051
C of V (%)	18	19	2
SAMPLE	**Ecorr**	**Rp**	**Icorr**
B_{11-1}	343.3	37.27	0.7
B_{12-1}	293.99	43.46	0.6
B_{13-1}	468.63	12.27	2.12
B_{14-1}	310.48	22.23	2.1
B_{15-1}	398.07	21.1	1.24
MEAN	362.89	27.27	1.35
STD DEV	71.23	12.43	0.73
C of V (%)	20	46	54

SAMPLE	Ecorr (uV)	Rp (kohms/cm2)	Icorr (μA/cm2)
A_{11-2}	551.87	29.23	0.89
A_{12-2}	485.81	40.2	0.65
A_{13-2}	385.57	20.96	1.24
A_{14-2}	451.29	19.45	1.34
A_{15-2}	489.83	483.55	0.6
MEAN	472.87	30.68	0.94
STD DEV	60.79	10.94	0.34
C of V (%)	13	36	36
SAMPLE	**Ecorr**	**Rp**	**Icorr**
A_{21-2}	398.99	14.21	1.83
A_{22-2}	494.9	20.84	1.25
A_{23-2}	361.79	37.37	0.7
A_{24-2}	460.13	21.01	1.24
A_{25-2}	526.96	19.54	1.33
MEAN	448.55	22.59	1.27
STD DEV	67.85	8.71	0.04
C of V (%)	15	39	31
SAMPLE	**Ecorr**	**Rp**	**Icorr**
A_{31-2}	489.44	11.13	2.34
A_{32-2}	450.21	10.99	2.29
A_{33-2}	429.94	10.66	2.44
A_{34-2}	588.83	7.82	3.33
A_{35-2}	372.84	21.2	1.23
MEAN	466.25	12.36	2.33
STD DEV	80.41	5.12	0.75
C of V (%)	17	41	32
SAMPLE	**Ecorr**	**Rp**	**Icorr**
B_{11-2}	334.72	31	0.84
B_{12-2}	298.11	43.14	0.6
B_{13-2}	478.08	14.18	1.84
B_{14-2}	298.53	30.59	2
B_{15-2}	396.17	31.72	0.82
MEAN	361.12	30.13	1.22
STD DEV	76.64	10.33	0.65
C of V (%)	21	34	53

Table 3: Statistical Analysis of Linear Polarization Results Using a Point Counter Electrode

SAMPLE	Ecorr	Rp	Icorr
B_{21-1}	396.29	33.04	0.79
B_{22-1}	543.88	13.13	1.98
B_{23-1}	609.91	30.3	0.86
B_{24-1}	453.67	61.63	0.42
B_{25-1}	465.62	17.72	1.47
MEAN	493.87	31.16	1.1
STD DEV	83.52	18.96	0.62
C of V (%)	17	61	56
SAMPLE	Ecorr	Rp	Icorr
B_{31-1}	336.63	22.51	1.16
B_{32-1}	269.32	17.45	1.49
B_{33-1}	285.29	19.17	1.36
B_{34-1}	418.41	39.6	0.66
A_{35-1}	413.62	13.2	1.97
MEAN	364.65	22.39	1.33
STD DEV	73.24	10.19	0.48
C of V (%)	20	46	36
SAMPLE	Ecorr	Rp	Icorr
C_{11-1}	473.9	27.16	0.96
C_{12-1}	528.61	33.67	0.77
C_{13-1}	483.25	17.18	1.52
C_{14-1}	488.24	22.78	1.14
C_{15-1}	470.88	23.43	1.54
MEAN	488.98	24.84	1.19
STD DEV	46.46	6.09	0.34
C of V (%)	10	25	28
SAMPLE	Ecorr	Rp	Icorr
C_{21-1}	375.3	10.62	2.45
C_{22-1}	520.57	19.84	1.31
C_{23-1}	531.8	18.48	1.41
C_{24-1}	495.54	18.87	0.53
C_{25-1}	427.21	15.21	1.71
MEAN	470.08	16.6	1.48
STD DEV	66.76	3.77	0.69
C of V (%)	14	23	47
SAMPLE	Ecorr	Rp	Icorr
C_{31-1}	477.5	15.13	1.72
C_{32-1}	463.21	18.8	1.39
C_{33-1}	439.78	20.92	1.25
C_{34-1}	639.74	13.29	1.96
C_{35-1}	406.04	23.29	1.12
MEAN	485.25	18.29	1.49
STD DEV	90.49	4.1	0.35
C of V (%	17	22	23

SAMPLE	Ecorr	Rp	Icorr
B_{21-2}	399.4	35.1	0.74
B_{22-2}	544.35	12.9	2.02
B_{23-2}	607.42	27.81	0.94
B_{24-2}	453.41	25	1.04
B_{25-2}	473.03	24.17	1.08
MEAN	495.52	24.99	1.16
STD DEV	81.28	18.2	0.53
C of V(%)	16	72	46
SAMPLE	Ecorr	Rp	Icorr
B_{31-2}	342.68	42.27	0.62
B_{32-2}	281.88	26.6	0.98
B_{33-2}	288.83	37.75	0.69
B_{34-2}	415.29	37.2	0.7
B_{35-2}	427.27	15.91	1.64
MEAN	371.19	31.95	0.93
STD DEV	71.87	10.65	0.42
C of V (%)	19	33	45
SAMPLE	Ecorr	Rp	Icorr
C_{11-2}	476.84	28.47	0.92
C_{12-2}	525.04	31.94	0.82
C_{13-2}	478.78	13.55	1.92
C_{14-2}	388.46	22.64	1.15
C_{15-2}	484.84	31.54	0.83
MEAN	470.19	25.63	1.13
STD DEV	49.97	7.71	0.46
C of V (%)	11	30	41
SAMPLE	Ecorr	Rp	Icorr
C_{21-2}	389.62	15.88	1.64
C_{22-2}	519.12	18.55	1.4
C_{23-2}	529.39	17.71	1.47
C_{24-2}	490.7	25.54	1.02
C_{25-2}	445.43	22	1.18
MEAN	474.85	19.94	1.34
STD DEV	57.7	3.84	0.24
C of V (%)	12	19	18
SAMPLE	Ecorr	Rp	Icorr
C_{31-2}	483.52	16.28	1.6
C_{32-2}	472.99	27.63	0.94
C_{33-2}	438.33	18.98	1.43
C_{34-2}	638.89	12.87	2.02
C_{35-2}	415.08	24.94	1.04
MEAN	489.76	20.14	1.41
STD DEV	87.72	6.09	0.44
C of V (%	17	30	31

* - Coefficient of variation %

Table 3(continued): Statistical Analysis of Linear Polarization Results Using Point Counter Electrode

Samples are aerated - 2 atm pressure

A11 - A35

A11 - A15 Control (Inhibitor N/A)
A21 - A25 - 2% CaCl2
A31 - A35 - 4% CaCl2

B11 - B35

B11 - B15 - 2% NaNO2
B21 - B25 - 2% NaNO2 + 2%CaCl2
B31 - B35 - 2% NaNo2 + 4%CaCl2

C11 - C35

C11 - C15 - 5% 3-5,dinitrobenzoic acid
C21 - C25 - 5% 3-5,dinitrobenzoic acid + 2% CaCl2
C31 - C35 - 5% 3-5,dinitrobenzoic acid + 4%CaCl2

Sample	Ecorr [V]	Icorr [µA/cm2]	Ba	Bc	Sample	Ecorr [V]	Icorr [µA/cm2]	Ba	Bc	Sample	Ecorr [V]	Icorr [µA/cm2]	Ba	Bc
A11-1	-0.7655	14.22	48.49E-3	25.95E-3	B11-1	-0.4886	-0.98	-14.55E-3	-42.66E-3	C11-1	-0.6878	4.57	52.33E-3	21.85E-3
A11-2	-0.7660	16.04	52.68E-3	27.59E-3	B11-2	-0.4997	-0.99	-14.55E-3	-42.55E-3	C11-2	-0.6908	4.70	50.01E-3	20.85E-3
A11-3	-0.7665	16.11	53.98E-3	28.01E-3	B11-3	-0.4761	-0.92	-13.59E-3	-46.71E-3	C11-3	-0.6911	4.71	51.76E-3	21.68E-3
A12-1	-0.7276	2.67	46.91E-3	18.11E-3	B12-1	-0.6027	-0.27	17.91E-3	-3.026v/de	C12-1	-0.7479	12.19	62.10E-3	25.34E-3
A12-2	-0.7310	3.11	49.31E-3	20.18E-3	B12-2	-0.6048	-0.30	18.91E-3	-3.027v/de	C12-2	-0.7568	12.79	61.08E-3	24.38E-3
A12-3	-0.7298	2.58	46.81E-3	18.05E-3	B12-3	-0.6089	-0.57	1000v/dec	1000v/dec	C12-3	-0.7890	12.99	61.08E-3	24.38E-3
A13-1	-0.6905	4.59	54.48E-3	20.09E-3	B13-1	-0.7252	4.94	45.72E-3	20.45E-3	C13-1	-0.7121	5.72	66.16E-3	16.23E-3
A13-2	-0.6867	5.20	59.03E-3	20.05E-3	B13-2	-0.7381	4.87	44.89E-3	21.03E-3	C13-2	-0.7113	5.54	65.35E-3	15.85E-3
A13-3	-0.6860	5.20	59.02E-3	20.05E-3	B13-3	-0.7420	4.92	44.89E-3	21.03E-3	C13-3	-0.7118	5.55	66.70E-3	15.90E-3
A14-1	-0.7119	6.19	61.60E-3	19.79E-3	B14-1	-0.4929	-0.81	-14.35E-3	-38.27E-3	C14-1	-0.6883	3.13	48.37E-3	18.14E-3
A14-2	-0.7128	6.19	61.43E-3	21.31E-3	B14-2	-0.4876	1.27	55.83E-3	9.89E-3	C14-2	-0.6991	3.58	48.96E-3	19.01E-3
A14-3	-0.7200	6.20	61.43E-3	21.31E-3	B14-3	-0.4858	1.27	58.90E-3	9.89E-3	C14-3	-0.6875	3.15	48.97E-3	18.56E-3
A15-1	-0.7804	12.20	48.59E-3	27.18E-3	B15-1					C15-1	-0.6963	4.31	58.13E-3	17.45E-3
A15-2	-0.7803	12.20	48.59E-3	27.18E-3	B15-2					C15-2	-0.6961	4.31	58.13E-3	17.45E-3
A15-3	-0.7799	12.61	49.76E-3	27.82E-3	B15-3					C15-3	-0.6928	4.11	56.05E-3	15.35E-3
Average	-0.7357	8.35	53.47E-3	22.84E-3	Average	-0.5794	1.03	20.91E-3	-9.77E-3	Average	-0.7106	6.09	57.01E-3	19.49E-3
A21-1	-0.7315	11.92	73.13E-3	21.36E-3	B21-1	-0.6303	-2.82	-15.19E-3	-50.87E-3	C21-1	-0.6386	3.22	67.15E-3	12.02E-3
A21-2	-0.7415	12.13	73.78E-3	22.15E-3	B21-2	-0.6307	-2.77	-15.19E-3	-50.87E-3	C21-2	-0.6385	4.87	68.95E-3	14.71E-3
A21-3	-0.7319	12.21	75.11E-3	23.81E-3	B21-3	-0.6301	-2.68	-15.19E-3	-50.87E-3	C21-3	-0.6423	4.92	69.91E-3	14.91E-3
A22-1	0.7739	10.73	42.79E-3	29.17E-3	B22-1	-0.8678	10.32	50.35E-3	22.39E-3	C22-1	-0.7913	10.52	81.40E-3	22.10E-3
A22-2	-0.7740	10.98	43.51E-3	29.87E-3	B22-2	-0.8699	10.13	49.94E-3	21.44E-3	C22-2	-0.7865	11.31	83.51E-3	22.10E-3
A22-3	-0.7745	11.01	43.98E-3	29.98E-3	B22-3	-0.8167	9.86	49.22E-3	22.98E-3	C22-3	-0.7869	11.64	90.15E-3	23.81E-3
A23-1	-0.5600	3.69	46.48E-3	23.19E-3	B23-1	-0.7532	3.29	42.89E-3	21.42E-3	C23-1	-0.7354	3.95	50.27E-3	17.09E-3
A23-2	-0.5563	4.67	55.49E-3	21.75E-3	B23-2	-0.7680	3.51	42.91E-3	21.56E-3	C23-2	-0.7358	3.96	51.27E-3	17.27E-3
A23-3	-0.5611	3.79	46.78E-3	23.59E-3	B23-3	-0.7558	3.48	42.99E-3	21.83E-3	C23-3	-0.7371	4.11	53.18E-3	19.35E-3
A24-1	-0.7893	7.64	46.17E-3	27.64E-3	B24-1	-0.6133	-10.46	0.1000v/d	0.1000v/d	C24-1	-0.7513	10.25	80.39E-3	24.03E-3

Table 4 : Raw Data of Linear Polarization Using a Cylindrical Counter Electrode

Sample	Ecorr [V]	Icorr [µA/cm2]	Ba	Bc	Sample	Ecorr [V]	Icorr [µA/cm2]	Ba	Bc	Sample	Ecorr [V]	Icorr [µA/cm2]	Ba	Bc
A24-2	-0.7898	7.85	47.19E-3	27.69E-3	B24-2	-0.6191	-16.26	0.1000v/d	0.1000v/d	C24-2	-0.7670	11.28	61.12E-3	23.74E-3
A24-3	-0.7880	7.32	46.11E-3	27.01E-3	B24-3	-0.6280	-18.89	0.1000v/d	0.1000v/d	C24-3	-0.7685	10.38	61.06E-3	23.76E-3
A25-1	-0.7847	14.77	55.89E-3	27.86E-3	B25-1	-0.7610	6.43	47.79E-3	33.93E-3	C25-1	-0.7491	9.76	54.66E-3	25.14E-3
A25-2	-0.7815	14.67	55.25E-3	27.54E-3	B25-2	-0.7610	6.13	44.21E-3	27.07E-3	C25-2	-0.7546	8.73	55.96E-3	24.79E-3
A25-3	-0.7832	14.69	54.83E-3	26.95E-3	B25-3	-0.7683	6.53	46.38E-3	29.11E-3	C-25-3	-0.7600	8.33	54.86E-3	23.55E-3
Average	-0.6249	9.87	53.77E-3	25.97E-3	Average	-0.7247	-0.15	30.93E-3	5.76E-3	Average	-0.7362	8.28	66.12E-3	20.56E-3
A31-1	-0.5172	2.96	58.92E-3	15.62E-3	B31-1	-0.7245	17.41	0.1000v/d	0.1000v/d	C31-1	-0.7493	18.37	45.69E-3	29.01E-3
A31-2	-0.5119	3.17	62.32E-3	14.78E-3	B31-2	-0.6595	13.59	0.1000v/d	0.1000v/d	C31-2	-0.7503	19.80	50.05E-3	30.41E-3
A31-3	-0.5087	3.12	62.33E-3	15.02E-3	B31-3	-0.6523	17.64	0.1000v/d	0.1000v/d	C31-3	-0.7503	19,80	50.05E-3	30.41E-3
A32-1	-0.7287	-14.43	0.1000v/d	0.1000v/d	B32-1	-0.7348	81.28	97.90E-3	24.40E-3	C32-1	-0.7410	-4.17	-23.99E-3	-40.08E-3
A32-2	-0.7291	-14.51	0.1000/de	0.1000v/d	B32-2	-0.0759	85.41	98.76E-3	25.11E-3	C32-2	-0.7458	-4.22	-25.11E-3	-42.71E-3
A32-3	-0.7299	-14.53	0.1000v/d	0.1000v/d	B32-3	-0.7593	85.51	98.79E-3	25.31E-3	C32-3	-0.7460	-4.22	-25.81E-3	-42.99E-3
A33-1	-0.7550	-18.50	0.1000v/d	0.1000v/d	B33-1	-0.4326	1.30	60.53E-3	19.28E-3	C33-1	-0.7964	9.26	48.96E-3	25.86E-3
A33-2	-0.7437	-17.74	3.23E-3	4.84E-3	B33-2	-0.4328	1.02	45.85E-3	17.26E-3	C33-2	-0.7831	8.77	46.31E-3	22.75E-3
A33-3	-0.7437	-12.72	0.1000v/d	0.1000v/d	B33-3	-0.4178	1.00	40.17E-3	15.63E-3	C33-3	-0.7981	9.40	49.11E-3	25.99E-3
A34-1	-0.8013	-26.01	-23.11E-3	-48.52E-3	B34-1	-0.5938	2.72	43.66E-3	21.64E-3	C34-1	-0.8209	-19.52	-22.73E-3	-38.26E-3
A34-2	-0.8056	-26.89	25.11E-3	50.01E-3	B34-2	-0.5941	2.73	43.78E-3	22.11E-3	C34-2	-0.8315	-19.71	-22.81E-3	-39.01E-3
A34-3	-0.8061	-27.03	26.80E-3	50.93E-3	B34-3	-0.5971	2.90	45.11E-3	23.01E-3	C34-3	-0.8617	-20.22	-25.01E-3	-41.61E-3
A35-1	-0.6961	-2.71	-15.89E-3	-48.02E-3	B35-1	-0.8469	5.38	37.88E-3	23.80E-3	C35-1	-0.7759	3.95	31.91E-3	19.10E-3
A35-2	-0.6859	-3.59	-16.57E-3	-53.03E-3	B35-2	-0.8511	5.48	37.93E-3	25.01E-3	C35-2	-0.7762	2.30	44.84E-3	16.50E-3
A35-3	-0.6846	3.48	-16.21E-3	53.00E-3	B35-3	-0.8541	5.50	38.01E-3	25.76E-3	C35-3	-0.7781	2.98	45.02E-3	17.16E-3
Average	-0.6974	-12.10	20.34E-3		Average	-0.5980	23.10	59.12E-3	22.05E-3	Average	-0.7805	-0.02	15.82E-3	-3.19E-3

Table 4 (contunued): Raw Data of Linear Polarization Using a Cylindrical Counter Electrode

A_{11} - A_{15} CONTROL (INHIBITOR Na)	B_{11} - B_{15} - 2% $NaNO_2$	C_{11} - C_{15} - 5% 3-5 DINITROBENZOIC ACID
A_{21} - A_{25} - 2% $CaCl_2$	B_{21} - B_{25} - 2% $NaNO_2$ +2% $CaCl_2$	C_{21} - C_{25} - 5% 3-5 DINITROBENZOIC ACID +2%$CaCl_2$
A_{31} - A_{35} - 4% $CaCl_2$	B_{31} - B_{35} - 2% $NaNO_2$ +4%$CaCl_2$	C_{31} - C_{35} - 5% 3-5 DINITROBENZOIC ACID +4%$CaCl_2$

SAMPLE	Ecorr AVG (V)	Icorr AVG µA /CM2	Icorr 28 cm2	SAMPLE	Ecorr AVG	Icorr AVG µA /CM2	Icorr 28 cm2	SAMPLE	Ecorr AVG	Icorr AVG µA /CM2	Icorr 28 cm2
A_{11-1} / A_{11-3}	-0.766	15.46	0.552	B_{11-1} / B_{11-3}	-0.4881	0.96	-0.034	C_{11-1} / C_{11-3}	-0.6899	4.66	0.166
A_{12-1} / A_{12-3}	-0.7295	2.79	0.099	B_{12-1} / B_{12-3}	-0.6055	0.38	-0.0136	C_{12-1} / C_{12-3}	-0.7645	12.66	0.0136
A_{13-1} / A_{13-3}	-0.6877	4.5	0.1607	B_{13-1} / B_{13-3}	-0.7351	4.91	0.1754	C_{13-1} / C_{13-3}	-0.7117	5.6	0.2
A_{14-1} / A_{14-3}	-0.7149	6.19	0.3211	B_{14-1} / B_{14-3}	-0.4888	1.12	0.04	C_{14-1} / C_{14-3}	-0.6916	3.29	0.1175
A_{15-1} / A_{15-3}	-0.7802	12.34	0.4407	B_{15-1} / B_{15-3}	-0.36	1.96	0.07	C_{15-1} / C_{15-3}	-0.6551	4.24	0.151
A_{21-1} / A_{21-3}	-0.735	12.09	0.4318	B_{21-1} / B_{21-3}	-0.6304	2.76	0.0986	C_{21-1} / C_{21-3}	-0.6398	4.34	0.155
A_{22-1} / A_{22-3}	-0.7741	10.91	0.3896	B_{22-1} / B_{22-3}	-0.8515	10.1	0.3607	C_{22-1} / C_{22-3}	-0.7882	11.16	0.399
A_{23-1} / A_{23-3}	-0.5591	4.05	0.1446	B_{23-1} / B_{23-3}	-0.759	3.43	0.1225	C_{23-1} / C_{23-3}	-0.7361	4.01	0.1432
A_{24-1} / A_{24-3}	-0.789	7.6	0.2714	B_{24-1} / B_{24-3}	-0.6191	17.87	-0.6382	C_{24-1} / C_{24-3}	-0.7623	13.03	0.4654
A_{25-1} / A_{25-3}	-0.7831	14.71	0.5253	B_{25-1} / B_{25-3}	-0.7634	6.36	0.2271	C_{25-1} / C_{25-3}	-0.7546	8.61	0.307
A_{31-1} / A_{31-3}	-0.3126	3.08	0.11	B_{31-1} / B_{31-3}	-0.6789	16.21	0.5789	C_{31-1} / C_{31-3}	-0.745	19.32	0.69
A_{32-1} / A_{32-3}	-0.7292	14.49	.-.5175	B_{32-1} / B_{32-3}	-0.7333	84.07	3.003	C_{32-1} / C_{32-3}	-0.7443	4.2	0.15
A_{33-1} / A_{33-3}	-0.7475	16.32	-0.583	B_{33-1} / B_{33-3}	-0.4277	1.11	0.0396	C_{33-1} / C_{33-3}	-0.7925	9.14	0.326
A_{34-1} / A_{34-3}	-0.8043	26.64	-0.951	B_{34-1} / B_{34-3}	-0.595	2.78	0.0992	C_{34-1} / C_{34-3}	-0.838	19.82	-0.708
A_{35-1} / A_{35-3}	-0.6889	3.26	-0.116	B_{35-1} / B_{35-3}	-0.8507	5.45	0.1946	C_{35-1} / C_{35-3}	-0.7767	3.08	0.11

Table 5: Summary of Linear Polarization Results Using a Cylindrical Counter Electrode

6.2. Impedance Behavior and Simulation of the Steel-Concrete Interface

The means and coefficient of variation were calculated for each series. The results were repeatable between tests on the same sample but the variation within a series was rather large. This was attributed to the use of a point counter electrode resulting in non-uniform current distribution.

The measurements were repeated to reduce the variations after storing the specimens in continuously aerated water and using a circular reference electrode as shown in Figure 29b. The results are given in Table 4 and a summary in Table 5. The variation of results between samples in some series is still rather large.

All the specimens in series A, B, and C were subjected to ACIS (Table 4) but only a restricted number of specimens, one from each group, was simulated to determine the various electrochemical properties. The specimen with the I corrosion closest to the mean value of the group was selected from each group. Experimental results obtained for some samples with extreme values of I_{corr} were also simulated and presented in Appendix B. The results of the mean specimen simulations are shown in Figures 31-33.

The impedance spectra obtained from the control concrete specimens (A series) and concrete specimens containing 5% sodium nitrite (B series) and dinitrobenzoic (C series) are shown in Figures 31-33, respectively. Data are presented in the plots of Real impedance vs. Imaginary impedance (Figures 31a&b-33a&b), and Bode plots, e.g. Phase angle vs. Log(frequency) (Figures 31c-33c) and Log(modulus) vs. Log(frequency) (Figures 31d-33d). Curves numbered 1, 2 , 3 correspond to chloride contents of 0, 2 and 4%. Examination of all the impedance spectra show the following common characteristics. Two partial arcs and an entire arc were observed in three frequency regions in the Real vs. Imaginary plots for all the concrete specimens. A tail of an arc depicted in the high frequency range (l00kHz and higher) was followed by a depressed arc at frequencies ranging from kHz to Hz. In the very low frequency region a large and incomplete arc corresponding to the surface corrosion process was observed. The regions corresponding to these three arcs can also be distinguished in the Bode plots where three peaks or partial

peaks of the phase angle shift were observed in the phase angle versus logarithmic frequency plots. Three slope changes in the logarithmic modulus, $|Z|$, versus logarithmic frequency plots were also observed.

The simulation results are given by the solid lines and shown in Figures 31-33. The enlarged Real versus Imaginary plots (Figures 31a-33b) are presented to show more clearly the fit of the simulation results. The Real versus Imaginary plot is not good enough to judge excellence of the simulation since the simulation of the high frequency portion can not be seen clearly. Therefore, presenting the simulation results in the Bode plot format is necessary. Excellent agreement between the cycles and solid line, especially in the log modulus $|Z|$ and phase angle versus log (frequency) plots, were obtained. This ensures the accuracy of the R_p and other R_c parameters (Figure 31-33).

The simulated Rc parameters are listed in Table 6.

Sampl	RC, Ω	CC, nF	1-α1	Ri, Ω	Ci, µF	1-α2	Rp, Ω	Cdl, m	1-α3
A14	315	2.03	0.95	243	146	0.47	6894	21.9	0.6
A22	190	4.55	0.99	139	135	0.57	3313	59.6	0.43
A32	110	1.24	1	156	649	0.37	1406	55.5	0.57
B15	500	7.41	0.8	320	148	0.43	11459	4.56	0.74
B22	275	1.62	0.99	368	150	0.49	3680	7.76	0.51
B35	150	4.14	1	224	165	0.52	6181	4.45	0.51
C13	247	36.2	0.8	242	116	0.54	8339	9.76	0.57
C25	130	7.9	1	440	180	0.4	5925	21.4	0.51
C33	80	0.96	1	264	349	0.36	1224	23	0.47

Table 6 - RC Parameters Determined from the Simulation

6.3. Characterization of the Steel/Concrete Interface

Concrete Matrix

The simulated R_c and C_c, values are plotted against the pre-mixed chloride content (Figures 34a-b). The values of concrete resistance, R_c, decrease with an increase of chloride content in the concrete mix as expected. However, the specimens containing sodium nitrite appear to have the largest concrete resistance values and those containing dinitrobenzoic acid smaller compared to the control samples, (Figure 34a). The acceleration effect of nitrite addition and retardation effect of dinitrobenzoic acid addition on cement hydration and concrete microstructural development may be the reason. The concrete matrix capacitance, C_c, is usually in the nF level depending on the liquid/solid geometric surface area and surface charge storage. It appears that the corrosion-inhibiting additives do not make a significant difference to the values of C_c which range between 0.9-9 nF except for C13. The a_1 values are close to unity as indicated in Table 6.

Interface Film

The observation of an interface film arc in all the experimental measurements suggest that all specimens have undergone a certain amount of steel corrosion. The simulated parameters, e.g., R_i, Ci and α_2 are plotted in Figure35a-c. Unlike R_c, the simulated Ri ranging from 150-450 Ohm does not decrease with the amount of pre-mixed chloride content. It is not clear what defines the interface film resistance, R_i. The parameter C_i does not appear to depend on chloride content except for specimens A32 and C33 which values are 649 and 349 μF respectively. The α_2 values vary from 0.36 to 0.57 indicating the presence of highly distorted arcs. This arc is meant to be an indicator of rebar corrosion. However, there is not a direct relation between this arc and the corrosion rate of the rebar. Use of this arc to represent the corrosion rate would not be accurate.

Steel Corrosion Process

C_{dl} and R_p can be evaluated using equivalent circuit simulation. The simulated parameters, e,g. Rp, C_{dl} and the a_3 are listed in Table 6 and plotted versus chloride content in Figures 36a-c. R_p decreases with an increase in the amount of pre-mixed chloride.

Large values of R_p were obtained from specimens containing sodium nitrite (except for specimen B22 which is considered to have undergone heavy corrosion since rust stains were observed on the top portion of the sample) and the control specimens appear to have small values. R_p is the most relevant parameter since it represents the corrosion resistance of the rebar and it can be used to evaluate the corrosion rate by applying the Stern-Geary equation. A large R_p represents a high corrosion resistance. The corrosion resistance of these specimens, with and without pre-mixed chlorides, appears to follow the sequence: nitrite>dinitrobenzoic acid >control. In contrast to R_p the double layer capacitance, C_{dl}, appears to increase with pre-mixed chloride content but the trend is not very clear. The control specimens, A14 and A32 have the largest C_{dl} values (21.9 and 55.5 mF). Specimens containing sodium nitrite have the lowest values (4.45 to7.76mF). With the geometrical area normalization the values of C_{dl} fall into the range of 159 $\mu F/cm^2$ to 1980 $\mu C/cm^2$ which are larger than the pure double layer capacitance ca. 40 $\mu F/cm^2$. The C_{dl} value here is not a pure double layer capacitor but the overall capacitance of a rough rebar surface with chemical adsorption species. It should also be noted that the values of $\alpha 3$ for all the specimens are larger than 0.4 except for B15 (which is 0.26). The value of $\alpha 3$ has been used to characterize the corrosion extent of the reinforcing steel qualitatively[97]. Insignificant corrosion is assumed when $\alpha 3 < 0.1$ and heavy corrosion when $\alpha_3 > 0.4$. This rule would indicate that severe corrosion has taken place in all these specimens.

6.4. Effectiveness of Corrosion Inhibitors

Sodium nitrite is a typical anodic corrosion inhibitor. It is thought that the nitrite ions compete with the chloride ions for ferrous ions and react with ferrous ions to produce ferric oxide:

$$2Fe^{2+} + 2OH^- + 2NO_2^- \Rightarrow 2NO\uparrow + Fe_2O_3 + H_2O$$

This reaction is more rapid than the transport of ferrous ions via chloride ion complex formation. Thus the nitrite ions aid in the production of the stable passive layer even in the presence of chloride ions. However, its full protection depends greatly on the concentration of aggressive ions such as chloride ion. Collins suggested a ratio of $Cl^-/NO_2 < 1.5$ for use in reinforced concrete [99]. An insufficient nitrite concentration has

bond with iron. This lowers the reactivity of iron atoms on the surface and facilitates passivation. The NO_2 group in dinitrobenzoic acid may provide additional protection but the effect is much more moderate than that of sodium nitrite. One of the drawbacks of this corrosion inhibitor is that it may have an adverse effect on concrete strength development.

Phase Angle Shift Characteristics

A decrease of the maximum phase angle shift of the steel surface kinetic arc has been used to describe the degree of surface corrosion of steel by Mansfeld. The decrease of phase angle shift was also observed in reinforced concrete specimens immersed in chloride solution. In this study, the maximum phase angle shift was obtained from simulation. The plot of phase angle shift versus chloride content is given in Figure 37, where specimens without premix chloride ions have the largest values of phase angle shift in the series. For example, the values of phase angle are 31.5, 44.8, and 32.9 degrees for specimens A14, B15 and C13 respectively. The B series (samples containing sodium nitrite) appear to have higher values of phase angle than control specimens and specimens containing dinitrobenzoic acid (except for specimen B22). The decrease of phase angle is attributed to the decrease of corrosion resistance of the rebar in concrete. This trend was obtained from both experiment and theoretical simulation but phase angle shift can not be used to distinguish between the effectiveness of the inhibitor.

6.5. Comparison of Linear Polarization and ACIS Results

For the ACIS specimens the corrosion rate was estimated through the polarization resistance, R_p, determined in the equivalent circuit simulation of the experimental spectra. Corrosion current density is calculated using the Stern-Geary equation expressed below:

$$I_{corr} = \frac{B}{R_p}$$

where B is a function of the anodic and cathodic Tafel Slopes β_a and β_c.

For the rebar corrosion, a B value of 33 or 50 mV has been utilized in the calculation. Comparison of corrosion current densities from the impedance spectra simulations and those determined by linear polarization measurements is illustrated on Fig. 38.

Figure 38a illustrates the corrosion current densities, calculated using B = 50 mV and R_p, obtained from the impedance spectra simulations, of all the reinforced concrete specimens containing pre-mixed chloride and corrosion inhibiting additives. It appears that the corrosion protection performance provided by sodium nitrite is better than that provided by dinitrobenzoic acid. These ASIS results were confirmed by the corrosion current densities determined by linear polarization measurement as indicated in Figure 38b. The corrosion current densities of the reinforced concrete specimens are in the order of : sodium nitrite < dinitrobenzoic acid< control in both cases with and without pre-mixed chlorides.

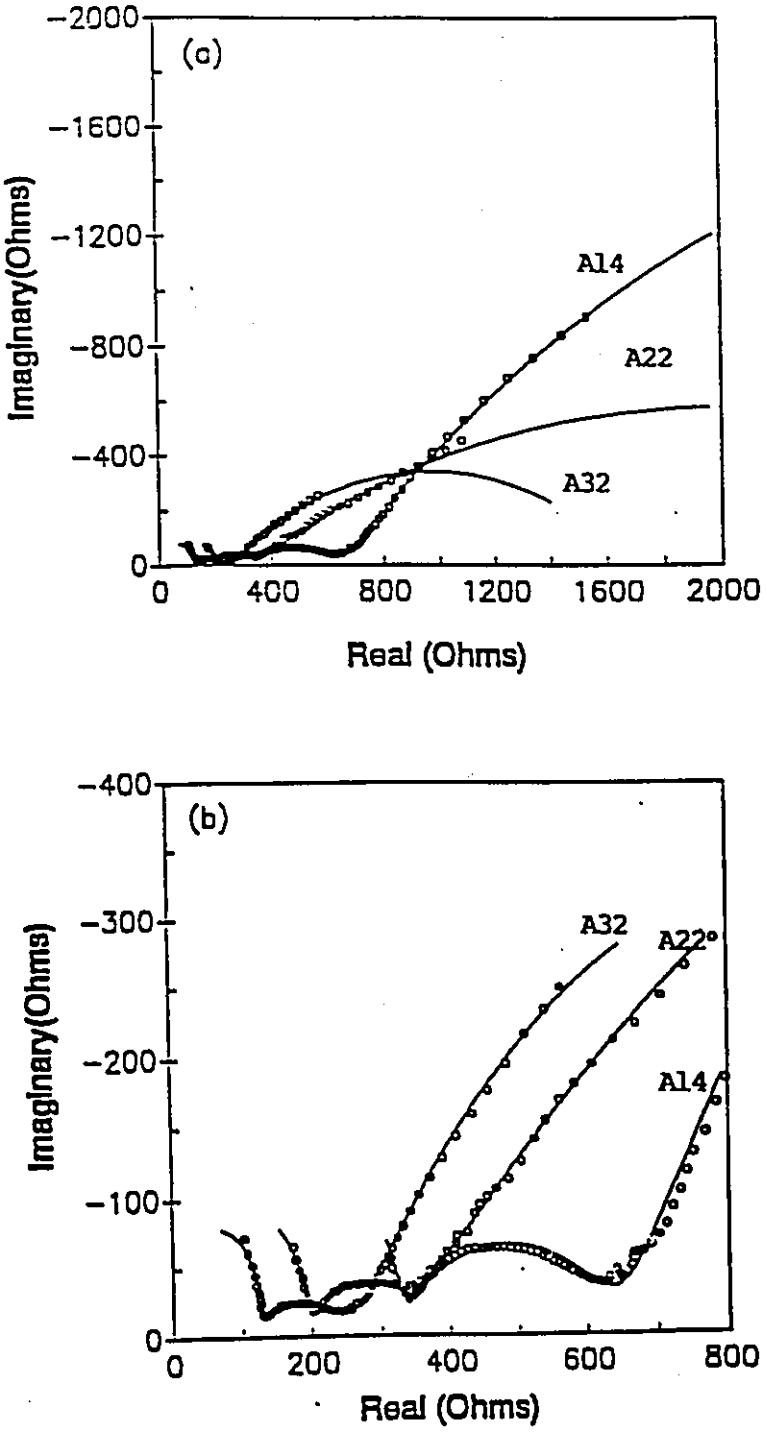

Fig. 31 a & b: Impedance spectra and simulation for the control reinforced concrete specimens. (a) real vs. imaginary Plot; (b) enlarged real vs. imaginary plot

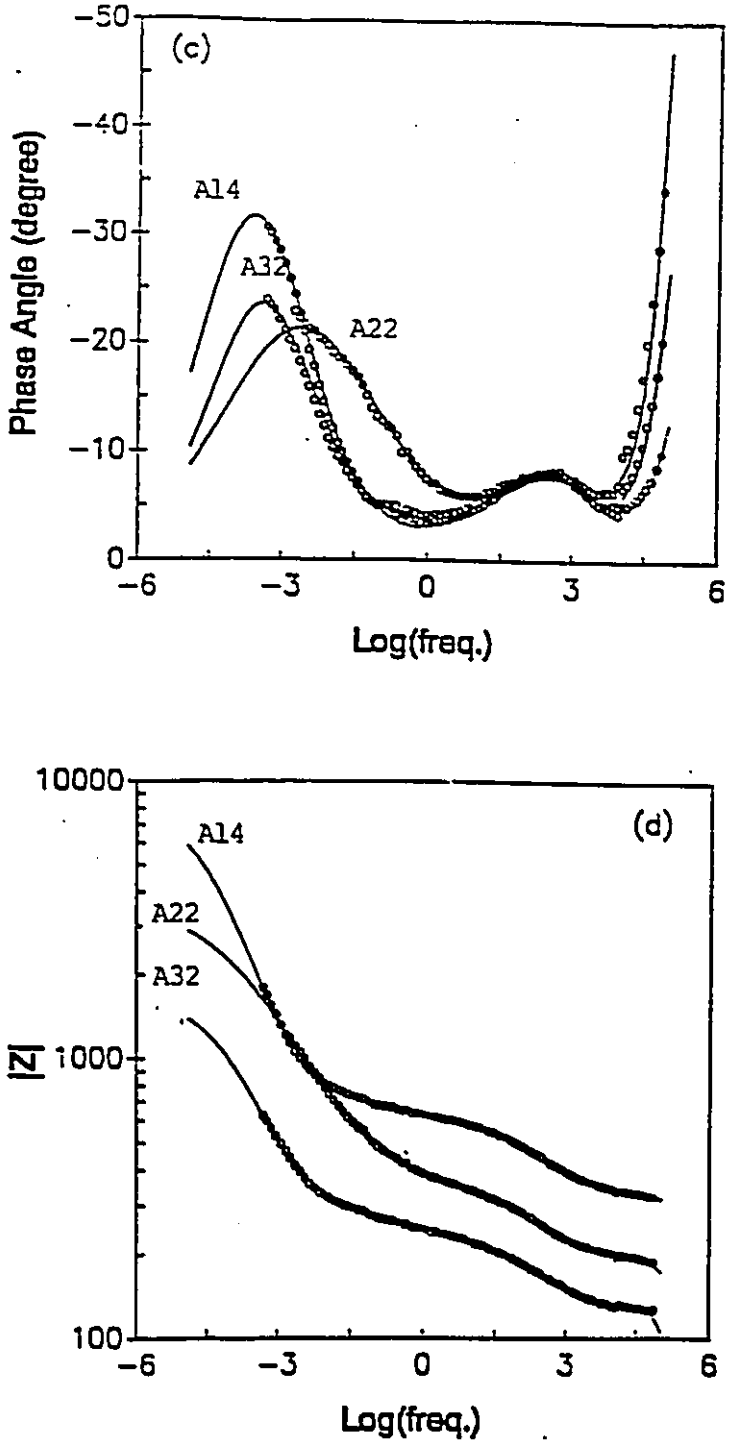

Fig. 31 c & d: Impedance spectra and simulation for the control reinforced concrete specimens. (c) phase angle vs. frequency plot and (d) modulus vs. frequency plot. Curves 1,2, and 3 correspond to the chloride contents of 0, 2 and 4%.

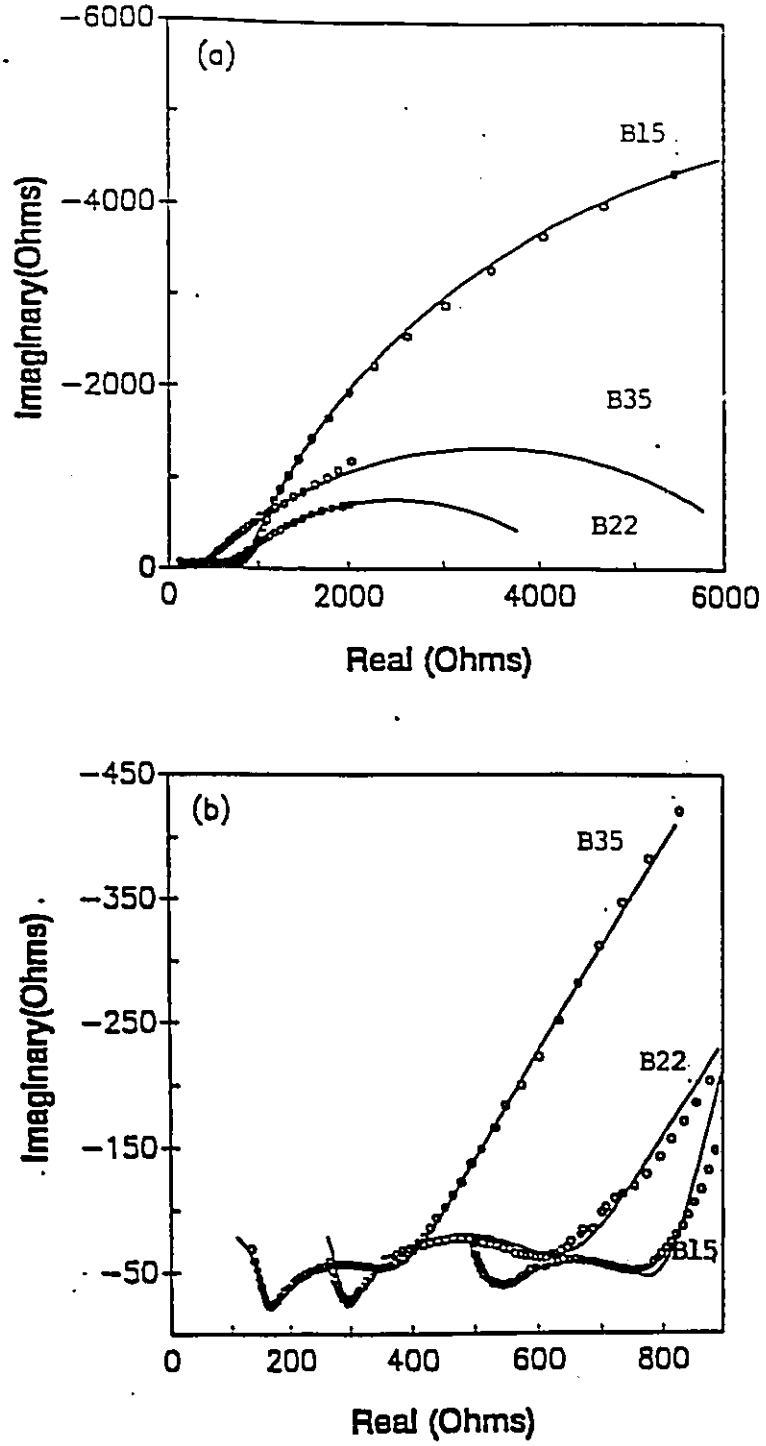

Fig. 32 a & b: Impedance spectra and simulation for the reinforced concrete specimens containing 5% sodium nitrite. (a) real vs. imaginary plot: (b) enlarged real vs. imaginary plot

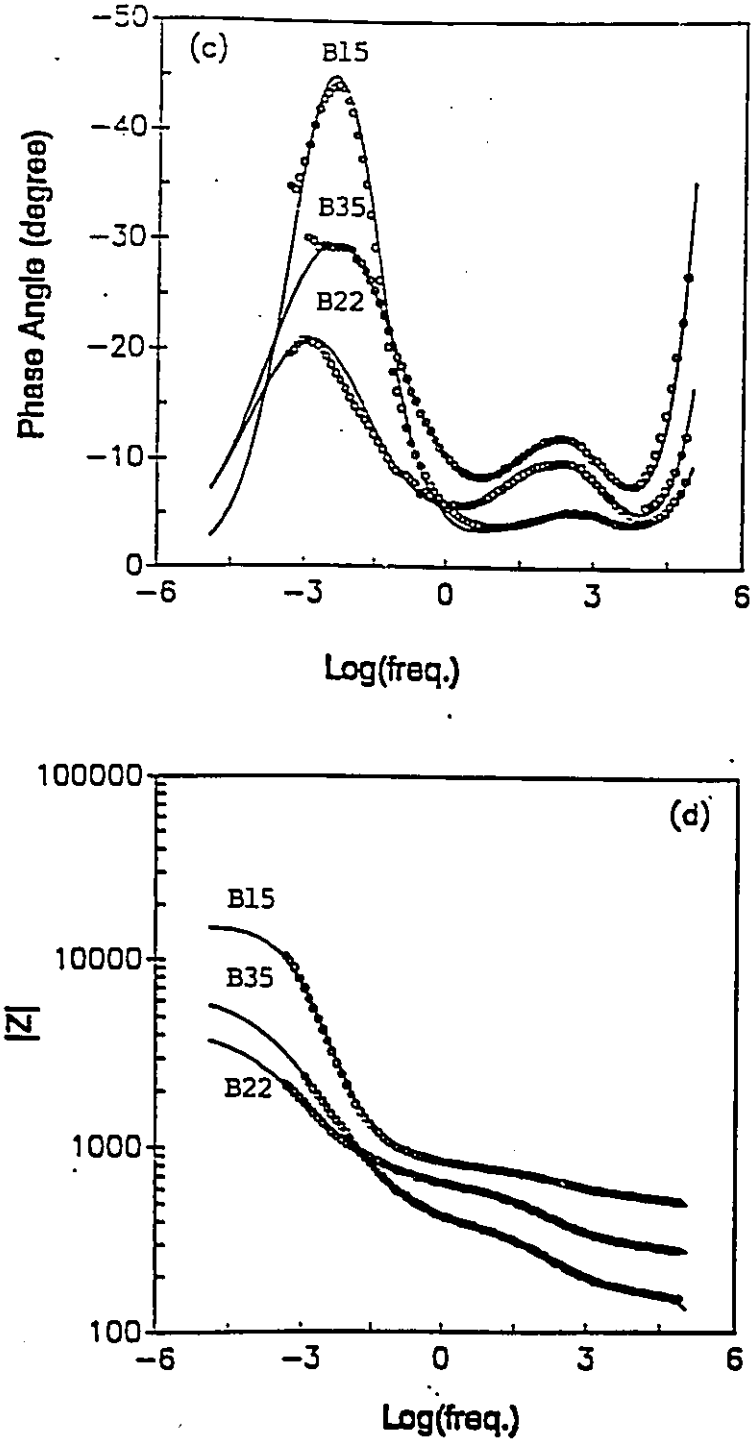

Fig. 32 c & d: Impedance spectra and simulation for the reinforced concrete specimens containing 5% sodium nitrite. (c) phase angle vs. frequency plot and (d) modulus vs. frequency plot

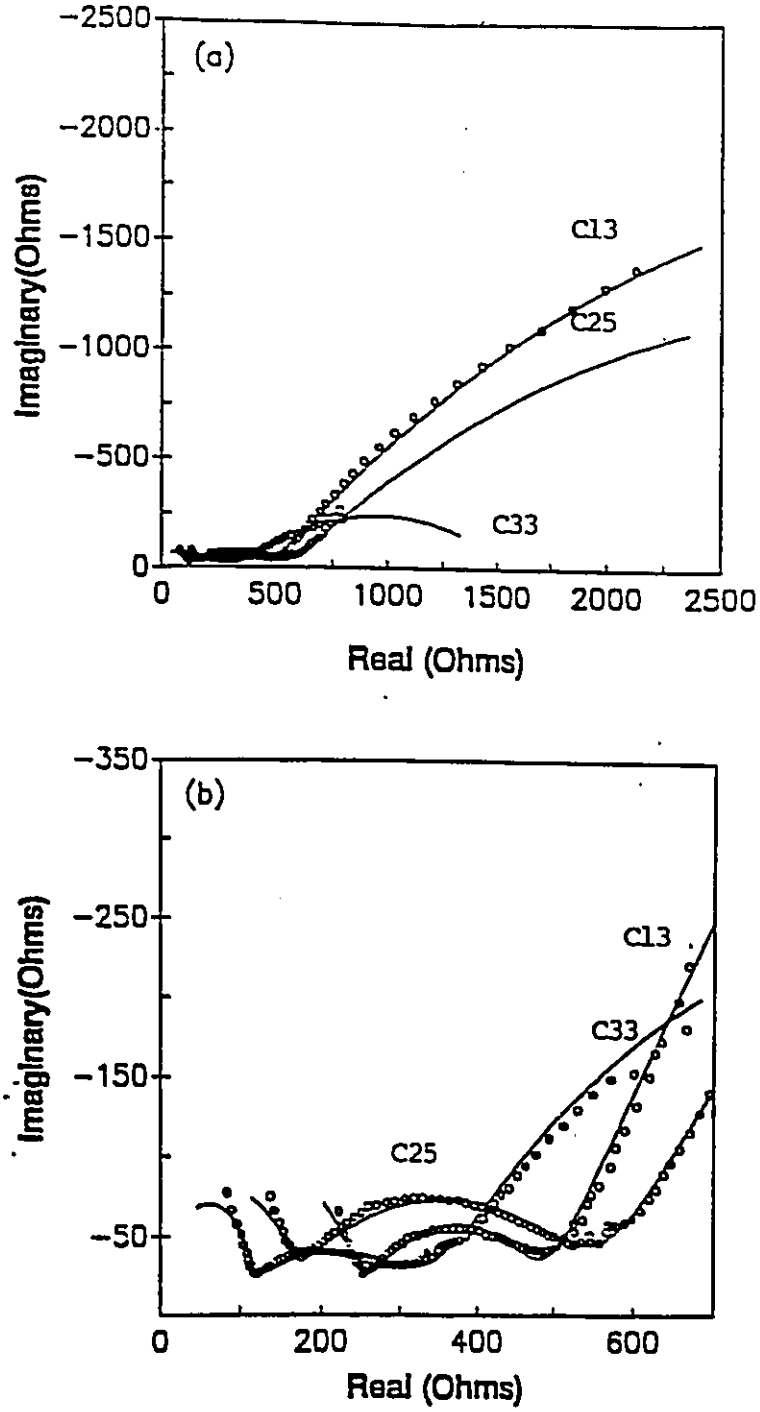

Fig. 33 a & b: Impedance spectra and simulation for the reinforced concrete specimens containing 5% dinitrobenzoic acid. (a) real vs. imaginary plot; (b) enlarged real vs. imaginary plot. Curves 1, 2 and 3 correspond to the chloride contents of 0, 2 and 4 %.

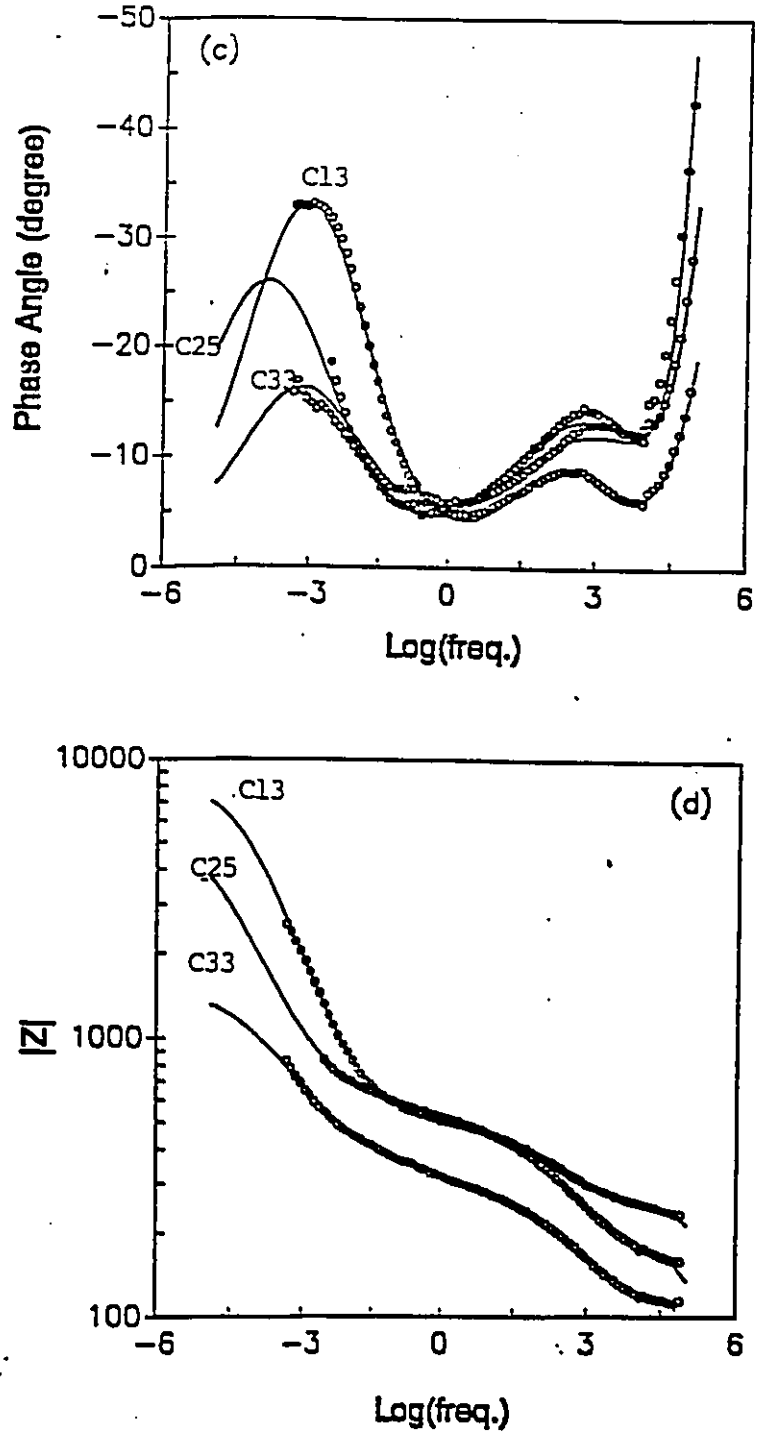

Fig. 33 c & d: Impedance spectra and simulation for the reinforced concrete specimens containing 5% dinitrobenzoic acid. (c) phase angle vs. frequency plot and (d) modulus vs. frequency plot.

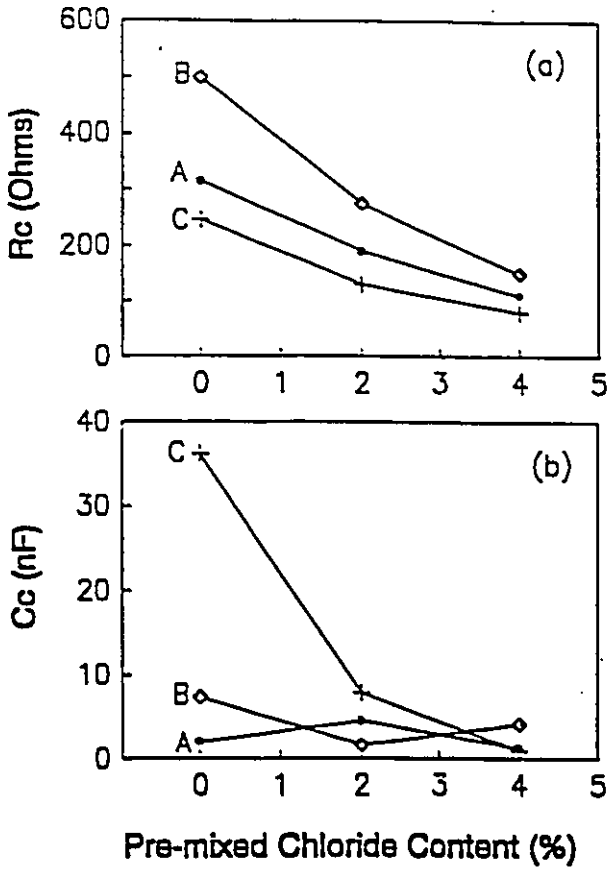

Fig. 34 a & b: (a) Plot of the R_C vs. percentage of pre-mixed chlorides and (b) C_C vs. percentage of pre-mixed chlorides.

Symbols represent: A - Control concrete; B - Concrete containing 5% sodium nitrite; and C - Concrete containing 5% dinitrobenzoic acid.

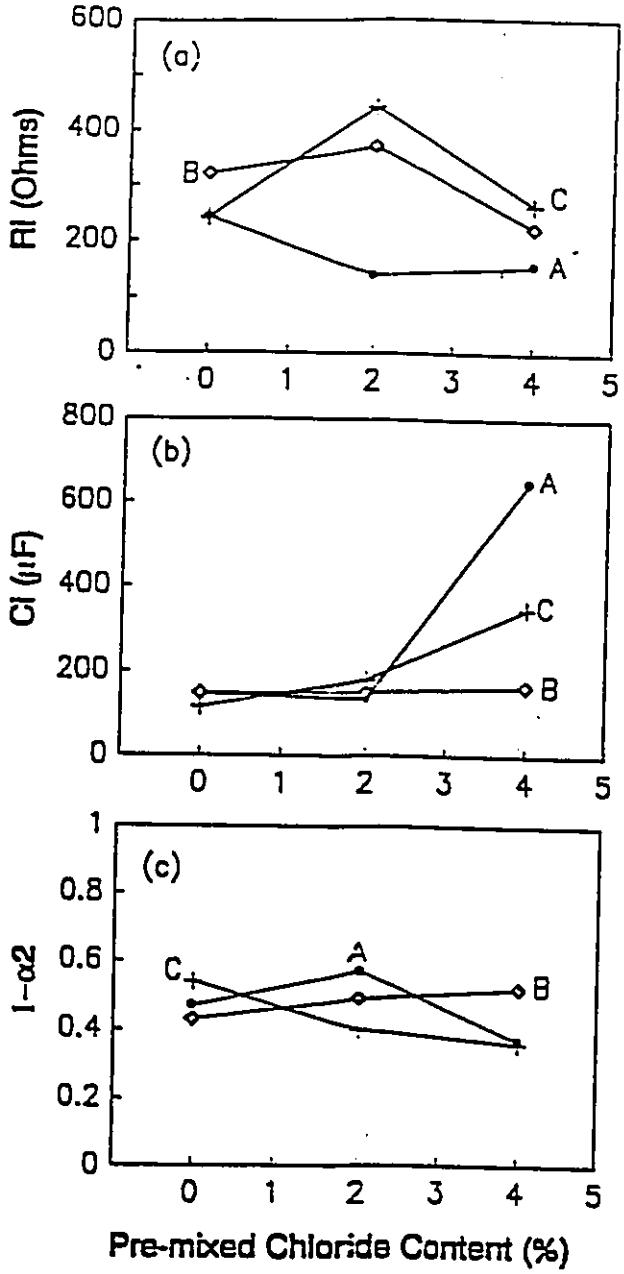

Fig. 35 a -c: (a) plot of the R_i vs. percentage of pre-mixed chlorides; (b) C_i vs. percentage of pre-mixed chlorides. Symbols represent: (A-) Control concrete; (B-) Concrete containing 5% sodium nitrite; and (C-) concrete containing 5% dinitrobenzoic acid

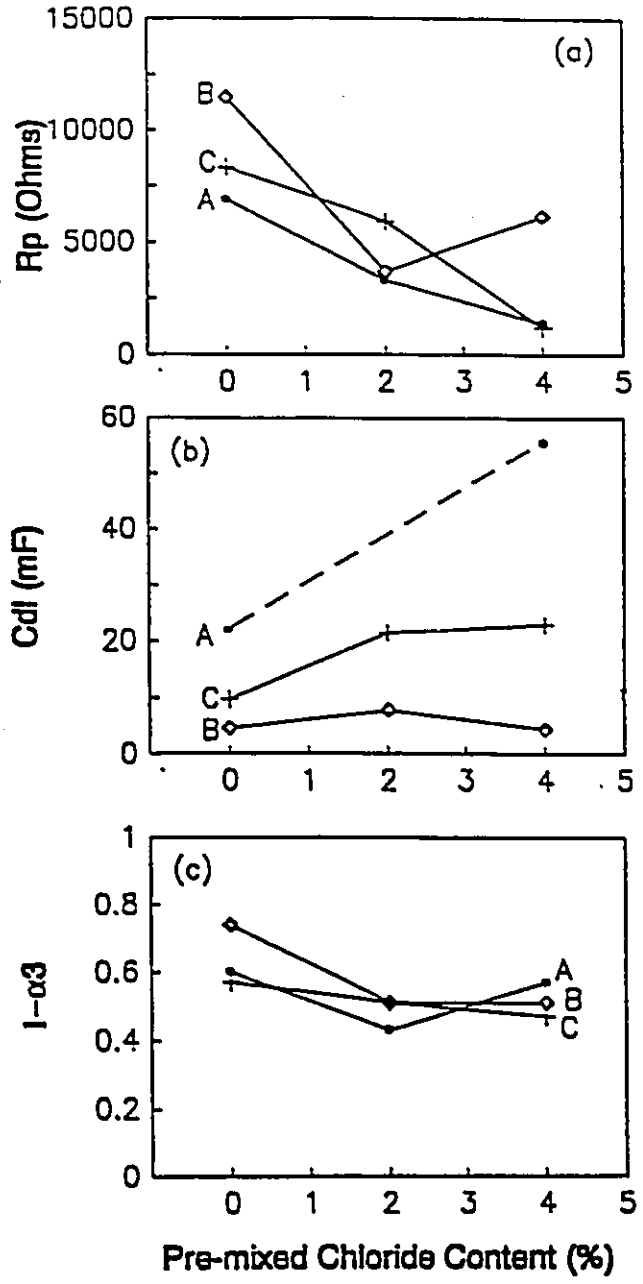

Fig. 36 a-c: (a) Plot of the R_p vs. percentage of pre-mixed chlorides; (b) C_{dl} vs. percentage of pre-mixed chlorides and (c) 1 - α_3 vs. percentage of pre-mixed chlorides. Symbols represent: (A-) Control concrete; (B-) Concrete containing 5% sodium nitrite; and (C-) Concrete containing 5% dinitrobenzoic acid.

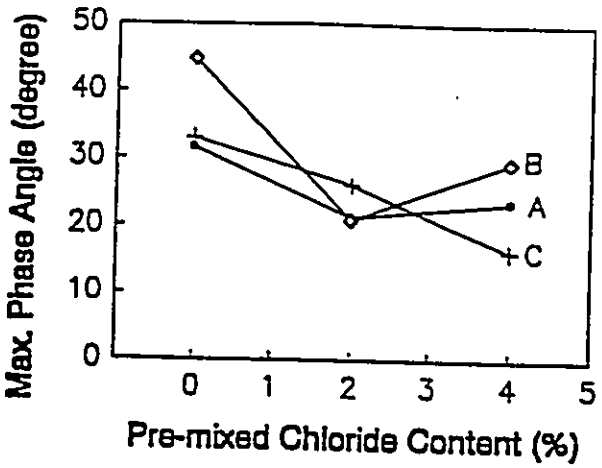

Fig. 37: (a) Plot of maximum phase angle shift vs. percentage of pre-mixed chlorides. Symbols represent: (A-) Control concrete; (B-) Concrete containing 5% sodium nitrite; and (C-) Concrete containing 5% dinitrobenzoic acid.

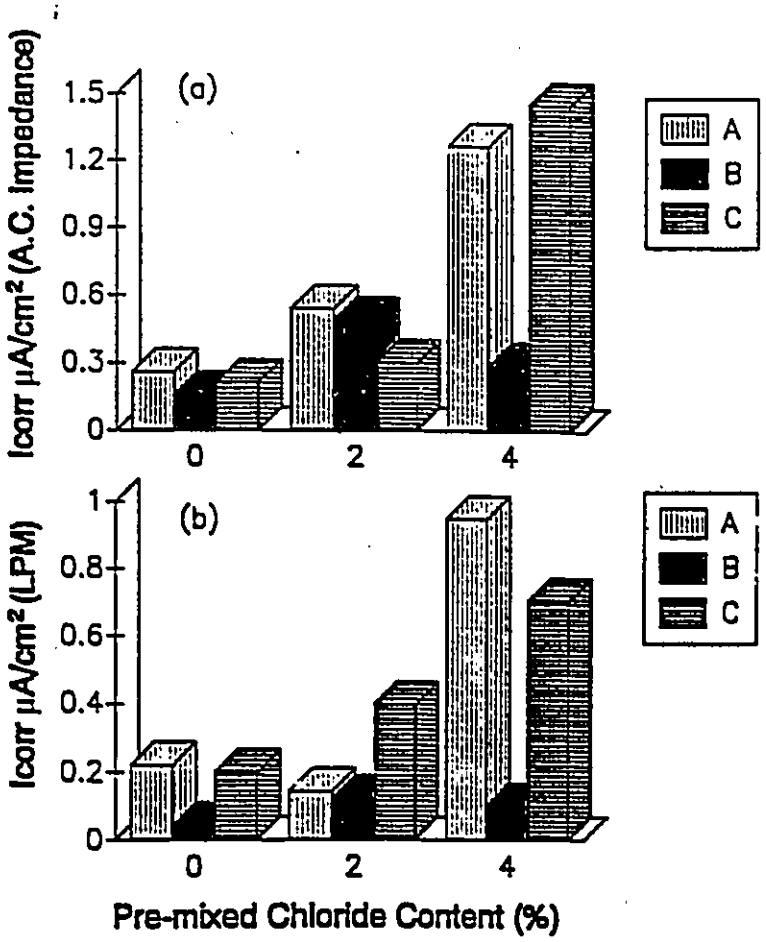

Fig. 38: Plot of corrosion current densities vs. percentage of pre-mixed chlorides. (a) corrosion current densities were calculated using Stern-Geary equation with B=50 mV and R_p obtained from the impedance spectra simulations; (b) corrosion current densities were determined by linear polarization measurements.

A - control samples

B - 2% $NaNO_2$ + 0, 2, 4% $CaCl_2$

C - 5% 3-5, Dinitrobenzoic acid

Chapter 7

7. Conclusions and Recommendations

The effectiveness of Sodium nitrite and dinitrobenzoic acid as corrosion inhibitors for reinforcing steel in 5 year old chloride contaminated concrete was investigated using linear polarization and AC impedance spectroscopy.

The linear polarization results are somewhat unreliable as shown by the large coefficients of variation within a sample set.

AC impedance spectroscopy was used to measure the impedance in a range of frequencies. Equivalent circuit models have to be used to interpret the impedance spectra. The RC parameters obtained from impedance simulation including the maximum phase angle shift and polarization resistance can be used to characterize the degree of rebar corrosion and evaluate the effectiveness of corrosion-inhibiting additives with and without the presence of pre-mixed chlorides. The distinct advantage of this method is its non-destructive characteristic. No polarization potential is applied. Possible damage of the steel-cement paste or concrete interface is avoided.

The extent of surface corrosion of the reinforcing steel is qualitatively described by the impedance data such as Real, Imaginary, phase angle shift, surface impedance and capacitive response with corrosion time. The phase angle shift in the low frequency region is believed to be sensitive to the surface corrosion of the reinforcing steel induced by chloride ion.

The results show that the corrosion protection performance provided by sodium nitrite is better than that provided by dinitrobenzoic acid. The corrosion current densities of the reinforced concrete specimens are in the order of : sodium nitrite<dinitrobenzoic acid< control in both cases with and without pre-mixed chlorides.

To understand which corrosion inhibition system performs the best it would be desirable to perform linear polarization tests with updated software using the current interrupt technique. It would also be desirable to perform a.c. impedance tests on more specimens. One reason this was not done in the current study was due to time constraints as each test takes approximately three hours.

The a.c. impedance measurement in the low frequency region gives information related to surface corrosion occurring in reinforced concrete. The rebar corrosion rate can be estimated through the equivalent circuit model simulation analysis. The results indicated that sodium nitrite is significantly more effective than dinitrobenzoic acid in inhibiting corrosion of reinforcing steel in concrete.

Needed Work

Future work should include investigation of performance durability of each selected corrosion-inhibiting admixture. The remaining concentration of the inhibitors should be analyzed subjecting the specimens to different aggressive environments and carrying out concentration analysis at different maturity levels of the concrete at 7, 28 days, 6 months, 1.5 years, 5 years.

The analysis procedure includes:

-preparation of concrete slices: a concrete cylinder at a selected maturity level will be cut into slices (thickness 12mm)

-extraction of inhibitor: concrete slices will be crushed to powder form and solvent will be used to extract the inhibitor (For example, a distilled water-based solution will be used for extraction of nitrite-based inhibitor)

-concentration analysis: the extracted solution will be subjected to test methods-potential cyclic-voltammetry, A.C. impedance spectroscopy , etc.

The remaining concentration of each inhibitor can be determined by comparing the calibration curves. Plots of concentration vs depth and hydration can be constructed.

NOTATION

COMMONLY USED ABBREVIATIONS

Å- angstrom (unit of wavelength measure)

ac- alternating current

atm- atmosphere

ca.- approximately

cm^2- square centimeter

E- electrode potential

emf- electromotive force

etc.- and so forth

eV- electronvolt

F- rictional loss

g- gram

h- Planck's constant

Hz- hertz(formerly cycles per second, cps)

K- Kelvin

kg- kilogram

kWh- kilowatt-hour

l- length

log- logarithm

m- meter

m^3- cubic meter

mg- milligram

mL- milliliter

mm^2- square millimeter

N- normality, as l*N*

oz- ounce

Q- energy of nuclear reaction

abs- absolute

A- ampere

°C- degree Celsius

cm- centimeter

cm^3- cubic centimeter

e.g.- example

esu- electrostatic unit

et seq.- and the following

°F- degree Fahrenheit

f- frequency

g •cal -gram-calorie

h- hour

I- electric current

kcal- kilogram-calorie

kW- kilowatt

L- liter

ln- natural logarithm

M- molecular weight;mass

m^2- square meter

MeV- million (or mega-)electronvolt

min- minute

mm- millimeter

mm^3- cubic millimeter

n- index of refraction

ppt- precipitate

satd- saturated

s- second

soln- solution

sq- square

t- time

W- watt

μ-micro- (10^{-6})

B- Stearn Geary factor

D- Diffusion coefficient

E_{corr}- Corrosion potential

F- Faraday constant

R- Gas constant

i_{corr}- Corrosion current density

R_{me}- Resistance of metal dissolution

R_p- polarization resistance

sin- sine

sp- specific

T- temperature

V- volt

Wh- watt-hour

μm- micrometer (micron)

C- Cathode capacitance

E- Electrical potential

E_H- Electrode potential *vs.* NHE

i^{+}_{Me}- Anodic current density of Me dissolution

Nomenclature and Conventions

There is a singular lack of agreement in nomenclature and sign conventions in the various electrochemical journals, texts, and reference works. Although a partial agreement was established by the IUPAC Stockholm Convention, older customs still persist in the literature. Various terms and conventions are operationally defined below as they are used in this work.

Electrode - a conductor at which the species of a redox system may be on equilibrium. Selected electrode systems are given in Table 7.

Anode - electrode at which an oxidation occurs.

cathode - electrode at which a reduction occurs.

Indicator electrode - an electrode whose potential changes during an experiment because of a change in the concentration of a reactant or product of an electrochemical reaction. An example is the change in the potential of a silver wire electrode during the titration of a halogen with silver nitrate. The Ag^+ - Ag(s) redox couple establishes the electrode potential. The electrode potential can be given by the Nernst equation. At 25°C, this is

$$E_{electrode} = E^\circ_{electrode} + 0.05916 \log [Ag^+]$$

Strictly speaking the activity of Ag^+ should be used instead of the concentration, E° is the standard electrode potential. Unless furthur qualified, numerical values of electrode potentials are assumed to be those observed at the standard temperature of 25°C.

Electrode potential - the potential difference between one electrode system and another system used as a reference

Table 7 - Selected Electrode Systems

System	Standard Electrode Potential Standard Reduction EMF E °, V Versus NHE	Example Electroanalytical Application
$MnO_4^- + 8H^+ + 5e^- = Mn^{2+} + 4H_2O$	+1.51	Redox titration
$Br_2(aq) + 2e^- = 2Br^-$	+1.087	Coulometric titration
$VO_2^+ + 2H^+ + e^- = VO^{2+} + H_2O$	+1.000	Polarography
$Ag^+ + e^- = Ag(s)$	+0.7995	Precipitation titration
$Fe^{3+} + e^- = Fe^{2+}$	+0.771	Redox titration
$C_6H_4O_2(s) + 2H^+ + 2e^- = C_6H_4O_2H_2(s)$	+0.6994	Acid- base titration (quinhydrone electrode)
$I_2(aq) + 2e^- = 2I^-$	+0.620	Redox titration
$H_3AsO_4 + 2H^+ + 2e^- = HAsO_2 + 2H_2O$	+0.559	Direct coulometry
$UO_2^{2+} + 4H^+ + 2e^- = U^{4+} + 2H_2O$	+0.334	Direct coulometry
$Hg_2Cl_2(s) + 2e^- = 2Hg(l) + 2Cl^-(sat'd)$	+0.242	Reference electrode (SCE)
$AgCl(s) + e^- = Ag(s) + Cl^-$	+0.197	Reference electrode, precipitation titration
$H^+ + e^- = ½ H_2(g)$	0.000	Reference electrode, (normal hydrogen electrode), acid-base titration
$Pb^{2+} + 2e^- = Pb(s)$	-0.126	Amperometric titration polarography
$Ni^{2+} + 2e^- = Ni(s)$	-0.24	Polarography
$Cd^{2+} + 2e^- = Cd(s)$	-0.403	Anodic stripping
$Zn^{2+} + 2e^- = Zn(s)$	-0.763	Electrogravimetry
$Sn^{4+} + 2e^- = Sn^{2+}$	-1.90	Coulometric titration

Reference electrode - an electrode system used as a reference point in electrochemical potential measurements. A very common reference electrode is the saturated calomel system generally known as the saturated calomel electrode (SCE)

$$Hg_2Cl_2(s) + 2e^- = 2Hg(l) + 2Cl^-$$

for which the Nernst equation is:

$$E_{Hg_2Cl_2(s),\ Hg\ (l)} = E^{\circ}_{Hg_2cl_2(s),\ Hg(l)} + 0.05916 \log \frac{1}{[Cl^-]^2}$$

If, during an isothermal experiment, the concentration of chloride ion in equilibrium with mercury metal and solid mercurous chloride (calomel) remains constant, the lectrode potential does not change.

In most electroanalytical analyses, temperature control of ± 0.25°C and the use of analytical reagents without further purification is satisfactory for preparing reference electrode systems.

Electromotive force (emf) - the driving force of a reaction expressed in electrical units. The emf of a cell is a measurable qunatity, simply the difference in potential between two wires of the same material attached to the two electrodes. The emf of a half-reation is a defined quantity.

Oxidation potential - the emf of a half-reaction written as an oxidation. (This is the sense in which Latimer uses the term.)

Reduction Potential - the emf of a half-reaction written as a reduction.

There is considerable confusion in the terms and sybology of electrode potentials, and the oxidation or reduction potentials. The potential of an actual electrode is an observed physical quantity; it is distinctly different from the latter two quantities, which are, in fact, defined quantities.

According to the IUPAC Stockholm Convention, an electrode potential is defined as the potential difference between the electrode in question and the normal hydrogen electrode. Although two totally different concepts are involved, the numerical value of the

standard electrode potential is identical to that of the emf of the redox couple written as a reduction and is opposite in sign to the emf of the same couple written as an oxidation.

It would be better if there were a more generally accepted agreement on the usage of all these terms. Unfortunately, this is not the case. In fact the symbol, E, is used for both an emf and for an electrode potential. For example, take the silver-silver ion system:

$Ag(s) = Ag^+ + e^-$

$E^\circ_{Ag(s),\,Ag^+} = -0.7995$ V This can be either a standard oxidation emf or a standard oxidation potential

Reduction half-reaction:

$Ag^+ + e^- = Ag(s)$

$E^\circ_{Ag^+,\,Ag(s)} = +0.7995$ V This can be either a standard reduction emf or a standard reduction potential

Standard electrode potential:

$$E^\circ_{Ag^+,\,Ag(s)} = +0.7995 \text{ V}$$

The symbol $E^\circ_{Ag^+,\,Ag(s)}$ is hence used for both the standard electrode potential and the standard reduction emf.

REFERENCES:

[1] Strategic Highway Research Program, Participant Workbook-National Workshop, Strategic Highway Research Program: Washington, DC, Sept 1985, p.TRA 4-1

[2] Strategic Highway Research Plans, Final Report, Technical Research Areas 43, TRA 4-1 - TRA 4-60, May 1986.

[3] Focus, Special Edition, Strategic Highway Research Program, Washington, DC, 18-20 Sept 1985.

[4] V.S. Ramachandran, and R.F. Feldman, in "Concrete Admixtures Handbook: Properties, Science and Technology", Ed. by V.S. Ramachandran, Noyes Publications, New Jersey, USA, Chapter 1, pp10-16, 1984.

[5] P. K. Mehta, "Concrete Structure, Properties and Materials", Prentice-Hall, Inc., Englewood Cliffs, New Jersey, Chapter 6, pp.170, 1984

[6] N.R. Buenfeld, J.B. Newman, "The Permeability of Concrete in a Marine Environment", Mag. Concr. Res., 36, 67-80 (1984).

[7]R. S. Barneyback, Jr. and S. Diamond, "Expression and Analysis of Pore Fluids from Hardened Cement Pastes and Mortars," Cem. Concr. Res., 11, 279-85 (1981).

[8]K. Byfors, C. M. Hansson, and J. Tritthart, "Pore Solution Expression as a Method to Determine the Influence of Mineral Additives on Chloride Binding," Cem. Concr.Res., 16, 760-70 (1986).

[9]C. L. Page and Ø. Vennesland, "Pore Solution Composition and Chloride Capacity of Silica-Fume Cement Pastes," Materiaux Construct., 16 [91] 19-25 (1983).

[10] C. M. Hansson, J. B. Markussen, and T. Frolund, "The Effect of Chloride Cation, Type on the Corrosion of Steel in Concrete by Chloride Salts," Cem. Concr. Res., 15 65-73 (1985).

[11]S. Diamond, "A Critical Comparison of Mercury Porosimetry and Capillary Condensation Pore Size Distributions of Portland Cement Pastes," Cem. Concr. Res., 1, 531-45 (1971).

[12]D. Pearson, A. J. Allan, C. G. Windsor, M. McN. Alford, and D. D. Double, "An Investigation of the Nature of Porosity in Hardened Cement Pastes using Small Angle Neutron Scattering," J Mater. Sci., 181, 430-38 (1983).

[13]D. H. Bager and E. J. Sellevold, "Ice Formation in Hardened Cement Paste, Part II-Drying and Resaturation on Room Temperaturc Cured Pastes," Cem. Concr. Res., 16, 835-44 (1986).

[14] C. le Sage de Fontenay and E. J. Sellevold; p. 425 in Durability of Building Materials and Components. STP 691. ASTM, Philadelphia, 1980.

[15]C. L. Page, "Microstructural Features of Interfaces in Fibre Cement," pp. 140-44 (April 1982). Composites.

[16]P.D. Cady and E.J. Cannon, "Condition Evaluation of Concrete Bridges Relative to Reinforcement Corrosion, Vloume 1:State of the Art of Existing Methods", National Research Council, Washington DC, SHRP 5-330, 1992.

[17]M. Pourbaix, Atlas of Electrochemical Equilibrium in Aqueous Solutions. Pergamon, London, 1976.

[18] C. L. Page, N. R. Page, and A. El Tarras, "Diffusion of Chloride Ions in Hardened Cement Paste," Cem. Concr. Res., 11, 395 (1981).

[19]M.G. Fontana, "Corrosion Engineering" Third edition, McGraw-Hill Book Company, U.S.A. 1986, pp 445-504

[20]C. M. Preece, F. O. Gronvold, and T. Frolund, "The Influence of Cement Type on the Electrochemical Behaviour of Steel in Concrete"; pp. 393-406 in Corrosion of Reinforcement in Concrete Construction. Edited by A. P. Crane. Ellis Horwood Ltd., Chichester, UK, 1983.

[21]A. Rosenberg, C.H. Hansson and C. Andrade "Mechanisms of Corrosion of Steel in Concrete", in Materials Science of Concrete I edited by J. Skalny, The American Ceramic Society, Inc., 1989, pp285-313.

[22]J. Tafel, Z. Physik. Chem., 50, 641 (1904).

[23]M. Stearn and A.L Geary, "EIectrochemical Polarization No,1: Theoretical Analysis of the Shape of Polarization Curves," J. Electrochem. Soc., 104 [1] 56-63 (1957).

[24]C. M. Hansson, H. Strunge, J. B. Markussen, and T. Frolund, "The Effect of Cement Type on the Diffusion of Chloride"; Paper No. 6 in Nordic Concrete Research, Publication No. 4 (1935).

[25] A. Nielsen, "Durability"; pp. 200-43 in Beton Bogen (The Concrete Book). Edited by Aa. D. Herholdt, Chr. F. P. Justesen, P. Nepper-Christensen, and A. Nielsen. Aalborg, Portland, 1985.

[26] A. M. Rosenberg, J. M. Gaidis, T. G. Kossivas, and R.W. Previte, "A Corrosion Inhibitor Formulated with Calcium Nitrite for Use in Reinforced Concrete"; pp.89-99 in Chloride Corrosion of Steel in Concrete. STP-629. ASTM, Philadelphia, 1977.

[27] M. Venuat, "Relationship Between Concrete Carbonation and the Corrosion of Reinforcement," Recentres CEFRACOR-77, JTBTP, October 1977.

[28] J.A. Gonzales, S. Algaba, and C. Andrade, "Corrosion of Reinforcing Bars in Carbonated Concrete," Br. Corr. J., 3, 135-39 (1980).

[29]C. Andrade, C. Alonso, P. Santos, and A. Macias, "Corrosion Behaviour of Steel During Accelerated Carbonation in Solutions Which Simulate the Concrete Pore Solution"; pp. 256-62 in 8th International Congress of Cement Chemistry, Rio de ,Janeiro, Brazil, Theme 4, 1986.

[30]C. Alonso and C. Andrade, "Effect of Cement Type and Mortar Composition on the Corrosion Rate of Bars Embedded in Carbonated Mortar," Materiales de Construccin, 37 [205] 5-15 (1987).

[31]A.W. Beeby, "Cracking, Cover and Corrosion of Reinforcement," Concr. Int., pp. 35-40 (February 1983).

[32]P. Schiessel, "Relation Between the Crack Width and the Amount of Corrosion at the Reinforcement," Betonwerk + Festigkeit-Technik, 2, 594-98 (1975).

[33] H. Woods, "Durability of Concrete Construction," p.102 in ACI Monograph No.4. American Concrete Institute/Iowa State University Press, Detroit, 1968.

[34]W.F. Perenchio, "Corrosion of Reinforcing Steel, in Concrete and Concrete Making Materials" - ASTM STP 169C, Edited by Paul Klieger and J.F. Lamond, ASTM, Philadelphia, 164-172 (1994).

[35]Griffin, D. F., "Corrosion Inhibitors for Reinforced Concrete," in Corrosion of Metals in Concrete, ACI SP-49. American Concrete Institute, Detroit, MI: (1975), p.95.

[36]Craig, R. J. and Wood, L.E., "Effectiveness of Corrosion Inhibitors and Their Influence on the Physical Properties of Portland Cement Mortars," Highway Research Record, No. 328, 1970, p.77.

[37]Treadaway, K. W. J. and Russell, A. D., Highways and Public Works, 36, September,1968, p. 40.

[38] Slater, John E., Corrosion of Metals in Association with Concrete, STP 818, American Society for Testing and Materials, Philadelphia, PA: (1983), p.53

[39]Berke, N. S., "Corrosion Inhibitors in Concrete," Concrete International, V. 13, July 1991.

[40]Berke, N. S., "Corrosion Inhibitors in Concrete," Corrosion/89 Paper No. 445, National Association of Corrosion Engineers, Houston, TX (1989), 10 pp.

[41]Treadaway, K.W. J., The Corrosion of Steel in Alkaline Chloride Solutions, D.Sc. Thesis University of Galford, April 1966.

[42]Arup, H., "The Mechanisms of the Protection of Steel by Concrete," in Corrosion of Reinforcement in Concrete Construction, A. P. Crane, ed., Elliss Horwood LTD., Chichester, England: (1983), p. 151.

[43]Arber, M. G. and Vivian, H.E., Australian J. Applied Science, 12, 1961, p.339.

[44]Hope, B. B. and Ip, K.C., Corrosion Inhibitors for Use in Concrete", ACI Materials Journal, November-December 1989, pp. 602-608.

[45]Rosenberg, A. M., Gaidis. J.M., Kossivas, T.G. and Previte, R.W., "A Corrosion Inhibitor Formulated with Calcium Nitrite for Use in Reinforced Concrete," ASTM STP No. 629, ASTM: Philadelphia (1977), p. 89.

[46]Berke, N. S., Pfeifer, D.E. and Weil,T.G., "Protection Against Chloride Induced Corrosion-A Review of Data and Economics on silica fume and Calcium Nitrite," Concrete International, December 1988.

[47]Berke, N.S. and Roberts, L.R.R., "Use of Concrete Admixtures to Provide Long-Term Durability from Steel Corrosion, Superplasticizers and Other Chemical Admixtures in Concrete, ACI SP 119, Malhotra, V. M., Ed., American Concrete Institute, 1989, pp. 383-403.

[48]Berke, N. S. and Sundberg, K. M., Corrosion/89 Paper No. 386, National Association of Corrosion Engineers, Houston, TX (I989), 14 pp.

[49]Gaidis, J. M. and Lundquist, J. T., and Rosenberg, A. M., Materials Perf., 18, 3, 1979, p.36.

[50]Gaidis, J. M. and Rosenberg, A. M., Materials Perf., 18, 11, 1979, p.45.

[51]Berke, N. S., "The Use of Anodic Polarization to Determine the Effectiveness of Calcium Nitrite as an Anodic Inhibitor," Corrosion Effect of Stray Currents and the Techniques for Evaluating Corrosion of Rebars in Concrete, ASTM STP-906, V. Chaker, ed., ASTM, Philadelphia: (1986), p. 78.

[52]Virmani, Y. P., Clear, K. C., and Pasko, T. J., "Time-to-Corrosion of Reinforcing Steel in Concrete Slabs, Vol. 5-Calcium Nitrite Admixture and Epoxy-Coated Reinforcing Bars as Corrosion Protection Systems," Report No. FHWA-RD-83-012, Federal Highway Administration, Washington, D.C., Sept. 1983, 71 pp.

[53]Virmani, Y. P., "Effectiveness of Calcium Nitrite Admixture as a Corrosion Inhibitor," Public Roads, Vol. 54, June 1990, pp. 171-181.

[54]Berke, N. S. and Rosenberg, A. M., "Technical Review of the Use of Calcium Nitrite in Concrete," Transportation Research Record 1211,1989, pp. 18-27.

[55]"Laboratory Performance of Corrosion Control Methods," Interim Report, Research Program Division of Planning, South Dakota Department of Transportation, Pierre, South Dakota, March 1984.

[56]Tomozawa, F., Masuda, Y., Tanaka, H., Fukushi, I., Takakura, M., Hori,

T., and Higashi, S., "An Experimental Study on Effectiveness of Corrosion Inhibitor in Reinforced Concrete Under High Chloride Content Conditions," Nihon Architecture Society, Oct. 1987.

[57]Nishibayashi, S., Hideshima, S., Negami, S. and Takada, M., "The Effect of Admixtures on the Durability of Concrete in an Undersea Environment," Performance of Concrete in Marine Environment, SP 109, V. M. Malhotra, ed., American Concrete Institute, Detroit: (1988), p.481.

[58]Tomozawa, F., Masuda, Y., Tanaka, H., Fukushi, I., Takakura, and M., Hori, T., "Experimental Study on the Effectiveness of Corrosion Inhibitor in Reinforced Concrete, RILEM Symposium on Concrete Durability, Barcelona, Spain, May 1990, pp. 382-391.

[59]Alonso, C., Acha, M., and Andrade, C. "Inhibiting Effect of Nitrites" Symposium of Concrete Durability, Barcelona, Spain, May 1990, p.219-228

[60]Berke, N. S., Dallaire, M. P., and Hicks, M. C., "Plastic, Mechanical, Corrosion, and Chemical Resistance Properties of Silica Fume (Microsilica) Concretes," in Fly Ash, Silica Fume, Slag, and Natural Pozzolans in Concrete, Proceedings Fourth International Conference, Istanbul, Turkey, May 1992, SP-132, ed.V. M. Malhotra, American Concrete Institute, Detroit pp. 1125-1149-1992.

[61]Berke, N.S., Shen,D. F. and Sundberg, K. M., "Comparison of the Polarization Resistance Technique to the Macrocell Corrosion Technique,"Corrosion Rates of Steel in Concrete ASTM STP 1045, Berke, N. S., Chaker, V. and Whiting, D., eds., American Society for Testing and Materials, Philadelphia, 1990, pp. 38-51.

[62]El-Jazairi, B. and Berke, N. S., "The Use of Calcium Nitrite as a Corrosion Inhibiting Admixture to Steel Reinforcement in Concrete," in Corrosion of Reinforcement in Concrete, Page, C. L., Treadaway, K. W. J., and Bamforth, P. B., editors, Elsevier Applied Science, London and New York, 1990, pp.571-585.

[63]Berke, N. S., Dallaire, M. P. and Hicks, M.C., "Effect of Calcium Nitrite on the Corrosion Fatigue of Steel Reinforcing in Cracked Concrete," Corrosion 91 Paper No. 550, National Association of Corrosion Engineers, Houston, 1991, 17 pp.

[64]Berke, N. S., Dallaire, M. P., Hicks, M. C. and Hoopes, R. J., "Corrosion of Steel in Cracked Concrete," Corrosion 93, Paper No. 322, NACE, Houston, TX, 1993.

[65]Briesmann,D., "Corrosion Inhibitors for Steel in Concrete," Civil Engineering Department, Munich Technical University, Munich, West Germany.

[66]Beeby A.W., Concrete International, Feb., 1983, p. 35.

[67]Margat,P.S. and Gurusamy K., Cement and Concrete Research, 17, 1987, p.385.

[68]Berke, N.S., "The Effects of Calcium Nitrite and Mix Design on the Corrosion Resistance of Steel in Concrete (Part 2, Long-Term Results)," Corrosion of Metals in Concrete, Proceeding of the Corrosion-87 Symposium on Corrosion of Metals in Concrete, NACE: Houston (1987), p.134.

[69]Berke, N.S., Hicks, M.C. and Hoopes, R.J., "Condition Assessment of Field Structures with Calcium Nitrite", to be presented at the P. Cady Symposium. Fall ACI Meeting, Minneapolis, MN, October 1993.

[70]Pourbaix, M., Atlas of Electrochemical Equilibria in Aqueous Solutions," Pergamon Press (1966).

[71]Figg, J., Concrete, V.14, No. 5, May 1980, pp. 34-36.

[72]Spellman, D. L. and Stratfull, R. F., Highway Research Board Bulletin 182, Washington, DC 1958, pp. I8-41.

[73]Locke, C.E. and Simon, A., "Corrosion of Reinforcing Steel in Concrete", Tonini, E.E. and Gaidis, J.M. editors, ASTM STP 713, Philadelphia, PA.

[74]Rechberger, P., Cement-Kalk-Gips, V. 36, 1983, pp. 582-590.

[75]Geronov, V., Tomov, T. and Georgiev, S., J. of Applied Electrochemistry,V.5, 1976, pp. 351-358.

[76]Dillard, J., Glanville, J., Osiroff, T. and Weyers, R., "Surface Characterization of Reinforcing Steel and the Interaction of Steel with Inhibitors in Pore Solution," TRB Paper No.910272, Transportation Research Board, Washington, D.C., 1991, 7 pp.

[77]Dressman, S., Osiroff, T., Dillard, J., Glanville, J. and Weyers, R., "A Screening Test for Rebar Corrosion Inhibitors," TRB Paper No. 910281, Transportation Research Board, Washington, D.C., 1991, 8 pp.

[78]Diamond, S., Cement and Concrete Aggregates, V. 8, No. 2, 1986, pp. 97-102.

[79]Martin, P. J. and Miksic, B. A., "Corrosion Inhibition in Reinforced Cement," Canadian Patent No. 1,258,473, August 1989.

[80]Nmai, C. K., Farrington, S. A. and Bobrowski, G. S., "Organic-Based Corrosion-Inhibiting Admixtures for Reinforced Concrete," Concrete International, pp. 45-51, April 1992.

[81]ASTM G 109-92, "Standard Test Method for Determining the Effects of Chemical Admixtures on the Corrosion of Embedded Steel Reinforcement in Concrete Exposed to Chloride Environments," ASTM Annual Book of Standards, Vol. 03.02, 1992.

[82]Berke, N.S., Hicks, M.C. and Tourney, P.G., "Evaluation of Concrete Corrosion Inhibitors," NACE 12th International Corrosion Congress, Houston, TX, Sept. 1993.

[83]Berke, N. S., Hicks, M. C. and Tourney, P.G., "Use of Laboratory Techniques to Evaluate the Long-Term Durability of Steel Reinforced Concrete Exposed to Chloride Ingress," CANMET/ACI Conference on Concrete Durability, Nice, France, May 1994.

[84]Bobrowski, G. S., Nmai, C. K. and Farrington, S. A., "Inhibiting Corrosion of Steel in Concrete: A New Approach," Master Builders Publication, Cleveland, OH.

[85]Nmai, C. K., "Effect of Chemical and Mineral Admixtures on the Corrosion of Steel in Concrete," Corrosion 92, Paper No. 201, NACE, Houston, TX, 1992.

[86]Rozenfeld, I. L., Corrosion Inhibitors, McGraw Hill Inc., New York, NY,1981.

[87]R.J. Craig and L.E. Wood, "Effectiveness of Corrosion Inhibitors and Their Influence on the Physical Properties of Portland Cement Mortars"; pp. 77-88 in Highway Research Record, No. 328. Highway Research Board, 1970.

[88]Arber, M.G. and Vivian, H.E., Australian J. Applied Science, 12, 1961, p.436.

[89]EG&G, Princeton Applied Research Application Note-140 "Linear Polarization" and Note-148 "Tafel Plot".

[90]C. Andrade, "Quantification of Durability of Reinforcing Steel", in Concrete Technology, New Trends, Industrial Applications, edited by A. Aguado, R. Gettu and S.P. Shah, E&FN SPON, an Imprint of Chapman & Hall, London, 1994, ppl57-175.

[91]American Society for Testing and Materials, Annual Book of Standards, ASTM, Vol. 03.02, Wear and Erosion; Metal Corrosion, Philadelphia, G5-87, G59-91, G96-90 and G102-89 1993.

[92]J. Flis, A. Sehgal, D. Li, Y.T. Kho, S. Sabotl, H. Pickering, K. Osseo-Asare and P.D. Cady, "Condition Evaluation of Concrete Bridges Relative to Reinforcement Corrosion, Volume 2: Method for Measuring the Corrosion Rate of Reinforcing Steel", National Research Council, Washington DC. SHRP-S-324, 1992.

[93]F. Wenger and J. Galland, "Analysis of Local Corrosion of Large Metallic Structures or Reinforced Concrete Structures by Electrochemical Impedance Spectroscopy", Electrochimica Acta 35 1573-1578 (1990).

[94]L. Lemoine, F. Wenger and J. Galland, "Study of the Corrosion of Concrete Reinforcement by Electrochemical Impedance Measurement, in Corrosion Rates of Steel in Concrete, ASTM STP 1065. Edited by N.S. Berke, V. Chaker and D. Whiting, Philadelphia, PA, ASTM, 1990, pp 118-133.

[95]K.S Cole and R.H. Cole, "Dispersion and Absorption in Dielectrics I. Alternating Current Characteristics", J. Chem. Phys., 9, 341-351 (1941).

[96]K.K S. Crentsil, F.P. Glasser and J.T.S. Irvine, " Electrochemical Characteristics of Reinforced Concrete Corrosion as Determined by Impedance Spectroscopy", British Corrosion Journal, 27, 113-318 (1992).

[97]K.K S. Crentsil, V.T. Yilmaz and F.P. Glasser, "Impedance Spectroscopy Analysis of the Influence of Superplasticizers on Steel Corrosion in OPC Mortar", Journal of Materials Science, 27, 3400-3404, (1992).

[98]L. Lemoine, F. Wenger and J. Galland, "Study of the Corrosion of Concrete Reinforcement by Electrochemical Impedance Measurement", "Corrosion Rates of Steel in Concrete", ASTM STP 1065. Edited by N.S. Berke, V. Chaker and D.

Whiting, Philadelphia, PA, ASTM, 1990, pp 118-133.

[99]F.Wenger, "Etude de la Corrosion de L'acier Doux dans le Beton par des Methodes Electrochimiques, Application au Controle des Ouvrages de Genie Civil", Metaux Corrosion Industrie, No.742, Juin 1978

[100] D.G. John, P.C. Searson and J.L. Dawson, "Use of AC Irnpedance Technique in Studies on Steel in Concrete in Immersed Conditions", Br. Corrosion J., 16, 102-106, (1981).

[101]L. Hachani, J. Carpio, C. Fiaud, A. Raharinaivo and E. Triki, "Steel Corrosion in Concrete Deteriorated by Chlorides and Sulphates: Electrochemical Study Using Impedance Spectrometry and Stepping down the Current Method", Cem. Concr. Res., 22, 56-66 (1992).

[102]L. Hachani, C. Fiaud, E. Triki and A. Raharinaivo, "Characteristics of Steel /Concrete Interface by Electrochemical Impedance Spectroscopy, British Corrosion Journal, 29, 122-127 (1994).

Bibliography:

[1] American Society for Testing and Materials, Annual Book of Standards, ASTM, Vol. 03.02, Wear and Erosion; Metal Corrosion, Philadelphia, G109-92 1992.

[2] C. Andrande, A. <acias, S. Feliu, M.L. Escudero and J.A. Gonzalez, "Quantitative Measurement of the Corrosion Rate Using a Small Counter Electrode in the Boundary of Passive and Corroded Zones of a Long Concrete Beam", in Corrosion Rates of Steel in Concrete, ASTM STP 1065. Edited by N.S. Berke, V> Chaker and D. Whiting Philadelphia, PA, ASTM, 1990, pp 134-142

[3] Baidis, J.M. and Rosenberg, A.M., "The Inhibition of Chloride-Induced Corrosion in Reinforced Concrete by Calcium Nitrite," Cement, Concrete, and Aggregates, 9 (1), 30-33, (1987)

[4] Berke, N.S. and Weil, T.G., "World Wide Review of Corrosion Inhibitors in Concrete", in Advances in Concrete Technology, Second Edition, edited by V.M. Malhorta, Published for Natural Resources Canada, 1983, pp891-915.

[5] N. Bonanos, B. C. H. Steele, E. P. Butler, W. B. Johnson, W. L. Worrell, D. D. MacDonald, and M. C. H. McKubre, " Application of Impedance Spectroscopy", Chpt. 4, Ed., McDonald, J. R., Wiley & Sons, NY, 1987.

[6] J.P. Broomfield, "Assessing Corrosion Damage on Reinforced Concrete Structures", in Corrosion and Corrosion Protection on Steel in Concrete, Proceedings of International Conference, University of Sheffield, U.K., Edited by R.N. Swamy, 1994, Vol. 1 pp 1-25.

[7] W.D. Collins, R.E. Weyers and I.L. Al-Qadi, "Chemical Treatment of Corroding Steel Reinforcement after Removal of Chloride-Contaminated Concrete" Corrosion, 49, 75 (1993).

[8] J.L. Dawson et al., "Electrochemical Methods for the Inspection and Monitoring of

Corrosion of reinforcing Steel in Concrete", in Corrosion of Reinforcement in Concrete Structures, edited by C.L. Page, K.W.J. Treadaway and P.B. Bamforth, Published for the Society of Chemical Industry by Elsevier, London, 1990, pp 358-371.

[9] EG&G, Princeton Applied Research Application Note-140 "Linear Polarization" and Note-148 "Tafel Plot".

[10] Ehrlich, S.G. and Rosenberg, A.M., "Methods of Steel Corrosion Control and Measurement in Concrete," in Materials Science of Concrete II, edited by J. Skalny and Mindess, The American Ceramic Society, Inc., 1991, pp 201-219.

[11]C.E. Locke, "Corrosion of Steel in Portland Cement Concrete: Fundamental Studies"; pp. 225-28 in Proceedings of the 8th International Congress on Metallic Corrosion, Toronto, 1986.

[12]D.D. Macdonald, Y.A. El-Tantawy, R.C. Rocha-Filho, M. Urquidi-Macdonald, "Evaluation of Electrochemical Impedance Techniques for Detecting Corrosion on Rebar in Reinforced Concrete", National Research Council, Washington DC. SHRP-ID/UFR-91-524, 1994.

[13] F. Mansfeld, M.W. Kendig and W.J. Lorenz, J. Electrochem. Soc., 132(2), 290-296, (1985).

[14] F. Mansfeld and H. Shih, J. Electrochem. Soc., 135(4), 1171-1172, (1988).

[15] F. Mansfeld, S.Lin, S.Kim, and H.Shih, J. Electrochem. Soc., 137(1), 78-82, (1990).

[16] F. Mansfeld, S. Lin, S. Kim, and H. Shih, Corrosion, 45(8), 615-630, (1989).

[17] Ping Gu, S. Elliott, J.J. Beaudoin, "Corrosion Resistance of Stainless Steel in Chloride Contaminated Concrete, (under preparation)

[18] Ping Gu, Yan Fu, Ping Xie, J.J. Beaudoin, "A Method for Evaluating the Corrosion Potential of a Cement Slurry to Reinforcing Steel" Cement and Concrete Research, 24 38-48 (1994).

[19] H. Shih and F. Mansfeld, Corrosion, 45(8), 610-614, (1989).

[20]M. Sluyters-Rehbach and J.H. Sluyters, in Electroanalytical Chemistry, Vol.4, ed., A.J. Bard, Marcel Dekker, New York, ppl-125 (1970).

[21]B. Sϕrensen, P.B. Jensen and E. Maahn, "The Corrosion Properties of Stainless Steel Reinforcement in Concrete, edited by C.L. Page, K.W.J. Treadaway and P.B. Bamforth, Elsevier Applied Science, New York, 1990 pp601-610.

[22] Van Daveer, J.R., Proceedings, American Concrete Institute, Vol 12.1975, pg 697.

[23] Xu Z., Gu P., Xie P. and Beaudoin J.J., 1993, "Application of A.C. Impedance Techniques in Studies of Porous Cementitious Materials, (II). Relationship between ACIS Behavior and the Porous Microstructure", Cem.Concr.Res., Vol. 23, No.4, pp853-862.

Appendix A

Linear Polarization Results for Complete Sample Set Using Point Counter Electrode

COMPLETE SET OF LINEAR POLARIZATION DATA WITH POINT COUNTER ELECTRODE

Sample #	Inhibitor	CaCl2	PROBE 1			PROBE2		
			E. Corrosion	Pol. Res.	I.Corrosion	E. Corrosion (uV)	Pol. Res. (kOhms cm²)	I.Corrosion (VA/cm²)
A11	N/A	N/A	-346.07	25.88	1.01	-551.93	19.23	0.49
A12	N/A	N/A	-483.7	31.78	0.89	-485.81	10.10	0.65
A13	N/A	N/A	-386.25	24.54	1.24	-385.57	20.98	1.24
A14	N/A	N/A	-445.53	17.65	1.48	-451.29	19.45	1.34
A15	N/A	N/A	-481.34	14.66	1.78	-469.83	43.55	0.6
A21	N/A	2%	-387.5	11.93	2.18	-398.99	14.21	1.83
A22	N/A	2%	-492.23	19.72	1.32	-494.9	20.84	1.25
A23	N/A	2%	-369.89	48.84	0.53	-361.79	37.37	0.7
A24	N/A	2%	-441.71	15.08	1.73	-460.13	21.01	1.24
A25	N/A	2%	-526.39	18.81	1.38	-526.98	19.54	1.33
A31	N/A	4%	-467.73	12.37	2.11	-489.44	11.13	2.34
A32	N/A	4%	-450.21	12.1	2.18	-450.21	10.99	2.19
A33	N/A	4%	-429.05	12.1	2.15	-429.94	10.86	2.44
A34	N/A	4%	-588.23	8.27	3.15	-588.66	7.82	3.33
A35	N/A	4%	-360.23	14.55	1.79	-372.84	21.2	1.23
B11	2%NaNo2	N/A	-343.3	37.27	0.7	-334.72	31	0.84
B12	2%NaNo2	N/A	-293.99	43.46	0.6	-298.11	43.14	0.6
B13	2%NaNo2	N/A	-468.63	12.27	2.12	-476.08	14.16	1.84
B14	2%NaNo2	N/A	-310.48	22.23	2.10	-296.53	30.59	2.00
B15	2%NaNo2	N/A	-398.07	21.1	1.24	-396.17	31.72	0.82
B21	2%NaNo2	2%	-396.14	31.04	0.79	-339.4	31.10	0.74
B22	2%NaNo2	2%	-543.88	13.13	1.98	-544.35	12.9	2.02
B23	2%NaNo2	2%	-609.91	30.3	0.86	-607.42	27.81	0.94
B24	2%NaNo2	2%	-453.87	61.63	0.42	-453.41	25	1.04
B25	2%NaNo2	2%	-485.62	17.72	1.47	-473.03	24.17	1.08
B31	2%NaNo2	4%	-336.63	22.51	1.16	-342.68	42.27	0.62
B32	2%NaNo2	4%	-289.32	17.45	1.49	-281.88	26.6	0.98
B33	2%NaNo2	4%	-285.29	19.17	1.36	-288.83	37.75	0.69
B34	2%NaNo2	4%	-418.41	35.6	0.66	-415.19	31.1	0.70
B35	2%NaNo2	4%	-415.62	13.2	1.97	-427.27	15.91	1.64
1B			-497.71	11.91	2.19	-509.32	15.02	1.73
2B		0.50%	-542.44	10.57	2.47	-547.74	12.48	2.09
3B		1%	-419.97	7.91	3.29	-450	12.64	2.03
4B		2%	-583.59	26.66	0.97	-583.36	26.81	0.97
5B		4%	-593.66	10.31	2.59	-593.78	10.17	2.56
C11	5% dinitrobenzoic acid	N/A	-473.9	27.16	0.98	-473.84	28.47	0.92
C12	5% dinitrobenzoic acid	N/A	-526.61	33.67	0.77	-525.04	31.94	0.82
C13	5% dinitrobenzoic acid	N/A	-483.25	17.18	1.52	-478.78	13.55	1.92
C14	5% dinitrobenzoic acid	N/A	-488.24	22.78	1.14	-388.48	22.84	1.15
C15	5% dinitrobenzoic acid	N/A	-470.88	23.43	1.54	-484.84	31.54	0.83
C21	5% dinitrobenzoic acid	2%	-375.3	10.62	2.45	-389.62	15.88	1.64
C22	5% dinitrobenzoic acid	2%	-520.57	19.84	1.31	-519.12	18.55	1.4
C23	5% dinitrobenzoic acid	2%	-531.8	18.46	1.41	-529.39	17.71	1.47
C24	5% dinitrobenzoic acid	2%	-495.54	88.87	0.53	-490.7	25.54	1.02
C25	5% dinitrobenzoic acid	2%	-427.21	15.21	1.71	-445.43	22	1.18
C31	5% dinitrobenzoic acid	4%	-477.5	16.11	1.75	-483.52	18.28	1.6

C32	5% dinitrobenzoic acid	4%	-463.21	18.8	1.39
C33	5% dinitrobenzoic acid	4%	-439.78	20.92	1.25
C34	5% dinitrobenzoic acid	4%	-639.74	13.29	1.98
C35	5% dinitrobenzoic acid	4%	-408.04	23.29	1.12
1C			-507.3	9.95	2.62
2C		0.50%	-541.14	22.04	1.16
3C		1%	-571.83	6.67	3.91
4C		2%	-488.54	15.4	1.69
5C		4%	-528.74	9.22	2.83
1D			-529.69	9.28	2.81
2D		0.50%	-568.52	13.79	1.89
3D		1%	-541.73	31.61	0.82
4D		2%	-513.83	16.44	1.58
5D		4%	-571.83	16.59	1.4
1			-549.66	7.29	3.57
2		0.50%	-234.09	85.41	0.31
3		1%	-358.94	38.779	0.67
4		2%	-346.98	38.13	0.68
5		4%	-405.88	26.58	0.98
6	2%NaNo2	0%	-453.34	35.47	0.73
7	2%NaNo2	0.50%	-582.4	75.51	0.35
8	2%NaNo2	1%	-249.94	28.48	0.91
9	2%NaNo2	2%	-534.06	81.9	0.3
10	2%NaNo2	4%	-489.81	26.15	1.29
11	5%dinitrobenzoic acid	0%	-451.29	58.55	0.44
12	5%dinitrobenzoic acid	0.50%	-424.55	101.12	0.28
13	5%dinitrobenzoic acid	1%	-479.45	48.99	0.53
14	5%dinitrobenzoic acid	2%	-554.63	18.74	1.39
15	5%dinitrobenzoic acid	4%	-479.08	18.24	1.43
16	4-aminobenzoic acid	0%	-503.03	18.68	1.38
17	4-aminobenzoic acid	0.50%	-493.73	41.9	0.62
18	4-aminobenzoic acid	1%	-520.9	57.03	0.46
19	4-aminobenzoic acid	2%	-334.58	22.49	1.16
20	4-aminobenzoic acid	4%	-379.21	31.5	0.83
21	5% diphenyl phosphite	0%	-484.41	22.62	1.16
22	5% diphenyl phosphite	0.50%	-490.21	23.11	1.13
23	5% diphenyl phosphite	1%	-547.77	8.72	2.99
24	5% diphenyl phosphite	2%	-514.07	29.41	0.89
25	5% diphenyl phosphite	4%	-420.96	13.61	1.89
26	5% 4-aminobenzoic acid	0%	-486.53	68.19	0.54
27	5% 4-aminobenzoic acid	0.50%	-349.23	53.0	0.49
28	5% 4-aminobenzoic acid	1%	-514.33	41.34	0.63
29	5% 4-aminobenzoic acid	2%	-535.65	11.95	2.16
30	5% 4-aminobenzoic acid	4%	-484.88	26.29	0.99
36	5% sodium hexametaphospate	0%	-536.15	16.04	1.44
37	5% sodium hexametaphospate	0.50%	-482.11	14.21	1.83
38	5% sodium hexametaphospate	1%	-566.39	13.63	1.91
39	5% sodium hexametaphospate	2%	-581.44	11.04	2.36
40	5% sodium hexametaphospate	4%	-608.19	9.28	2.81
41	same as 40 plus 2% NaNo2	0.50%	-588.99	14.26	1.83
42	same as 40 plus 2% NaNo3	1%	-598.11	10.95	2.38
43	same as 40 plus 2% NaNo4	2%	-521.85	22.81	1.14
44	same as 40 plus 2% NaNo5	4%	-508.98	11.27	2.31
45	5% sodium molybdate	0%	-538.99	3.988	11.88
46	5% sodium molybdate	0.50%	-493.78	24.05	1.08
47	5% sodium molybdate	1%	-422.07	28.4	1.08
48	5% sodium molybdate	2%	-520.1	17.09	1.52
49	5% sodium molybdate	4%	-502.17	6.82	3.82
50	5% sodium molybdate		-568.39	9.3	2.8

-472.99	27.63	0.94
-438.33	18.98	1.43
-638.69	12.67	2.02
-415.08	24.94	1.04
-518.62	13.53	1.99
-544.24	24.59	1.06
-574.18	6.97	3.74
-495.85	15.3	1.7
-564.21	11.33	2.3
-598.94	10.58	2.46
-572.36	15.25	1.71
-542.23	27.57	0.94
-507.72	13.98	1.66
-453.33	24.67	1.06
-388.22	23.66	1.1
-248.25	91.23	0.29
-381.65	37.9	0.69
-359.21	40.58	0.64
-408.11	23.99	0.98
-484.61	46.99	0.53
-600.41	59.71	0.44
-246	24.7	0.3197
-500.83	31.38	1.2
-489.19	19.29	1.81
-446.2	93.93	0.28
-423.07	108.66	0.24
-476.31	43.63	0.59
-551.98	16.52	1.58
-491.82	20.09	1.3
-517.79	27.46	0.95
-492.8	53.93	0.48
-514.95	23.93	1.09
-345.08	35.83	0.73
-382.76	24.51	1.08
-469.27	24.36	1.07
-484.31	25.26	1.9
-551.34	11.86	2.9
-519.44	23.09	1.13
-448.52	20.52	1.27
-510.18	23.11	0.91
-530.6	15.11	1.96
-516.38	19.95	1.31
-536.7	13.95	1.87
-485.6	21.76	1.2
-535.91	16.94	1.54
-465.87	13.12	1.99
-566.63	13.56	1.92
-581.37	11.01	2.37
-611.4	10.58	2.47
-587.5	13.55	1.92
-567.68	11.58	2.48
-524.44	23.16	1.12
-514.81	13.55	1.92
-540.58	4.1634	6.28
-495.47	26.3	0.99
-427	41.88	0.62
-522.45	17.38	1.5
-503.93	6.38	4.1
-568.74	10.52	2.48

Appendix B

Experimental Data and Simulation of Samples with Extreme Values

Appendix B

A.C. Impedance

A 14-1

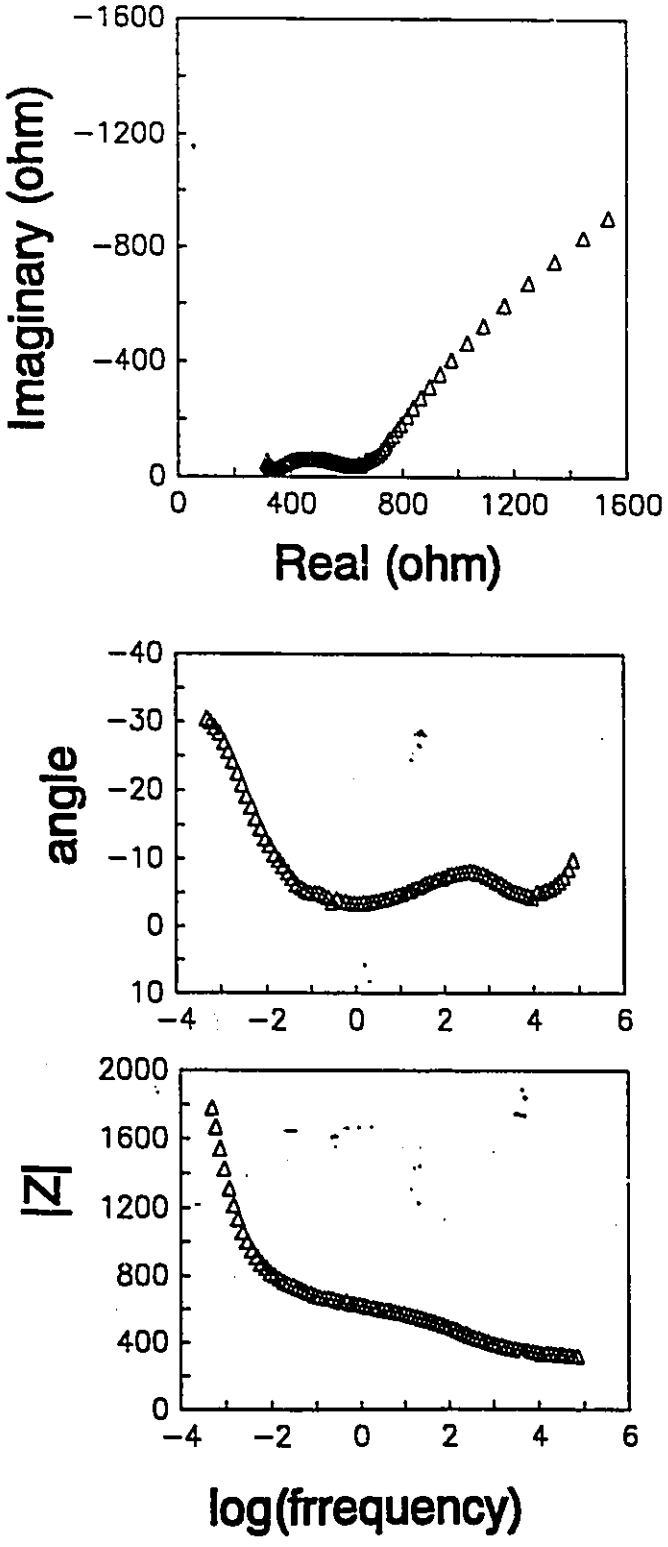

Appendix B

A.C. Impedance

A 23-1

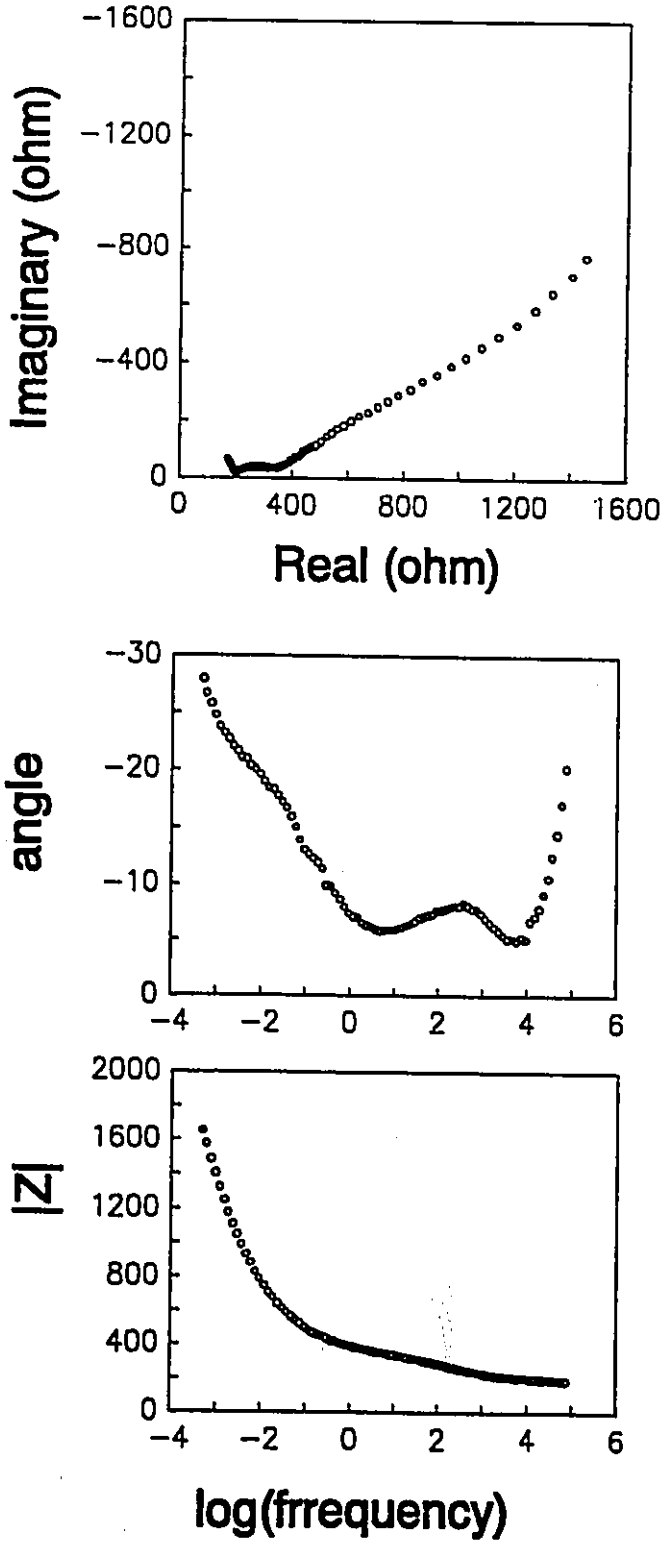

Appendix B

A.C. Impedance

A 34-1

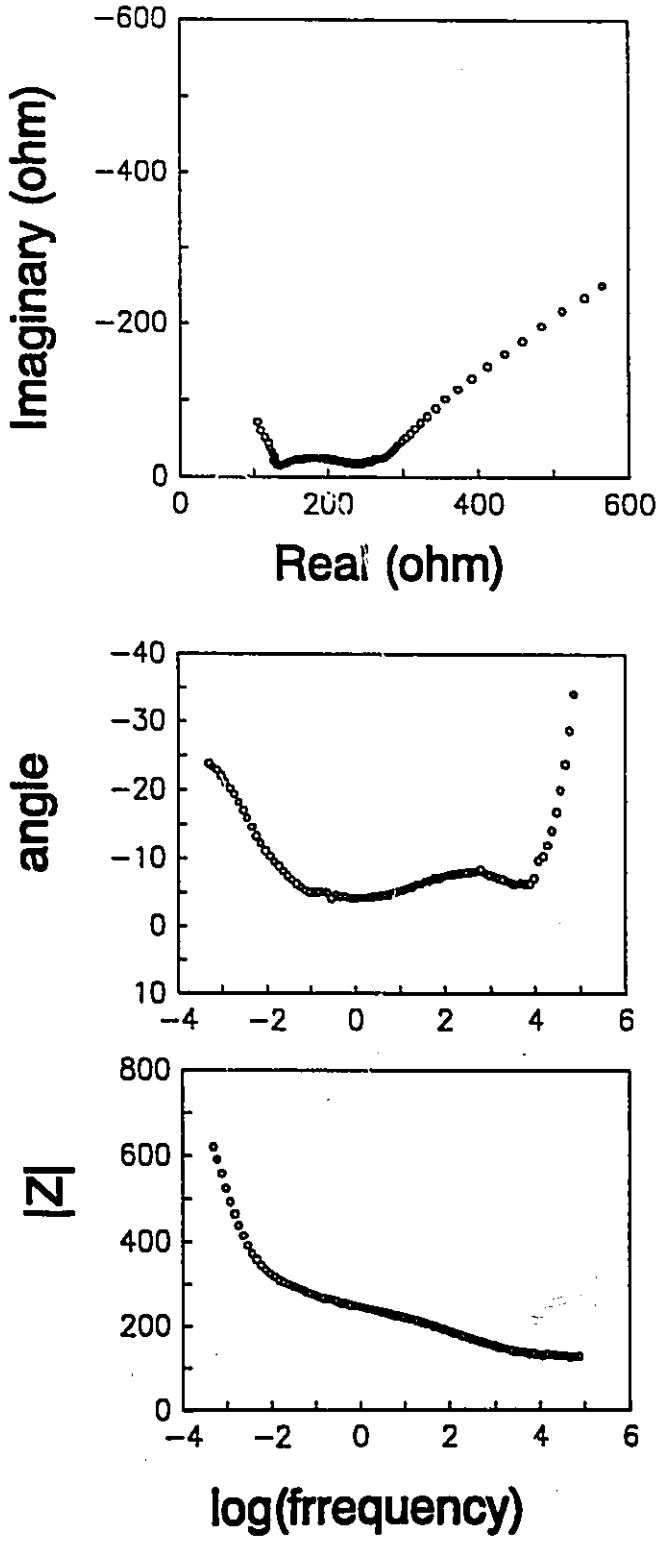

Appendix B

A.C. Impedance

B 14-1

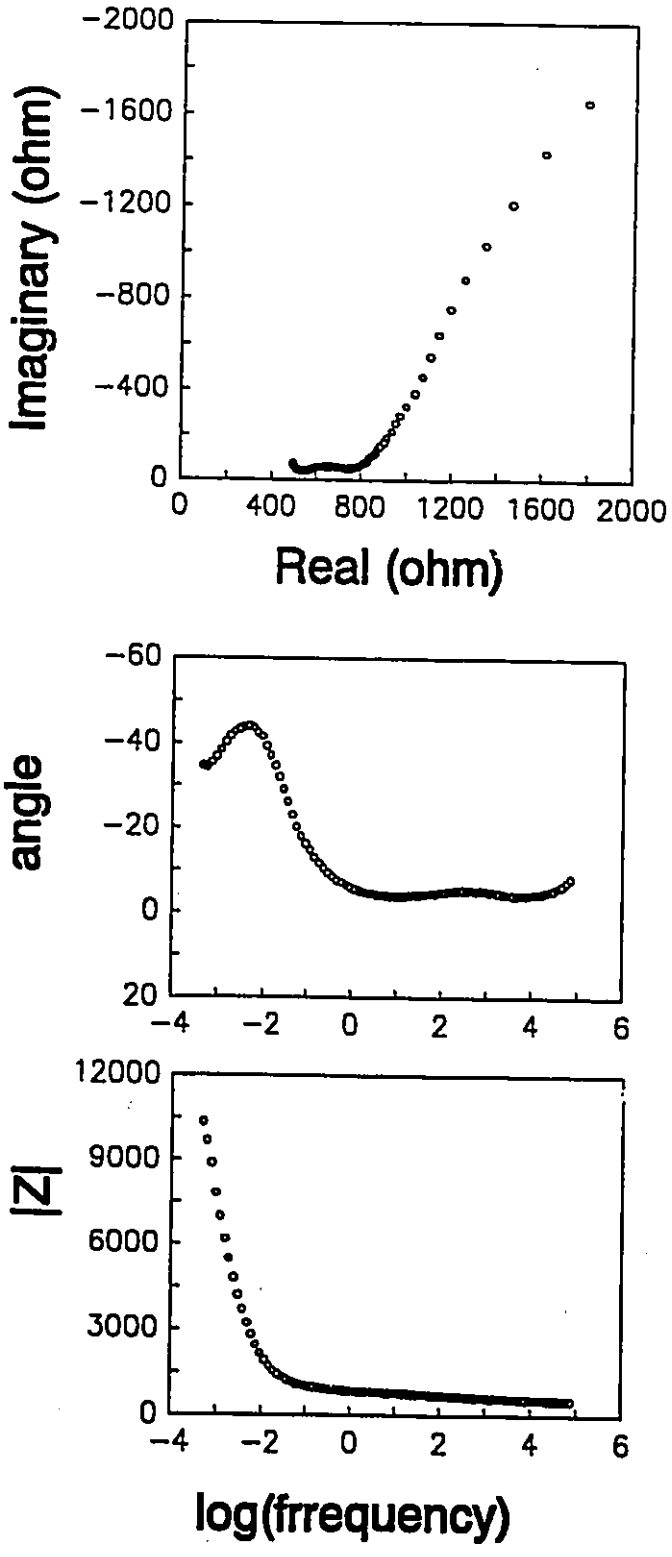

Appendix B

A.C. Impedance

B 21-1

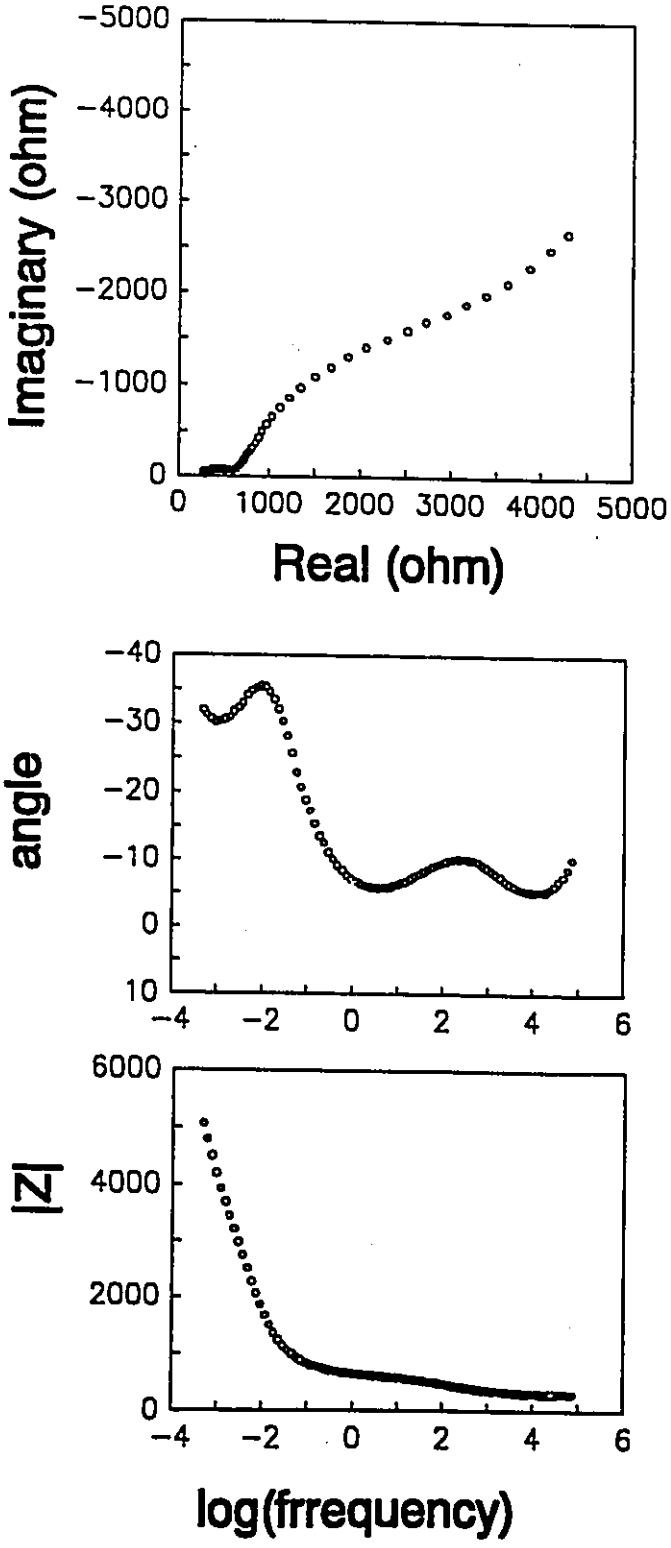

Appendix B

A.C. Impedance

B 34-1

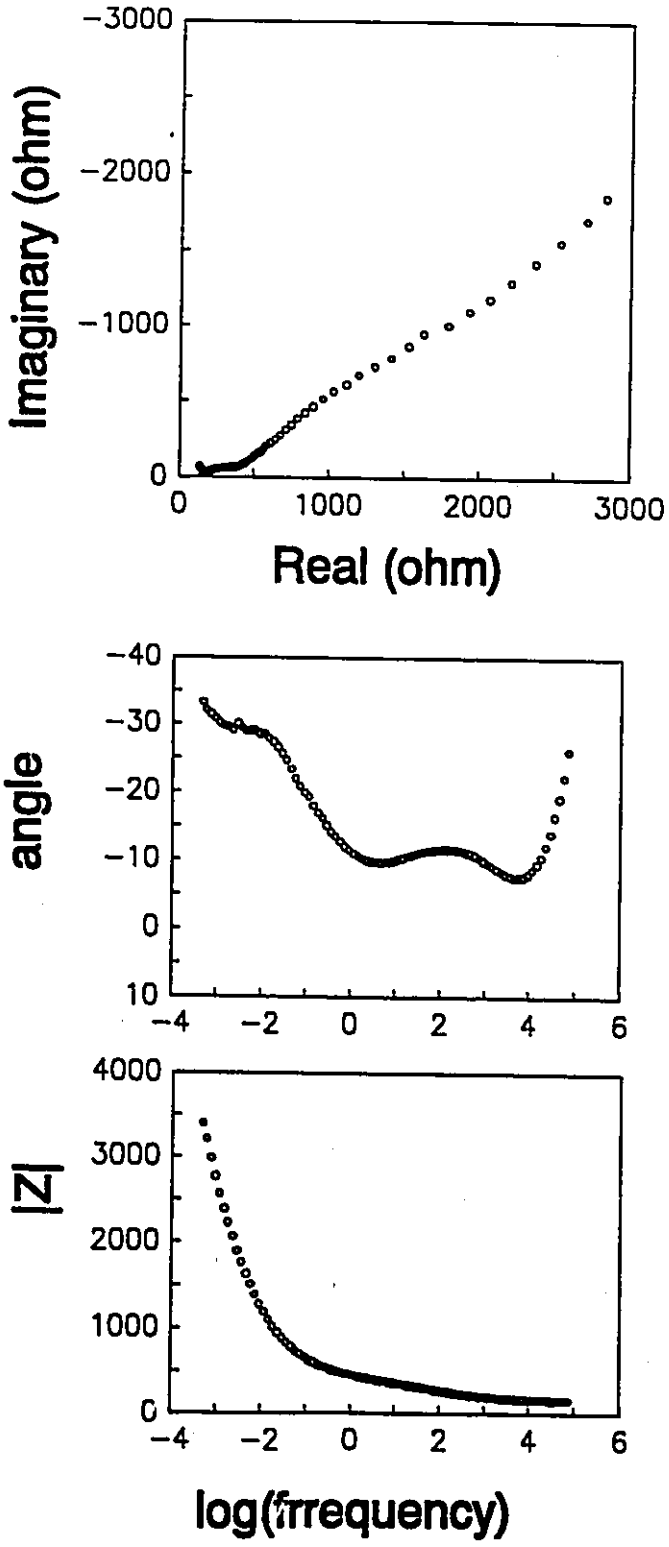

Appendix B

A.C. Impedance

C 11-1

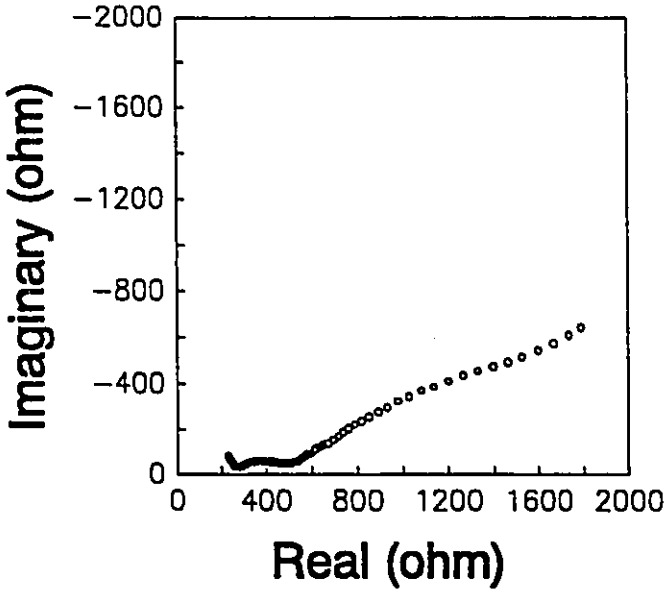

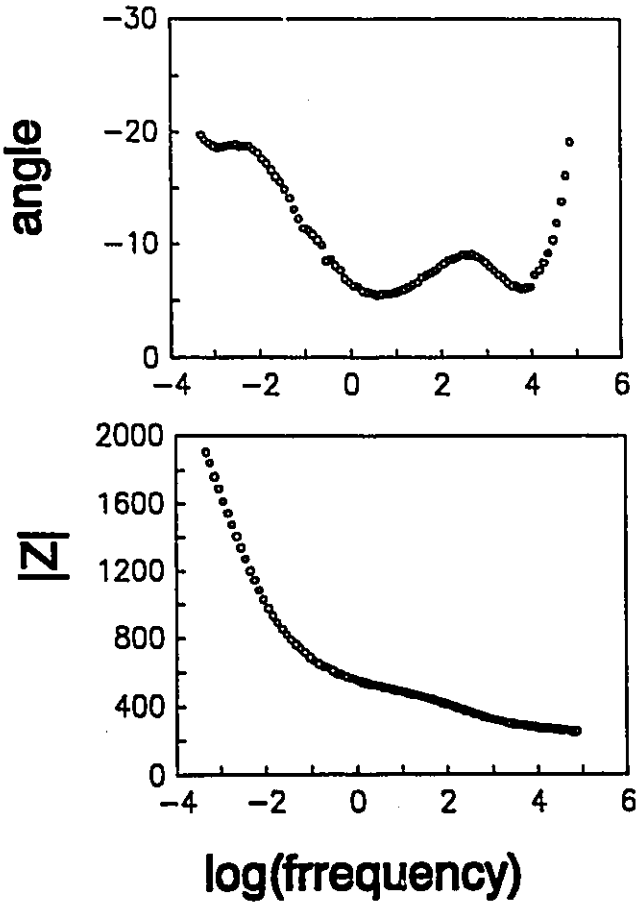

Appendix B

A.C. Impedance

C 22-1

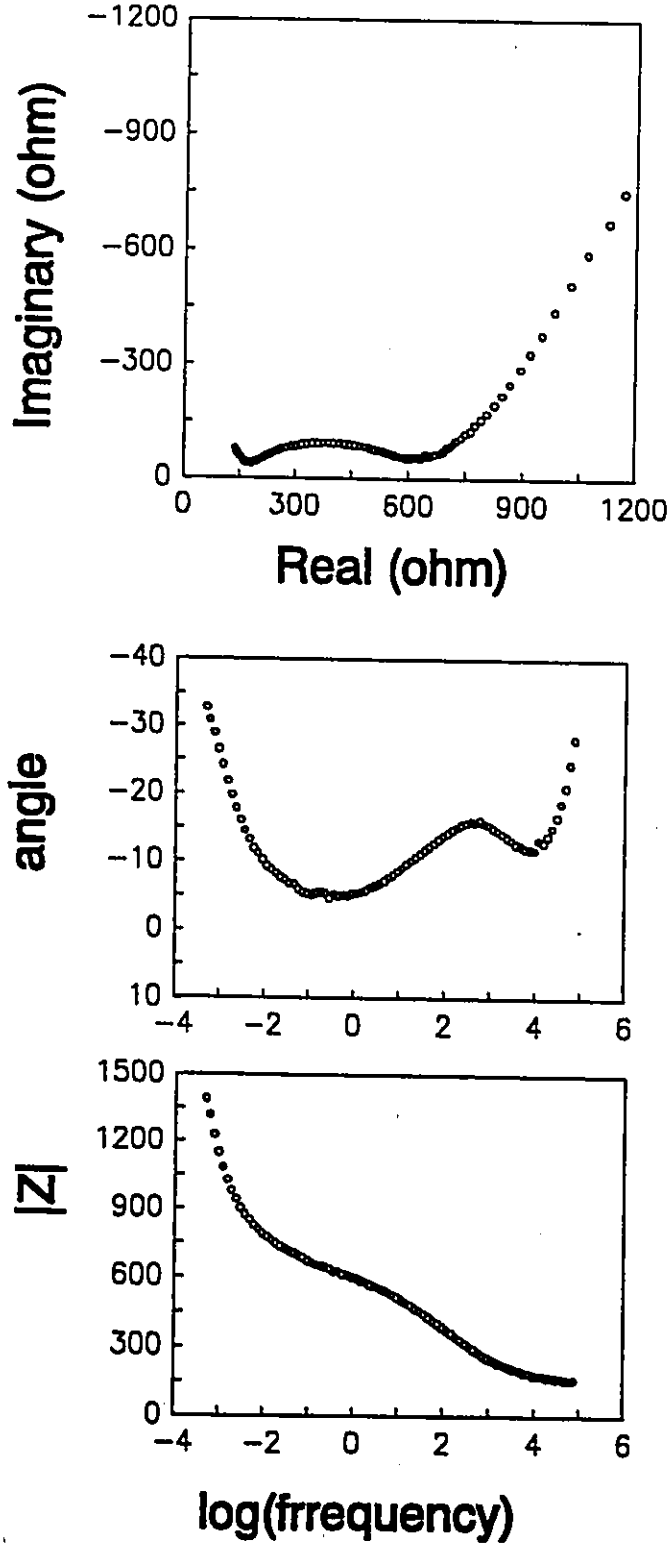

Appendix B

A.C. Impedance

C 34-1

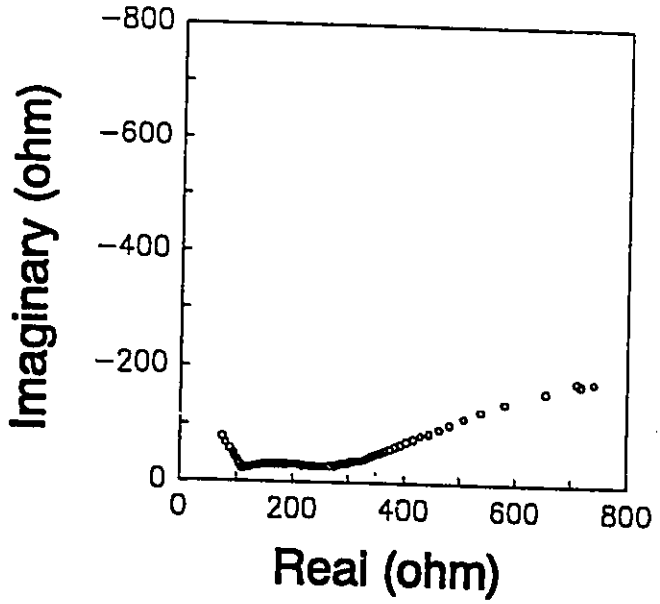

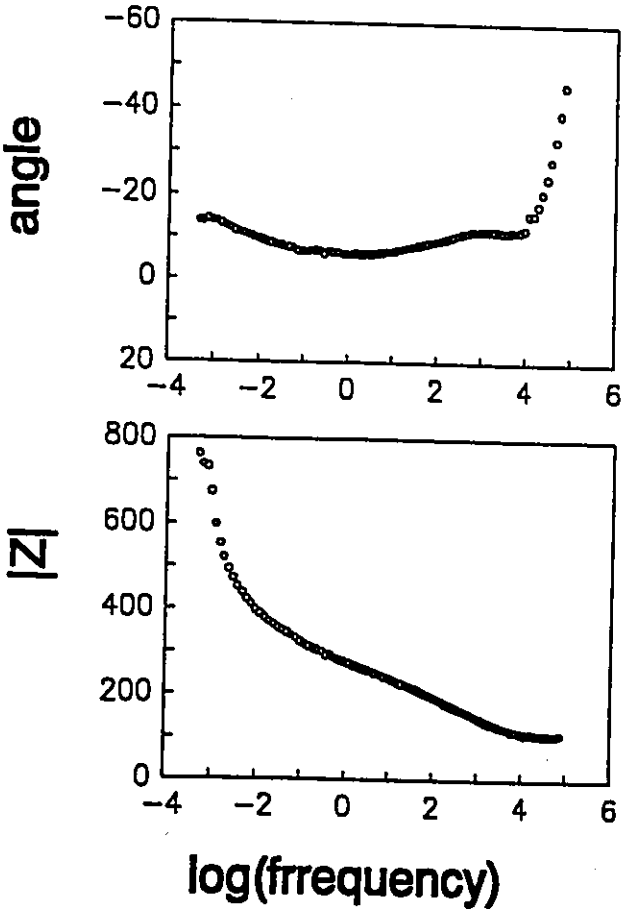

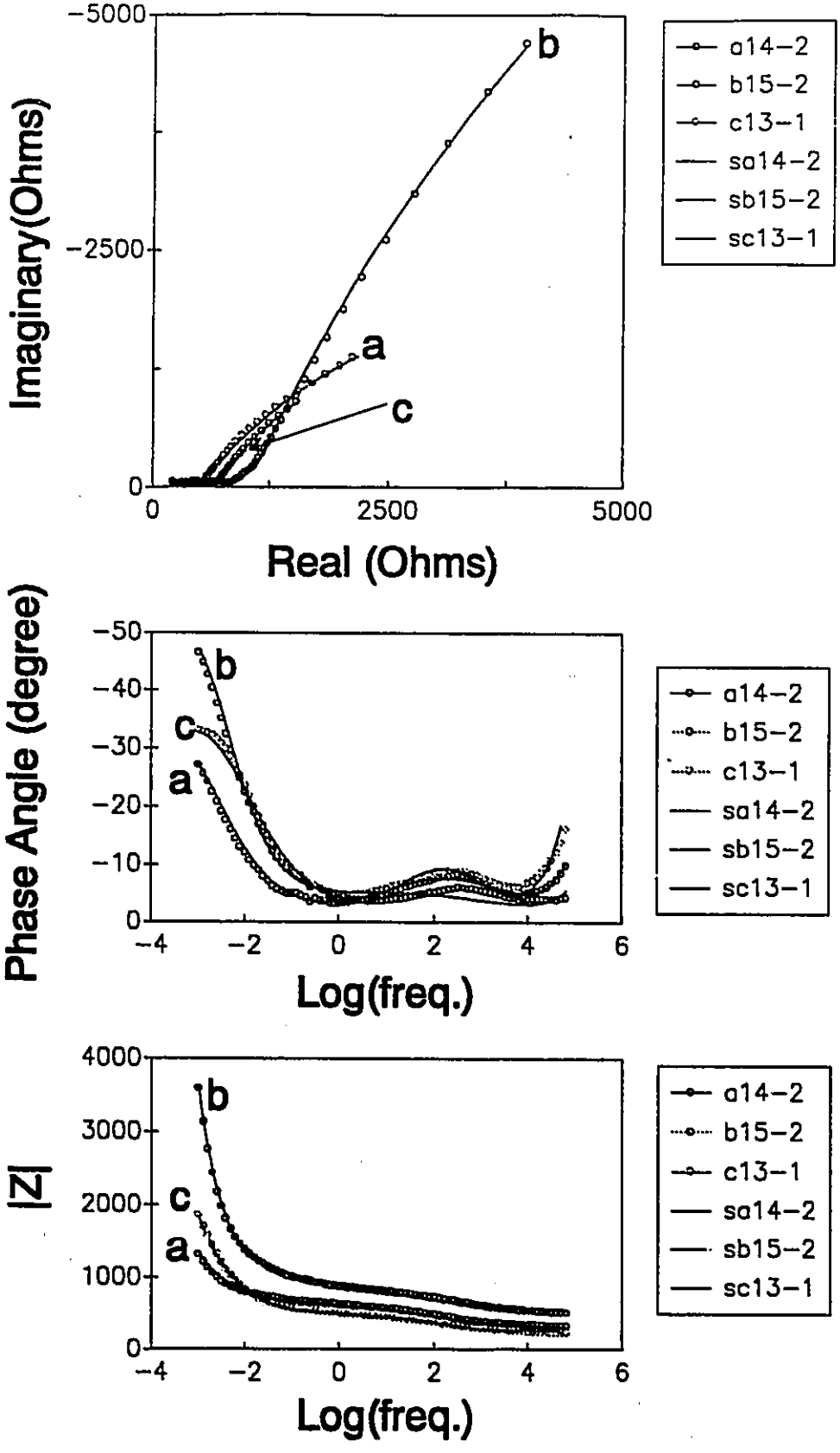

Fig. 39: Plots for the corrosion systems without inhibitor.

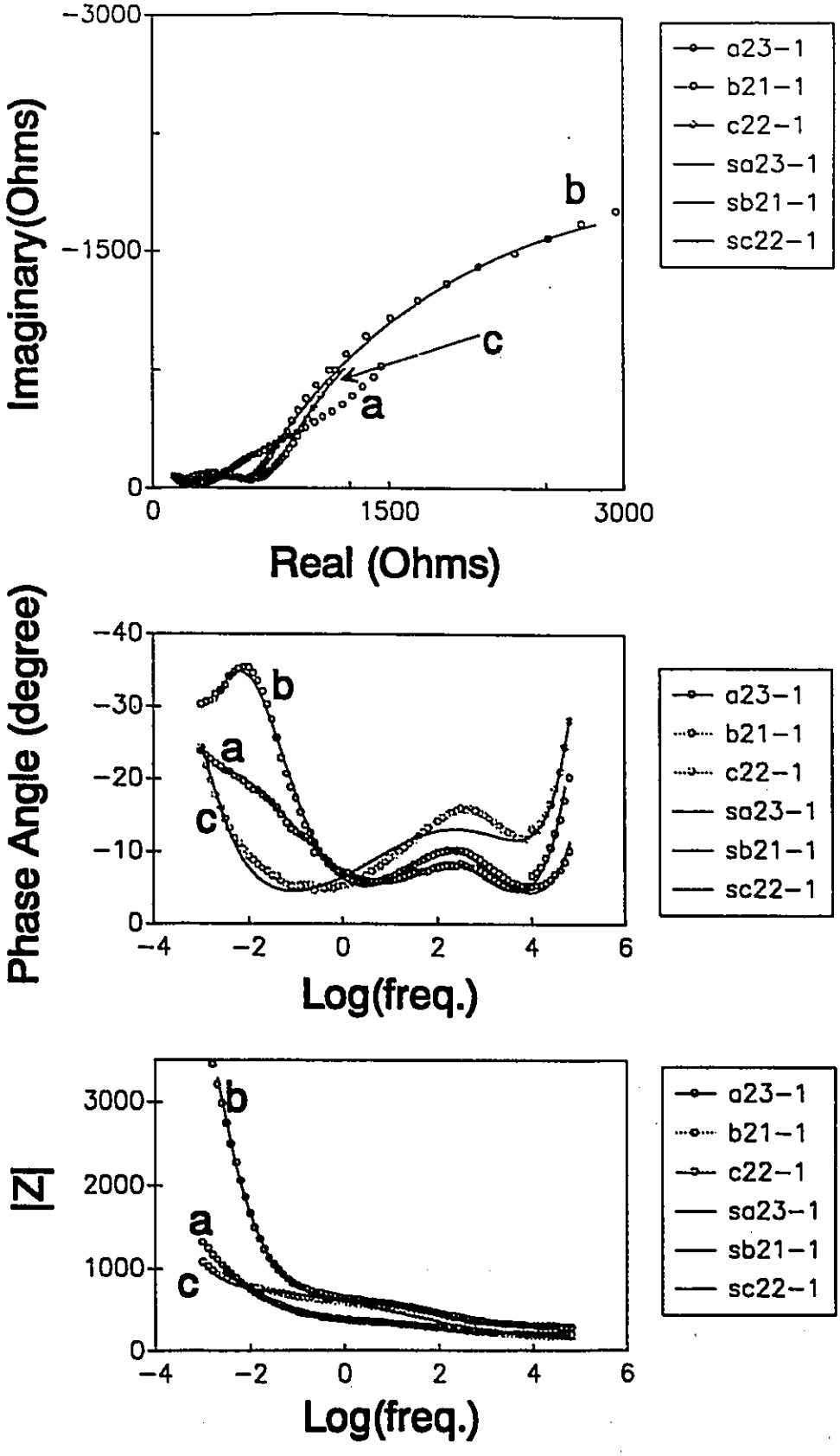

Fig. 40: Plots for the corrosion systems with 2% $NaNO_2$ and 2-4% $CaCl_2$

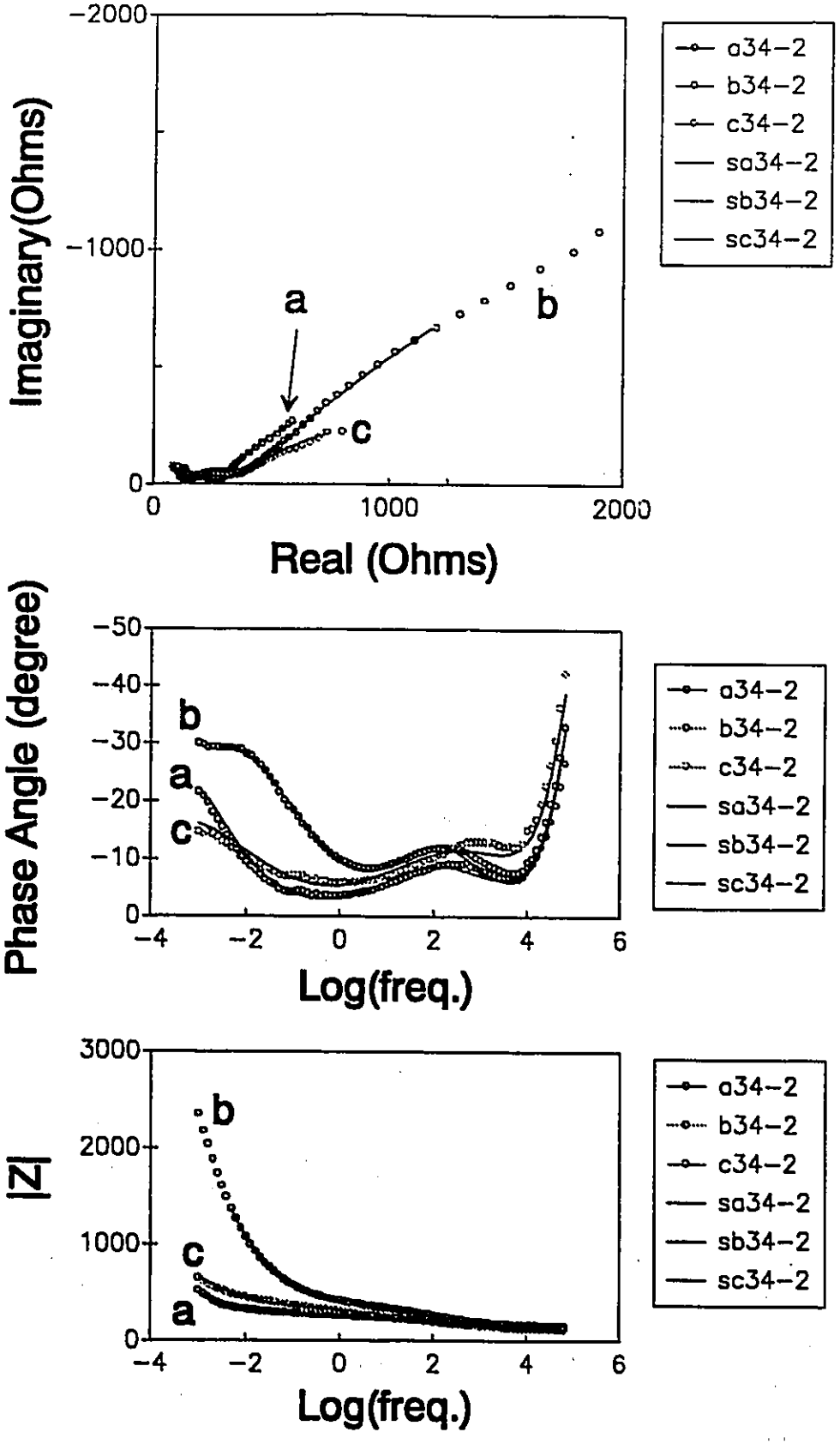

Fig. 41: Plots for the corrosion systems with 5% 3-5, dinitrobenzoic acid and 2-4% $CaCl_2$; (-) - optimum fit of the theoretical transfer function of the system; s- simulation.

Appendix C

Graphical Display of A.C. Impedance and Tabular Data Using a Digital Plotter

A14 Test #1
October 11, 1995

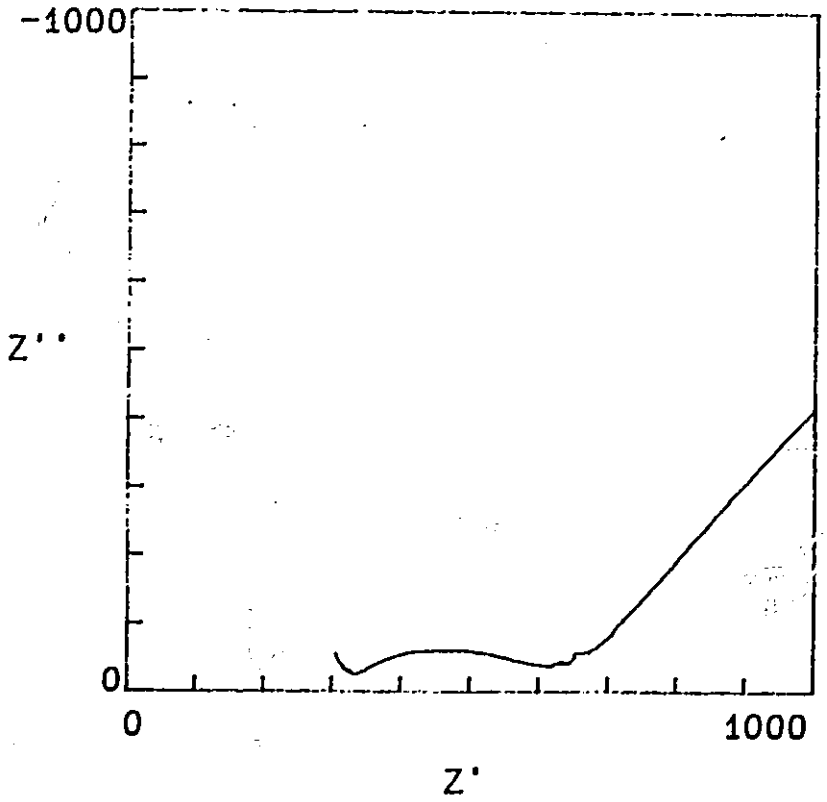

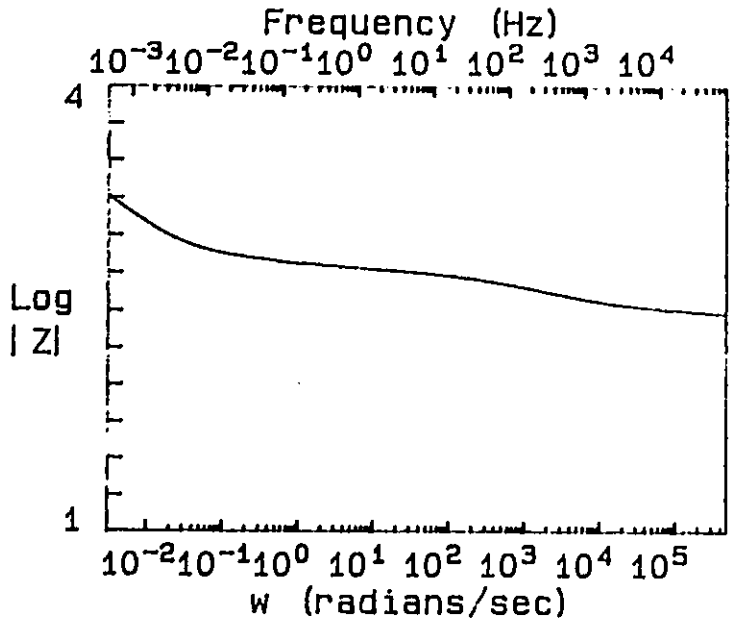

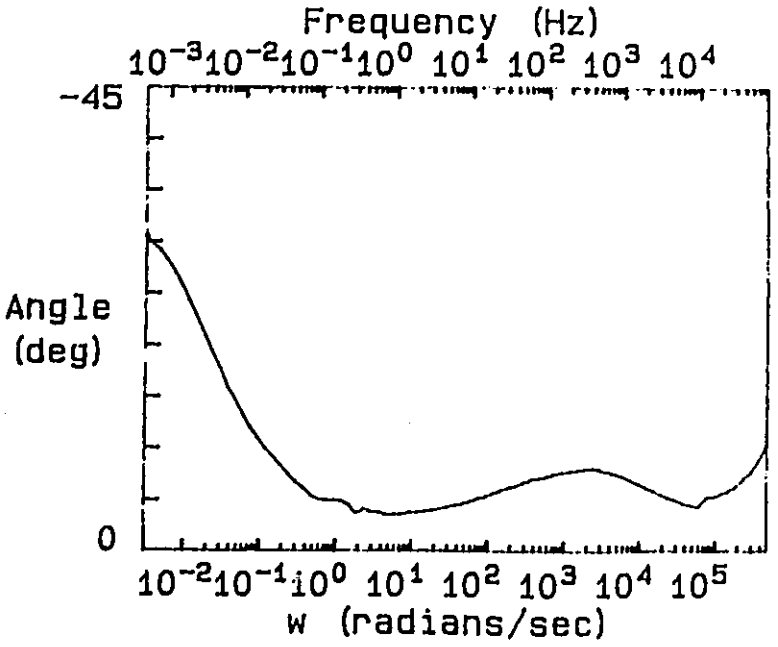

A14 Test #2
October 11, 1995

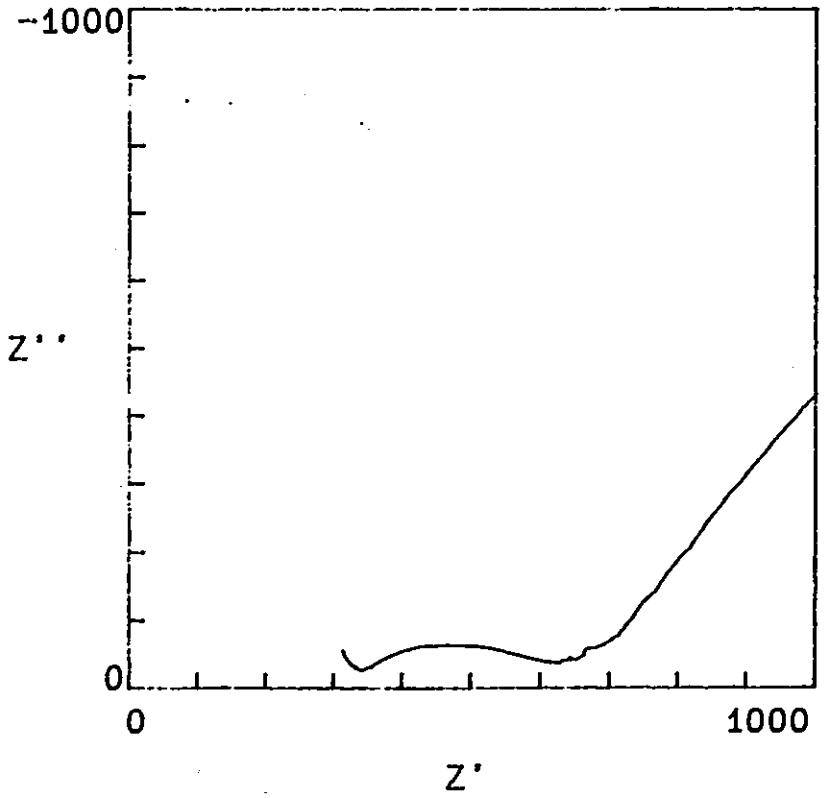

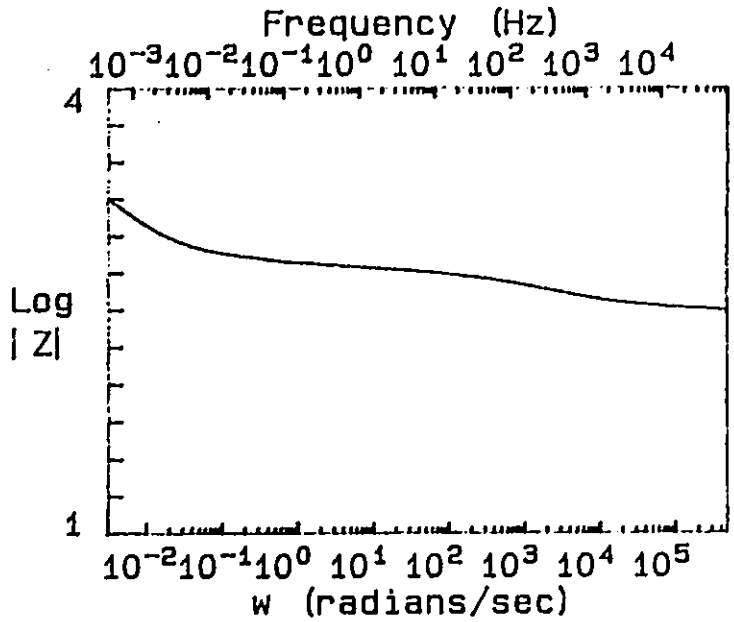

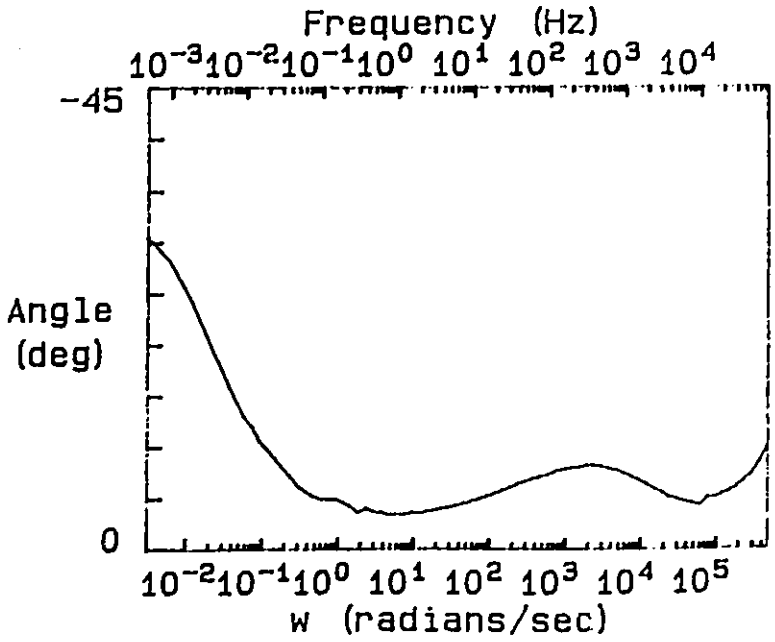

A23 Test #1
October 5, 1995

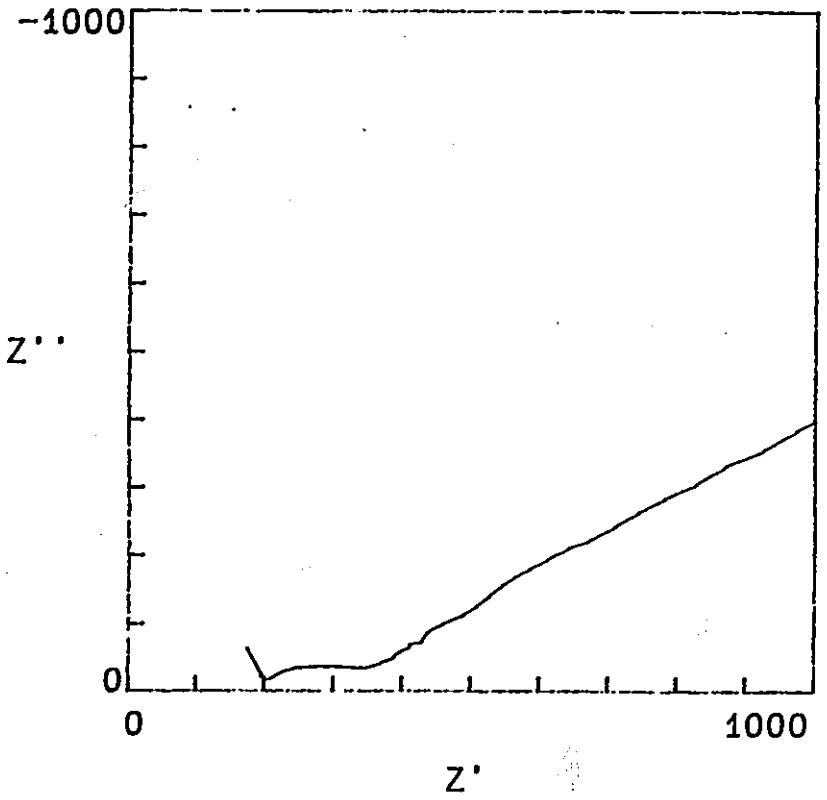

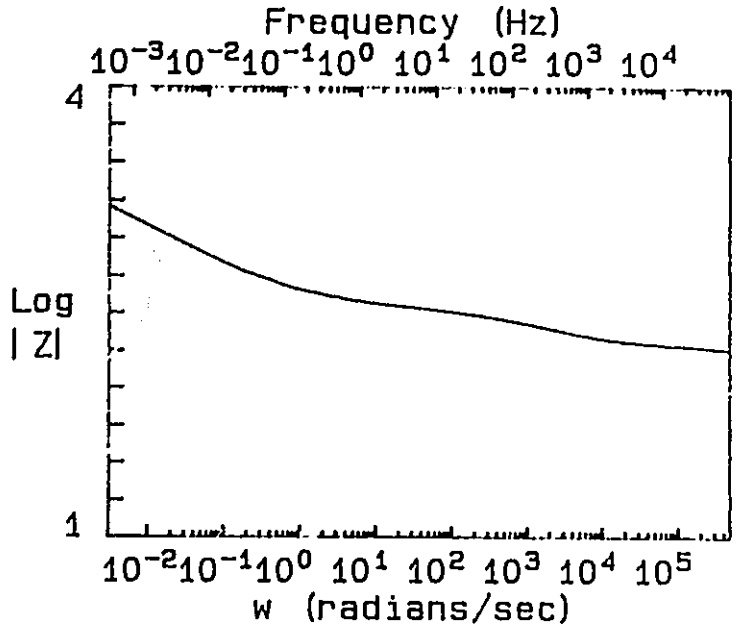

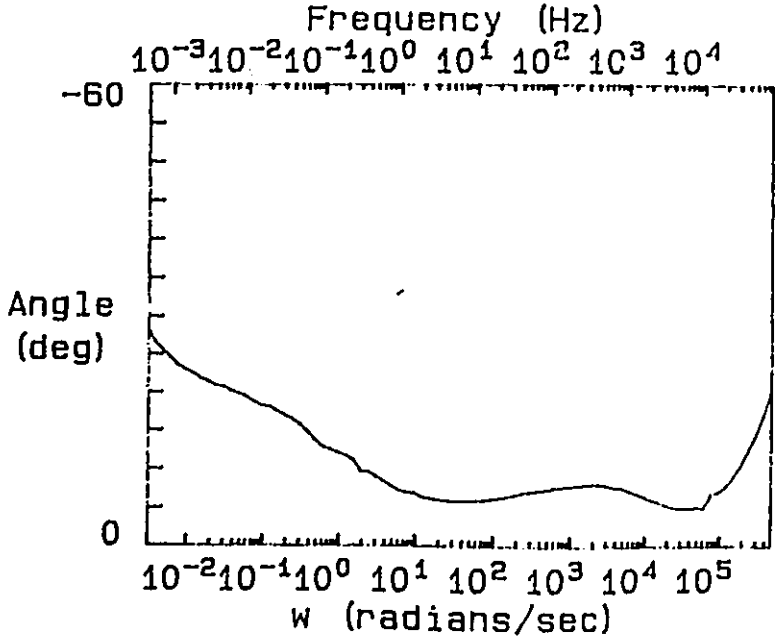

A23 Test #2
October 5, 1995

Frequency 75000 to 0.0001

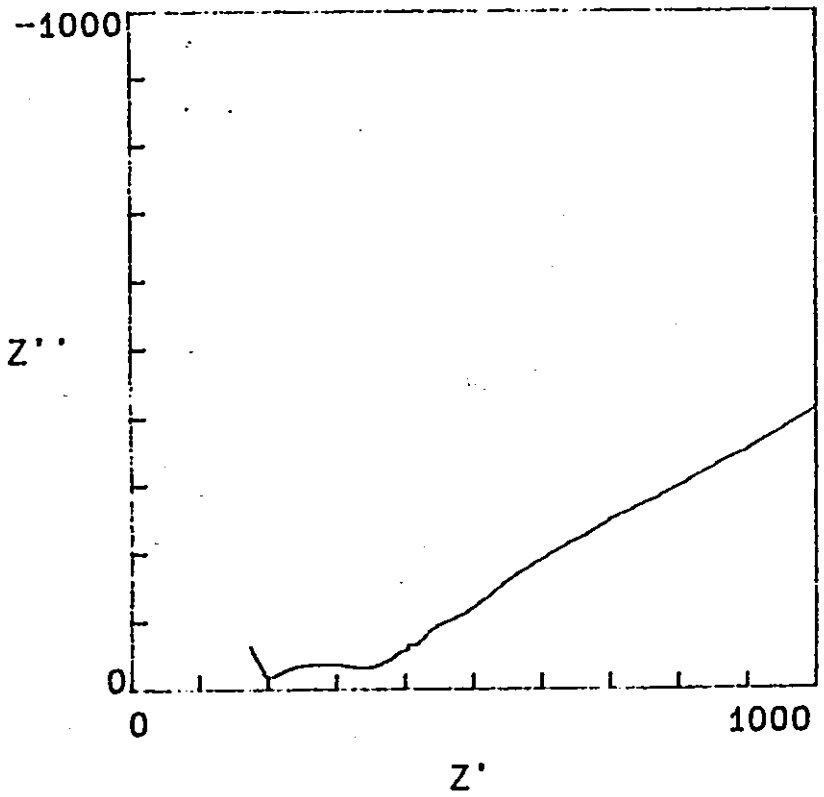

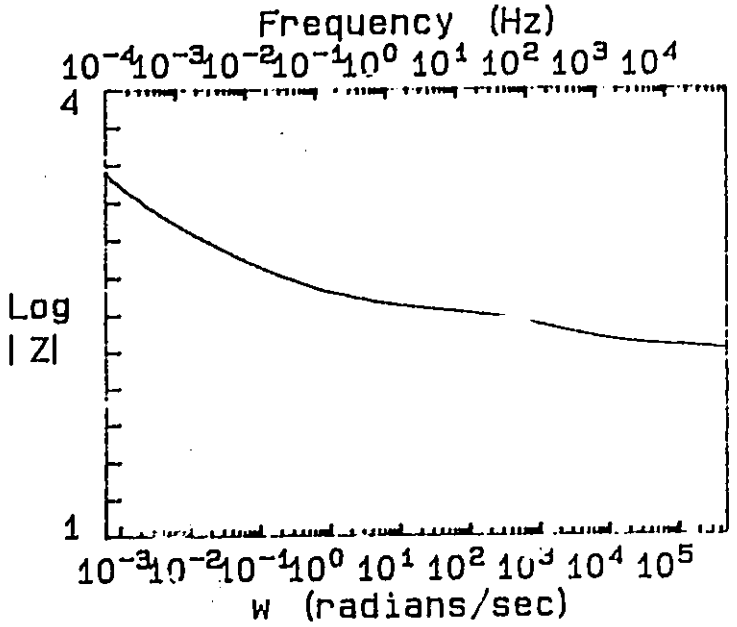

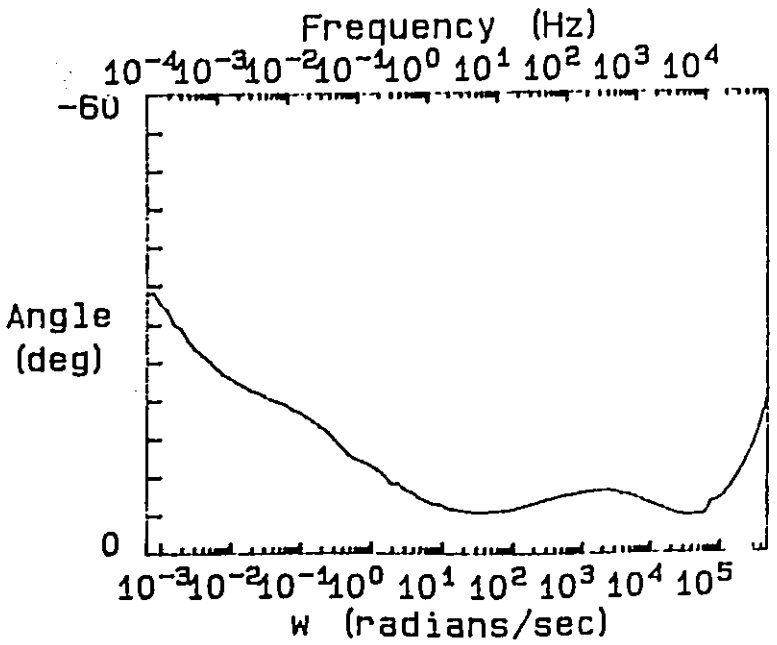

A34 Test #1
October 3, 1995

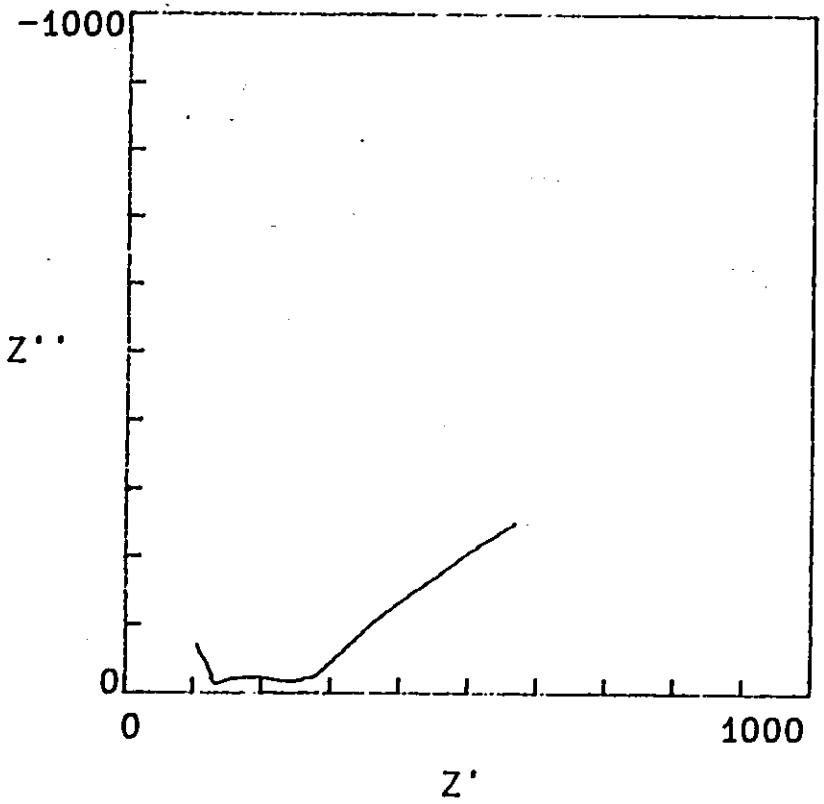

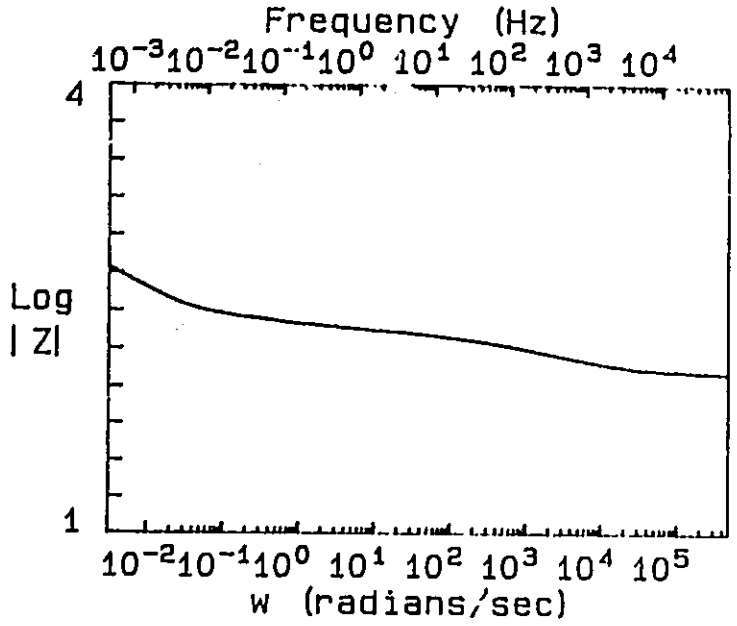

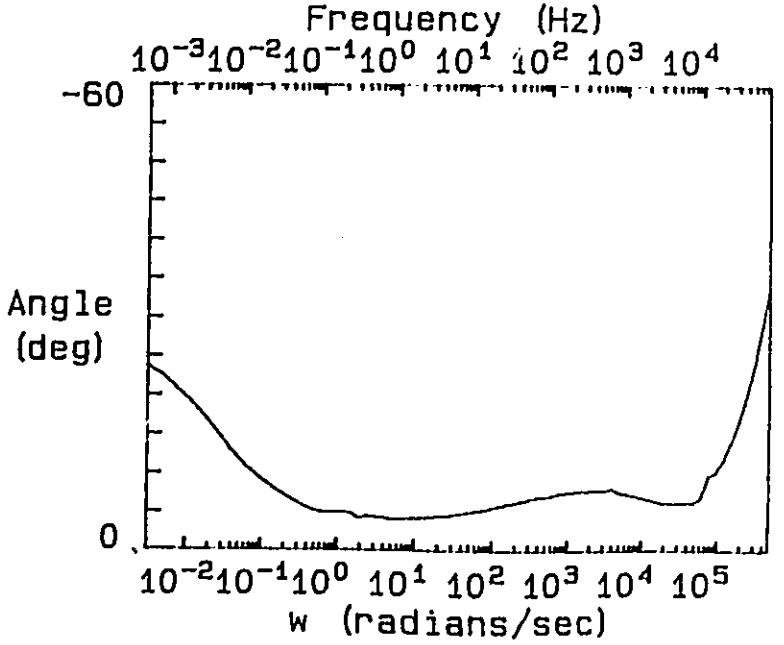

A34 Test #2
October 3, 1995

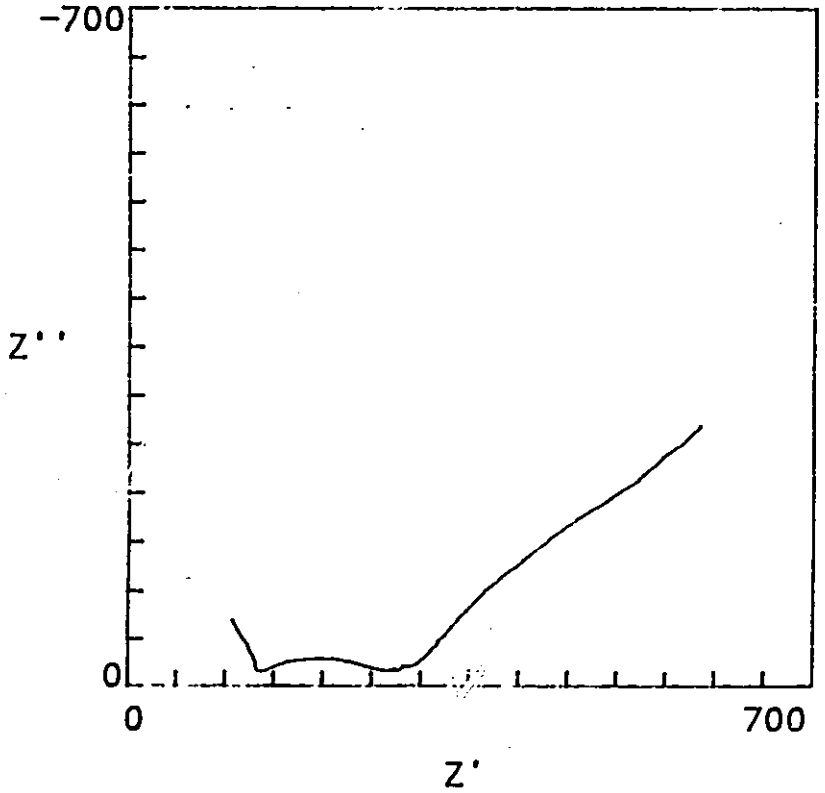

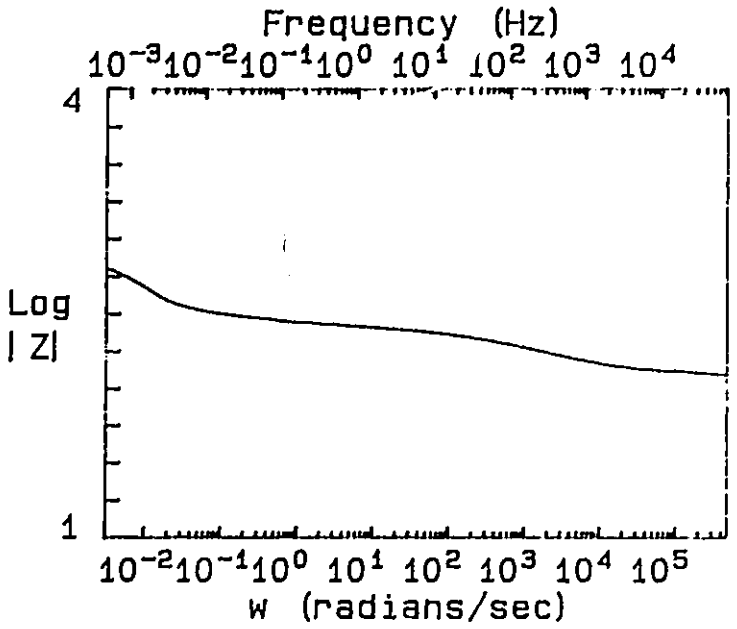

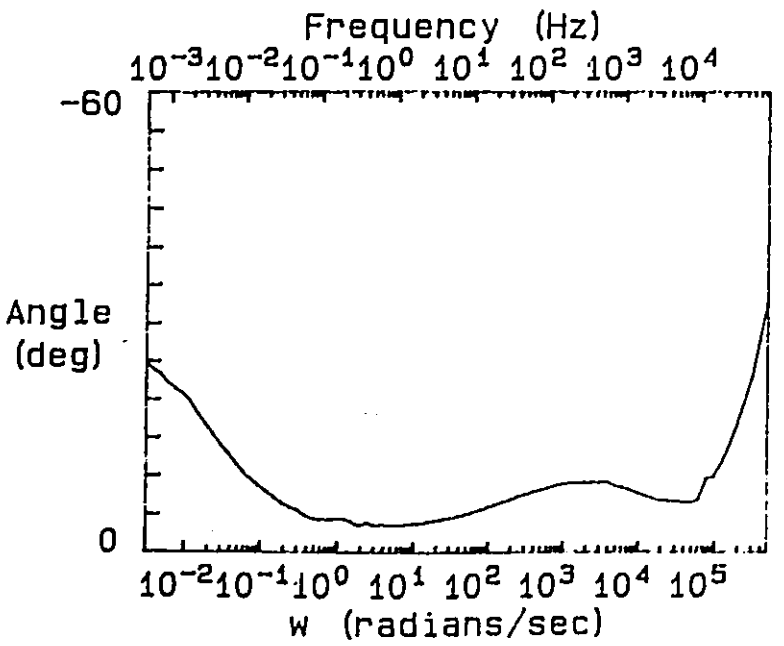

B14 Test #1
October 23, 1995

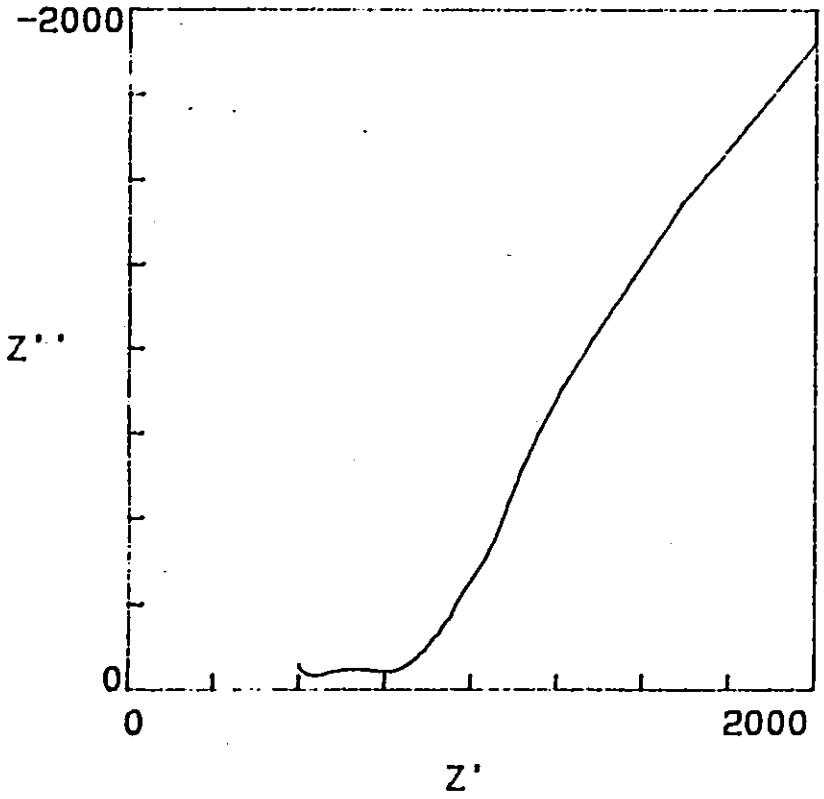

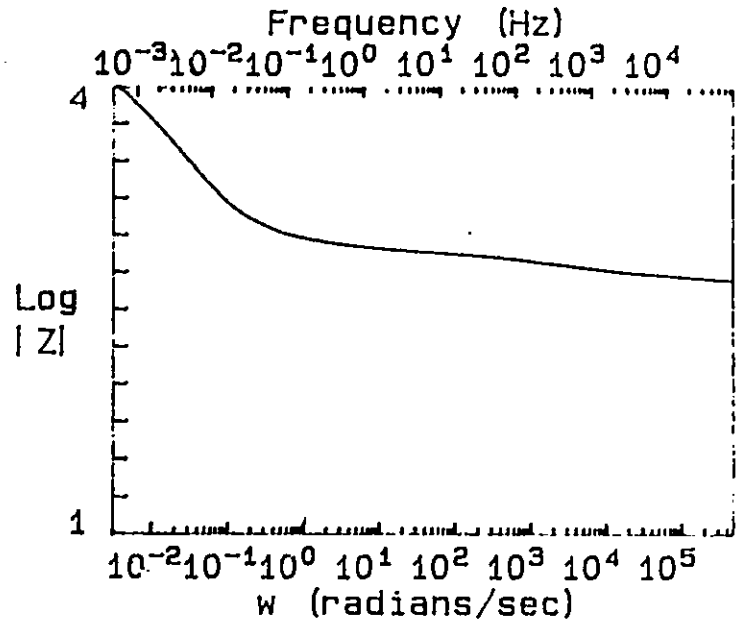

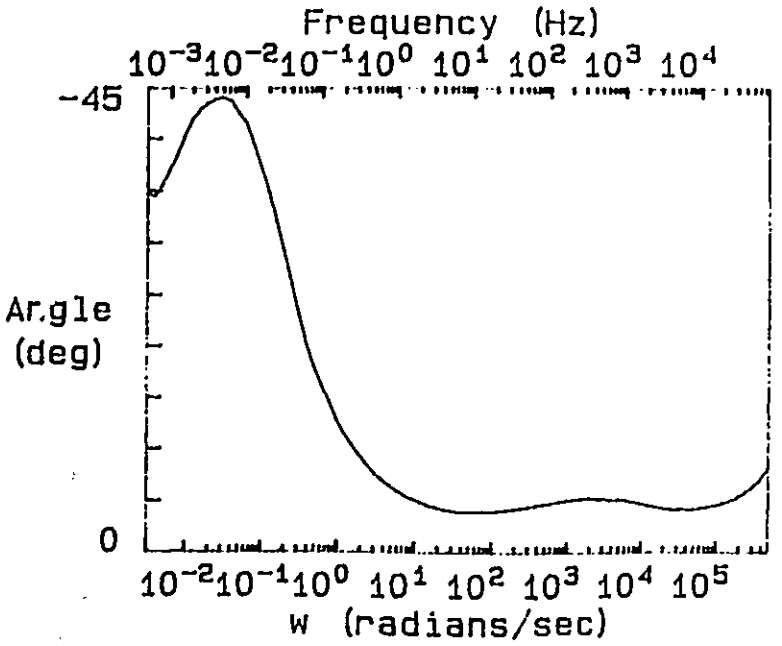

B15 Test #1
October 11, 1995

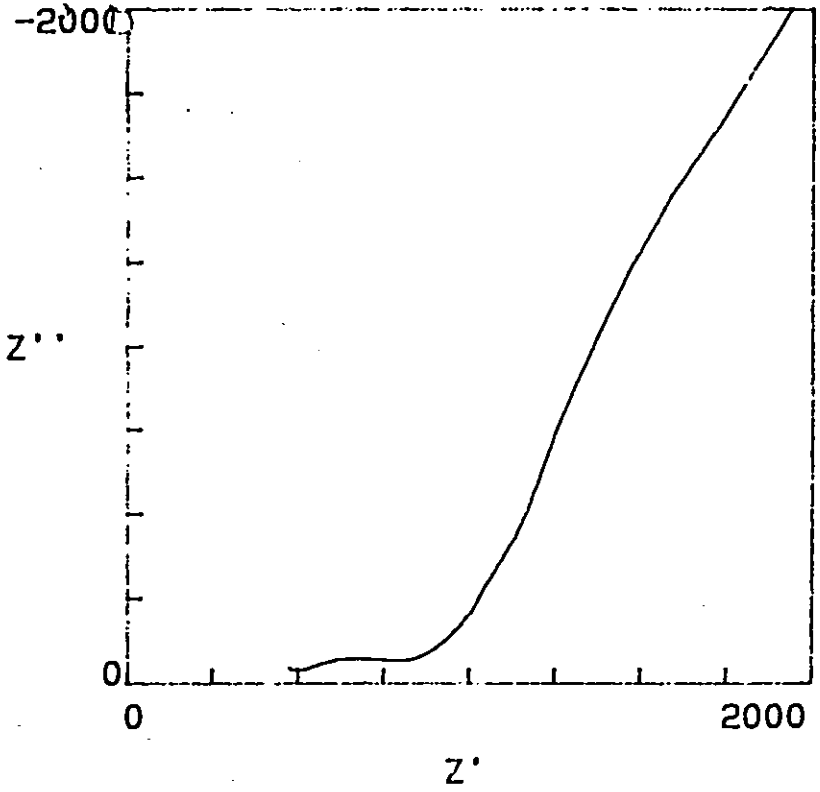

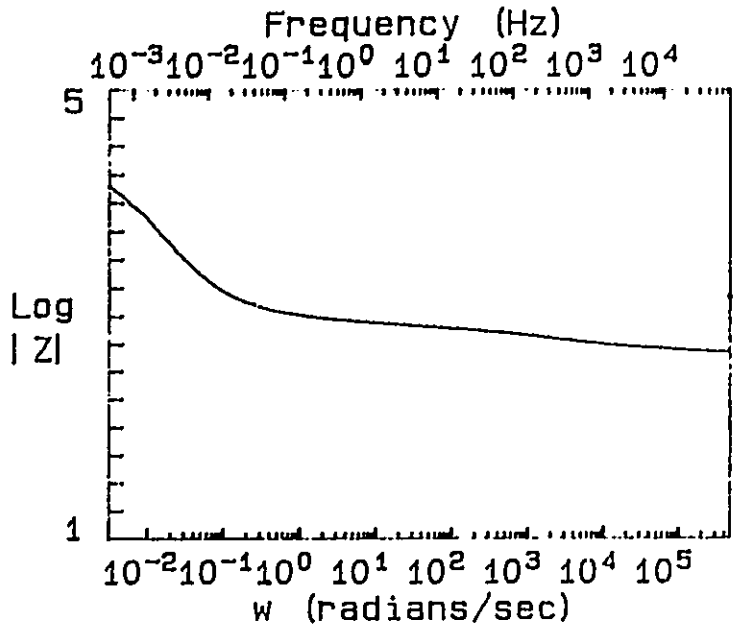

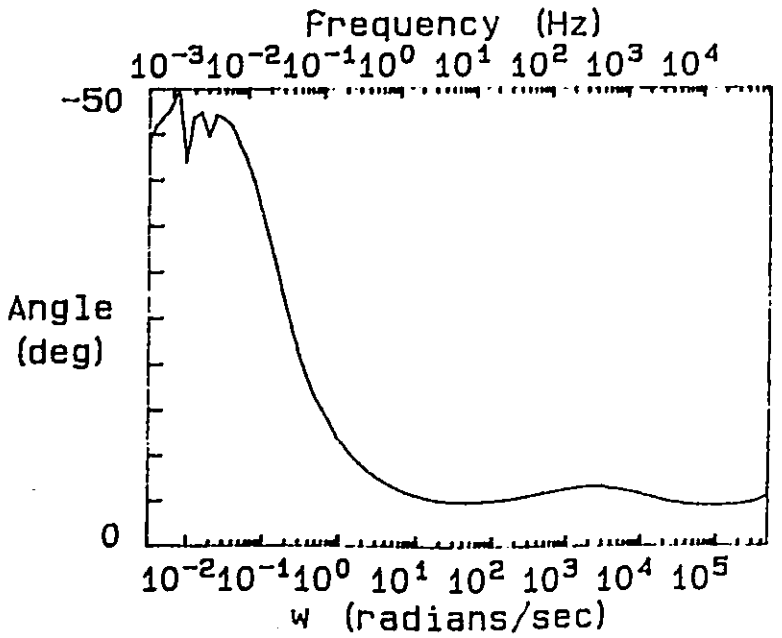

Bi5 Test #2
October 12, 1995

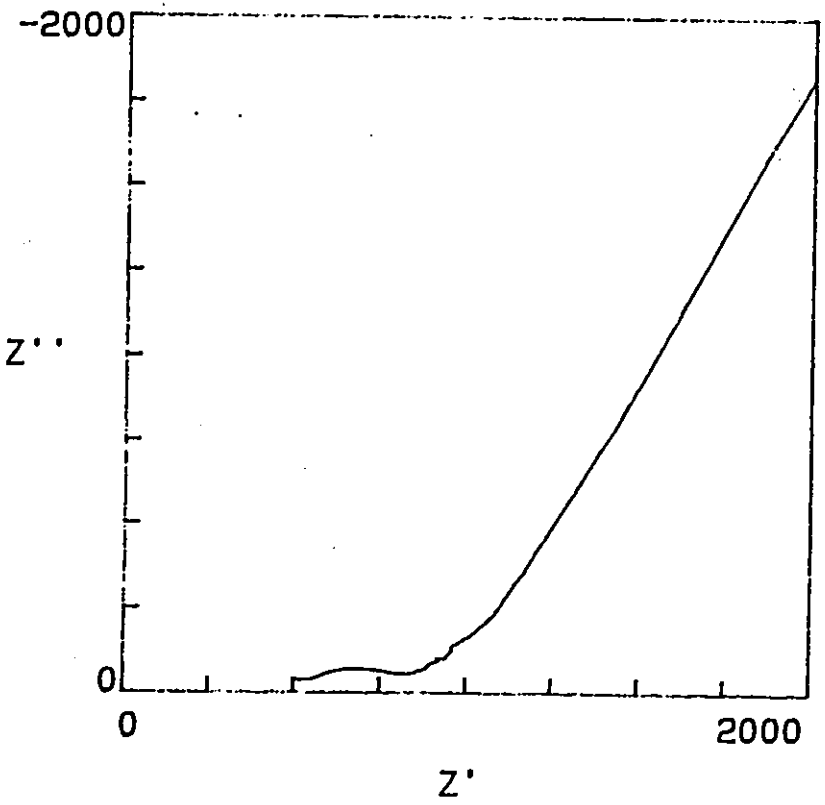

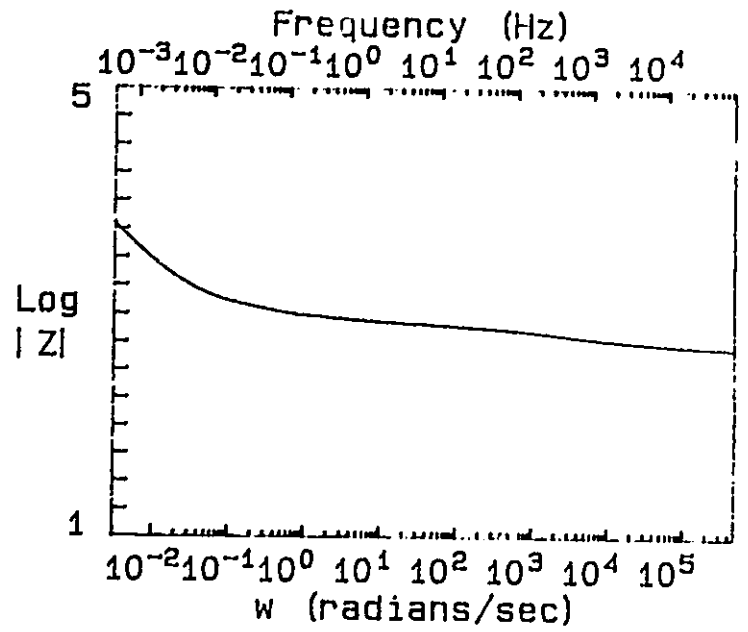

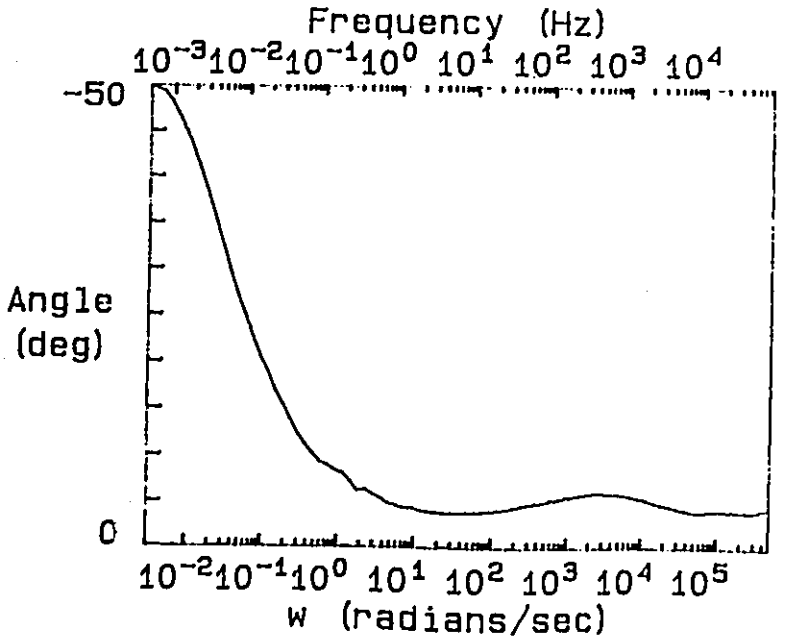

B21 Test #1
October 13, 1995

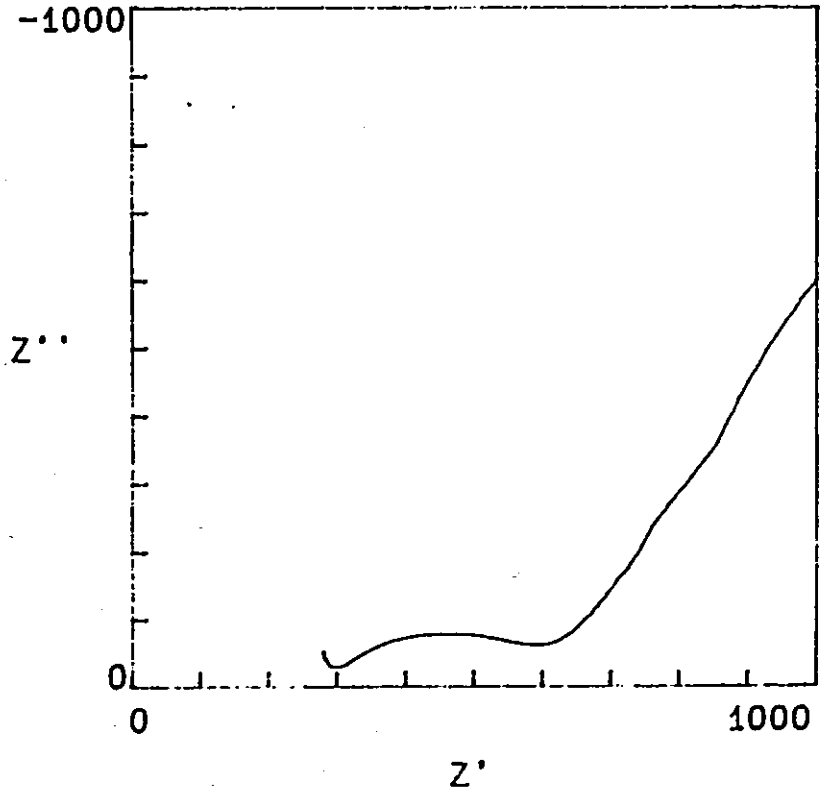

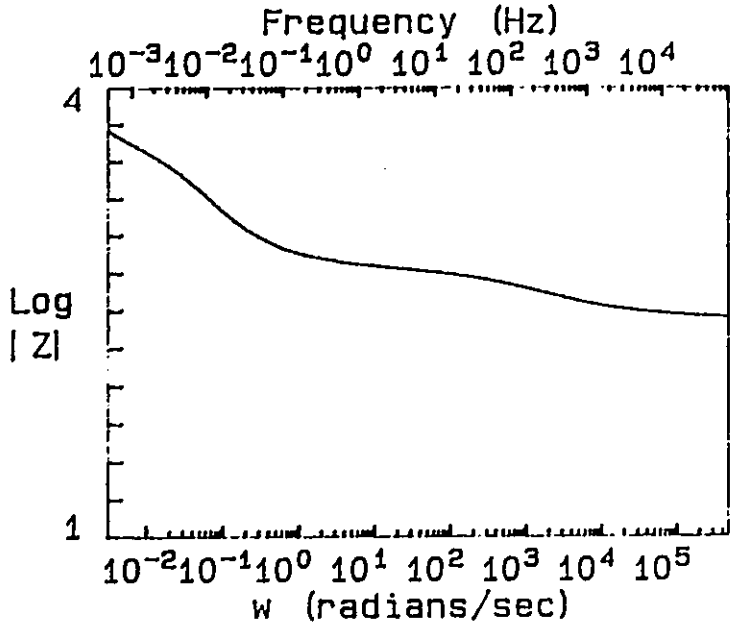

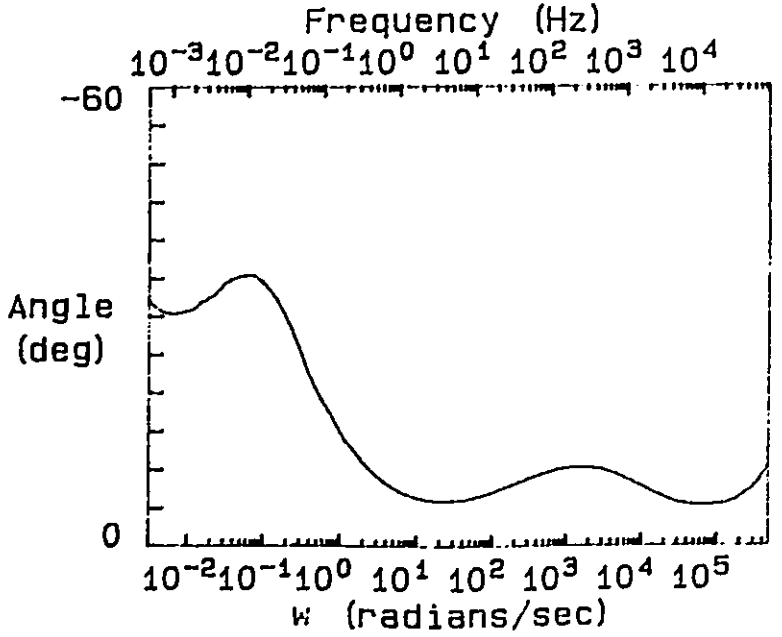

B34 Test #1
October 3, 1995

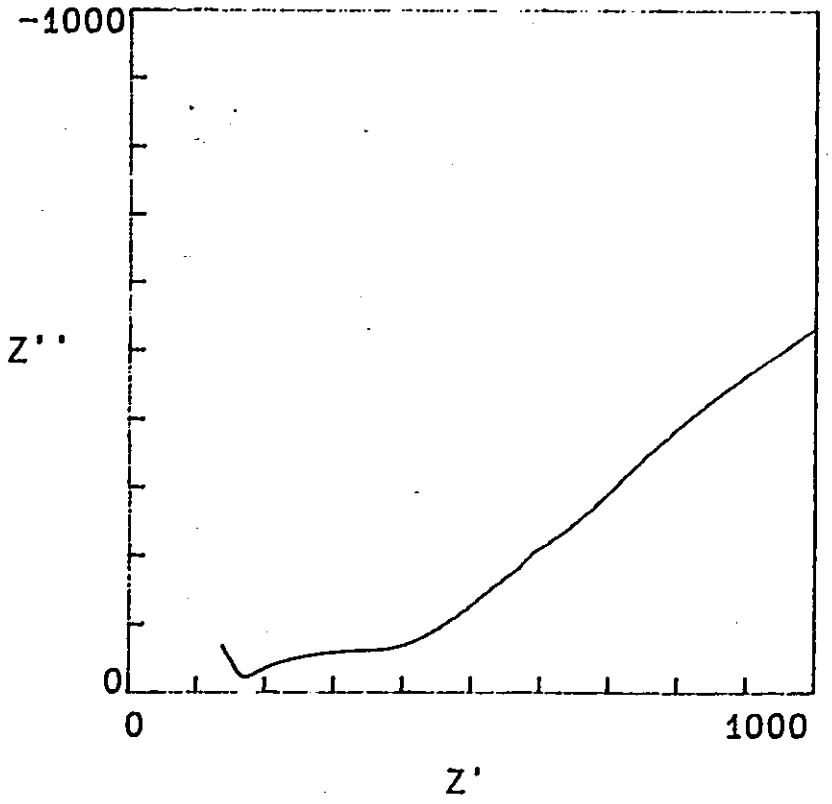

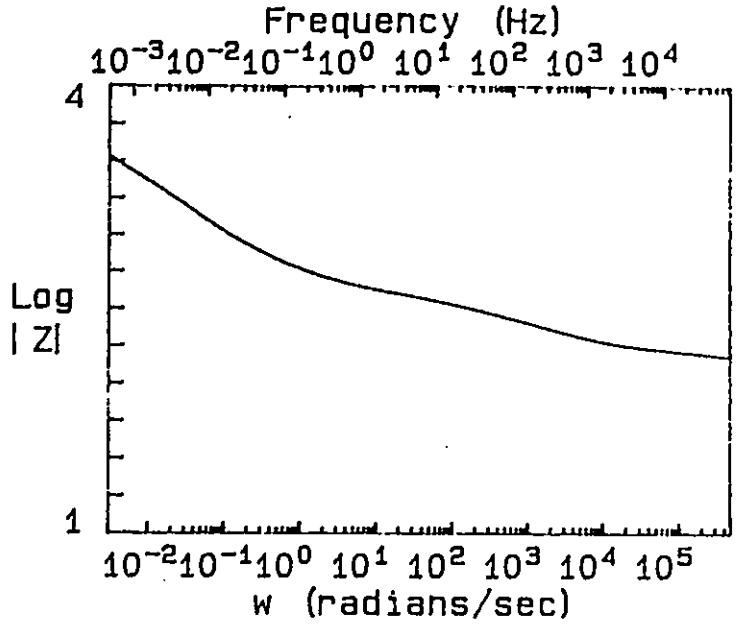

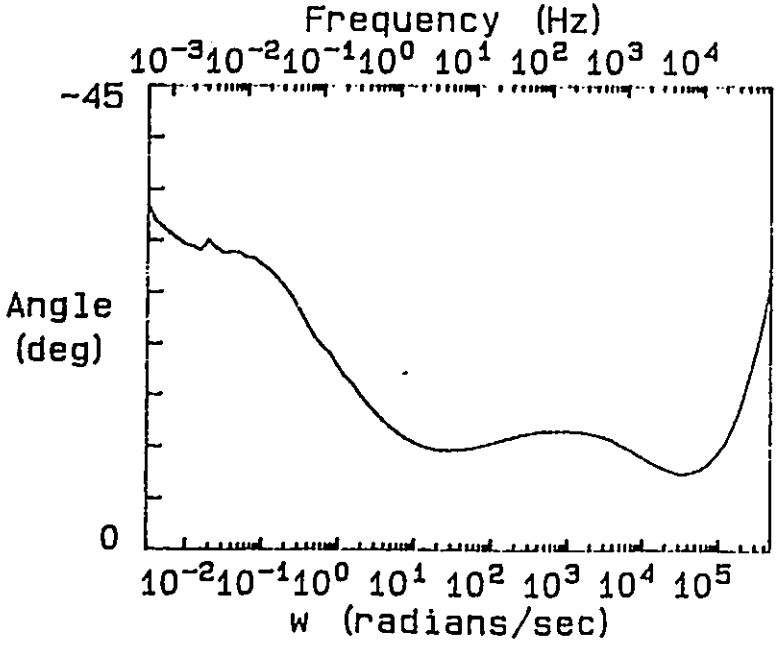

C11 Test #2
October 20, 1995

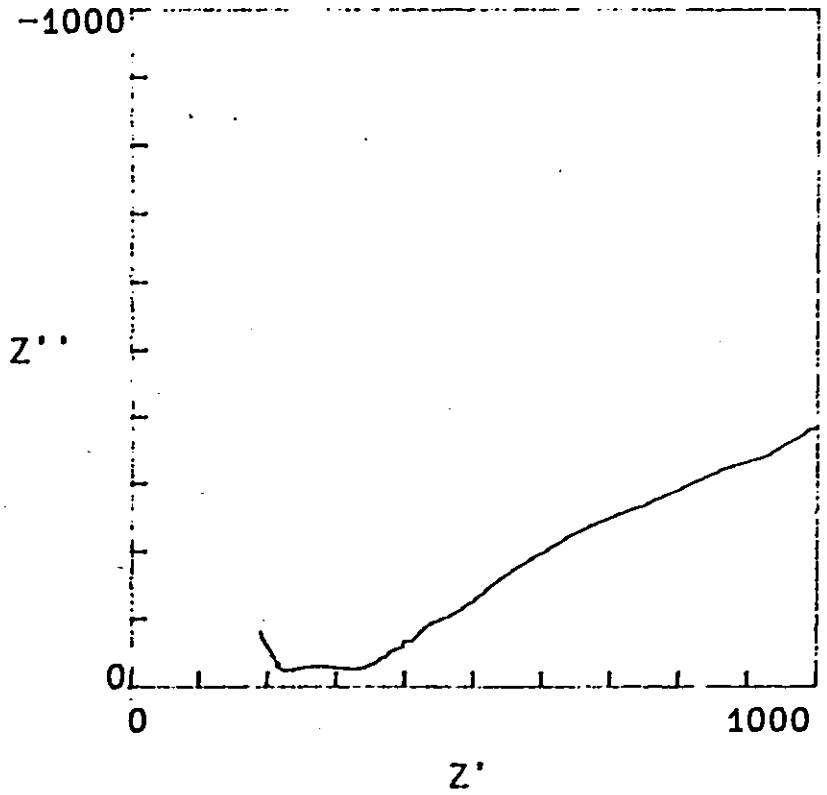

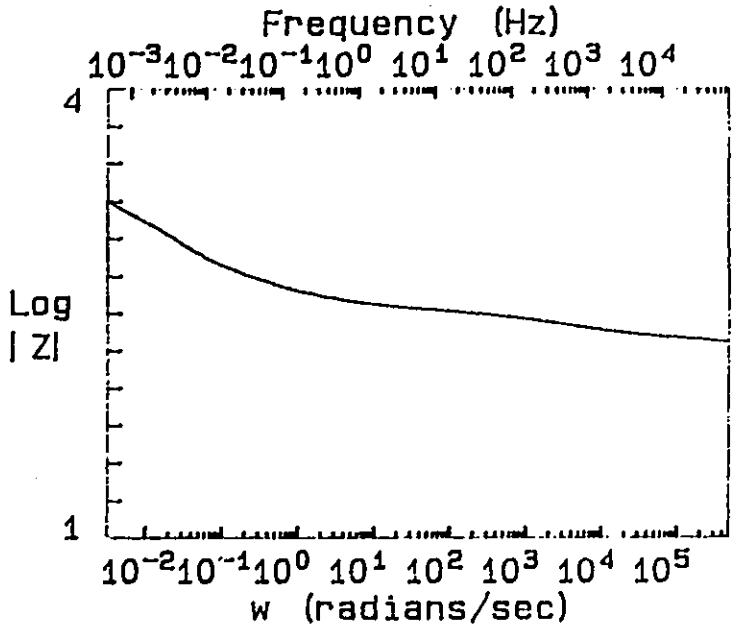

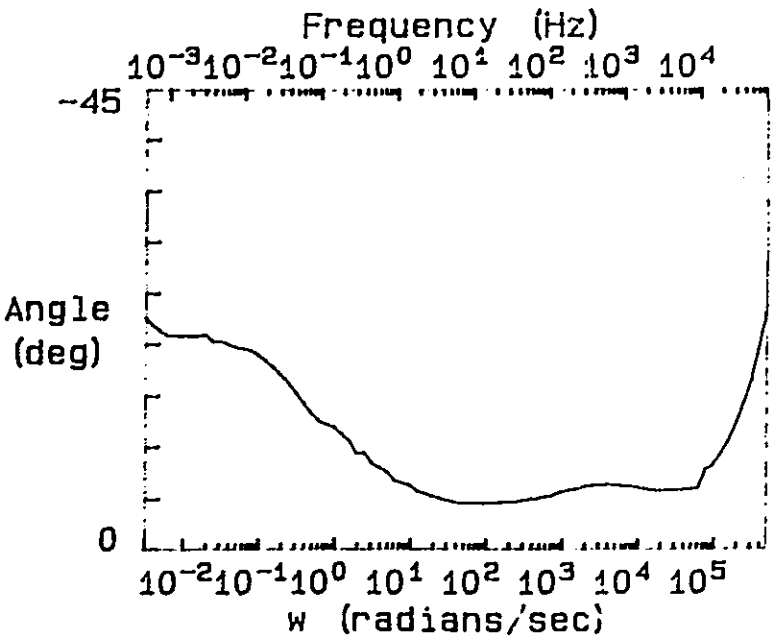

C11 Test #1
October 20, 1995

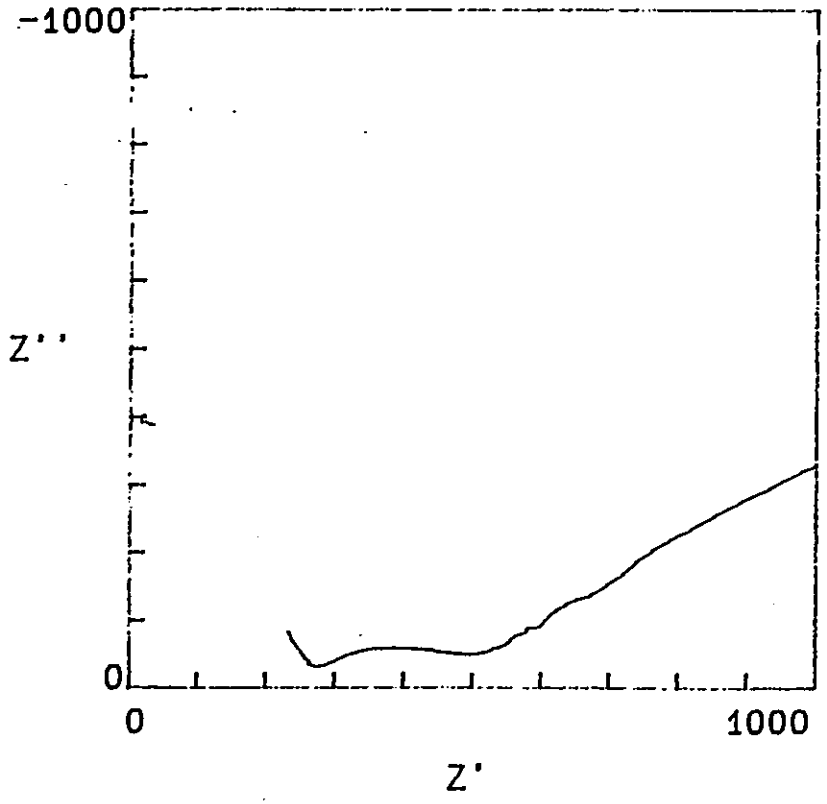

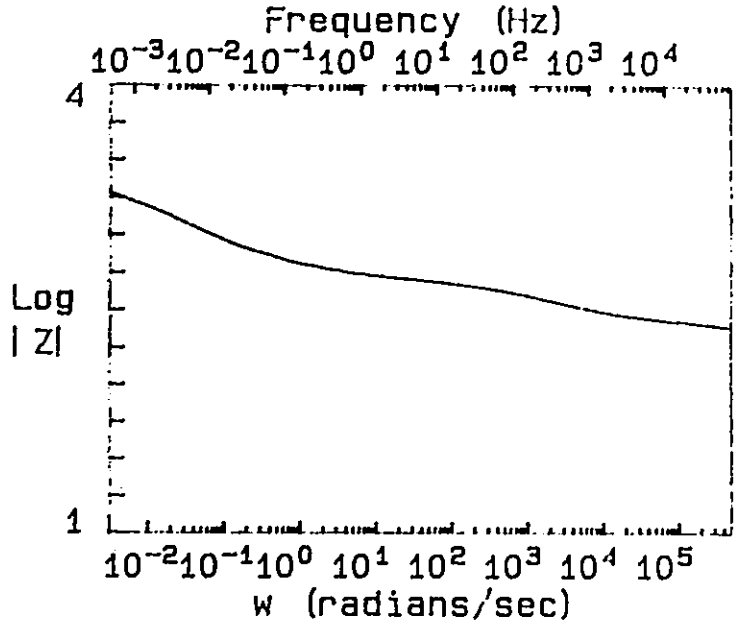

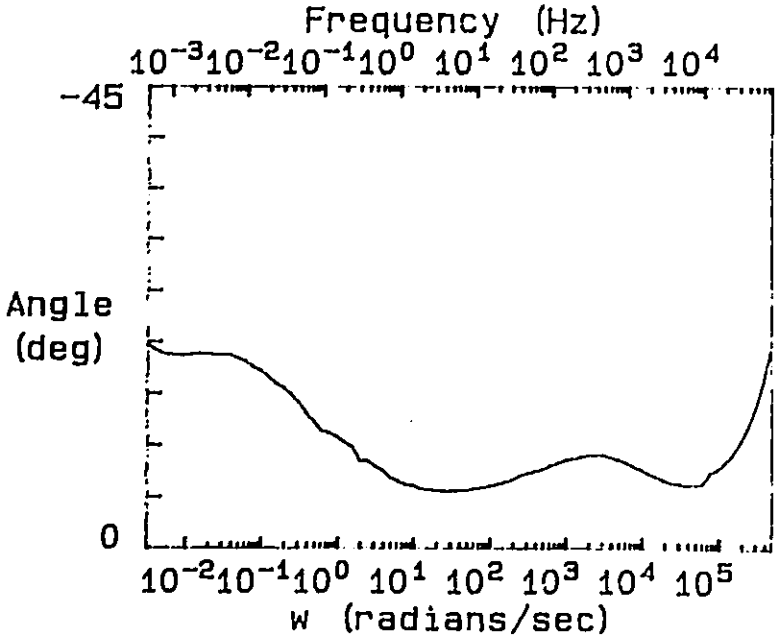

B34 Test #2
October 4, 1995

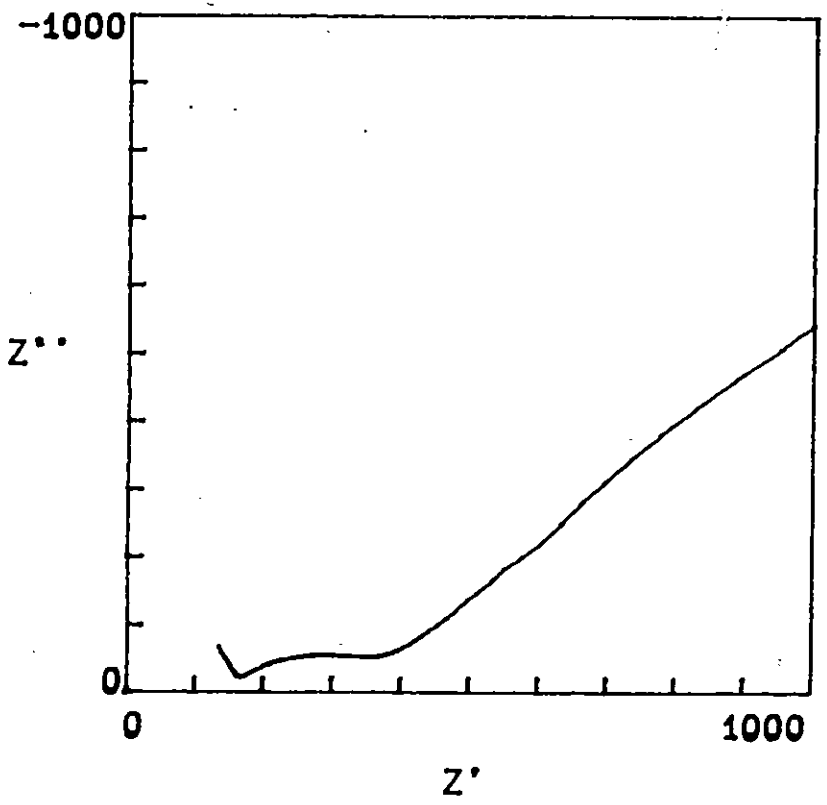

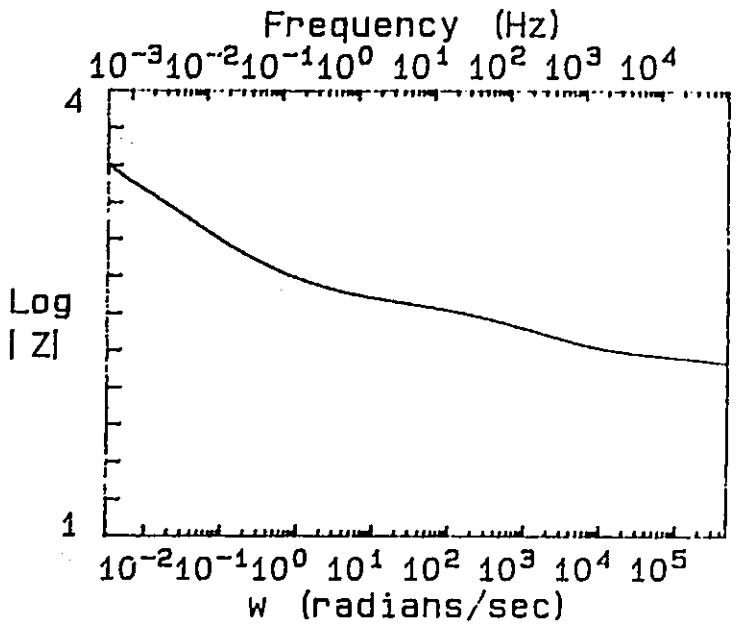

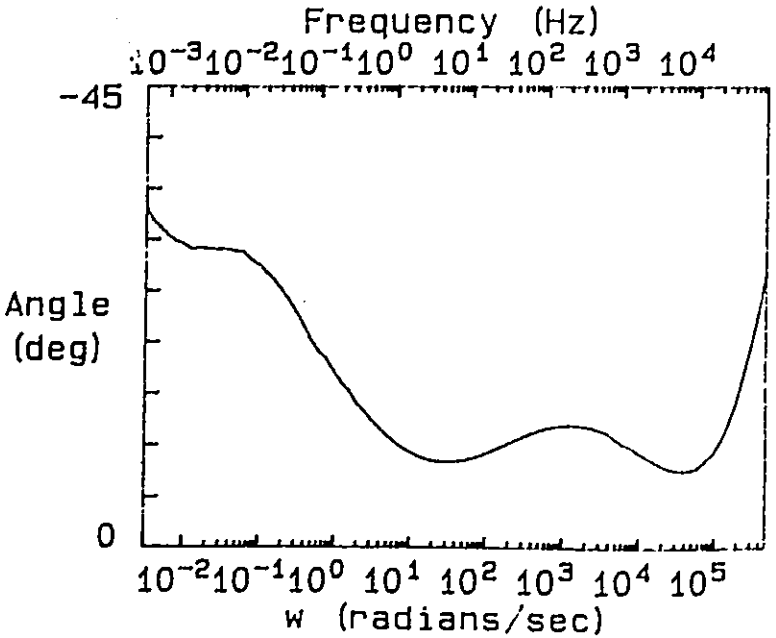

C22 Test #1
October 10, 1995
. . . . . .

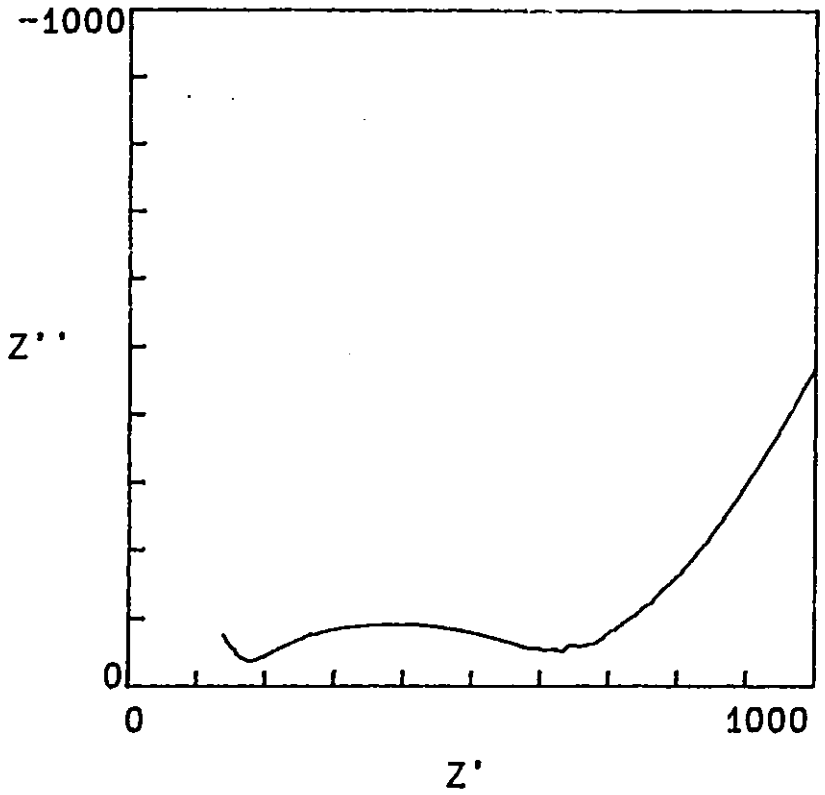

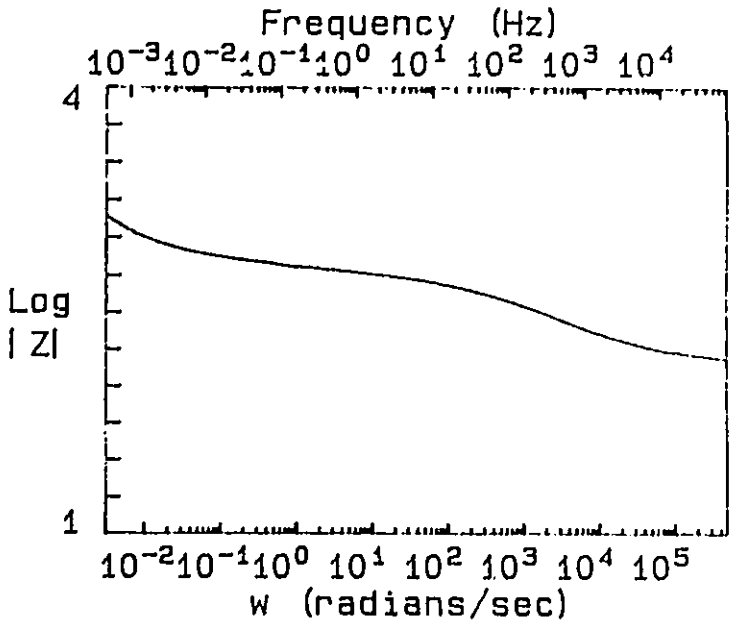

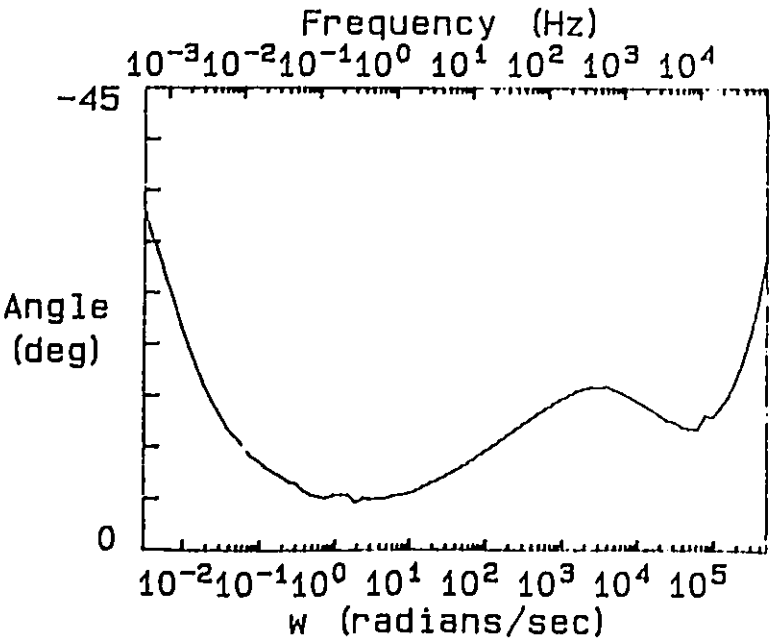

C22 Test #2
October 10, 1995

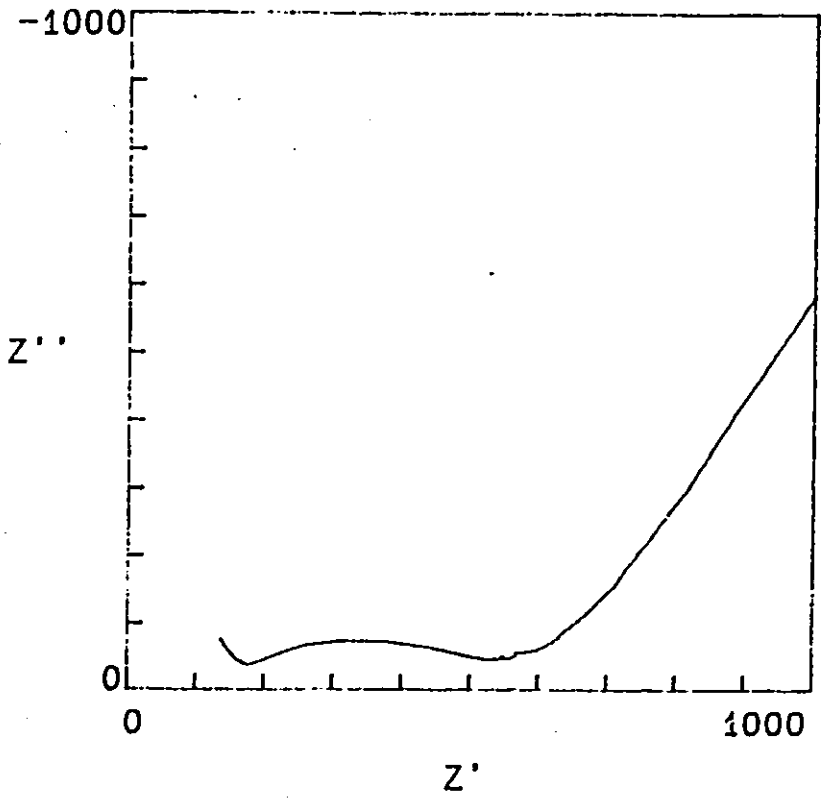

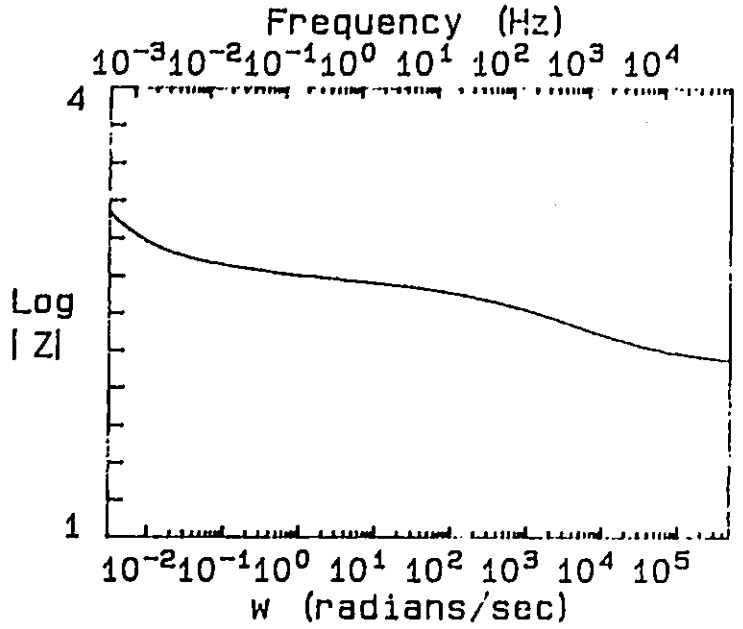

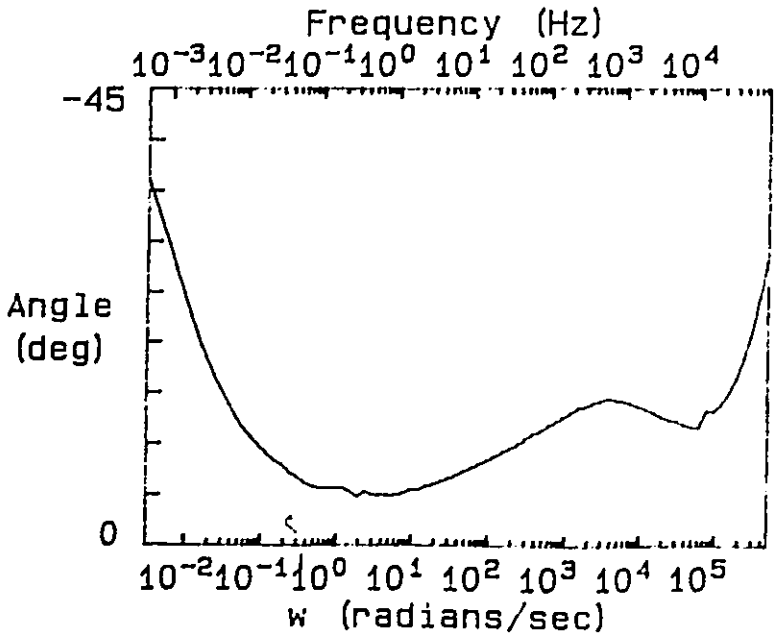

C34 Test #1
October 4, 1995

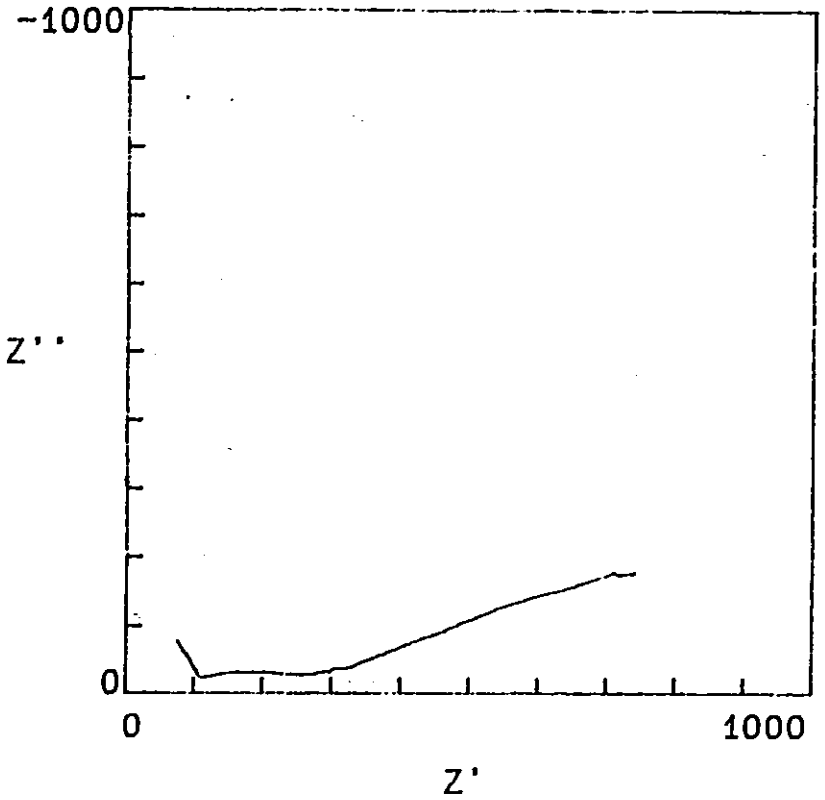

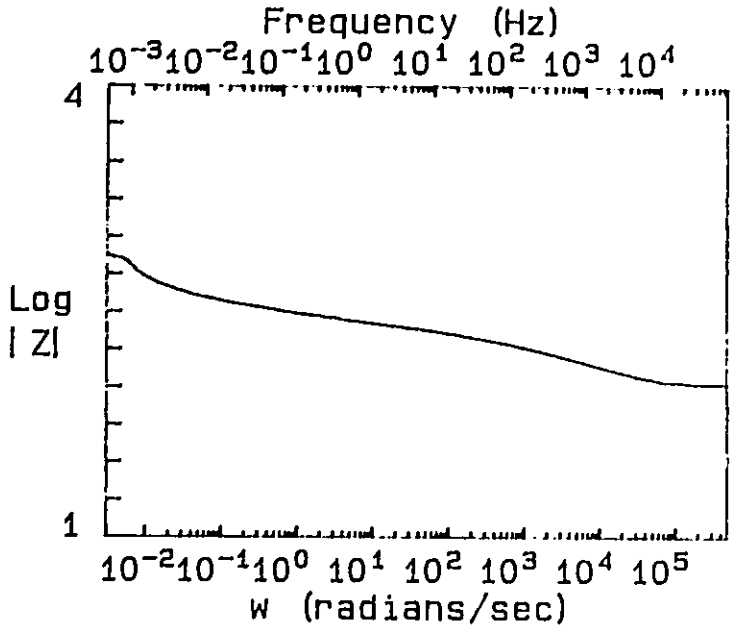

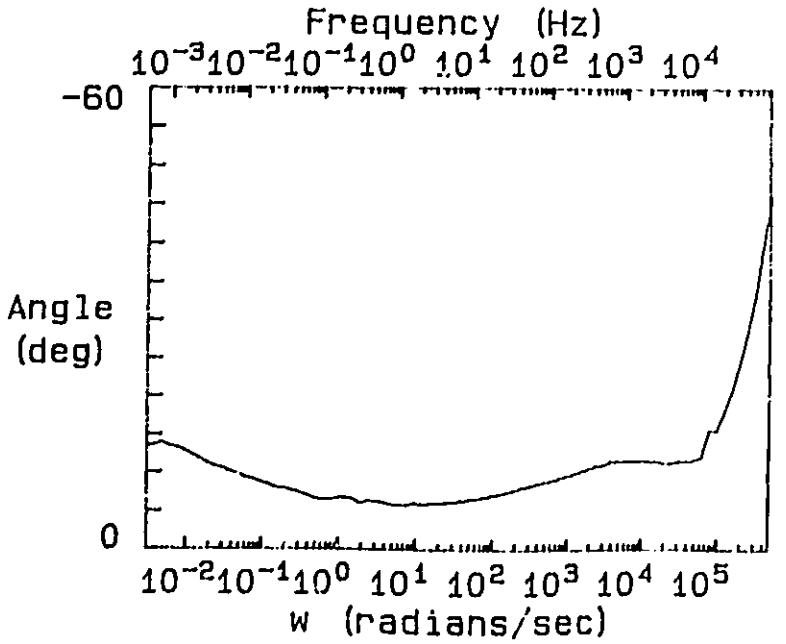

C34 Test #2
October 4, 1995

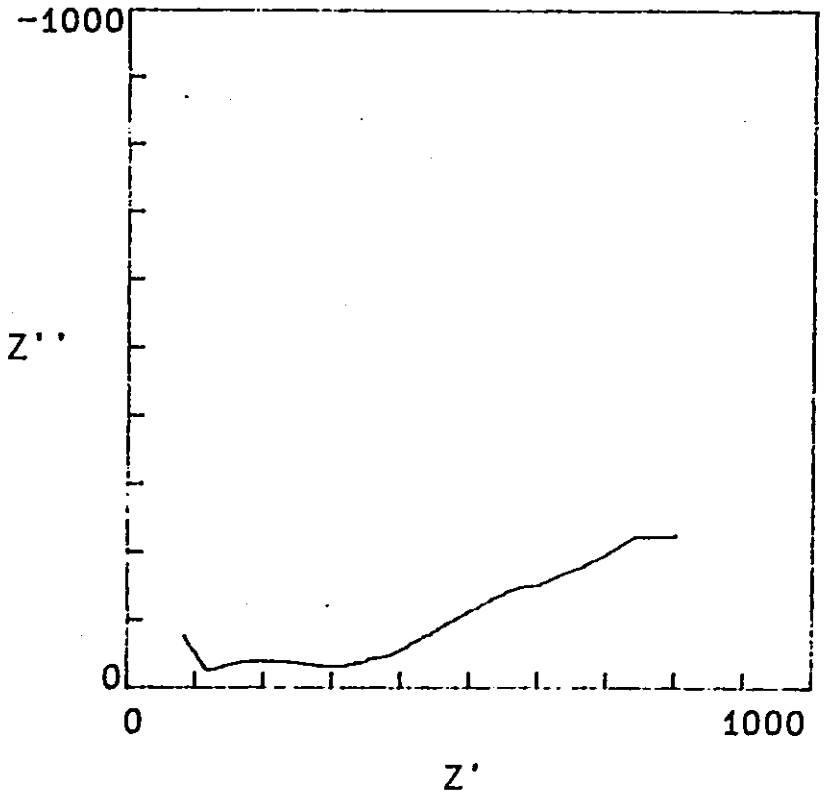

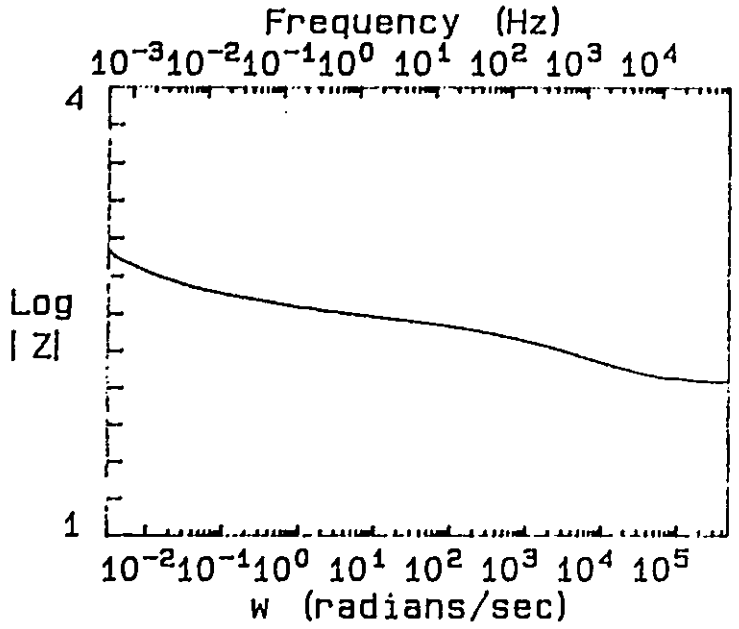

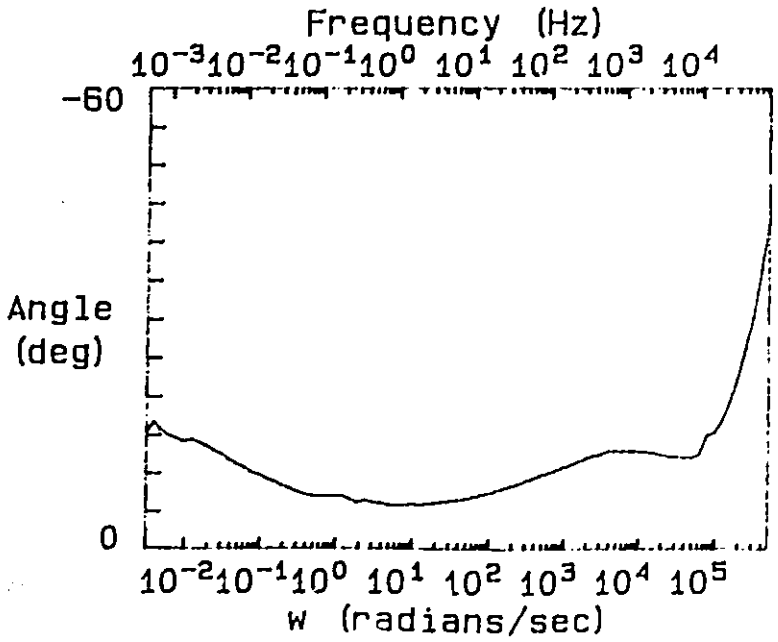

A.C. Impedance

Freq: +0.1000

Sample	Z'	Z"	Angle	Log|Z|
A11-1	425.3500	-27.2580	-3.6681	2.6296
A11-2	429.3100	-29.3970	-3.9172	2.6338
A11-3	431.1000	-28.9340	-3.8397	2.6356
A12-1				
A12-2	829.6700	-180.8300	-12.2956	2.9290
A12-3	825.4100	-177.9500	-12.1662	2.9265
A13-1				
A13-2	742.2700	-94.9000	-7.2858	2.8741
A13-3	739.0600	-95.4790	-7.3613	2.8723
A14-1	647.4500	-56.2080	-4.9617	2.8128
A14-2	648.3100	-55.7400	-4.9141	2.8134
A14-3				
A15-1	496.1500	-68.4900	-7.8596	2.6997
A15-2	491.7000	-66.4200	-7.6931	2.6956
A15-3	488.7900	-66.3190	-7.7267	2.6931
A21-1	549.7900	-79.9690	-8.2758	2.7447
A21-2	544.6800	-78.6750	-8.2191	2.7406
A21-3	545.7900	-78.4900	-8.1845	2.7415
A22-1	353.1800	-54.6670	-8.7987	2.5531
A22-2	357.5800	-54.7570	-8.7062	2.5584
A22-3	359.1500	-55.8630	-8.8411	2.5605
A23-1	508.3300	-175.3900	-19.0361	2.7306
A23-2	506.6901	-174.7200	-19.0255	2.7291
A23-3	505.1801	-173.0200	-18.9059	2.7275
A24-1	426.8900	-52.7000	-7.0376	2.6336
A24-2	435.8600	-53.1280	-6.9496	2.6425
A24-3	443.1200	-54.7140	-7.0389	2.6498
A25-1	366.8300	-33.8470	-5.2717	2.5663
A25-2	368.6800	-32.9020	-5.0997	2.5684
A25-3	370.0800	-33.9060	-5.2347	2.5701
A31-1	328.0900	-144.7400	-23.8051	2.5546
A31-2	334.7100	-145.1400	-23.4430	2.5621
A31-3	339.7600	-147.8400	-23.5153	2.5688
A32-1	315.7200	-72.6790	-12.9637	2.5105
A32-2	317.3900	-74.5900	-13.2251	2.5133
A32-3	318.7200	-74.7220	-13.1944	2.5150
A33-1	265.4900	-41.6740	-8.9209	2.4293
A33-2	273.6000	-44.6760	-9.2740	2.4428
A33-3	279.2800	-45.7310	-9.2994	2.4518
A34-1	263.3500	-27.1580	-5.8878	2.4228
A34-2	273.8900	-30.3090	-6.3147	2.4402
A34-3	277.6700	-30.9930	-6.3689	2.4462
A35-1	376.0300	-153.2900	-22.1785	2.6086
A35-2	381.2600	-155.5300	-22.1924	2.6146
A35-3	383.7000	-156.3800	-22.1738	2.6174
B11-1				
B11-2	832.8401	-195.5600	-13.2143	2.9321
B11-3	835.5500	-196.9100	-13.2607	2.9337

A.C. Impedance

Sample	Z'	Z''	Angle	Log|Z|
B12-1				
B12-2	931.4901	-235.2000	-14.1709	2.9826
B12-3	924.8500	-238.5900	-14.4656	2.9801
B13-1	721.2501	-93.1091	-7.3559	2.8617
B13-2	720.6000	-92.9810	-7.3524	2.8590
B14-1	979.7200	-287.9100	-16.3765	3.0091
B14-2	979.2401	-284.7700	-16.2148	3.0085
B14-3	980.4301	-286.2600	-16.2764	3.0092
B15-1				
B15-2	922.6600	-188.0900	-11.5222	2.9739
B15-3	927.8201	-188.9000	-11.5079	2.9763
B21-1	642.7300	-210.9500	-18.1703	2.8302
B21-2	656.1801	-211.5100	-17.8660	2.8385
B21-3	658.7500	-212.1600	-17.8519	2.8402
B22-1	495.8700	-73.5580	-8.4378	2.7001
B22-2	496.3600	-72.6770	-8.3301	2.7004
B22-3	497.5500	-73.6280	-8.4176	2.7015
B23-1	695.7600	-133.0300	-10.8244	2.8503
B23-2	704.6500	-135.5500	-10.8687	2.8559
B23-3	709.2100	-134.3700	-10.7283	2.8584
B24-1	621.6100	-111.5700	-10.1754	2.8004
B24-2				
B24-3	623.7700	-11.1300	-10.1018	2.8018
B25-1	533.7900	-75.3390	-8.0337	2.7317
B25-2	539.2100	-77.3790	-8.1664	2.7362
B25-3	597.6100	-77.8560	-7.4226	2.7801
B31-1	418.6300	-205.7400	-26.1723	2.6688
B31-2	418.0700	-204.3900	-26.0536	2.6678
B31-3	417.7500	-203.2400	-25.9434	2.6670
B32-1	449.1100	-198.8900	-23.8863	2.6912
B32-2	456.9400	-199.8200	-23.6198	2.6979
B32-3	462.8100	-202.2600	-23.6066	2.7034
B33-1	534.5800	-316.0300	-30.5905	2.7931
B33-2	551.4600	-318.7100	-30.0253	2.8041
B33-3	555.0601	-318.7100	-29.8640	2.8062
B34-1	520.6700	-209.7200	-21.9390	2.7492
B34-2	532.2900	-211.6800	-21.6866	2.7580
B34-3	535.9700	-212.4700	-21.6244	2.7608
B35-1	476.1800	-80.0710	-9.5452	2.6838
B35-2	486.8900	-81.5260	-9.5056	2.6934
B35-3	501.9900	-87.8250	-9.9237	2.7072
C11-1	605.3600	-163.7900	-15.1398	2.7974
C11-2	614.2200	-167.3900	-15.2443	2.8039
C11-3	617.4100	-165.7200	-15.0247	2.8057
C12-1	491.8900	-31.9510	-3.7165	2.6928
C12-2	492.1500	-31.5580	-3.6689	2.6930
C12-3	491.7000	-31.4400	-3.6714	2.6926
C13-1	551.4800	-72.7880	-7.5188	2.7453
C13-2	554.5800	-71.6400	-7.3606	2.7476
C13-3	558.7500	-73.8670	-7.5309	-2.7510

A.C. Impedance

Sample	Z'	Z''	Angle	Log|Z|
C14-1	695.7000	-180.1700	-14.5193	2.8565
C14-2	697.8201	-176.8000	-14.5779	2.8466
C14-3	674.1000	-175.2200	-14.5706	2.8429
C15-1	787.0800	-153.7400	-11.0524	2.9041
C15-2	791.8901	-155.5400	-11.1124	2.9069
C15-3	795.4801	-151.0500	-10.7516	2.9083
C21-1	532.5800	-103.7300	-11.0215	2.7345
C21-2	533.9600	-104.8100	-11.1053	2.7357
C21-3	530.5300	-103.2300	-11.0110	2.7328
C22-1	572.2101	-60.6310	-6.0485	2.7600
C22-2	575.3000	-61.3210	-6.0842	-2.7623
C22-3	574.6600	-59.4700	-5.9084	2.7617
C23-1	510.2200	-104.0700	-11.5285	2.7166
C23-2	500.4601	-102.4500	-11.5693	2.7003
C23-3	485.8100	-101.5500	-11.5750	2.7042
C24-1	566.2401	-44.9430	-4.5381	2.7543
C24-2	566.1400	-45.9210	-4.6373	2.7543
C24-3	564.1400	-46.3390	-4.6958	2.7528
C25-1	374.5500	-55.3210	-8.4018	2.5782
C25-2	372.5600	-55.4950	-8.4723	2.5760
C25-3	372.1400	-55.3390	-8.4582	3.5755
C31-1	260.1100	-45.2260	-9.8636	2.4216
C31-2	264.0000	-45.8800	-9.8589	2.4281
C31-3	265.0201	-45.8960	-9.8250	2.4297
C32-1	396.5200	-137.0200	-19.0629	2.6228
C32-2	407.8300	-145.0500	-19.5786	2.6363
C32-3	408.1900	-145.7700	-19.6523	2.6369
C33-1	398.2500	-99.1140	-13.9755	2.6132
C33-2	418.7100	-104.1700	-13.9709	2.6350
C33-3	419.9400	-103.5400	-13.8565	2.6360
C34-1	336.6900	-47.8060	-8.0813	2.5316
C34-2	342.2200	-49.8960	-8.2952	2.5389
C34-3	344.8000	-50.6390	-8.3550	2.5422
C35-1	324.9900	-149.9100	-24.7627	2.5538
C35-2	329.7400	-152.9700	-24.8871	2.5605
C35-3	331.2400	-156.8500	-24.8701	2.5641

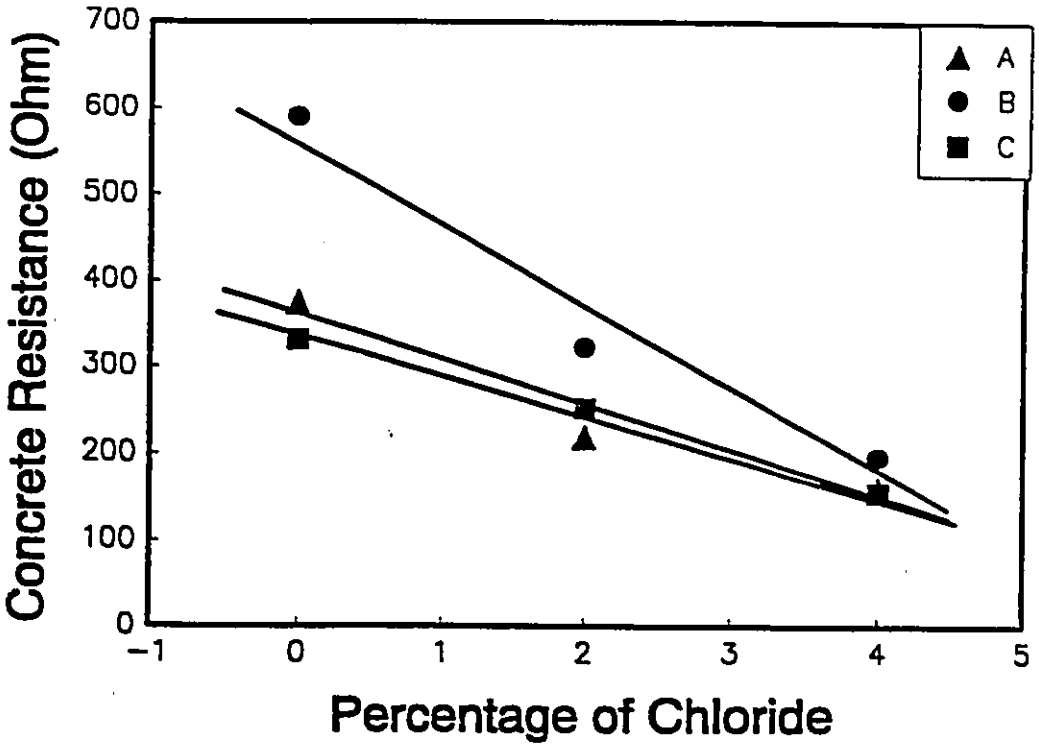

CONCRETE RESISTANCE OF THE TEST SAMPLES CONTAINING DIFFERENT PERCENTAGE OF CHLORIDE; A – CONTROL CONCRETE; B – CONCRETE CONTAINING 5% SODIUM NITRITE; C – CONCRETE CONTAINING 5% DINITROBENZOIC ACID